ABSTRACT

Photochemical Modification of Proteins and Tissue Surface
using 1,8-naphthalimides; DNA Enzyme Cofactors

Gabriela Uzcategui, Ph.D.

Mentor: Robert R. Kane, Ph.D.

Our lab has long had an interest in the potential biomedical applications of naphthalimide photochemistry, including especially the use for the bonding and modification of fresh tissue. Photochemical tissue bonding represents a possible tool for the repair of tissues such as cornea, skin grafts, tendons and heart valves. Accordingly, this dissertation reports extensive mechanistic and structure-activity (SAR) studies that were performed using 4-substituted naphthalimide derivatives as sensitizers and soluble proteins or fresh tissues as substrates. The initial studies were focused on the crosslinking and modification of soluble proteins as models for tissue surfaces, and used RNAse A and lysozyme. More recent studies have been aimed at extending these studies to the modification of fresh tissue surfaces. Bovine pericardium tissue, pig skin and bovine knee meniscal tissue were used as substrates in these experiments. It was demonstrated that compounds containing dopamine, histidine, hydrazide and tyramine showed the most promising incorporation in both protein and tissue models, and similar trends were observed in both the protein models and the tissue experiments. Mechanistic studies

suggested multiple photochemical mechanisms, and SAR studies identified promising naphthalimides.

In a second research project small organic compounds were synthesized and studied as cofactors for the discovery of DNA enzymes. The goal was to isolate DNA enzymes that catalyzed the cleavage of a ribonucleotide phosphoester substrate assisted by the synthetic cofactor. Another goal was to develop a broader understanding of how these cofactors function by potential candidates with different structural characteristics and then identifying which characteristics enhance the catalytic activity of the DNA enzymes. Concentration, and the time of interaction of the cofactors with the DNA enzyme during the *in vitro* selection process, played an important role in the catalytic activity of the species.

Photochemical Modification of Proteins and Tissue Surface
using 1,8-naphthalimides; DNA Enzyme Cofactors

by

Gabriela Uzcategui, B.S.

A Dissertation

Approved by the Department of Chemistry and Biochemistry

_____
Patrick J. Farmer, Ph.D. Chairperson

Submitted to the Graduate Faculty of
Baylor University in Partial Fulfillment of the
Requirements for the Degree
of
Doctor of Philosophy

Approved by the Dissertation Committee

_____
Robert R. Kane, Ph.D. Chairperson

_____
Kevin G. Pinney, Ph.D.

_____
Charles M. Garner, Ph.D.

_____
Sung-Kun Kim, Ph.D.

_____
Bessie W. Kebaara, Ph.D.

Accepted by the Graduate School
August 2010

_____
J. Larry Lyon, Ph.D., Dean

Page bearing signatures is kept on file in the Graduate School.

TABLE OF CONTENTS

LIST OF FIGURES xi

LIST OF SCHEMES xx

LIST OF TABLES xxii

LIST OF ABBREVIATIONS xxiii

ACKNOWLEDGMENTS xxvii

DEDICATION xxix

CHAPTER ONE 1

Introduction 1

Protein modification 1

Photochemistry 9

Type I mechanism. Electron transfer 12

Type II mechanism. Energy transfer 14

Amino Acid Redisues with singlet oxygen 15

Distinguishing between Type I and Type II processes 19

Photosensitizers 20

Current research goals and strategies 31

CHAPTER TWO 32

Reagents and material 32

Instrumentation and analytical techniques 32

Photochemical protein crosslinking 32

NMR analysis …….. 33

LC-MS ……... 33

SDS-PAGE Electrophoresis ……... 33

Western Blots …… 34

Synthetic procedure ……... 34

Synthetic procedure of 1,8-naphthalimides (Sensitizers) …… 34

*2-[2-(Diethylamino)ethyl]-1H-benz[de]isoquinoline-1,3(2H)-dione (**NP5**)* ... 34

*6-Bromo-2-[2-(diethylamino)ethyl]-1H-benz[de]isoquinoline-1,3(2H)-dione (**NP6**)* ……..……..... 35

*2-[2-(Diethylamino)ethyl]-6-ethylsulfanyl-1H-benz[de]isoquinoline-1,3(2H)-dione (**NP7**)* …… 36

*2-[2-(Diethylamino)ethyl]-6-ethoxy-1H-benz[de]isoquinoline-1,3(2H)-dione (**NP8**)* ……..……... 37

*2-[2-(Diethylamino)ethyl]-6-ethylamino-1H-benz[de]isoquinoline-1,3(2H)-dione (**NP9**)* …… 38

Synthetic procedure of the biotin labeled derivatives …… 39

*5-(2-Oxo-hexahydro-thieno[3,4-d]imidazol-4-yl)-pentanoic acid (5-hydrazinocarbonyl-pentyl)-amide (Biotin-LC-hydrazide, **BD1**)* ……..... 39

*5-(2-Oxo-hexahydro-thieno[3,4-d]imidazol-4-yl)-pentanoic acid [2-(3,4-dihydroxy-phenyl)-ethyl]-amide (Biotin-dopamine, **BD2**)* ……..……... 40

*3-(1H-Indol-3-yl)-2-[5-(2-oxo-hexahydro-thieno[3,4-d]imidazol-4-yl)-pentanoylamino]-propionic acid methyl ester (Biotin-tryptophan methyl ester, **BD3**)* ……..……... 41

*3-(1H-Indol-3-yl)-2-[5-(2-oxo-hexahydro-thieno[3,4-d]imidazol-4-yl)-pentanoylamino]-propionic acid (Biotin-tryptophan, **BD4**)* ……..…… 42

*3-(1H-Imidazol-4-yl)-2-[5-(2-oxo-hexahydro-thieno[3,4-d]imidazol-4-yl)-pentanoylamino]-propionic acid (Biotin-histidine, **BD5**)* …….. 43

*4-Methylsulfanyl-2-[5-(2-oxo-hexahydro-thieno[3,4-d]imidazol-4-yl)-pentanoylamino]-butyric acid (Biotin-methionine, **BD6**)* …….. 44

*4-Hydroxy-1-[5-(2-oxo-hexahydro-thieno[3,4-d]imidazol-4-yl)-pentanoyl]-pyrrolidine-2-carboxylic acid methyl ester (Biotin-hydroxyproline methyl ester, **BD7**)* 45

*4-Hydroxy-1-[5-(2-oxo-hexahydro-thieno[3,4-d]imidazol-4-yl)-pentanoyl]-pyrrolidine-2-carboxylic acid (Biotin-hydroxyproline, **BD8**)* 46

*5-(2-Oxo-hexahydro-thieno[3,4-d]imidazol-4-yl)-pentanoic acid[2-(4-hydroxy-phenyl)-ethyl]-amide (Biotin-tyramine, **BD9**)* 47

Experimental conditions for protein and tissue modification 48

Photochemical modification of proteins 48

SDS-PAGE analysis 48

Western Blotting analysis 49

Preparation of the Western blotting solutions 51

Tissue experiments 52

Mass spectral analysis of digested RNase A 53

CHAPTER THREE 55

Results and Discussion 55

Synthesis of sensitizers 55

Selection of proteins 56

Modification of RNAse A and Lysozyme with naphthalimide derivatives 58

Optimization of Lysozyme crosslinking 62

Effect of free amino acids on protein crosslinking 65

RNase A and Lysozyme inhibition studies with amino acids 68

Synthesis of biotin labeled derivatives 70

Stability studies of biotin side amino acid chain compounds 71

Incorporation of biotin labeled derivatives into proteins 75

Inhibition studies using biotin labeled compounds ……..…….. 82

Influence of sodium azide (NaN_3) and superoxide dismutase (SOD) on the photosensitized reactions of RNase A and Lysozyme….…… 85

Formation of persistent reactive intermediates in the naphthalimide-sensitized photochemical reactions of RNase A and Lysozyme ……...……. 89

Mass Spectral Analysis of Digested RNase A using as Sensitizer Naphthalimide ***NP8*** …….. 91

Tissue Modification Experiments ……...……... 97

Photochemical Incorporation of Biotin Derivatives into Pericardium Tissue …... 98

Photochemical Incorporation of Biotin Derivatives into Meniscus Tissue ……..... 102

Photochemical Incorporation of Biotin Derivatives into Pericardium Tissue – Second Approach …..……. 106

Photochemical Incorporation of Biotin Derivatives into Fetal Pig Skin ……... 112

CHAPTER FOUR ……. 114

Conclusions and future directions …… 114

CHAPTER FIVE …… 117

Introduction …….. 117

DNA Enzymes and In vitro Selection …….. 117

Amino acids as cofactor for obtaining DNA enzymes ……. 128

Current Research Goals and Strategies …… 133

CHAPTER SIX …….. 134

Reagents and material …….. 134

Instrumentation and analytical techniques ……..... 136

Polymerase chain reaction (PCR) …… 136

Agarose and PAGE Electrophoresis ……. 136

Radioactive labeling of DNA 136

NMR analysis 136

Synthethic procedure 137

Synthesis of DNA enzyme cofactors 137

*Trityl-[2-(1-trityl-1H-imidazol-4-yl)-ethyl]-amine (**C1**, diprotected histamine)* 137

*2-(1-trityl-1H-imidazole-4-yl)-ethylamine (**C2**, monoprotected histamine)* 138

*Fmoc-3-amino-N-[2-(1-trityl-1H-imidazol-4-yl)-ethyl]-propionamide (**C3**)* .. 139

*3-amino-N-[2-(1-trityl-1H-imidazol-4-yl)-ethyl]-propionamide (**C4**)* 140

*2-amino-3-(1-trityl-1H-imidazol-4-yl)-N-{2-[2-(1-trityl-1H-imidazol-4-yl)ethylcarbamoyl]-ethyl}-propionamide (**C5**)* 141

*2-Amino-3-(1H-imidazol-4-yl)-N-{2-[2-(1H-imidazol-4-yl)ethylcarbamoyl]-ethyl}-propionamide (**C6**)(histidine cofactor)* 142

*2-Amino-6-carbamimidoyl-hexanoic acid (2-(1H-imidazol-4-yl)-1-{2-[2-(1H-imidazol-4-yl)-ethylcarbamoyl]-ethylcarbamoyl}-ethyl)-amide (**C7**) (Arginine cofactor)* 143

*4-Amino-4-(2-(1H-imidazol-4-yl)-1-{2-[2-(1H-imidazol-4-yl)-ethylcarbamoyl]-ethylcarbamoyl}-ethylcarbamoyl)-butyric acid (**C8**)(Glutamic acid cofactor)* 144

*N-(2-(1H-imidazol-4-yl)-1-{2-[2-(1H-imidazol-4-yl)-ethylcarbamoyl]-ethylcarbamoyl}-ethyl)-isonicotinamide (**C9**) (Isonicotinic cofactor)* 145

Experimental conditions for DNA enzyme isolation 146

In vitro selection technique 146

PCR and in vitro selection conditions using α-dATP ^{32}P as DNA marker 148

Purification by agarose gel of the α-^{32}P dATP labeled DNA after third PCR amplification 151

QIAEX II Gel Extraction Protocol for radiolabeled DNA 152

Quantification of radioactive DNA by Liquid Scintillation Counter 153

Labeling of 5' position of DNA by γ-^{32}P (forward reaction) …….. 153

Purification of γ-^{32}P labeled DNA …….. 154

DNA polyacrylamide gel electrophoresis …….. 155

Autoradiography of radioactive labeled DNA gel …….. 155

CHAPTER SEVEN ……... 157

Results and Discussion ……. 157

Synthesis of DNA enzyme cofactors …….. 157

*In vitro selection studies using glutamic acid cofactor **C8** (DNA **R1**)* …….. 161

In vitro selection of DNA enzyme using imidazole moiety cofactors …….. 164

*Self cleavage experiment using pool of DNA **R2** and DNA **R3***…….. 168

In vitro selection studies using metal-cofactors……**....** 169

*In vitro selection studies using Lu(III)/ADA complex as cofactor (DNA-**R4**).…..* 171

*In vitro selection studies using Lu(III)/ADA complex as cofactor (DNA-**R5**)*…. 172

*In vitro selection studies using Lu(III)/ADA complex as cofactor (DNA-**R6**).…..* 173

*Comparative data of in vitro selection results for pools of DNA **R4**, **R5** and **R6** .* 173

CHAPTER EIGHT …… 175

Conclusions and future directions …… 175

APPENDIX …..……. 176

Selected NMR Spectra ……. 177

REFERENCES …….. 212

LIST OF FIGURES

Figure 1. Part of a polypeptide chain formed by the bonding of amino acids (n = 50-300) …… 1

Figure 2. Examples of photosensitizers compounds …….. 10

Figure 3. Structure of Rose Bengal …… 11

Figure 4. Modified Jablonski diagram to show origin of Type I and Type II processes …… 18

Figure 5. Structure of Thionine …….. 18

Figure 6. Endoperoxide and products produced during photo-oxygenation of tryptophan ……... 19

Figure 7. Hematoporphyrin Derivatives …… 21

Figure 8. Cyanine dyes …….. 22

Figure 9. Hypericin …… 22

Figure 10. Photothiazine Dyes ……... 23

Figure 11. Xanthenes Dyes …… 23

Figure 12. 1,8-Naphthalimide and bisnaphthalimide derivatives …….. 25

Figure 13. Naphthalimides used in the study by previous members of our group … 27

Figure 14. Photosensitizers used for photochemical modification of RNase A …… 28

Figure 15. Resonance structure showing charge separation …….. 29

Figure 16. Structure of naphthalimide and 4-substituent derivatives …… 30

Figure 17. Structure of **NP5** ……... 34

Figure 18. Structure of **NP6** ……... 35

Figure 19. Structure of **NP7** ……... 36

Figure 20. Structure of **NP8** ……... 37

Figure 21. Synthetic procedure of **NP9** ……. 38

Figure 22. Structure of compound **BD1** ……. 39

Figure 23. Structure of compound **BD2** ……. 40

Figure 24. Structure of compound **BD3** ……. 41

Figure 25. Structure of compound **BD4** ……. 42

Figure 26. Structure of compound **BD5** ……. 43

Figure 27. Structure of compound **BD6** ……. 44

Figure 28. Structure of compound **BD7** ……. 45

Figure 29. Structure of compound **BD8** ……. 46

Figure 30. Structure of compound **BD9** ……. 47

Figure 31. Western blotting apparatus ……... 50

Figure 32. First approach used for the tissue modification experiments ……... 53

Figure 33. Second approach used for the tissue modification experiments ……... 53

Figure 34. Coomassie blue SDS-PAGE of protein selection studies using RNase A (**RN**), Aprotinin (**AP**), Myoglobin (**MY**), Lysozyme (**LY**) (0.235 mM), **NP5** (0.5 mM), light exposure time: 5 minutes……...……... 57

Figure 35. Coomassie blue SDS-PAGE of RNase A (0.235 mM), **NP(5-9)** (0.5 mM), light exposure: 5 minutes, and light intensity: 2000 mW Hg lamp…….. 58

Figure 36. Coomassie blue SDS-PAGE of Lysozyme (0.235 mM), **NP(5-9)** (0.5 mM), light exposure: 5 minutes, and light intensity: 2000 mW Hg lamp …… 59

Figure 37. Protein Chip provided with the Agilent 2100 bioanalyzer ……... 59

Figure 38. Analysis of RNase A (0.235 mM) crosslinking using Agilent 2100 bioanalyzer. (a) Gel-like representation (b) Electropherogram …….. 60

Figure 39. Analysis of Lysozyme (0.235 mM) crosslinking using Agilent 2100 bioanalyzer. (a) Gel-like representation (b) Electropherogram …….. 61

Figure 40. Comparative protein percentage crosslinked for RNase A and Lysozyme when SDS-gel and protein chips were used ……... 62

Figure 41. Coomassie blue SDS-PAGE of the reaction of Lysozyme (6.44 mg/mL = 0.448 mM and 3.22 mg/mL = 0.235 mM) with **NP5** (1.0 mM and 0.5 mM), with variying light exposure (5, 10, 30 min at 2000 mW Hg lamp) …… 63

Figure 42. Coomassie blue SDS-PAGE of crosslinking of Lysozyme (0.235 mM) with naphthalimide derivatives **NP(5-9)** (0.5 mM), light exposure: 30 minutes and light intensity: 2000 mW Hg lamp …….. 64

Figure 43. Comparison of crosslinking trends for RNase A and Lysozyme with naphthalimide derivatives …… 64

Figure 44. Oxidative reactions and possible crosslinking pathways of tyrosine and DOPA in mussel adhesive proteins ……..... 66

Figure 45. Inhibition of RNase A crosslinking by dopamine. 0.235 mM RNase A; 0.5 mM **NP5**; 0, 0.05, 0.1, 0.25, 0.5, or 1 mM dopamine; 5 min irradiation at 2000 mW …… 67

Figure 46. Inhibition of lysozyme crosslinking by dopamine. 0.235 mM lysozyme; 0.5 mM **NP5** or **NP7**; 0, 0.05, 0.1, 0.5, or 1 mM dopamine; 5 min. irradiation at 2000 mW ……..…….. 67

Figure 47. Structure of (a) lysine, (b) tryptophan, (c) histidine, (d) tyramine and (e) methionine …… 68

Figure 48. Crosslinking inhibition studies (a) RNase A (0.235 mM) and (b) lysozyme (0.235 mM); **NP(5-9)** (0.5 mM); lysine (1.5 mM). Photolysis was 5 min for RNase A and 30 min for Lysozyme at 2000 mW ……..... 69

Figure 49. Crosslinking inhibition studies (a) RNase A (0.235 mM) and (b) lysozyme (0.235 mM); **NP(5-9)** (0.5 mM); histidine (1.5 mM). Photolysis was 5 min for RNase A and 30 min for lysozyme at 2000 mW ……..…... 69

Figure 50. Biotin labeled derivatives (**BD1**-**BD9**) ……. 72

Figure 51. Structure of D-(+)-Biotin …….. 74

Figure 52. Analysis of biotin stability by ^{1}HNMR . 1 mM Biotin and 0.5 mM sensitizers (**NP5-NP9**) were dissolved in PBS containing 10% D_2O and exposed to 0 or 5 min of light irradiation using Hg lamp (2000 mW) … 74

Figure 53. Analysis of biotin stability by ^{1}HNMR . 1 mM Biotin and 0.5 mM sensitizer **NP6** were dissolved in PBS containing 10% D_2O and exposed to 0 or 5 min of light irradiation using Hg lamp (2000 mW). **(1)** Biotin + **NP6** + 5 min hν, **(2)** Biotin + **NP6** + 0 min hν, **(3)** Biotin + 5 min hν 75

Figure 54. Dependence of biotin- dopamine (**BD2**) incorporation on time of light irradiation. [RNase A]: 0.235 mM, [**NP5**]: 0.5 mM, [**BD2**]: 0.05 mM ... 77

Figure 55. Incorporation of biotin-dopamine (**BD2**) or biotin-tyramine (**BD9**) in RNase A at various concentrations with **NP5** as sensitizer. [RNase A]: 0.235 mM .……..... 77

Figure 56. Dependence of biotin- amino acid side chains incorporation on type of sensitizer. [RNase A]: 0.235 mM, [**NP(5-9)**]: 0.5 mM, [**BD2**],[**BD9**]: 0.05 mM, 5 min light irradiation. (a) Western blot gel, (b) Coomassie blue gel ……. 77

Figure 57. Dependence of biotin-dopamine incorporation on type of sensitizer. (a) Normalized % **BD2** incorporated into RNase A, (b) % RNase A crosslinked in the presence of biotin-dopamine **BD2** …….. 78

Figure 58. Dependence of biotin- tyramine incorporation on type of sensitizer. (a) Normalized % of **BD9** incorporated into RNase A; (b) % RNase A crosslinked in the presence of **BD9** ……. 78

Figure 59. Normalized incorporation of biotin derivatives into proteins; (a) RNase A; (b) lysozyme. [RNase A], [Lysozyme]: 0.235 mM, [**NP5-NP9)**]: 0.5 mM, [**BD**]: 0.025 mM, irradiation 2000 mW for 5 min. for RNase A and 30 min. for lysozyme……..... 79

Figure 60. Incorporation of biotin labeled derivatives using NP6 as sensitizer. a) RNase A, (b) Lysozyme. [protein]: 0.235 mM, [**NP6**]: (0.5 mM), [**BD**]: 0.025 mM, 5 min (RNase A) and 30 min (lysozyme) of light irradiation at 2000 mW…….. 80

Figure 61. Solvent-accessible surfaces of amino acid residues in RNase A. (a) Tyrosine; (b) Histidine; (c) Lysine ...…….... 81

Figure 62. Solvent-accessible surfaces of amino acid residues in lysozyme. (a) Tyrosine; (b) Tryptophan; (c) Histidine; (d) Lysine …… 82

Figure 63. Inhibition gels of RNase A and lysozyme (0.235 mM) using **NP6** (0.5 mM) as sensitizer, [**BD**]: 0.025 mM and 5 minutes of light exposure.(a) RNase A, (b) lysozyme …….…….. 82

Figure 64. Inhibition of crosslinking for (a) RNase A; (b) lysozyme. [RNase A], [Lysozyme]: 0.235 mM, [**NP5**-**NP9**]: 0.5 mM, [**BD**]: 0.025 mM, 5 minutes of light irradiation for RNase A and 30 minutes of exposure for Lysozyme .……. 84

Figure 65. Azide influence on incorporation of biotin derivatives in photosensitized reactions of RNase A usine **NP5** and **NP9**. **BD1**: Biotin-Hydrazide, **BD2**: Biotin-Dopamine, **BD4**: Biotin-Tryptophan, **BD5**: Biotin-Histidine, **BD6**: Biotin-Methionine, **BD8**: Biotin-Hydroxyproline, **BD9**: Biotin-Tyramine …… 86

Figure 66. RNase A and lysozyme crosslinking photosensitized by **NP8** in the presence of SOD ……... 87

Figure 67. Influence of SOD on incorporation of biotin-tyramine (**BD9**) in RNase A and lysozyme using **NP8.** [**BD9**]: 0.025 mM, [**NP8**]: 0.5 mM, [RNase A] and [Lysozyme]: 0.235 mM ……. 87

Figure 68. Effect of preactivation on the incorporation of biotin derivatives into RNase A using **NP8** as sensitizer ……...…… 90

Figure 69. Incorporation of preactivated biotin derivatives into RNase A and lysozyme ……..…… 90

Figure 70. Full scan TIC MS of digested RNase A ……... 92

Figure 71. Full scan TIC MS of digested RNase A. Retention times and masses of the major peaks. a) 9.91 min; b) 10.93 min; c) 13.60 min; d) 14.02 min.. 93

Figure 72. Peptide sequence for the major four peaks identified for digested RNase A ……..**.....** 93

Figure 73. Full scan TIC MS of digested RNase A modified using **NP8** as sensitizer in presence of biotin-dopamine (**BD2**)……..…... 95

Figure 74. Full scan TIC MS of digested RNase A modified using **NP8** as sensitizer in presence of biotin-histidine (**BD5**) …….. 95

Figure 75. Full scan TIC MS of digested RNase A modified using **NP8** as sensitizer in presence of biotin-hydrazide (**BD1**) …… 96

Figure 76. Amino acid residues present in the peptide sequences for peaks with retention time of 9.98 min (479.216 uma) and 10.93 min (802.9892 uma) ……..……... 97

Figure 77. Pericardium tissue coated with a solution of **NP5** or **NP7** (0.5 mM) combined with various biotin derivatives (0.1 mM), irradiated for 5 min. (mercury lamp, 2000 mW) ……...……... 99

Figure 78. Pericardium tissue coated with a solution of **NP6** combined with various biotin derivatives (0.1 mM) and irradiated for 5 min. (mercury lamp, 2000 mW) ……...……... 100

Figure 79. Pericardium tissue coated with a solution of **NP8** (0.5 mM) combined with various biotin derivatives (0.1 mM) and irradiated for 5 min. (mercury lamp, 2000 mW) .……. 101

Figure 80. Pericardium tissue coated with a solution of **NP5** or **NP9** (1 mM) combined with various biotin derivatives (0.1 mM) and irradiated for 5 min. (mercury lamp, 2000 mW)……...…… 102

Figure 81. Collagen network in meniscus ……...…….. 103

Figure 82. Meniscal tissue coated with a solution of **NP** combined with various biotin derivatives (0.1 mM) and irradiated for 5 min. (mercury lamp, 2000 mW) ……..…….. 104

Figure 83. Meniscal tissue, with and without pretreatment using chABC, coated with a solution of **NP5** or **NP9** (0.5 or 1 mM) combined with various biotin derivatives (0.05 mM) and irradiated for 5 min. (mercury lamp, 2000 mW) .…….. 105

Figure 84. Incorporation of biotin-dopamine (**BD2**) (0.5 mM) in pericardium tissue using **NP5-NP9** (0.5 mM) and 15 minutes of light irradiation…... 107

Figure 85. Incorporation of biotin-histidine (**BD5**) in pericardium tissue using **NP5-NP9** and 15 minutes of light irradiation.…… 108

Figure 86. Incorporation of biotin-tyramine (**BD9**) in pericardium tissue using **NP5-NP9** and 15 minutes of light irradiation.……..… 109

Figure 87. Incorporation of biotin-hydrazide (**BD1**) in pericardium tissue using **NP5-NP9** and 15 minutes of light irradiation …..…… 109

Figure 88. Incorporation of biotin-dopamine (**BD2**) and biotin-tyramine (**BD4**) in pericardium tissue using **NP7** and **NP8** as sensitizers and 15 minutes of light irradiation.…… 110

Figure 89. Time dependence in the incorporation of biotin-dopamine (**BD2**) (0.5 mM) in pericardium tissue using **NP8** (0.5 mM) as sensitizer …..…….. 111

Figure 90. Incorporation of biotin-dopamine (**BD2**) (0.5 mM) and biotin-hydrazide (**BD1**) (0.5mM) in pericardium tissue using **NP8** (0.5 mM) as sensitizers ……. 111

Figure 91. The incorporation of **BD2** (0.5 mM) in pig skin using **NP8** (0.5 mM) as sensitizer …….. 112

Figure 92. Incorporation of biotin-hydrazide (**BD1**) (0.5mM) in pig skin using **NP8** (0.5 mM) as sensitizer.……. 113

Figure 93. Incorporation of biotin-hydrazide (**BD1**) (0.5 mM) and biotin-dopamine (**BD2**) (0.5 mM) in pig skin using as sensitizers **NP (5-9)** (0.5 mM) and 3 minutes of light irradiation ……... 113

Figure 94. Part of DNA and RNA structure ……..…… 118

Figure 95. Amino acid side chains that most commonly recognized as catalytic residues …… 118

Figure 96. RNA cleavage reaction …… 121

Figure 97. Two hypothetical chemical mechanisms for catalysis of RNA cleavage by divalent metals. a) Mechanism involving a divalent metal hydroxide that functions as a general base. b) Mechanism involving a divalent metal cation that functions as a Lewis acid ……. 122

Figure 98. 10-23 RNA cleaving DNA enzyme ……. 123

Figure 99. DNA nanomotor based on 10-23……..…… 124

Figure 100. 8-17 RNA cleaving DNA enzyme …….. 125

Figure 101. A Pb^{2+} biosensor based on 8-17……... 126

Figure 102. Bipartite II RNA cleaving DNA enzyme ……...… 127

Figure 103. 16.2-11 DNA enzyme ……...…….. 127

Figure 104. 9_{25}-11 RNA cleaving DNA enzyme ……... 128

Figure 105. Four classes of histidine-dependent deoxyribozymes …… 130

Figure 106. Proposed acid/base mechanism for the cleavage of RNA catalyzed by RNase A ……... 131

Figure 107. Examples of the catalytic cores of several ribozyme mimics. (A) First example of wholly synthetic ribozyme mimic, a major-groove-directed terpy conjugate. (B) A major-groove-directed bipyridine conjugate. (C) A minor-groove-directed bipyridine conjugate. (D) A minor-groove-directed terpy conjugate ……... 132

Figure 108. Imidazole ribozyme mimics ...……..... 132

Figure 109. Structure of **C1** ……... 137

Figure 110. Structure of **C2** ……... 138

Figure 111. Structure of **C3** ……... 139

Figure 112. Structure of **C4** ……... 140

Figure 113. Structure of **C5** ……... 141

Figure 114. Structure of **C6** ……... 142

Figure 115. Structure of **C7** ……... 143

Figure 116. Structure of **C8** ……... 144

Figure 117. Structure of **C9** ……... 145

Figure 118. *In vitro* selection using coenzymes ……...…… 147

Figure 119. Percentage of DNA-**R1** cleaved per round of selection in the *in vitro* selection experiment of DNA enzymes with cofactor **C8** .……. 164

Figure 120 Imidazole cofactors ……..... 165

Figure 121. Percentage of DNA cleaved during the *in vitro* selection of DNA-**R2** enzymes by mixture of cofactor **C10-C13** (50 mM of cofactors concentration)…….…... 166

Figure 122. Percentage of DNA-**R3** cleaved during the *in vitro* selection of DNA enzymes by variation of mixture of cofactor **C10-13** concentration… 167

Figure 123. Self cleavage procedure ……..……... 169

Figure 124. Structure of ADA ……... 170

Figure 125. Percentage of DNA cleaved during the *in vitro* selection of DNA **R4** enzymes by Lu(III)/ADA complex when the incubation time was varied after the 6^{th} round ……. 171

Figure 126. Percentage of DNA **R5** cleaved during the *in vitro* selection of DNA enzymes by Lu(III)/ADA complex (10 μM cofactor, 16 hours incubation) ……... 172

Figure 127. Percentage of DNA **R6** cleaved during the *in vitro* selection of DNA enzymes by Lu(III)/ADA complex (1 mM cofactor, 16 hours incubation) ……... 173

Figure 128. Comparative plot of percentage of DNA cleaved for pool of DNA enzymes **R4**, **R5**, and **R6** ……. 174

LIST OF SCHEMES

Scheme 1. Reaction of N-maleimides with protein amino groups …… 2

Scheme 2. Alkylation of reduced protein with biotin derivatives ……. 3

Scheme 3. Dansylation, Edman and Sanger reaction …… 4

Scheme 4. The reaction of formaldehyde with proteins …… 5

Scheme 5. Reductive alkylation of diphtheria toxoid primary amines …….. 6

Scheme 6. Modification of amino groups by cyanate ……... 7

Scheme 7. Type I reaction involves ……..……. 13

Scheme 8. Example of electron transfer …… 13

Scheme 9. Reaction of superoxide radical ……. 14

Scheme 10. Type II mechanism ……. 14

Scheme 11. Reaction of unsaturated lipids with singlet oxygen ……... 14

Scheme 12. Oxidation of cholesterol (Oxidation gives predominantly the 7α and 7β hydroperoxides) …….. 15

Scheme 13. Photochemical oxidation of tryptophan ……. 16

Scheme 14. Photochemical oxidation of histidine ……. 16

Scheme 15. Photochemical oxidation of methionine ……. 17

Scheme 16. Photochemical oxidation of purine bases ……... 17

Scheme 17. Synthesis of **NP5** (X=H), **NP6**(X=Br), **NP7**(X=SCH2CH3) ……. 55

Scheme 18. Synthesis of **NP7** …… 56

Scheme 19. Synthesis of **NP8** …… 56

Scheme 20. Synthesis of **NP9** …… 56

Scheme 21. Synthetic procedure of **BD(2-9)** ……. 72

Scheme 22. Involvement of biotinylated compounds in photosensitized reaction … 76

Scheme 23. Superoxide reaction catalyzed by superoxide dismutase (SOD) ……..... 88

Scheme 24. Oxidation of naphthalimide (Sens) radical anion by oxygen …… 88

Scheme 25. Procedure of protein modification changing the order of reagent addition ……..…….. 89

Scheme 26. Protection of histamine dihydrochloride with triphenyl chloride …….. 158

Scheme 27. Diprotection of deprotected histamine ……... 158

Scheme 28. Coupling reaction with β-alanine-fmoc …….. 159

Scheme 29. Synthetic procedure for intermediate **C5** ……..... 159

Scheme 30. Synthetic procedure for cofactor **C6** ……...…... 160

Scheme 31. Synthetic procedure for cofactor **C7** …….. 160

Scheme 32. Synthetic procedure for cofactor **C8** …….. 161

Scheme 33. Synthetic procedure for cofactor **C9** …….. 162

TABLE OF TABLES

Table 1. Photo-oxygenation of tryptophan under various conditions …… 19

Table 2. Relative rate of RNase A crosslinking based on resonance parameter …… 29

Table 3. Inhibition of RNase A crosslinking by free amino acids and derivatives 70

Table 4. Inhibition of lysozyme crosslinking by free amino acids and derivatives ... 70

Table 5. Potentially reactive amino acid residues present in RNase A and Lysozyme ……. 81

Table 6. Application of DNA enzyme *in vitro* and *in vivo* …… 129

Table 7. Primers and oligonucleotides used in *in vitro* selection …….. 135

Table 8. PCR reaction mixture ……. 148

Table 9. Second PCR reaction mixture …… 150

Table 10. Third PCR reaction mixture ……... 151

Table 11. Reaction mixture for γ-^{32}P DNA labeling ……..... 154

Table 12. Incubation time used in the *in vitro* selection experiment when 50 mM of cofactor **C8** was employed for isolating DNA enzymes.…… 163

Table 13. Reaction time used in the *in vitro* selection used for 50 mM of cofactor **C10-C13** ……..…….. 166

Table 14. Conditions used in the *in vitro* selection of DNA **R3** by mixture of cofactor **C10-C13** ……..…..…… 167

Table 15. Reaction time used in the *in vitro* selection used for 10 μM of cofactor Lu(III)/ADA …… 171

LIST OF ABBREVIATIONS

General abbreviations

A – Deoxyadenosine

ADA - carbamoylmethyl-carboxymethyl-amino-acetic acid

α-^{32}P dATP – alpha ^{32}P deoxyadenine triphosphate

AMP – Adenosine monophosphate

ATP – Adenosine triphosphate

γ-^{32}P ATP – gamma ^{32}P adenine triphosphate

BD – Biotin derivative

BHT – 3,5-Di-t-butyl-4-hydroxytoluene

Boc- Di-tert-butyl dicarbonate

BOP - benzotriazole-1-yl-oxy-tris(dimethylamino)phosphoniumhexafluorophosphate

Cys – Cysteine

chABC - Chondroitinase ABC

DCM – Dichloromethane

DMF – Dimethylformamide

DMSO – Dimethyl sulfoxide

DNA – Deoxyribonucleic acid

EDTA- Ethylenediaminetetraacetic acid

EI – Electron impact

Erg1 – Equaline epoxidase

+ ESI – Positive electrospray ionization

- ESI – Negative electrospray ionization

EtOAc – Ethyl acetate

FRET - Fluorescence resonance energy transfer

Fmoc – Fluorenylmethyloxyl carbonyl

HEPES – 4-(2-hydroxyethyl)-1-piperazine-ethane sulfonic acid

Hex – Hexane

His – L-Histidine

HIV-1 - Human immunodeficiency virus

HRP - Horseradish peroxidase

HRMS – High resolution mass spectrometry

LCMS – liquid chromatography mass spectroscopy

MAPs – Mussel adhesive protein

MeOH – Methanol

NEt_3 – Triethylamine

NP – Naphthalimide

OtBu – Butyl ester

PAGE – Polyacrylamide gel electrophoresis

PBS – Phosphate buffered saline

PCR- Polymerase chain reaction

PEG - Poly(ethylene glycol)

PTB – Photochemical tissue bonding

PyBOP - benzotriazol-1-yl-oxytripyrrolidinophosphonium hexafluorophosphate

R- Purine

RNA – Ribonucleic acid

RNase A – Ribonuclease A

Sens – Sensitizer

SDS- Sodium dodecyl sulfate

SOD – Superoxide dismutase

TAE – Tis/acetate/EDTA

TBE – Tris/borate/EDTA

TBS – Tris buffered saline

TIC MS – Total ion chromatogram mass spectra

TFA – Trifluoroacetic acid

TLC – Thin layer chromatography

Trp – Tryptophan

Trt – Triphenyl

Trt-Cl – Triphenyl chloride

Tyr – Tyrosine

U – Deoxyuridine

uma – Unit of mass atomic

VEGFR2 – Vascular endothelial growth factor receptor

Y- Pyrimidine

Spectroscopy

^{1}H NMR – Proton nuclear magnetic resonance

^{13}C NMR – Carbon nuclear magnetic resonance

NMR	nuclear magnetic resonance
δ	chemical shift
ppm	parts per million
J	coupling constant
Hz	hertz
MHz	megahertz
s	singlet
d	doublet
dd	doublet of doublets
t	triplet
q	quartet
m	multiplet

ACKNOWLEDGMENTS

First of all I would like to start by expressing my gratitude to my family; for always believing in me, since none of this could have been achieved without their support and love. To my brother Freddy and my mom, who show me every single day, no matter how far apart we are that the distance only matters to the mind, but not to the heart. You really mean the world to me. To my beloved dad who made me a stronger person, taught me the meaning of forgiveness, and showed me that it is never too late to become a better person or to give love. Thanks for changing yours and my life at the same time; you will live forever in my thoughts and heart. I miss you more than ever.

Being away from home could not have been possible without having my husband Fernando by my side; I am such a lucky person to have somebody like you in my life, you are the smartest, sweetest and most wonderful person I have ever known; thanks for all the patience, help and understanding you give me every day.

I would like to thank my mentor Dr. Kane and also Dr. Manzanares for giving me the opportunity of being part of this institution, for the guidance, the support, and the time that they have dedicated to me. To the other members of my dissertation committee, Dr. Pinney, Dr. Garner, Dr. Kim and Dr. Kebaara for helping me to complete this last requirement of my Ph.D.

I am thankful to all the members of my group, past and present; Jose, Ae Gyeong, Drew, Josh, Joanna, Matt, Robert, Dustin, Brittany, Becca, Kat, Diane, Lisa and the rest

of the undergrad students for cheering me up and drawing a smile on me every time I was feeling sad, and for making my days in the lab enjoyable.

I am blessed to have my special friends, Jose Boquin, Robert Hazlitt, Beth Martine, David Camejo and Ivanna Laboren. You came into my life in the moment I needed the most to offer me support; thank you for being my shoulder to cry on; especially in these past months; which I considered have been the hardest ones for me. Thanks for listening, for comforting me, for all of the advice, and for being there for me. I really appreciate your friendship; thanks for the help in the lab, for the concerts, the movies, the conversations, the driving lessons, and all of those wonderful moments that we shared together; I enjoyed every single second beside you, I will never forget you and I wish you all a bright future.

Special thanks to my family-in-law for all the support and love and to my Venezuelan friends Juan, Maryuri, Alejandro, Mieke, Otsmar and Jenny for being wonderful people to be around. To Andrea Johnson for being such an angel to me; and also to all of the professors and staff members at Baylor University that have contributed to my academic education.

DEDICATION

To the memory of

Freddy Alejandro Uzcategui Oraa

CHAPTER ONE

Introduction

Protein Modification

Proteins are polypeptides (amino acids linked through amide bonds; Figure 1) which play key roles in virtually all biological processes. Nearly all catalyst in biological systems are proteins which are called enzymes. Proteins are responsible for chemical transformations in cells, and are involved in a wide range of functions including transport and storage of some essential nutrients, motion and coordination in muscle, mechanical support, and immune protection.

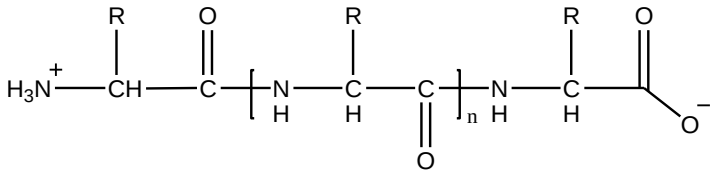

Figure 1. Part of a polypeptide chain formed by the bonding of amino acids (n = 50-300).

Examples of the aforementioned functions of proteins include the following:

a) Transport and storage: For example, hemoglobin transports oxygen in erythrocytes, whereas myoglobin transports oxygen in muscle. Iron is carried in the plasma blood by transferrin, and is stored in the liver as a complex with ferritin, a different protein.
b) Coordinated motions: Muscle contraction is accomplished by the sliding motion of two kinds of protein filaments. Muscular tension is generated through the action of actin and myosin cross-bridge cycling.

c) Mechanical support: Collagen and elastin are fibrous protein that provides the highly tensile strength of skin and bones while keratin is found in hard or filamentous structures such as hair, nails, feathers, hooves, and some animal shells.

d) Immune protection: Since antibodies are highly specific proteins that recognize and combine with foreign substances provides protection against viruses, bacteria, and cells from other organisms.[1]

Since proteins play an important role as the building blocks of life the synthetic modification of protein has been widely used in research and technology. The chemical modification of proteins has assumed a prominent role[1-4] in the investigation and explotation of protein structure. Proteins have been modified intentionally for structure-function relationship studies or for development of new and improved products. These modifications include simple organic reactions such as oxidations, reductions, and nucleophilic (Scheme 1) and electrophilic substitutions.

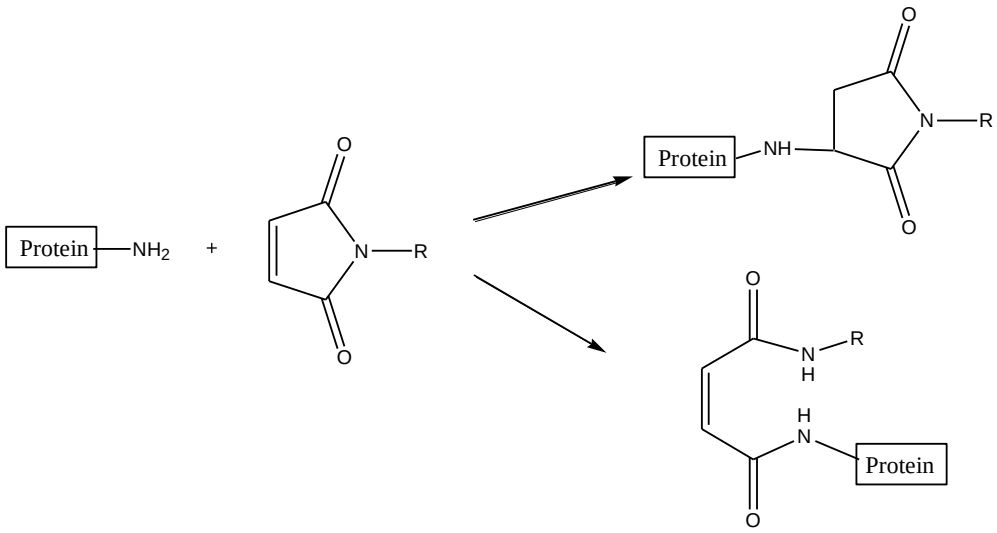

Scheme 1. Reaction of N-maleimides with protein amino groups.[5]

Another common synthethic modification of proteins is the attachment of prosthestic groups, for example, conjugation to poly(ethylene glycol) (PEGylation). PEGylation is frequently used in the manufacture to biopharmaceuticals since the covalent attachment of PEG to drug or therapeutic protein can "mask" the agent from the host's immune system, increase its hydrodynamic size (size in solution), and prolong its circulatory time by reducing renal clearance. Another prothestic group often used is biotin, which is often attached to reduced sulfhydryl groups on a protein to permit the isolation of modified peptides[6] (Scheme 2).

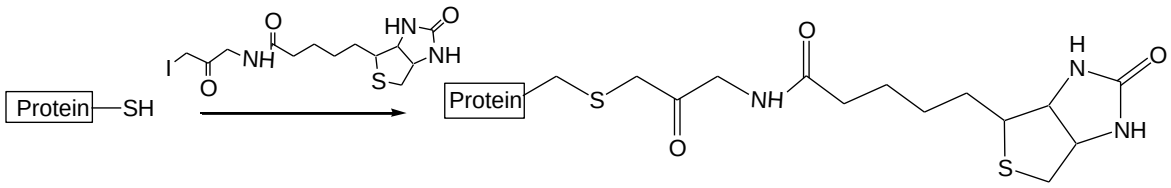

Scheme 2. Alkylation of reduced protein with biotin derivatives.

Other examples of protein modifications include reactions that are useful for the identification of specific functional groups/amino acids. For example, the dansylation reaction involves the reaction of primary amines (the N-terminal amino acid and lysine), the Edman degradation, which reveals the N-terminal amino acid, and arylation of proteins using the Sanger reagent 1-fluoro-2,4-dinitro-benzene (Scheme 3).

Even before scientists recognized the distinctive chemical features of proteins, workers were using chemical modification in such areas as leather tanning and fabric dyeing.

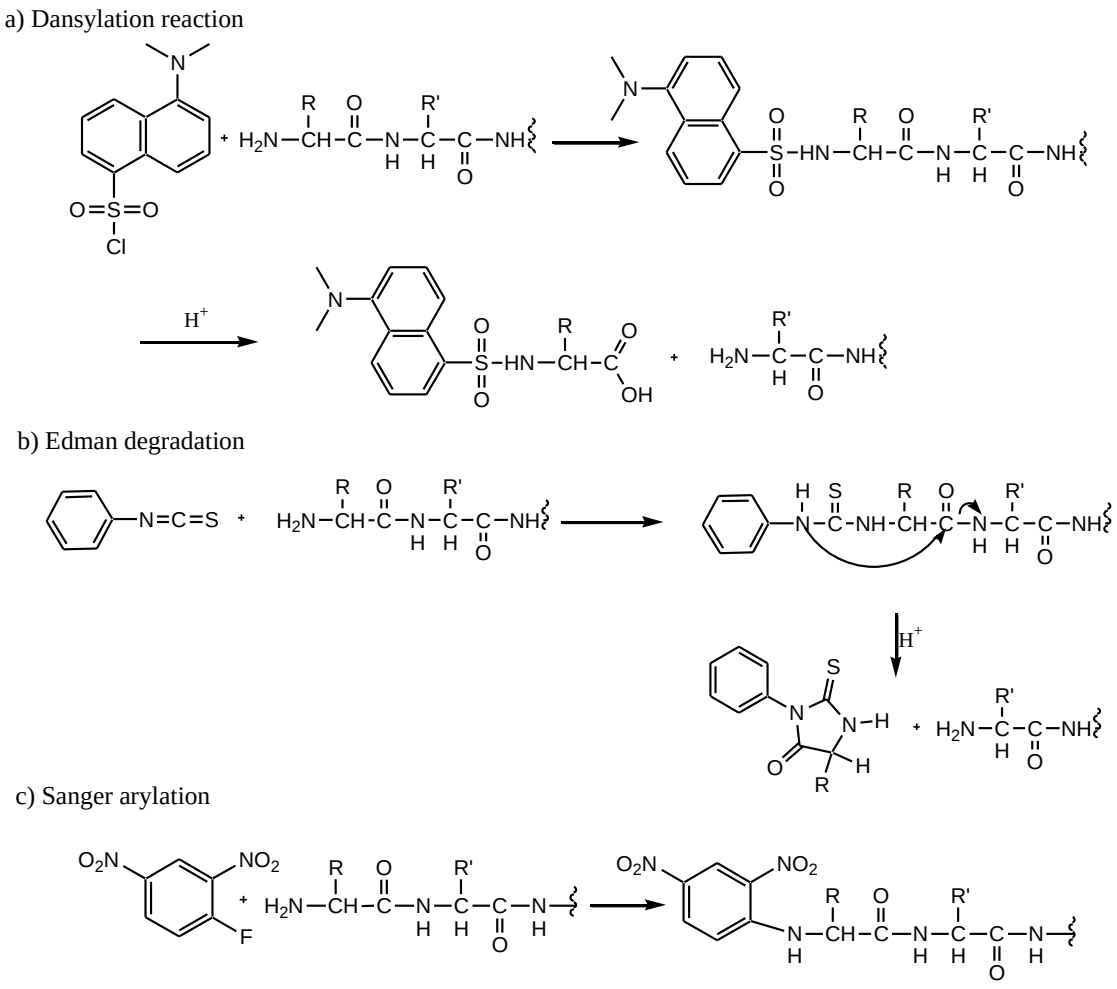

Scheme 3. Dansylation, Edman and Sanger reaction.

Older procedures using organic compounds (e.g., formaldehyde; Scheme 4) and inorganic salts (e.g., chromates) have been refined and extended on the basis of a modern understanding of how they function. For example, formaldehyde is often replaced by glutaraldehyde, a reagent for cross-linking proteins.[7] Glutaraldehyde is a cross-linker reagent that links covalently reacts with amino groups, sulfhydryl groups and possibly with aromatic ring structures in protein molecules creating more stable structure.

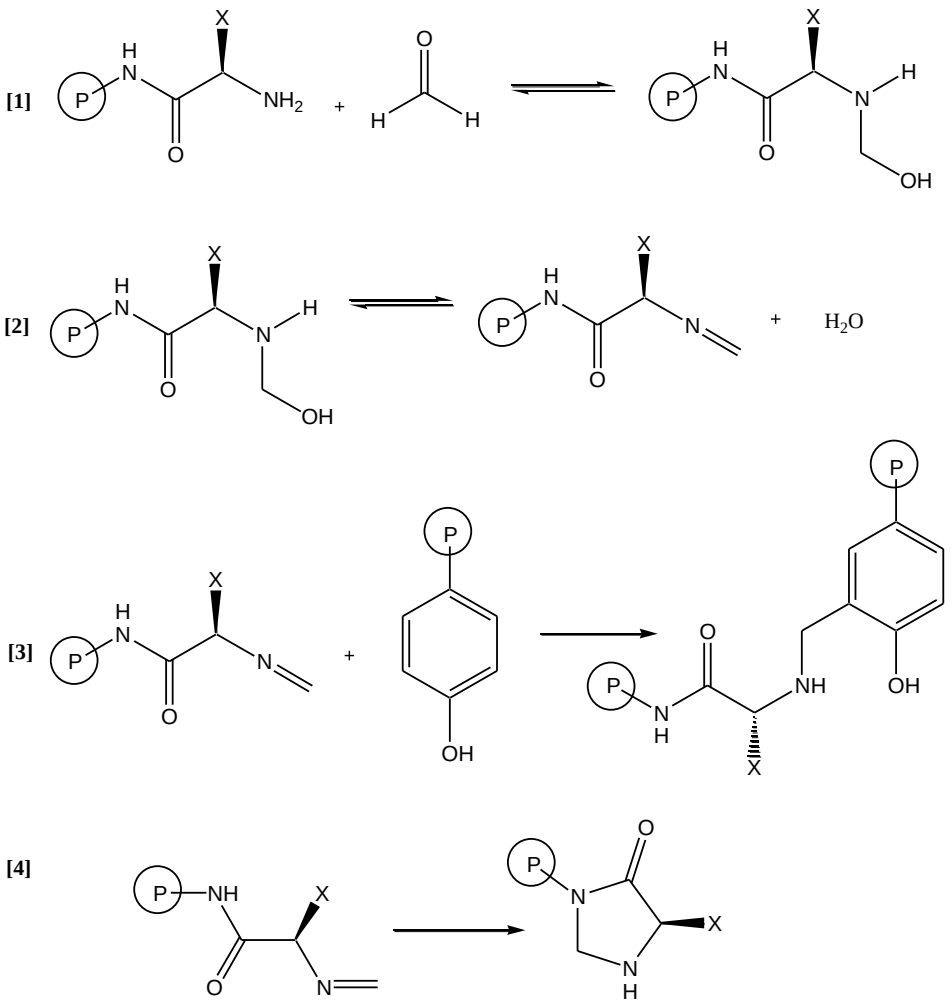

Scheme 4. The reaction of formaldehyde with proteins. The reaction starts with the formation of methylol adducts on amino groups. The methylol adducts of primary amino groups are partially dehydrated, yielding labile Schiff bases, which can form crosslinking with several amino acid residues, for example with tyrosine. After addition of formaldehyde, a 4-imidazolidinone adduct can be formed at the N-terminal site of the protein, probably via a Schiff base intermediate.

Not even the proteins that are injested escape chemical modification. In early times this normally was the result of treating food with acid or alkali, and it may be a result of the long acceptance of such procedures that their consequences in terms of alterations to protein structure are ignored by many today. The ancient Mayan practice of treating corn and other grains with alkali preserved the food, but it was valued also for its

pleasing effect as improving the flavor and texture of the product.[8] In nutritional terms alkali treatment had the mixed effect of causing losses of some amino acids but increasing the digestibility therefore providing a valuable benefit to these people.

Another historically important application of the modification of proteins is the use of formaldehyde in the production of toxoids, bacterial toxins whose toxicity has been weakened or suppressed while their immunogenicity is maintained.[9] This procedure was developed in the first part of the century mainly by trial and error and often depends on treating the proteins with formaldehyde for several weeks at temperatures close to 40 ^{o}C. For example, diphtheria toxoid is treated with formaldehyde and glycine to afford intramolecular cross-links and formaldehyde-glycine attachments. The intramolecular cross-links occur between formylated lysine residues and susceptible amino acids including arginine, asparagine, glutamine, histidine, tryptophan and tyrosine. To determine the reactivity of each individual lysine residue with formaldehyde, diphtheria toxin was treated with formaldehyde and $NaCNBH_3$ (Scheme 5).[10] This treatment results

Scheme 5. Reductive alkylation of diphtheria toxoid primary amines.

in the toxin being changed in such a manner that it retains its capacity to elicit an immune response when injected into an animal or person, but lacks the capacity for the damage that is associated with the native toxin. Imprecise as this procedure seems today, the satisfactory results obtained through strict quality control have resulted in its continuing use and the production of many millions of doses of life-saving vaccines.

Some drugs and toxic compounds owe their activity to an ability to form covalent products with important target substances.[11-13] Among these targets are enzymes and other important proteins such as hemoglobin. For a number of years, the covalent modification of the α-amino groups of hemoglobin with cyanate was studied intensively as a possible means of therapy for the sickle cell trait (Scheme 6). Unfortunately, orally administered cyanate had forbidding side effects in volunteer patients and did not appear to reduce the incidence of the disorder's "painful crisis".[14]

It is difficult to devise a precise system by which chemical modifications of protein can be classified. A useful division could be classified those as two groups: (a) those that are performed intentionally for specific purposes and (b) those that can be described as deteriorative or incidental to the processing, storage, or aging of protein-containing materials.

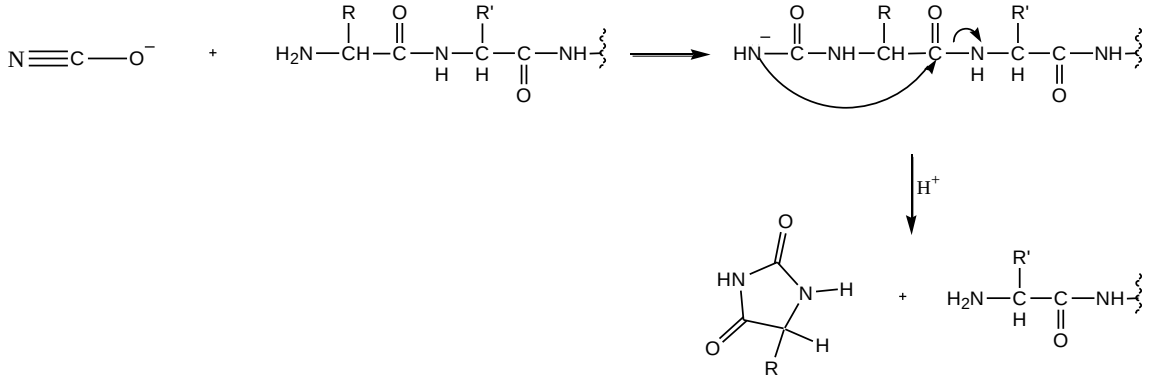

Scheme 6. Modification of amino groups by cyanate.

Specific modifications of proteins result from adding a selected reagent to the pure protein or crude protein-rich material. This may be done in the course of a fundamental study in protein chemistry or as a step in the production of a bulk protein

product for practical purposes. The same chemical modification can be useful in both processes.

The molecular properties of a protein respond continuously to changes in the disposition of its constituent amino acids. Changes in the ionization of functional groups lead in turn to adjustments in the complex network of attractive and repulsive forces that maintain the molecule's integrity, and the proteins structure. Since many chemical modification reactions are governed in a major way by the protein's overall structure, as well as by the disposition of the individual group or class of groups to be modified, it follows that such modifications are extremely sensitive to the conditions under which they are performed. Careful selection of the conditions is an essential step in the design of any chemical modification experiment.

An important feature of the reactions that are described above for the individual amino acid side groups is that they mostly depend on reagents much milder than the majority used in general organic chemistry. Among the more important factors affecting reactions with proteins, pH is the most important since it controls the distribution of potentially reactive side chains between reactive and unreactive ionization states. Temperature is another parameter that must be dealt with carefully since it, too, may affect the microenviroment of reactive groups. Some competitive side reactions may be minimized or prevented by thoughtful choices of temperatures. An additional complexity is added since many typical reagents are insoluble or only sparingly soluble in aqueous solution and require some organic solvent to assist dissolution. Few organic solvents can be used because they tend to denature proteins and frequently result in precipitation.

Working with membrane-bound proteins is exceptionally challenging, although they can sometimes be solubilized with the aid of detergents.

Photochemistry

Photochemical processes have been intimately related to the development of man and his environment even before his appearance on the planet. It is believed that certain stages in the generation of the building units for the macromolecules of life occurred on the primordial earth under the influence of the sun's rays.[15] Subsequently the evolution of the process of photosynthesis, the conversion of carbon dioxide into carbohydrate, rendered life in its present form possible. Finally the evolution of all life of an advanced form would be drastically different if the photochemical process of vision had not been developed.

Photochemical reactions in the laboratory have been known for almost as long as chemistry has been studied. Most of the observations were accidental and remained uninterpreted, and only at the end of the nineteenth century was any systematic approach made. After that and because of the work of Ciamician, Silber, and Paterno, the organic chemist at last paid serious attention to the possibilities of the chemical action of the light.[15]

The effect of photosensitized reactions on living organisms was discovered in 1898 at the Ludwin-Maximillian University in Munich where Raab and von Tappeiner were examining the effect of dyes on paramecia (a group of unicellular protozoa). They observed that the paramecia were killed in the presence of daylight when low concentrations of acridine (Figure 2) were used as photosensitizer, while the paramecia survived in the presence of acridine in the dark. The result stimulated research in this area

and several years later von Tappeiner and Jesionek extended these studies and proposed various dermatological applications for photosensitizers including the compound eosin Y (Figure 2). It is now appreciated that the biological effects are due to photosensitized reactions with important biomolecules including proteins, nucleic acids, and lipids. Specifically relevant to this dissertation, proteins are often modified, and this modification often includes the crosslinking of proteins to other molecules (including other proteins).

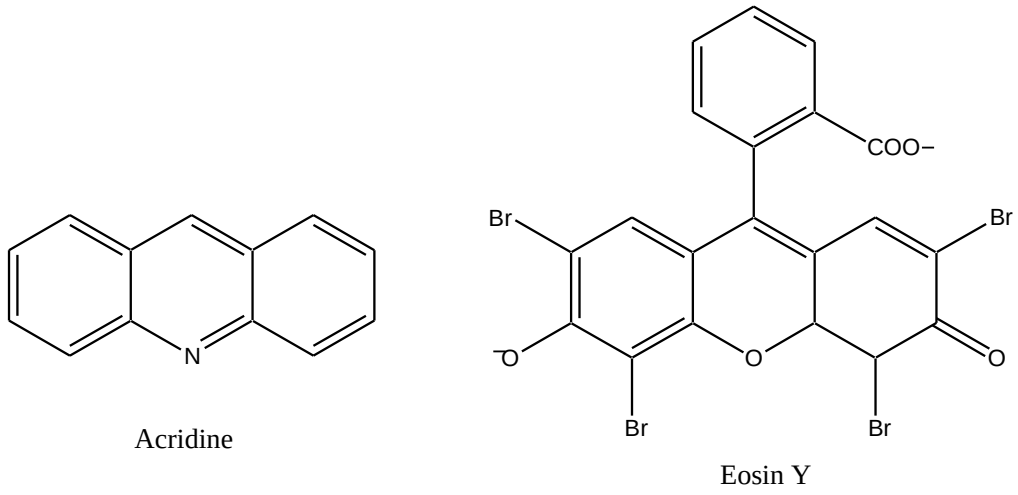

Acridine

Eosin Y

Figure 2. Examples of photosensitizers compounds.

Although certain amino acids including tryptophan, tyrosine, histidine, cysteine, and methionine are vulnerable to photosensitized crosslinking, it has been suggested that photochemical crosslinking in proteins is usually nonspecific, and that actual crosslinking sites cannot usually be readily determined.[16] Even photochemical protein crosslinking most often proceeds by multiple mechanisms and produces heterogeneous product mixtures, photoactivated processes have recently been used in medical applications including the production of bioprosthetic devices such as heart valves[17] with enhanced

thermal stability. Recently, photo-activated processes studied for applications such as the bonding of collagen-rich tissues such as skin grafts[18] and tendon specimens[19] as a surgical repair, and for the lamination of collagen gel on muscle layers in bioengineered esophageal tissues.[20] Photochemical tissue bonding using rose bengal (Figure 3) as a photosensitizer has been shown to be rapid without compromising cell viability at temperatures far below the denaturation temperature of collagen.[18,20]

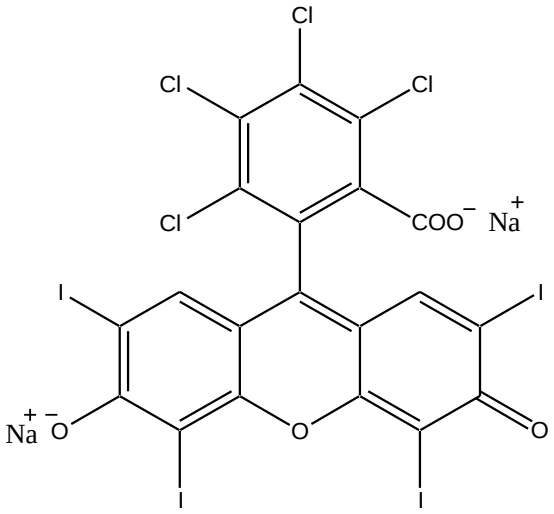

Figure 3. Structure of rose bengal

The two major mechanisms of photosensitized reactions are referred to as Type I (direct) and Type II (indirect) processes. We shall use the generally accepted definitions for these general mechanisms. According to Schenck, "Type I photosensitization is characterized by electron transfer to/from the excited sensitizer (including simultaneous transfer of a proton corresponding to the transfer of a hydrogen atom), resulting in a free radical pathway, while Type II photosensitization is characterized by energy transfer from the excited sensitizer".[15]

With the advent of the quantum theory and modern photochemistry, it became obvious that limits on the photobiological processes were set by the absorption spectrum of the light-absorbing substances or photosensitizers. For a substance to be an efficient photosensitizer, it must be capable of being excited, upon exposure to light, to a relatively long-lived, energy-rich form termed the *triplet state*.[21, 22] Organic photosensitizer molecules in the dark almost always exist in the ground state; in this state, the molecule has no unpaired electron spin. Upon absorption of a photon, an electron in the sensitizer shifts to a higher orbital that could undergo fast spin inversion to generate the *triplet state*, containing two unpaired electrons (type I reaction).[23, 24] The metastable triplet state of the photosensitizer can then collide with certain biomolecules, such as molecular oxygen, with the subsequent transfer of energy (type II reaction)[22, 24] and the return of the photosensitizer to the ground state to carry on another interaction with a photon. The transfer of energy from the triplet photosensitizer to molecular oxygen results in the generation of the highly toxic activated oxygen molecule singlet oxygen ($^1O_2$), which has a very short lifetime in biological systems (<40 nanoseconds) and a short radius of action (<0.02 mm).[25]

Type I Mechanism. Electron Transfer.

In this mechanism the excited state of the photosensitizer generates a radical species by electron transfer from (or to) a substrate, or by hydrogen atom abstraction from a substrate (Scheme 7). This type of direct mechanism is sometimes responsible for the covalent modification of proteins, such as by hydrogen atom abstraction followed by radical coupling.[26]

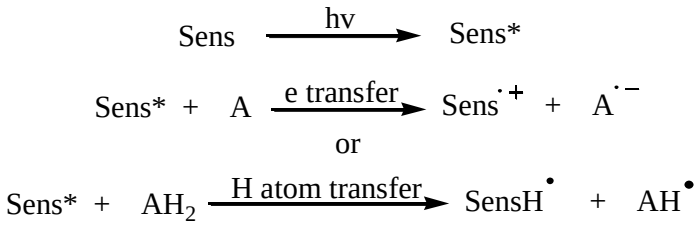

Scheme 7. Type I reaction involves.

A common example of electron transfer to dioxygen, giving the superoxide radical anion. This can follow two general routes: a) the direct electron-transfer reaction form the excited singlet state of the sensitizer to dioxygen, or b) electron transfer to dioxygen from a radical anion produced from reaction of the excited triplet state of the sensitizer with an oxidizable substrate (Scheme 8):

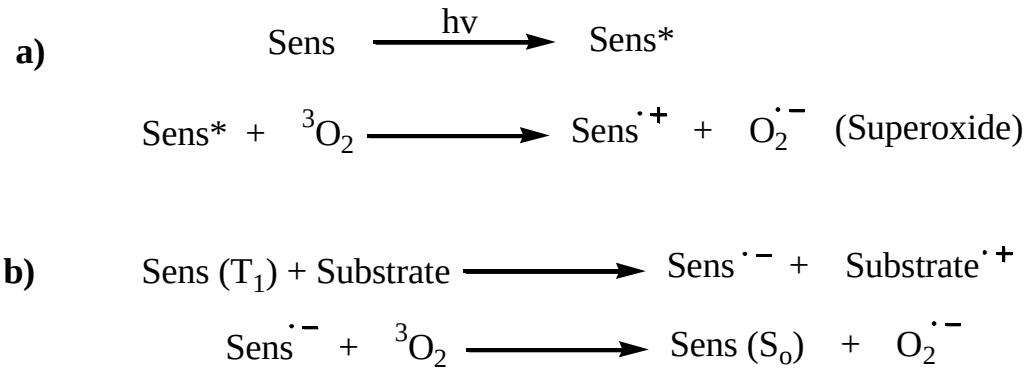

Scheme 8. Example of electron transfer.

Superoxide itself is not particularly reactive, and is readily oxidized back to dioxygen. However the protonated form of this compound, the hydroperoxyl radical, undergoes a spontaneous dismutation which can also be catalyzed by a widely distributed enzyme system (superoxide dismutases), producing ground state dioxygen and hydrogen peroxide (Scheme 9).

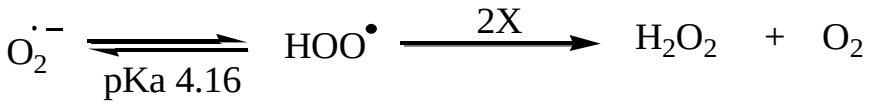

Scheme 9. Reaction of superoxide radical.

Type II Mechanism. Energy Transfer.

In the second general mechanism, electronic excitation energy is transferred from the excited triplet of the sensitizer to another molecule, which returns the sensitizer to its ground state. The other molecule is most often triplet dioxygen, which results in the production of highly reactive singlet oxygen (Scheme 10). Rose Bengal, mentioned above as a useful photosensitizer for tissue engineering, is thought to primarily use a singlet oxygen mechanism.

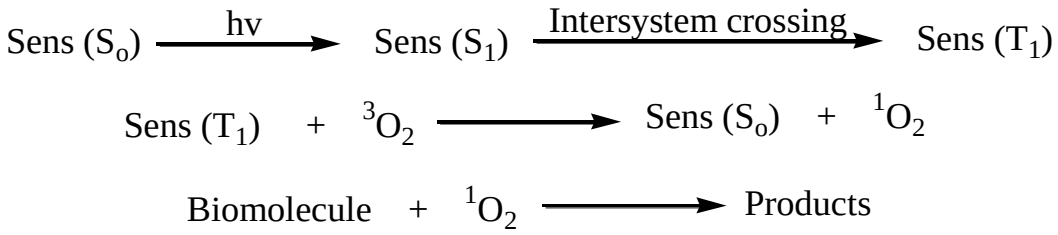

Scheme 10. Type II mechanism.

Many biomolecules have the ability to undergo facile reactions with singlet oxygen. Two examples are shown below in Schemes 11 and 12.

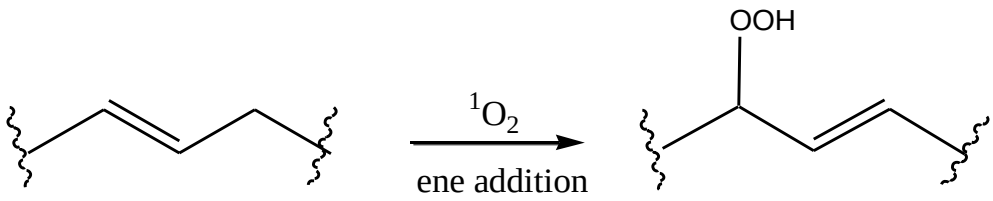

Scheme 11. Reaction of unsaturated lipids with singlet oxygen.[15]

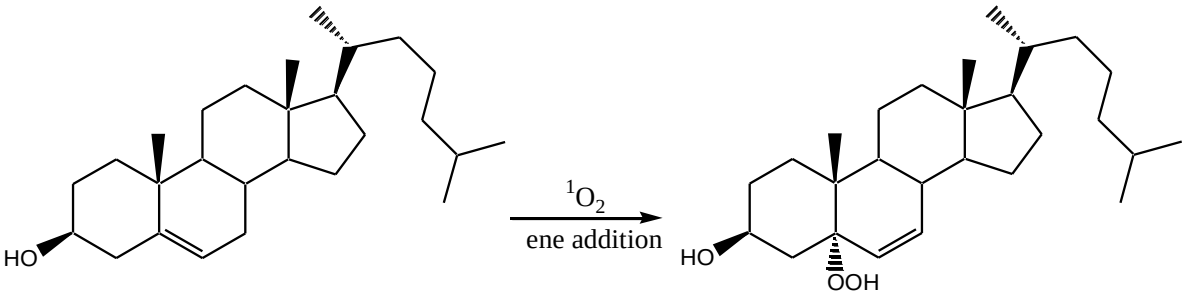

Scheme 12. Oxidation of cholesterol (Oxidation gives predominantly the 7α and 7β hydroperoxides).[15]

Amino Acid Reactions with Singlet Oxygen (Schemes 13-15)

Many proteins form intermolecular and/or intramolecular crosslinked when illuminated in the presence of a certain photosensitizer (photodynamic crosslinking or sensitized photocrosslinking). Significant work has been performed to elucidate the mechanism of these crosslinking reactions using model systems involving free amino acids, amino acids derivatives and amino acids bound to sepharose gels. These studies suggest that the intermolecular photochemical oxidation crosslinking of proteins often involves the reaction of single oxygen with amino acid residues such as L-histidine (His), cysteine (Cys), tryptophan (Trp), and tyrosine (Tyr) in one protein molecule. This initial reaction results in the formation of species that react non-photochemically with a reactive amino acid residue in another protein molecule to form the crosslink. The photosensitized formation of intramolecular crosslinks has also been observed in some proteins. Although the crosslinking of proteins with most photosensitizers requires oxygen, it is more efficient under anaerobic conditions in several cases.[15] The photodymanic loss of activity of certain enzymes is associated with the destruction of tryptophan (e.g. in chymotrypsin), histidine and methionine (e.g. in phosphoglucomutase) residues.[15]

a) Tryptophan

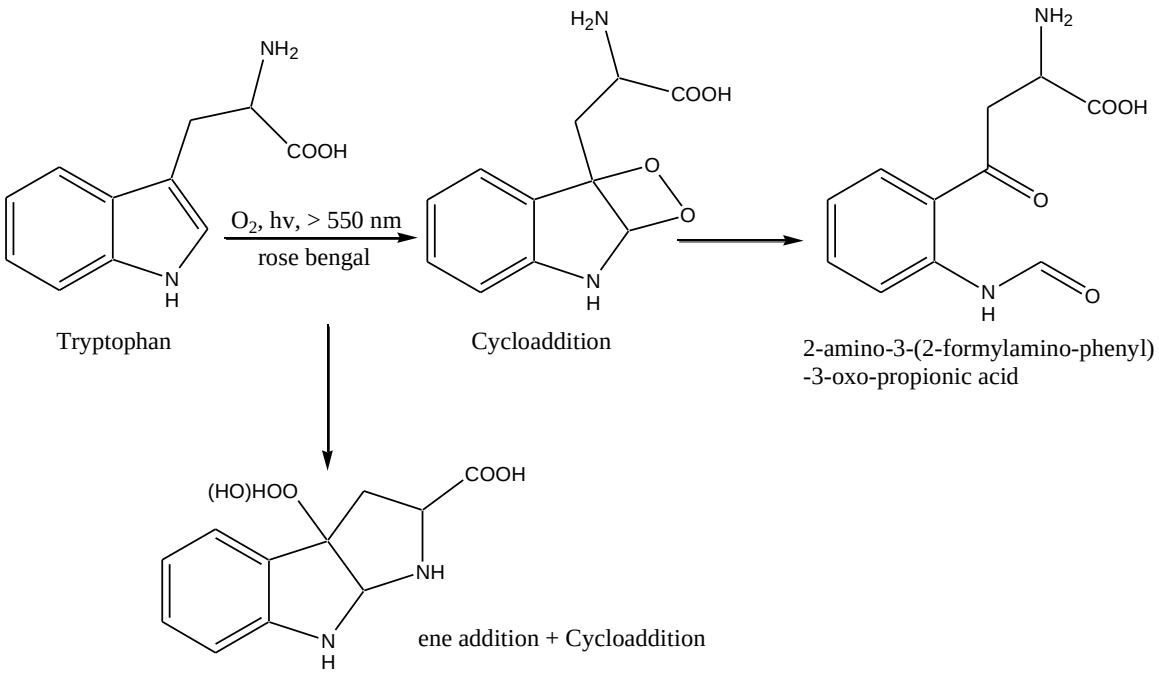

Scheme 13. Photochemical oxidation of tryptophan.[15]

b) Histidine

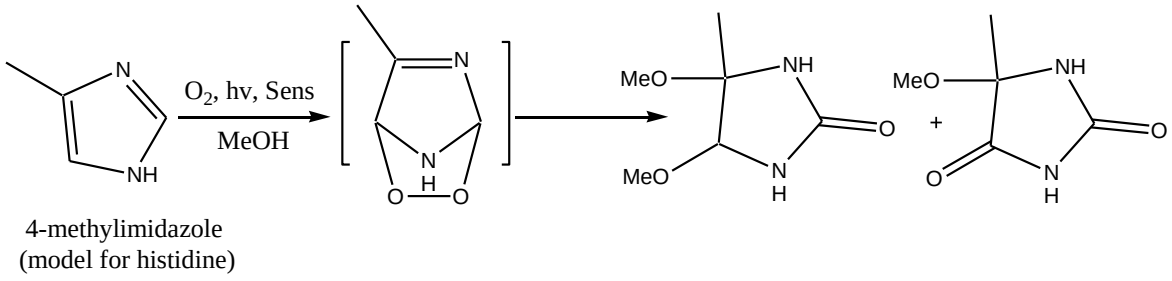

4-methylimidazole
(model for histidine)

Scheme 14. Photochemical oxidation of histidine.[15]

c) Methionine

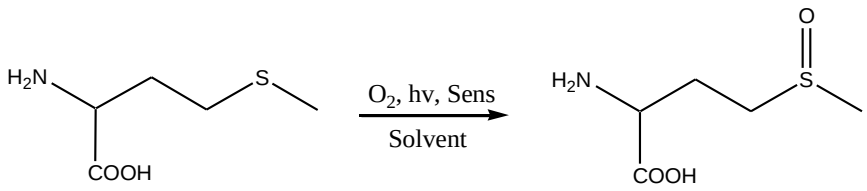

Methionine

Scheme 15. Photochemical oxidation of methionine.[15]

Nucleic acids also undergo photochemical modification by both Type I and Type II pathways. The precise mechanisms for these reactions are not obvious. One important reaction is the selective destruction of guanine residues which can be selectively destroyed in DNA (both solution and in cells) on irradiation with certain sensitizers (Scheme 16).[15]

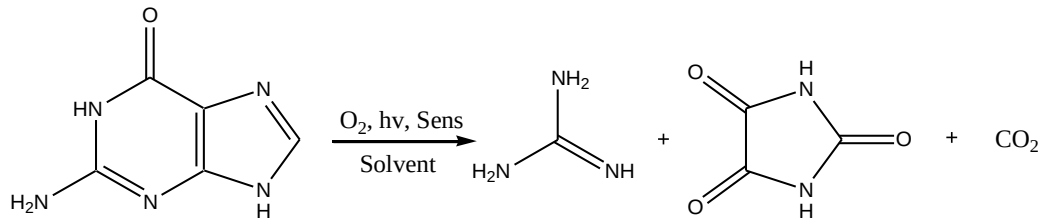

Guanine Guanidine Parabanic acid

Scheme 16. Photochemical oxidation of purine bases.[15]

Both Type I and Type II processes may occur together. It is often helpful to describe the situation in terms of a modified Jablonski diagram, as shown in Figure 4, where the left hand of the diagram refers to the sensitizer and the right hand refers to dioxygen molecular species.

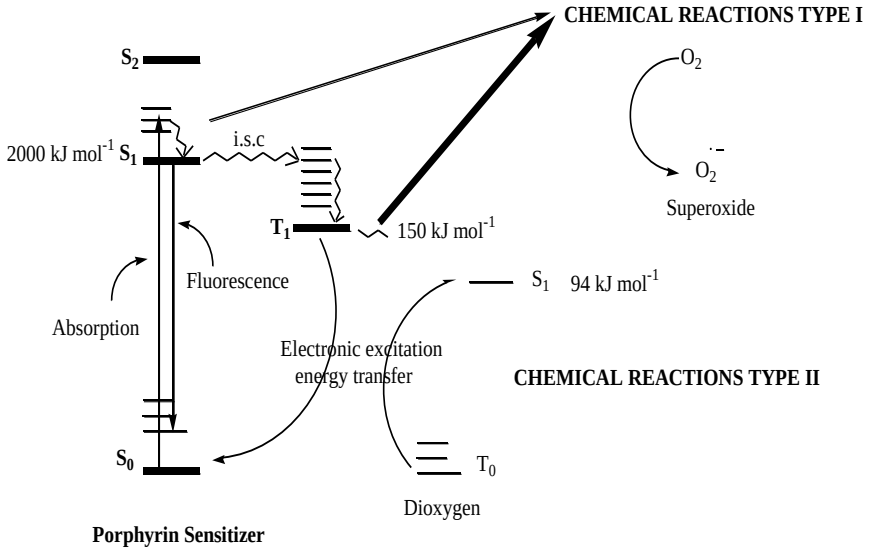

Figure 4. Modified Jablonski diagram to show origin of Type I and Type II processes.

Tryptophan provides an example where Type I and Type II reactions can give the same product, but in different proportions (Table 1). This example is instructive because it shows the close relationship between the two processes.[15] Chemically generated $^1O_2$ from an endoperoxide was reacted with tryptophan and the products obtained from this reaction were compared with those obtained from rose bengal and thionine-sensitized photooxidations (Figures 3 and 5). It was found that the reaction mechanism was highly dependent on the sensitizer with the reaction sensitized by rose bengal proceeding exclusively by the Type II ($^1O_2$) mechanism, while with thionine as the photosensitizer the reaction with tryptophan proceeds by a combination of $^1O_2$ (Type II) and Type I mechanism (Table 1).

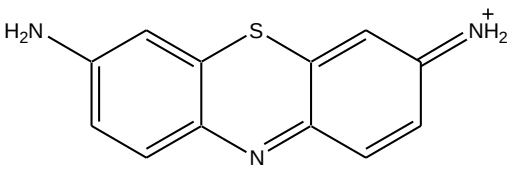

Figure 5. Structure of Thionine

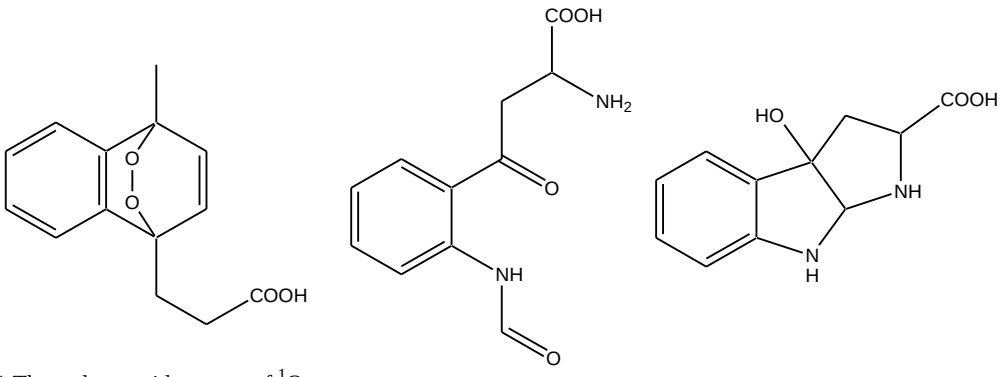

* The endoperoxide source of $^1O_2$ * **A** is N-formylkynurenine * **B** is the hydroxy tricyclic product

Figure 6. Endoperoxide and products produced during photo-oxygenation of tryptophan

Table 1. Photo-oxygenation of tryptophan under various conditions

Source of $^1O_2$	Conditions	% Product Yield		Reaction Type deduced
		A*	B*	
Endoperoxide (Figure 4)*	35 ^oC	23	42	Type II
Rose Bengal/O_2	>300 nm	30	1	Type II, + photodecomposition of B
Rose Bengal/O_2	>500 nm	23	44	Type II
Thionine/O_2	>550 nm	22	23	Type I + Type II

Distinguishing between Type I and Type II Processes

Distinguishing between the two mechanism types is rarely straightfoward, and some of the so-called distinguishing tests (such as lifetime in deuteriated solvents, quenching by azide, and detection of spin-trapped hydroxyl radical) do not reliably

distinguish between singlet oxygen and superoxide intermediates. Clearly, considerable care is needed both in experiment and interpretation, and the use of several lines of experimentation is most persuasive. At this time the most reliable methods appear to be.[27]

i. Luminescence detection of singlet oxygen in Type II reaction.

ii. Characterization of products in the reaction of cholesterol: the 5α-hydroperoxide is formed by a Type II reaction, while a mixture of the 7α- and 7β-hydroperoxides is formed in a Type I reaction.

iii. Quenching of the reaction by BHT, or mannitol is characterized by a Type I mechanism.

iv. Quenching by 9,10-diphenylanthracene with formation of the endoperoxide suggests a Type II mechanism.

Photosensitizers

Since the biomolecular photochemistry of these compounds typically is very toxic to exposed cells, photodynamic therapy has long been promoted as a potential binary anti-cancer modality. The pioneering work in this area used mixtures of porphyrins as the sensitizers (Figure 7)[28,29] and was led by Tappeiner and Jesionek in 1903 and Lipson and Schwatz in 1960, compounds including photofrin, purpurins, xanthenes, phthalocyanines, oxazines, cyanines, chlorins and others have been tested as binary photoactivated anti-cancer agents *in vitro* and *in vivo* with some success.[30,21-35]

Hematoporphyrin was the first photosensitizer to receive regulatory approval in Canada in 1993 and has received subsequent approval in the U.S., Europe, and Japan for a number of indications including cervical cancer, endobronchial cancer, esophageal cancer, bladder cancer, and gastric cancers.[36] As successful as hematoporphyrin has been,

it still suffers from many drawbacks, which have stimulated subsequent research for better photosensitizers. Hematoporphyrin and its commercial variants comprise the first generation of photosensitizers. A number of "second generations" photosensitizers have since been developed. These compounds are generally well-characterized single substances (not mixtures) that are designed to exhibit improved activity and selectivity.[15]

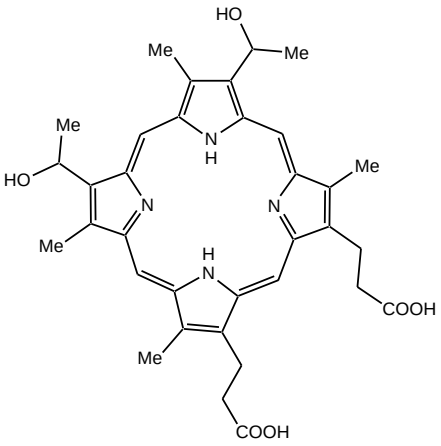

Hematoporphyrin

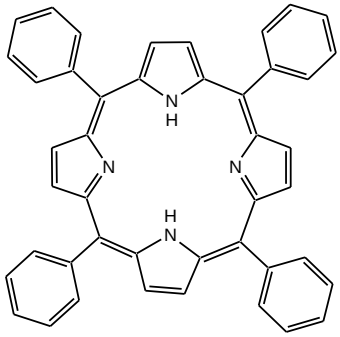

Tetraphenylporphyrin

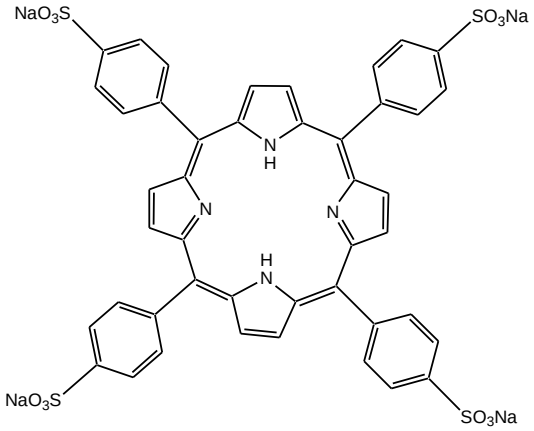

Tetraphenylporphyrin tetrasulfonate

Figure 7. Hematoporphyrin Derivatives.

One class of second generation photosensitizers is the cyanine dyes such as Merocyanine 540 and Indocyanine green which have demonstrated significant

phototherapeutic activities (Figure 8). Hypericin have been studied for its anticancer and photovirucidal activity (Figure 9).[15]

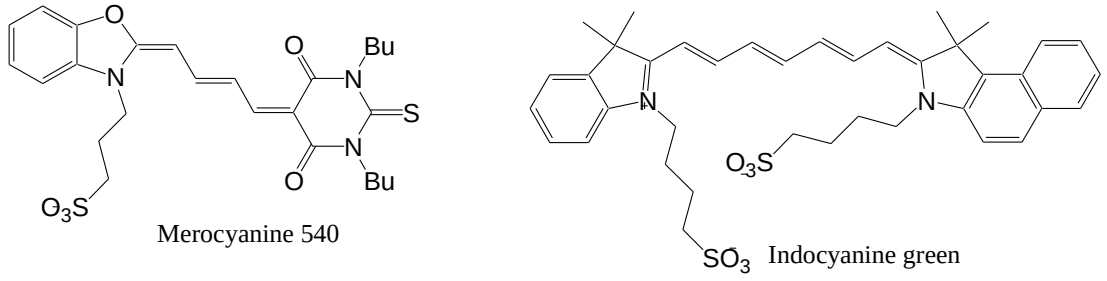

Merocyanine 540 Indocyanine green

Figure 8. Cyanine dyes.

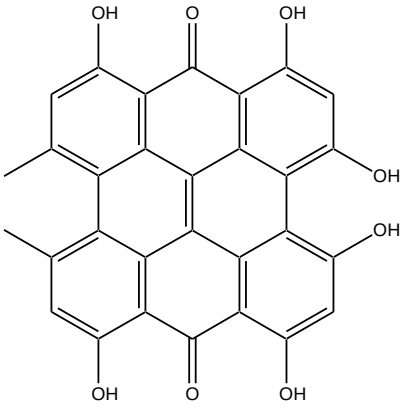

Hypericin

Figure 9. Hypericin.

Several photothiazine dyes (Figure 10), typified by methylene blue and toluidine blue, have long been commercially available as dyes, and there is a considerable literature on the use of these dyes, to stain and visualize cancerous lesions *in vivo* as an aid in diagnosis. These species have been demonstrated to have photomicrobicidal properties and well established as good singlet oxygen sources. This is especially true in

the case of methylene blue, which is frequently employed in aqueous systems to identify tryptophan at or near the active site of an enzyme.[15]

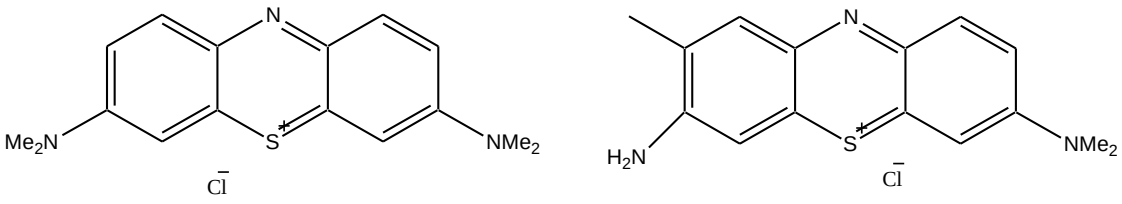

Methylene Blue Toluidine Blue

Figure 10. Photothiazine Dyes.

The xanthenes dyes, for example, fluorescein, rose bengal (Figure 11) and eosin (Figure 2), are excellent photosensitizers for singlet oxygen formation and are perhaps the most commonly used compounds when singlet oxygen is required in organic synthesis.[15]

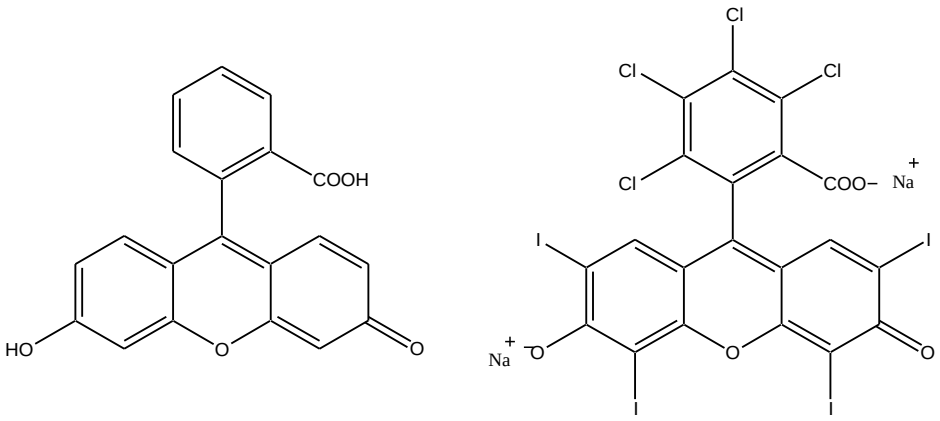

Fluorescein Rose Bengal

Figure 11. Xanthenes Dyes.

Photosensitizers having an added targeting mechanisms and in an early stage of development and can be considered the "third generation". Undoubtedly new photosensitizers will continue to appear especially as other targets become apparent. An

example of this is the porphycenes, which are being developed with topical delivery for dermatological and periodontal disease.[37,15-17]

Naphthalenic imides constitute a very versatile class of photosensitizing compounds which have been recently studied in numerous contexts. Studies of substituted 1,8-naphthalimides and bisnaphthalimides,[38] such as mitonafide, amonafide and elinafide (Figure 12), have revealed dramatic anticancer activity,[39,40] without photochemical excitation and members of both series have already entered into clinical trials.[41] Although the precise mechanism of their tumoricidal efficacy has not yet been fully understood, several lines of evidence suggest that it is linked to their ability to intercalate into DNA with high affinity and sequence specificity.[42] Sulfonated naphthalimides and bisnaphthalimides have also been reported to be very promising antiviral agents with selective *in vitro* activity against the human immunodeficiency virus, HIV-1.[43] In addition to the above "dark" properties, photochemical activation of these naphthalenic derivatives has been used to further broaden the range of biological applications. In this respect, brominated mono- and bisnaphthalimides have been proposed as good candidates for the photochemotherapeutic eradication of enveloped viruses in blood and blood products.[44-46] These photosensitizers have also been used for the photochemical repair of tissue and in these matters naphthalenic imides have been reported to be most effective.

The combination of high photoactivity and DNA-intercalation has prompted the use of some naphthalenic derivatives as sequence-specific DNA-photonucleases.[47] Depending on the chemical structure of the compound used, various mechanisms have been proposed, involving free radical formation,[48] photogeneration of carbocation,[49]

electron-transfer from oxidizable guanine residues (G),[50] or hydrogen abstraction from thymine,[51] although no single mechanism has been definitively implicated.

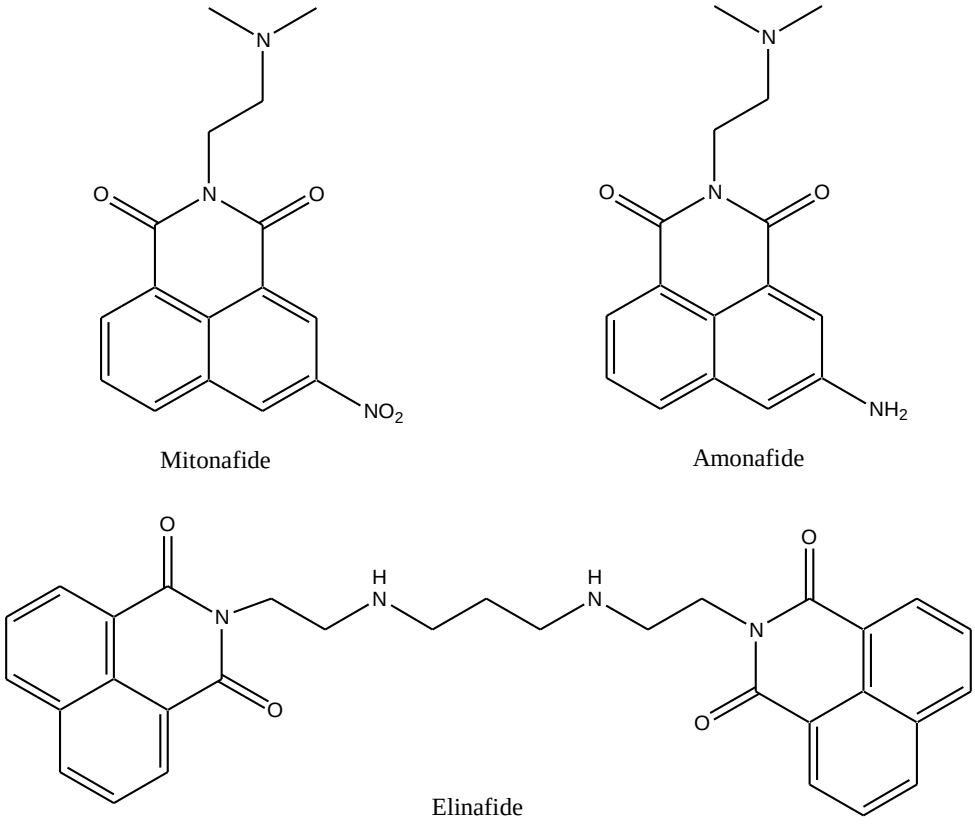

Figure 12. 1,8-Naphthalimide and bisnaphthalimide derivatives.

In 1993 Judy and Matthews reported that photoexcitation of the bichromophoric derivatives efficiently induced the cross-linking of proteins such as collagen.[52-54] This discovery led to their investigation of the potential application of these compounds in light-induced tissue-bonding of meniscal cartilage, articular cartilage and cornea.[55,56] Our group had the privilege to collaborate with Matthews and Judy on this photochemical tissue bonding (PTB), which was found to have potential in areas such as corneal repair, skin incision repair and skin grafts, tendon repair, nerve repair, and blood vessel repair.

Tissue repair is an obvious requirement following traumatic injury or surgical procedures. For most situations, tried and tested methods of mechanical bonding (such as sutures, clips, and staples) provide a cheap, rapid and efficient means of repair. However, in some situations these approaches are not particularly useful. Disadvantages include the placement of a foreign body in the tissue with resultant potential for inflammation and scarring, as well as the difficulty of suturing very small wounds. There are also a number of tissues that do not lend themselves easily to mechanical repair. Cornea is a particular example where suture repair is not optimal for a variety of reasons. Microsurgery in blood vessel and nerve repair is also difficult due to the necessity of tightly sealing off the tissue environment.[57] Thus, there is a possibility that a suitable, less invasive technology for tissue repair will be of value for specific applications.

Following up our initial studies with Matthews and Judy, our lab has demonstrated that a wide variety of naphthalimides produce, upon photochemical activation, mechanical bonds between a variety of tissue surfaces. One application of particular interest has been the bonding of tears in the avascular zone of menisci. Menisci are collagen-rich fibrocartilaginous tissues that support up to 90% of the load across the knee joint and participate in important functions including shock absorption, joint stabilization, hyperextension prevention, and lubrication of the knee. In fact, *ex vivo* and *in vivo* work demonstrated the significant potential of photochemically activated naphthalimides for the repair of meniscal lesions.[58-60]

In a related structure activity study the relative strengths of photochemically-catalyzed bonds in meniscal tissue by a variety of photoactive naphthalimides (Figure 13) were measured.[61] The bond strengths produced by these compounds (under the conditions

of these tests) ranged from 0.47 kg/cm^2 (for compound 3) to 1.38 kg/cm^2 (for compound 11), with an average background bond strength of 0.29 kg/cm^2 for control samples (irradiation/PBS with no naphthalimide). Although these bonds were much weaker than a simple mattress suture (10.2 kg/cm^2 in human meniscus),[62] they were comparable to those previously reported for naphthalimide mediated photochemical bonding of cartilage[47,56] and skin[63] and also to bonds formed in porcine aorta (~1.1 kg/cm^2) using an albumin/indocyanine green thermal welding strategy.[64]

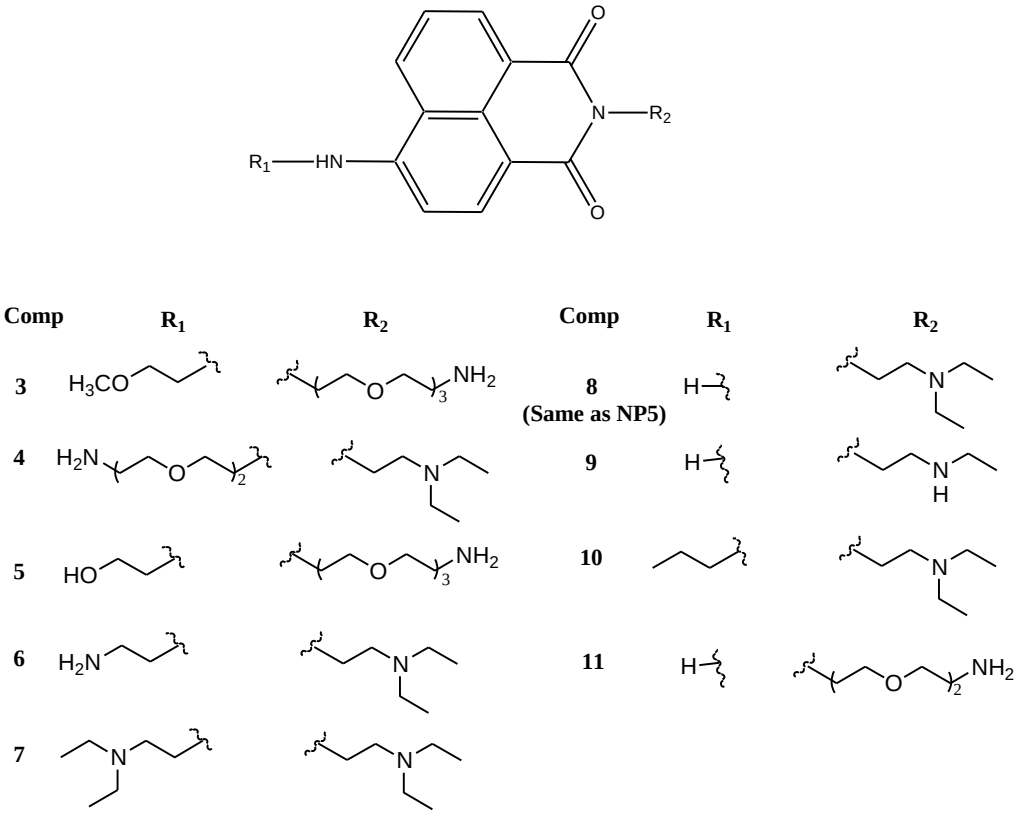

Figure 13. Naphthalimides used in the study by previous members of our group.

Since certain naphthalimide compounds can crosslink soluble proteins on photochemical activation the idea that these compounds might have also the potential to mediate the formation of tissue bonds was proposed. As tissue bonding experiments are

difficult and time consuming, our focus moved to evaluating the crosslinking of soluble protein by naphthalimides with various substituents at the 4-position. It could be anticipated that the most active photochemical protein crosslinkers would also exhibit enhaced tissue bonding. In any event, the photochemical crosslinking of a simple model protein (RNase A) was studied using a variety of water-soluble 1,8-naphthalimides based on the parent compound **NP5**, and including compounds C-4 substituents such as bromo (**NP6**), ethylsulfanyl (**NP7**), ethoxy (**NP8**), and ethylamino (**NP9**) (Figure 14).

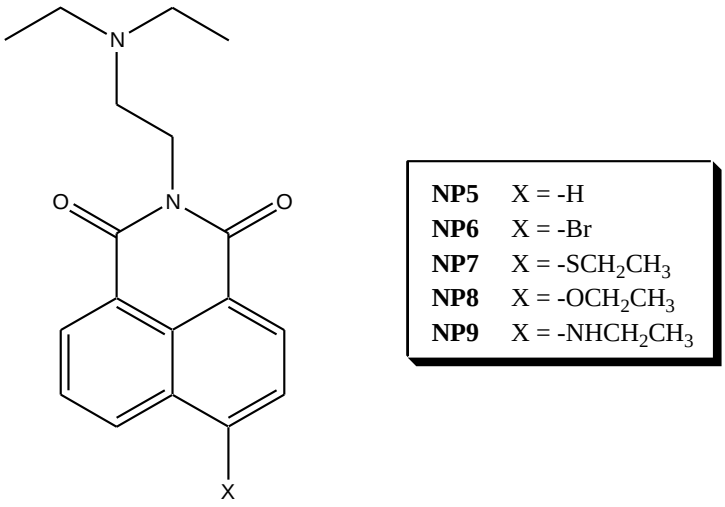

Figure 14. Photosensitizers used for photochemical modification of RNase A.

In preliminary experiments in our lab Woods reported[64] that the photosensitized crosslinking of RNase A was most favored when the unsubstituted compound **NP5** was employed, while the ethylamino-substituted naphthalimide **NP9** gave the least oligomerization. This trend is consistent with the trend of charge separation in the first excited singlet state[66] of these compounds which can be understood by examining their ability to participate in resonance delocalization (Figure 15). A simple examination of resonance parameters shows that as the R^+ values for the substituents become more

negative, and charge separation becomes more favored, the rate of protein crosslinking decreases (Table 2).[61]

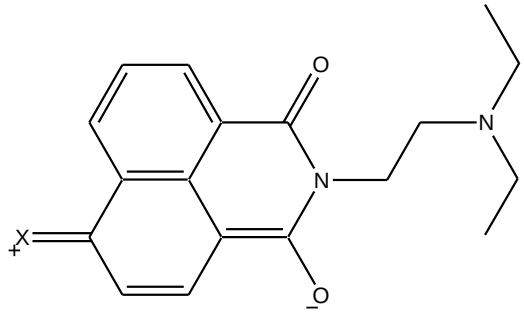

Figure 15. Resonance structure showing charge separation.

Table 2. Relative rate of RNase A crosslinking based on resonance parameter.[61]

Compound Susbtituent (a)	NP5 (H-)	NP6 (Br-)	NP7 (RS-)	NP8 (RO-)	NP9 (RNH-)
Relative initial rate of RNase crosslinking	56	17	9	3	1
Resonance Parameter R^+(b)	0.00	-0.30	-0.83	-1.07	-1.78

a) The alkyl substituents used in deriving the resonance parameter were methyl groups, not ethyl.
b) Other parameter sets show that this change would have a minimal impact on the absolute numbers, and none at all on the trend[62].

The ease by which the excited-state properties of naphthalimides can be readily tuned by altering the nature of the group at the 4-position makes them an attractive platform for study. Unsubstituted naphthaimides posses a nonpolar π,π^* state while the introduction of electron-donating or -withdrawing substituents (amino or nitro groups)

induces a polar charge-transfer excited state.[67] The compounds with charge transfer character are especially interesting due to their strong oxidizing or reducing capacity. The photochemical characteristics of these species has resulted in their studied in organic materials,[68] such as donor/acceptor systems for solar cells, sensors for metal ions and protons,[68-70]

A recent theoretical and experimental study of the photochemical properties of unsubstituted and 4-substituted naphthalimides (Figure 16) was reported by Kucheryavy and coworkers.[71] Compounds with the substituents by -SMe, -NO_2, and -NMe_2 exhibited a large red shift with broad and structureless absorption and emission bands. They attributed this behavior to the charge-transfer excited states, in which electronic donation are from the lone pairs of electrons present in the 4 substituent toward the aromatic ring. The effect of chloro substitution is minor, as its inductive electron withdrawing tends to cancel out its resonance electron donation, and so the character of its excited state is very similar to the parent unsubstituted naphthalimides. A similar result was observed by previous members of our group[72] in which they reported maximum absorption values of several 4-substituted-1,8-naphthalimides derivatives and found that the 4-bromo and 4-unsubstituted derivatives have the shortest absorption values.

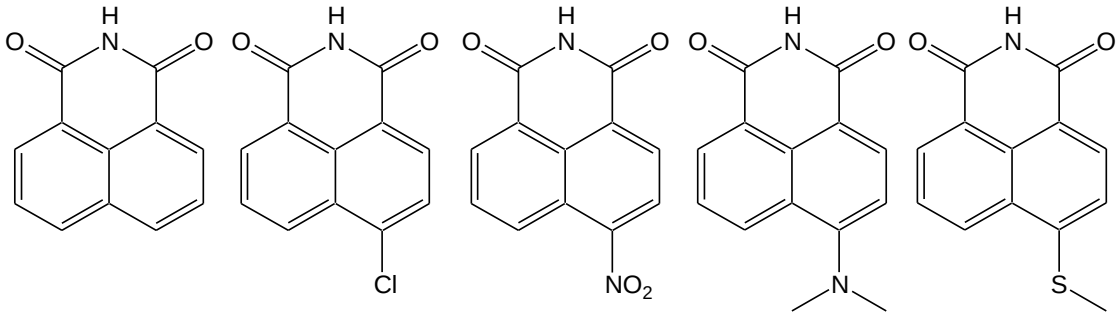

Figure 16. Structure of naphthalimide and 4-substituent derivatives.

Current Research Goals and Strategies

Our lab has long had an interest in the potential biomedical applications of naphthalimide photochemistry, including especially the use for tissue bonding and modification. Accordingly, this dissertation reports extensive structure-activity studies that were performed in the hopes of identifying features that will allow us to develop improved photosensitizing compounds. Our initial studies were focused on protein crosslinking and modification as a model for tissue surfaces. Results from these studies can also contribute to the understanding of the photochemical mechanisms of naphthalimide-induced protein modification and crosslinking. With our results from solution protein photochemistry in hand, we have now begun preliminary studies aimed at extending these studies to the modification of fresh tissue surfaces. Bovine pericardium tissue, pig skin and bovine knee meniscal tissue were used substrates for the tissue modification experiments.

CHAPTER TWO

Materials and Methods

Reagents and Materials

RNAse A (USB Company), Lysozyme (VWR), D-(+)-Biotin (VWR), Z-amino acids were obtained from commercial sources and used as received. Methylene chloride, methanol, ethyl acetate were obtained from commercial sources and distilled prior to use. Anhydrous ethanol, DMF and DMSO were used as received. SDS-Polyacrylamide gels were obtained from two sources, PRCST IGEL 4-20% Tris-Glycine-SDS (VWR) and 4-20% Precise Protein Gels Tris-HEPES-SDS (Thermo Scientific-Pierce). Materials and solutions for Western Blots were purchased mainly from Bio-Rad, VWR and Thermal Fischer Scientific Inc. All other reagents were provided from commercial suppliers such as Sigma-Aldrich, VWR, and Acros and were used as received. Pericardium tissue and pig skin were purchased from Animal Technology (Tyler, TX), fresh bovine knee tissue was harvested and supplied by a local slaughterhouse within a few hours of the death of the animal.

Instrumentation and Analytical Techniques

Photochemical Protein Crosslinking

Photochemical crosslinking modification of RNAse and Lysozyme was achieved using an EFOS Novacure mercury lamp with a 400-500 nm filter as the light source. The

light intensity was set up to 2000 mW and was routinely measured with an EFOS Novacure radiometer

NMR Analysis

A Bruker 500 MHz NMR was used for ^{1}H, GCosy and ^{13}C analysis of the naphthalimides and the biotin-derivatives synthesized for the purpose of this investigation.

LC-MS

Mass spectrometry was carried out by the Baylor University mass spectroscopy center. High resolution mass spectra (HRMS) were obtained using electron impact (EI) ionization on a VG Prospec Micromass Spectrometer on electrospray ionization (+ESI) technique on a Thermo Scientific LTQ Orbitrap Discovery Mass Spectrometer.

SDS-PAGE Electrophoresis

Sodium dodecyl sulfate polyacrylamide gel electrophoresis was performed using a Bio-Rad Mini-Protean Three cell electrophoresis system connected to a VWR 150 power supply. Ten-well Precast 4-20 % SDS-gels were purchased from VWR and Thermo-Pierce. An Omega 10 imager provided documentation of gels or biological samples requiring UV A, B, or C transillumination, white light transillumination, and/or UV A or C EPI-lighting was used to visualize the coomassie blue gels after electrophoresis.

Western Blots

The incorporation of biotinylated compounds was determined by western blotting. SuperBlock blocking buffer and conjugated InmunoPure Avidin-Horseradish Peroxidase were obtained from Pierce. North2South Chemiluminescent Substrate (HRP) kit (Thermo Scientific) was used to visualize the reagents. A gel imager from Ultralum INC with a 12 bit Hamamatsu integrating monochrome CCD digital camera was used for imaging.

Synthetic Procedures

Synthetic Procedure of 1,8-naphthalimides (Sensitizers)

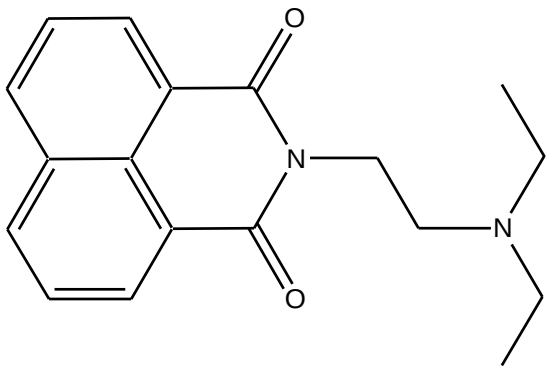

Figure 17. Structure of **NP5**.

2-[2-(Diethylamino)ethyl]-1H-benz[de]isoquinoline-1,3(2H)-dione (**NP5**, Figure 17). Naphthalimide 5, which has previously been reported by our group[65] and by other authors,[73] was prepared by a reaction of 1,8-naphthalic anhydride with *N*,*N*-diethylethylenediamine using 90% ethanol as solvent. *N*,*N*-diethylethylenediamine (0.156 mL, 1.11 mmol, 1.1 equivalents) was added to a stirred suspension of 1,8-naphthalic anhydride (200 mg, 1.01 mmol) in ethanol (10 mL). The suspension was stirred at room temperature in the dark for one hour until the solid fully dissolved forming a dark brown

solution. The ethanol was then removed under reduced pressure. Flash column chromatography (silica gel, 95:5 DCM/ CH_3OH; Rf = 0.20) yielded the pure product as a light yellow solid (119 mg, 40% yield): ^{1}H NMR (500 MHz, $CDCl_3$) δ 1.09 (t, 6H, *J* = 5.0 Hz), 2.65 (q, 4H, *J* = 5.0 Hz), 2.77 (m, 2H), 4.27 (m, 2H), 7.72 (t, 2H, *J* = 5.0 Hz), 8.2 (d, 2H, *J* = 10.0 Hz), 8.58 (d, 2H, *J* = 10.0 Hz); ^{13}C NMR (125 MHz, $CDCl_3$) δ 12.28, 38.01, 47.72, 49.92, 122.62, 126.68, 128.04, 131.09, 131.52, 133.63, 164.09.

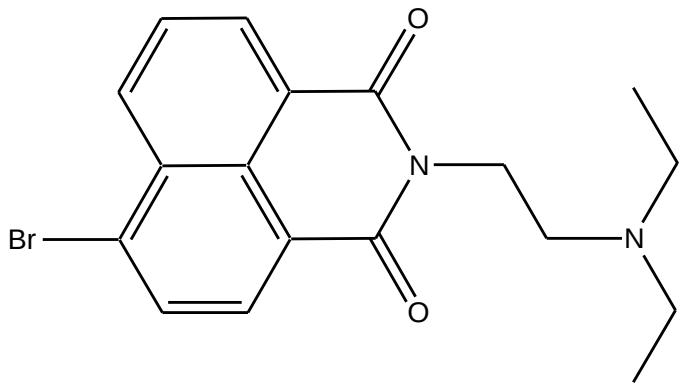

Figure 18. Structure of **NP6**.

6-Bromo-2-[2-(diethylamino)ethyl]-1H-benz[de]isoquinoline-1,3(2H)dione (**NP6**, Figure 18). Brominated naphthalimide derivative previously syntesized by Wood[65] was obtained by adding *N*,*N*-diethylethylenediamine (0.56 mL, 3.97 mmol, 1.1 equivalents) to a stirred suspension of 4-bromo-1,8-naphthalic anhydride (1.00 g, 3.61 mmol, 50 mL) in ethanol. The suspension was stirred under nitrogen atmosphere at room temperature in the dark for 2 hours and then the ethanol was removed under reduced pressure. Flash column chromatography (silica gel, 9.5:0.5 DCM/CH_3OH, Rf: 0.27) yielded the pure product as a light yellow solid (1.06 g, 78% yield): ^{1}H NMR (500 MHz, $CDCl_3$) δ 1.07 (t, 6H, *J* = 5.0 Hz), 2.64 (q, 4H, *J* = 5.0 Hz), 2.76 (m, 2H), 4.25 (t, 2H, *J* = 10.0 Hz), 7.80 (dd, 1H, *J* = 10.0, 5.0 Hz), 7.99 (d, 1H, *J* = 10.0 Hz), 8.36 (d, 1H, *J* = 5.0 Hz), 8.51 (d,

1H, *J* = 10.0 Hz), 8.61 (d, 1H, *J* = 5.0 Hz); ^{13}C NMR (125 MHz, $CDCl_3$) δ 12.24, 38.17, 47.60, 49.92, 122.14, 123.03, 128.02, 128.92, 130.10, 130.48, 131.21, 131.87, 133.22, 163.47.

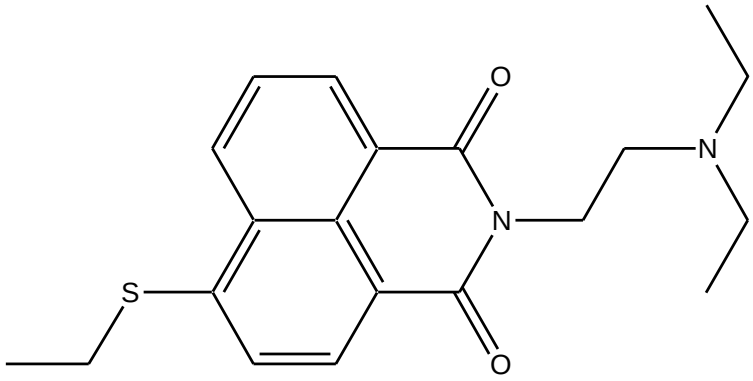

Figure 19. Structure of **NP7**.

2-[2-(Diethylamino)ethyl]-6-ethylsulfanyl-1H-benz[de]isoquinoline-1,3(2H)dione (**NP 7**, Figure 19). The preparation of this sensitizer, previously reported by our group,[65] was achieved by a two step synthetic procedure. The first step produced 4-ethylsulfanyl-1,8-naphthalic anhydride. Anhydrous potassium carbonate (1.9 equivalents, 0.95 g, 6.84 mmol) and ethanethiol (1.07 mL, 0.89 g, 14.4 mmol, 4 equivalents) were added to a solution of 4-bromo-1,8-naphthalic anhydride (1.0 g, 3.6 mmol, 50 mL) in anhydrous DMF. The solution was placed under nitrogen atmosphere, stirred at room temperature in the dark for 19 hours and then poured onto ice water (300 mL) to give a yellow suspension. This Suspension was stirred for 2 hours and the yellow solid was recovered by vacuum filtration. Recrystallization from ethanol afforded the pure product as a yellow solid (0.72 g, 78% yield). For the second step two equivalents of *N*,*N*-diethylethylenediamine (0.79 mL, 0.69 g, 5.58 mmol) were added to a suspension of 4-ethylsulfanyl-1,8-naphthalic anhydride (0.72 g, 2.79 mmol) in ethanol (17 mL). The

mixture was stirred at room temperature under nitrogen in the dark for 3 hours; by the end of the reaction time all the solid was completely dissolved. Removal of the solvent and excess amine under vacuum gave the pure product (0.99 g, 99% yield), ^{1}H NMR (500 MHz, $CDCl_3$) δ 1.08 (t, 6H, *J* = 5.0 Hz), 1.47 (t, 3H, *J* = 5.0 Hz), 2.03 (s, 1H), 2.65 (q, 4H, *J* = 10.0 Hz), 2.77 (t, 2H, *J* = 5.0 Hz), 3.17 (q, 2H, *J* = 5.0 Hz), 4.26 (t, 2H, *J* = 10.0 Hz), 7.51 (d, 1H, *J* = 10.0 Hz), 7.71 (dd, 1H, *J* = 10.0, 5.0 Hz), 8.44 (d, 1H, *J* = 10.0 Hz), 8.53 (d, 1H, *J* = 10.0 Hz), 8.59 (d, 1H, *J* = 10.0 Hz); ^{13}C NMR (125 MHz, $CDCl_3$) δ 12.23, 13.54, 26.36, 37.99, 47.63, 49.84, 118.91, 122.62, 123.16, 126.53, 128.37, 129.51, 130.05, 130.70, 131.48, 145.17, 164.05.

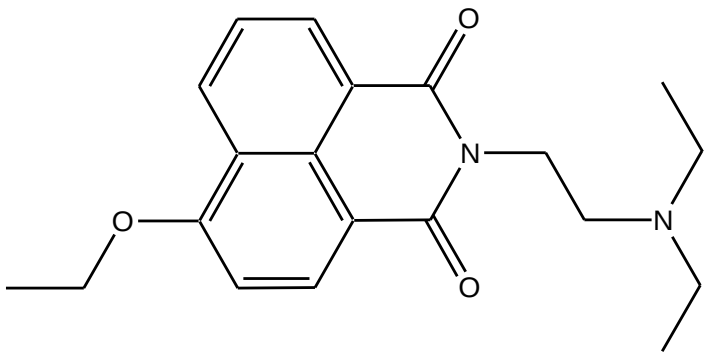

Figure 20. Structure of **NP8**.

2-[2-(Diethylamino)ethyl]-6-ethoxy-1H-benz[de]isoquinoline-1,3(2H)-dione (**NP8**, Figure 20).[65] **NP6** (300 mg, 0.80 mmol) was dissolved in ethanol (8 mL), followed by the addition of eight equivalents of sodium ethoxide (6.39 mmol, 435.0 mg, 2.39 mL of a 21% (wt) solution in ethanol) and $CuSO_4 \cdot 5H_2O$ (0.10 mmol, 24.9 mg, 0.125 equivalents). The solution was refluxed while stirring for eight hours, and then was stirred for additional 10 hours at room temperature. The solution was then diluted with DCM (50 mL), washed three times with 1M NaOH, washed once with saturated NaCl,

dried over $MgSO_4$, and filtered. Removal of the solvents under reduced pressure yielded the crude product, which was purified by silica gel flash column chromatography (9.7:0.3 DCM/CH_3OH, Rf: 0.21) to give the pure product as a yellow oil (164 mg, 60% yield): ^1H NMR (500 MHz, $CDCl_3$) δ 1.06 (t, 6H, *J* = 5.0 Hz), 1.55 (t, 3H, *J* = 5.0 Hz), 2.62 (q, 4H, *J* = 10.0 Hz), 2.73 (m, 2H), 4.20 (m, 2H), 4.26 (q, 2H, *J* = 10.0 Hz), 5.26 (s, 1H), 6.89 (d, 1H, *J* = 10.0 Hz), 7.57 (dd, 1H, *J* = 10.0, 5.0 Hz), 8.39 (d, 1H, *J* = 5.0 Hz), 8.44 (t, 2H, *J* = 10.0 Hz). ^{13}C NMR (125 MHz, $CDCl_3$) δ 12.31, 14.61, 37.76, 47.65, 49.82, 53.51, 64.63, 105.60, 114.51, 122.16, 123.30, 125.59, 128.58, 129.25, 131.28, 133.33, 159.96, 163.85, 164.41.

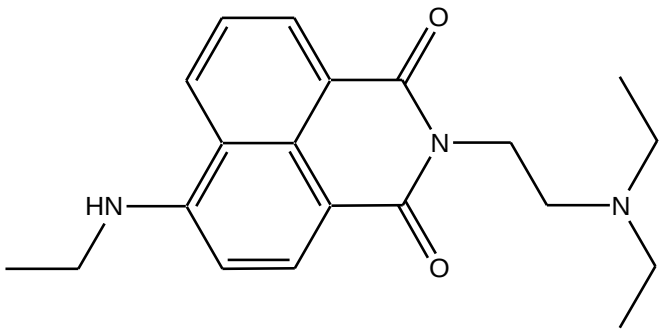

Figure 21. Synthetic procedure of **NP9**.

2-[2-(Diethylamino)ethyl]-6-ethylamino-1H-benz[de]isoquinoline-1,3(2H)-dione (**NP9**, Figure 21).[65] **NP6** (0.52 g, 1.39 mmol), was combined with DMSO (15 mL) and ethylamine (2 equivalents, 2.78 mmol, 179.07 mg of a 70% solution in water) in a sealed flask. The solution was heated to 150 ^oC in a sand bath and stirred for 8 hours, followed by additional 13 hours at room temperature. The solvents were then removed under vacuum and the crude product purified by flash chromatography (silica gel, 9:1 DCM/CH_3OH, Rf: 0.43) to give an orange solid (36.2 mg, 50% yield from **NP6**). ^1H

NMR (500 MHz, $CDCl_3$) δ 1.12 (t, 6H, J = 5.0 Hz), 1.45 (t, 3H, J = 5.0), 2.68 (q, 4H, J = 10.0 Hz), 2.79 (m, 2H), 3.43 (m, 2H), 4.27 (t, 2H, J = 5.0 Hz), 5.23 (s, 1H), 6.70 (d, 1H, J = 10.0 Hz), 7.59 (t, 1H, J = 10.0 Hz), 8.08 (d, 1H, J = 10.0 Hz), 8.44 (d, 1H, J = 10.0 Hz), 8.56 (d, 1H, J = 5.0 Hz); ^{13}C NMR (125 MHz, DMSO) δ 11.26, 14.12, 37.33, 37.98, 47.36, 49.43, 104.14, 107.84, 120.52, 122.18, 124.59, 129.20, 129.92, 131.08, 134.77, 151.06, 163.38, 164.31.

Synthetic Procedure of the Biotin Labeled Derivatives

Biotin-labeled compounds are very useful to determine the capability of the naphthalimide compounds used as sensitizers to link specific functional groups to proteins. These experiments were designed to investigate at both the reaction of photochemically activated protein with the biotin-derivatives and the condensation of photochemically activated biotin-derivatives with native protein.

Biotin-LC-Hydrazide (**BD1**) was obtained from commercial sources (Pierce). The remainder of the biotinylated compounds used for this investigation were synthesized and characterized as is described.

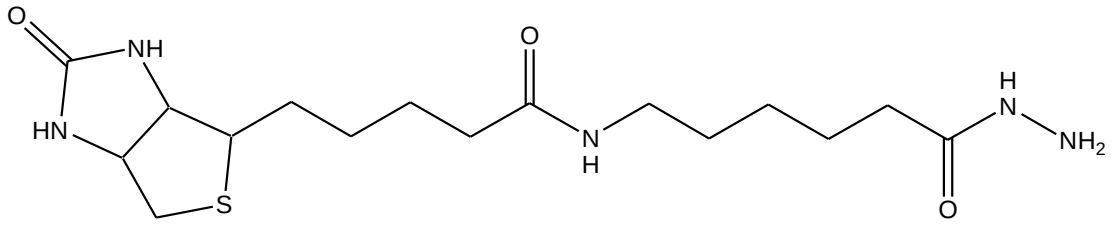

Figure 22. Structure of compound **BD1**.

5-(2-Oxo-hexahydro-thieno[3,4-d]imidazol-4-yl)-pentanoic acid (5-hydrazinocarbonyl-pentyl)-amide (Biotin-LC-Hydrazide, **BD1**, Figure 22). The biotin-

LC-hydrazide reagent was commercially obtained from Pierce Company and prepared as a 2 mM stock solution in DMSO. The product was used without further purification and diluted as necessary.

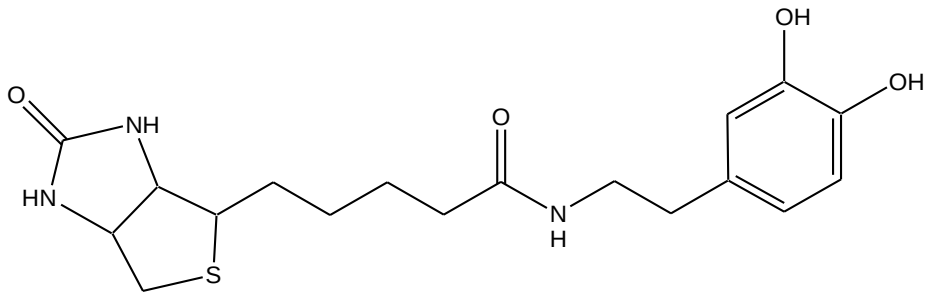

Figure 23. Structure of compound **BD2**.

5-(2-Oxo-hexahydro-thieno[3,4-d]imidazol-4-yl)-pentanoic acid [2-(3,4-dihydroxy-phenyl)-ethyl]-amide (Biotin-Dopamine, **BD2**, Figure 23). Synthesis of biotin-dopamine has been reported before by other authors. [74,75] In the synthetic procedure carried out by us, biotin (1.3 g, 5.3 mmol) and benzotriazole-1-yl-oxy-tris-(dimethylamino)-phosphonium hexafluorophosphate (BOP) (2.3 g, 5.3 mmol) were dissolved in DMF (10 mL) anhydrous at room temperature; NEt_3 (0.5 mL, 3.6 mmol) was then added to the solution which was stirred for 5 minutes. In another flask, dopamine (1.0 g, 5.3 mmol) was dissolved in DMF (5 mL) and NEt_3 (0.5 mL, 3.6 mmol) was added to the mixture. The dopamine solution was then added dropwise to the solution containing the biotin, and the reaction was stirred for 24 hours at room temperature under nitrogen atmosphere. The crude reaction mixture was evaporated, and dissolved in EtOAc (10 mL) and washed with water. Excess of water remaining in the EtOAc layer was removed with $MgSO_4$ and then the solvent was evaporated under vacuum affording the product as a creamy-colored solid (yield: 51 %). Purification of the product was

achieved by column chromatography (silica gel, 9.5:0.5 CH_2Cl_2/ CH_3OH). The new compound was obtained as a greenish precipitate with an Rf: 0.27 and yield of 47%. ^{1}H NMR (500 MHz, DMSO): δ, 1.28 (m, 2H), 1.48 (m, 4H), 2.03 (t, 2H, *J* = 7.0 Hz), 2.10 (dd, 1H, *J* = 5.0 Hz, 7.5 Hz), 3.08 (m, 1H), 3.15 (td, 2H, *J* = 6.5 Hz, 7.0Hz), 4.12 (s, 1H), 4.30 (m, 1H), 6.42 (m, 3H), 6.56 (m, 2H), 7.79 (s, 1H). ^{13}C NMR (125 MHz, DMSO): δ, 9.62, 25.76, 28.48, 31.15, 35.17, 46.05, 55.87, 59.67, 61.49, 111.26, 116.42, 119.62, 123.41, 130.70, 143.95, 145.49, 163.22, 172.32. HRMS(ESI+) calculated for $C_{18}H_{25}N_3O_4S$ ($[M+H]^+$, was 380.163. Positive electrospray ionization HRMS(ESI+) found 380.164 (Δ ppm: 1.05). Negative electrospray ionization HRMS(ESI-) calculated for $C_{18}H_{24}N_3O_4S$ ($[M-H]^+$, was 378.149 and the found 378.149 (Δ ppm: -1.79).

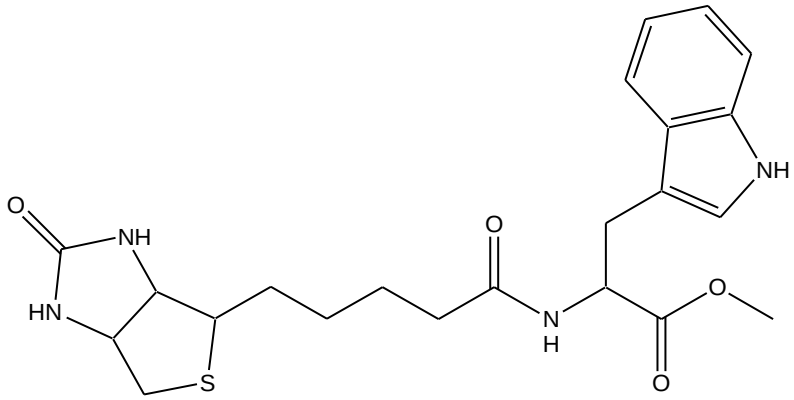

Figure 24. Structure of compound **BD3**.

The compound 3-(1H-Indol-3-yl)-2-[5-(2-oxo-hexahydro-thieno[3,4-d]imidazol-4-yl)-pentanoylamino]-propionic acid methyl ester (Biotin-Tryptophan methyl ester, **BD3**, Figure 24). Biotin-tryptophan methyl ester is a known compound reported by Gu and coworkers.[76] Our synthetic procedure involved a solution of tryptophan methyl ester (1.0 g, 3.9 mmol) dissolved in DMF (5 mL) and NEt_3 (0.5 mL, 3.6 mmol) was added dropwise to a flask containing a mixture of biotin (1.0 g, 3.9 mmol), BOP (1.7 g, 3.9

mmol), and NEt_3 (0.5 mL, 3.6 mmol) dissolved in DMF (10 mL). The solution was stirred for 24 hour at room temperature under nitrogen atmosphere. The reaction mixture was then dissolved in water (20 mL) and extracted with EtOAc (20 mL). Evaporation of the ethyl acetate layer afforded crude product of the biotin-tryptophan methyl ester compound as a yellow oil which was purified by column chromatography (9.5: 0.5 CH_2Cl_2/ CH_3OH) with yield of 25 % and Rf: 0.45. ^{1}H NMR (500 MHz, DMSO): δ, 1.25 (m, 2H), 1.52 (m, 4H), 2.18 (t, 2H, *J* = 7.2 Hz), 2.52 (d, 1H, *J* = 12.6 Hz), 2.66 (d, 1H, *J* = 9.4 Hz), 2.96 (s, 3H), 3.30 (d, 2H, *J* = 5.76 Hz), 4.02 (dd, 1H, *J* = 4.7 Hz, 7.5 Hz), 4.18 (td, 1H, *J* = 5.4 Hz, 11.5 Hz), 4.95 (dt, 1H, *J* = 6.1 Hz, 7.6 Hz), 5.75 (s, 1H), 6.56 (s, 1H), 6.85 (d, 1H, *J* = 5.0 Hz), 7.08 (m, 2H), 7.35 (d, 1H, *J* = 7.9 Hz), 7.58 (d, 1H, *J* = 7.9 Hz). ^{13}C NMR (125 MHz, DMSO): δ, 13.18, 20.04, 24.33, 26.51, 30.44, 34.40, 35.49, 39.38, 51.39, 54.64, 59.09, 60.84, 108.43, 110.35, 117.32, 117.65, 120.86, 122.64, 126.42, 135.26, 163.32, 172.34.

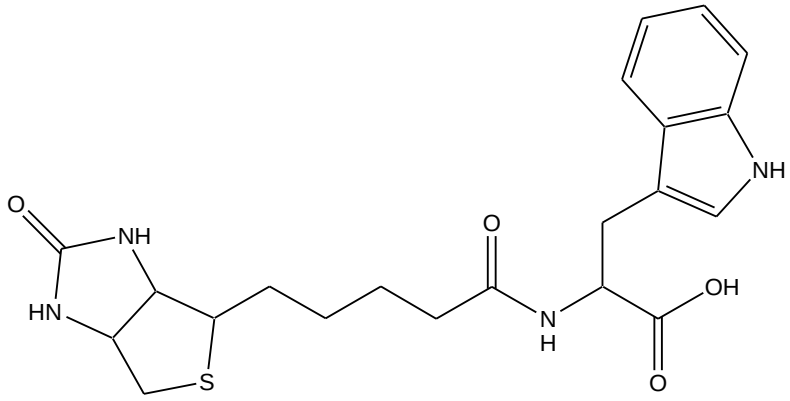

Figure 25. Structure of compound **BD4**.

Biotin-tryptophan or also called 3-(1H-Indol-3-yl)-2-[5-(2-oxo-hexahydro-thieno[3,4-d]imidazol-4-yl)-pentanoylamino]-propionic acid (**BD4**, Figure 25)(reported compound by Gu[76]). 0.4 g of **BD3** (0.95 mmol) from the previous synthetic procedure

was dissolved in 1M HCl/acetone (5 mL) and the reaction was allowed to stir for 72 hours at 70 ^{o}C using a sand bath reflux. The compound was purified using column chromatography (silica gel, 9.5: 0.5 CH_2Cl_2/CH_3OH) which resulted in a fine creamy white solid with Rf: 0.29 and yield: 97%. ^{1}H NMR (500 MHz, DMSO): δ, 1.25 (m, 2H), 1.52 (m, 4H), 2.18 (t, 2H, *J* = 7.2 Hz), 2.52 (d, 1H, *J* = 12.6 Hz), 2.66 (d, 1H, *J* = 9.4 Hz), 3.30 (d, 2H, *J* = 5.76 Hz), 4.02 (dd, 1H, *J* = 4.7 Hz, 7.5 Hz), 4.18 (td, 1H, *J* = 5.4 Hz, 11.5 Hz), 4.95 (dt, 1H, *J* = 6.1 Hz, 7.6 Hz), 5.75 (s, 1H), 6.56 (s, 1H), 6.85 (d, 1H, *J* = 5.0 Hz), 7.08 (m, 2H), 7.35 (d, 1H, *J* = 7.9 Hz), 7.58 (d, 1H, *J* = 7.9 Hz), 10.49 (s, 1H). ^{13}C NMR (125 MHz, DMSO): δ, 20.04, 24.33, 26.51, 30.44, 34.40, 35.49, 39.38, 51.39, 54.64, 59.09, 60.84, 108.43, 110.35, 117.32, 117.65, 120.86, 122.64, 126.42, 135.26, 163.32, 172.34. Positive electrospray ionization HRMS(ESI+) calculated for $C_{21}H_{26}N_4O_4S$ ($[M+H]^+$) was 431.175 and HRMS(ESI+) found 431.175 (Δ ppm: 0.32). Negative electrospray ionization HRMS(ESI-) calculated for $C_{21}H_{25}N_4O_4S$ ($[M-H]^+$) was 429.160 and the found 429.160 (Δ ppm: 0.44).

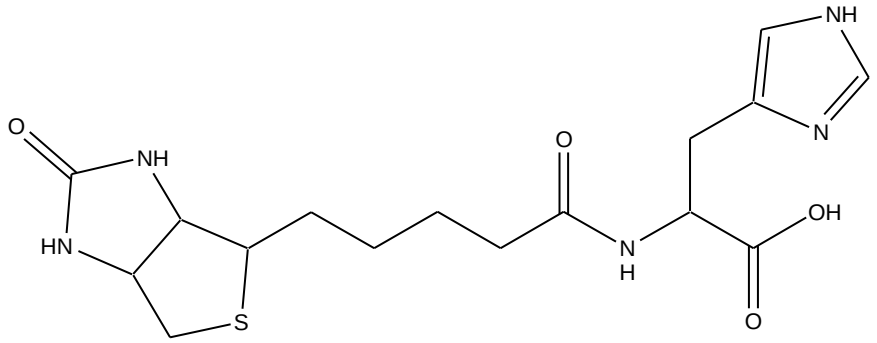

Figure 26. Structure of compound **BD5**.

3-(1H-Imidazol-4-yl)-2-[5-(2-oxo-hexahydro-thieno[3,4-d]imidazol-4-yl)-pentanoylamino]-propionic acid (Biotin-Histidine, **BD5**, Figure 26). A solution of histidine (0.3 g, 2.05 mmol) and NEt_3 (0.3 mL, 1.8 mmol) in chloroform (5 mL) was

prepared and added dropwise to another solution containing biotin (0.5 g, 2.05 mmol), BOP (0.91 g, 2.05 mmol), and NEt_3 (0.25 mL, 1.8 mmol) in DMSO (5 mL). The mixture was stirred for 24 hour at room temperature under nitrogen atmosphere. The solvent was then removed using vacuum distillation and the crude product was purified by column chromatography (silica gel, 5:5 CH_2Cl_2/ CH_3OH). The purified compound was obtained as a creamy white solid with Rf: 0.28 (UV(-), I_2(+)) and with a 54% yield. ^{1}H NMR (500 MHz, DMSO): δ, 1.26, 1.44, 1.59 (m, 6H), 2.05 (t, 2H, *J* = 7.5 Hz), 2.58 (d, 2H, *J* = 12.5 Hz), 2.82 (dd, 1H, *J* = 5.0 Hz, 12.5 Hz), 3.08, 3.11 (m, 3H), 4.12 (m, 1H), 4.31 (td, 1H, *J* = 5.0 Hz, 7 Hz), 4.56 (dt, 1H, *J* = 9.0 Hz, 14.0 Hz), 6.39 (d, 2H, *J* = 9.0 Hz), 7.30 (s, 1H), 8.22 (d, 1H, *J* = 8.5 Hz), 8.82 (s, 1H). ^{13}C NMR (125 MHz, DMSO): δ, 25.59, 27.45, 28.49, 35.31, 37.90, 51.47, 55.83, 59.66, 61.48, 117.34, 130.61, 134.37, 163.18, 172.68, 172.79. Positive electrospray ionization HRMS(ESI+) calculated for $C_{16}H_{23}N_5O_4S$ ($[M+H]^+$) 382.154, HRMS(ESI+) found 382.154 (Δ ppm: 0.34).

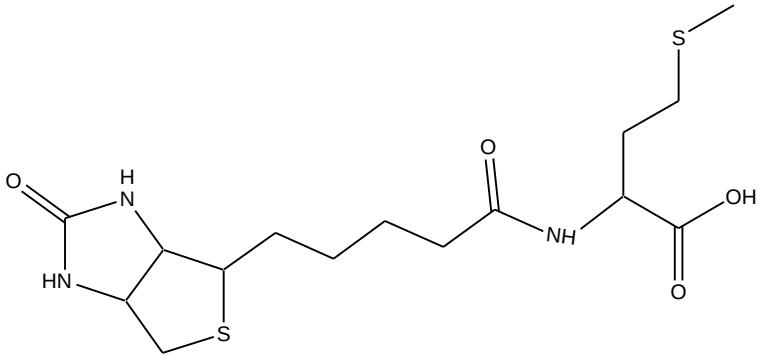

Figure 27. Structure of compound **BD6**.

4-Methylsulfanyl-2-[5-(2-oxo-hexahydro-thieno[3,4-d]imidazol-4-yl)-pentanoylamino]-butyric acid (Biotin-Methionine, **BD6**, Figure 27)(reported compound by Gu[76]). Methionine (0.3 g, 2.1 mmol) and NEt_3 (0.3 mL, 1.8 mmol) were dissolved in DMSO (5 mL) and added dropwise to a solution containing biotin (0.5 g, 2.05 mmol),

BOP (0.91 g, 2.05 mmol), and NEt_3 (0.3 mL, 1.8 mmol) also in DMSO (5 mL). The reaction was stirred for 24 hours at room temperature. The product was then evaporated and purified with a silica column starting with a mixture of 8:2 CH_2Cl_2/CH_3OH, without applying air to the column. After elution of UV(+) impurities the polarity of the column was changed to 6:4 CH_2Cl_2/CH_3OH, which eluted pure compound exhibiting one spot in the TLC with Rf: 0.72 (UV(-), I_2(+)). The compound was obtained as a yellow oil that, after drying, gave an orange/beige solid with a 42 % yield. ^{1}H NMR (500 MHz, D_2O): δ, 1.29, 1.44, 1.52, 1.54 (m, 7H), 1.81 (m, 1H), 1.97 (s, 3H), 2.19 (t, 2H, *J* = 5.5 Hz), 2.45 (m, 2H), 2.64 (d, 1H, *J* = 13.0 Hz), 2.89 (dd, 1H, *J* = 5.0 Hz, 13.0 Hz), 3.22 (m, 2H), 4.22 (m, 1H), 4.29 (m, 1H), 4.49 (m, 1H). ^{13}C NMR (125 MHz, D_2O): δ, 14.06, 24.36, 24.98, 27.52, 27.71, 27.86, 29.71, 30.75, 35.23, 39.63, 53.50, 55.21, 55.30, 60.19, 61.99. Positive electrospray ionization HRMS(ESI+) calculated for $C_{15}H_{25}N_3O_4S_2$ ($[M+H]^+$) was 376.135. HRMS(ESI+) found 376.136 (Δ ppm: -0.45). Negative electrospray ionization HRMS(ESI-) ($[M-H]^+$) calculated for $C_{15}H_{24}N_3O_4S_2$ was 374.121 and the found 374.120 (Δ ppm: -2.22).

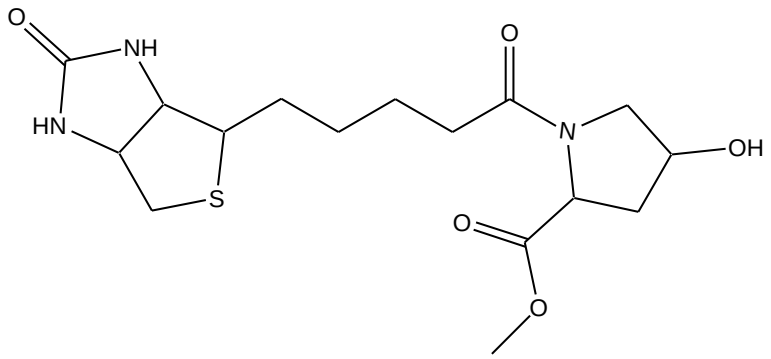

Figure 28. Structure of compound **BD7**.

4-Hydroxy-1-[5-(2-oxo-hexahydro-thieno[3,4-d]imidazol-4-yl)-pentanoyl]-pyrrolidine-2-carboxylic acid methyl ester (Biotin-hydroxyproline methyl ester, **BD7**,

Figure 28). Hydroxyproline methyl ester (0.4 g, 2.1 mmol) and NEt_3 (0.3 mL, 1.8 mmol) were dissolved in DMSO (5 mL) and added dropwise to a solution containing biotin (0.5 g, 2.1 mmol), BOP (0.91 g, 2.1 mmol) and NEt_3 (0.3 mL, 1.8 mmol) dissolved in DMSO (7 mL). The reaction was allowed to stir for 24 hours at room temperature. Biotin-hydroxyproline methyl ester was isolated as a brown oil by column chromatography (silica gel, 8:2 CH_2Cl_2/ CH_3OH), Rf: 0.84 (UV(-), I_2(+)), 43% yield.^{1}H NMR (500 MHz, DMSO): δ, 1.33, 1.49, 1.60 (m, 6H), 1.63 (m, 1H), 2.24 (t, 2H, *J* = 6.5 Hz), 2.5 (s, 3H), 2.57 (d, 1H, *J* = 12.5 Hz), 2.83 (dd, 1H, *J* = 5.0 Hz, 12.5 Hz), 3.12 (m, 1H), 3.34 (m, 5H), 4.14 (m, 1H), 4.25 (t, 1H, *J* = 7.5 Hz), 4.30 (t, 1H, *J* = 6.5 Hz), 6.37 (s, 1H), 6.46 (s, 1H). Positive electrospray ionization HRMS(ESI+) calculated for $C_{16}H_{25}N_3O_5S$ ($[M+H]^+$) were 372.158. HRMS(ESI+) found 372.159 (Δ ppm: 0.78).

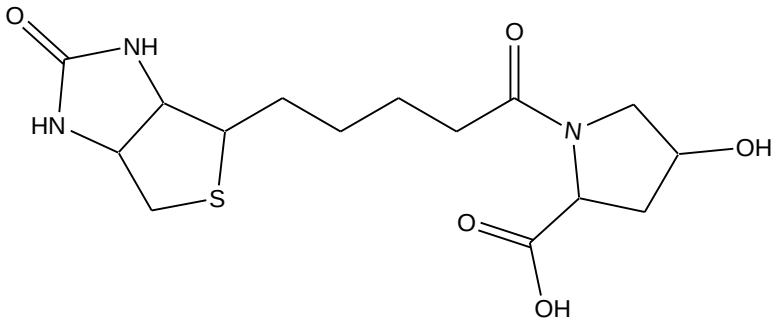

Figure 29. Structure of compound **BD8**.

4-Hydroxy-1-[5-(2-oxo-hexahydro-thieno[3,4-d]imidazol-4-yl)-pentanoyl]-pyrrolidine-2-carboxylic acid (Biotin-Hydroxyproline, **BD8**, Figure 29). A portion of the previously synthesized **BD7** was dissolved in 1M HCl/Acetone solution and stirred for 72 hours at 70 ^oC under reflux. The desired product was then purified by column chromatography (silica gel, 8:2 CH_2Cl_2/ CH_3OH) which gave a brown solid with Rf: 0.49 (UV(-), I_2(+)) and 43 % yield. ^{1}H NMR (500 MHz, D_2O): δ, 1.34, 1.51, 1.62 (m, 6H),

2.10 (m, 2H), 2.32 (m, 1H), 2.67 (d, 1H, *J* = 13.0 Hz), 2.89 (d, 1H, *J* = 9.0 Hz), 3.23 (s, 1H), 3.48 (m, 5H), 4.22 (m, 1H), 4.37 (m, 1H), 4.55 (m, 1H). ^{13}C NMR (125 MHz, D_2O): δ, 24.11, 27.61, 33.14, 33.85, 36.64, 39.69, 52.27, 53.26, 55.24, 59.76, 61.95, 74.55, 165.36, 173.79, 175.89. Positive electrospray ionization HRMS(ESI+) calculated for $C_{15}H_{23}N_3O_5S$ ($[M+Na]^+$) 380.125, HRMS(ESI+) found 380.125 (Δ ppm: 0.53). Negative electrospray ionization HRMS(ESI-) ($[M-H]^+$) calculated for $C_{15}H_{22}N_3O_5S$ was 356.128 and the found 356.129 (Δ ppm: 1.91).

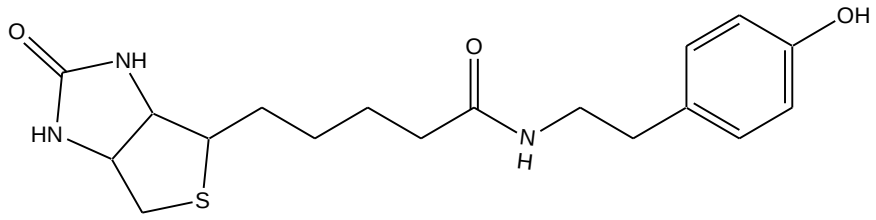

Figure 30. Structure of compound **BD9**.

5-(2-Oxo-hexahydro-thieno[3,4-d]imidazol-4-yl)-pentanoic acid[2-(4-hydroxy-phenyl)-ethyl]-amide (Biotin-Tyramine, **BD9**, Figure 30). A solution of tyramine (0.3 g, 2.1 mmol) and NEt_3 (0.3 mL, 1.8 mmol) was dissolved in DMSO (10 mL) and transferred dropwise to a solution containing biotin (0.5 g , 2.1 mmol), BOP (0.9 g, 2.1 mmol) and NEt_3 (0.3 mL, 1.8 mmol), also dissolved in DMSO (10 mL). The mixture was stirred for 24 hours at room temperature. The crude product was isolated by evaporation of the solvent under vacuum distillation, which was purified using column chromatography (silica gel, 4:1 CH_2Cl_2/ CH_3OH). The pure compound was obtained as a white light cream powder with a Rf: 0.43 and 40 % yield. ^{1}H NMR (500 MHz, DMSO): δ, 1.27, 1.45, 1.59 (m, 6H), 2.01 (t, 2H, *J* = 7.0 Hz), 2.54 (t, 2H, *J* = 6.5 Hz), 2.58, (d, 1H, *J* = 5.0 Hz), 2.82 (dd, 1H, *J* = 5.0 Hz, 12.5 Hz), 3.07 (m, 1H), 3.18 (dt, 2H, *J* = 7.0 Hz, 14.0 Hz),

4.12 (t, 1H, *J* = 5.0 Hz), 4.29 (t, 1H, *J* = 7.5 Hz), 6.35 (s, 1H), 6.42 (s, 1H), 6.65 (d, 2H, *J* = 8.0 Hz), 6.97 (d, 2H, *J* = 8.0 Hz), 7.79 (t, 2H, *J* = 5.5 Hz), 9.15 (s, 1H). ^{13}C NMR (125 MHz, DMSO): δ, 19.02, 25.76, 28.49, 28.64, 34.87, 35.67, 36.93, 40.88, 46.17, 55.89, 59.66, 61.49, 115.51, 129.90, 130.00, 156.04, 164.19, 172.32. Positive electrospray ionization HRMS(ESI+) calculated for $C_{18}H_{25}N_3O_3S$ ($[M+H]^+$) was 364.168. Negative electrospray ionization HRMS(ESI+) ($[M-H]^+$) found 364.169 (Δ ppm: 0.55).

Experimental Conditions for Protein and Tissue Modification

Photochemical Modification of Proteins

Solutions (total volume 100 μL) containing the indicated concentration of protein, sensitizer (naphthalimide), biotin-derivatives, and any other additives were prepared in microcentrifuge tubes (1.5 mL) and positioned in a room-temperature water bath to minimize heating of the sample. The light guide of the mercury lamp (filtered to 400-500 nm) was positioned approximately 5 mm above the top of the sample and the samples were irradiated at the reported energy for the indicated time period. The concentration of proteins was 0.235 mM (3.22 mg/mL for RNAse A), and final concentration of 0.5 mM of sensitizer and 0.025 mM of the biotin-derivatives were used for the majority of the experiments. The duration of sample irradiation was usually 5 minutes for RNAse and 30 minutes for lysozyme.

SDS-PAGE Analysis

Immediately after the completion of the experiment a 10 μL aliquot of the sample was added to a tube containing 10 μL of 2X reducing SDS-tris-HCl loading buffer. Samples were denaturated by heat for 3-5 minutes at approximately 100 ^{o}C followed by

centrifugation for 30 seconds, and 10 μL was loaded onto a 4-20% polyacrylamide gel. For the NuSep gels a 1X Tris-glycine-SDS running buffer was used while a 1X Tris-HEPES-SDS running buffer was used for the Thermo Scientific-Pierce gels. Electrophoresis was carried out at 150 V for 50 min (Tris-Glycine-SDS gels) and/or 25 minutes (Tris-HEPES-SDS). Gels were then stained with a coomassie blue G-250 solution for 1 hour and destained by washing several times with a solution of 5:10:85 glycerol/acetic acid/water.

1X Tris-glycine- SDS was prepared by dilution of a 10X Tris-Glycine-SDS buffer solution which was prepared by dissolving Tris-base (29 g , 0.23 mol), glycine (144 g, 1.9 mol) and sodium dodecyl sulfate (10 g), ultra pure (0.03 mol) into a 1L of water. In the same way, the 10X Tris-HEPES-SDS buffer solution was prepared by mixing in Tris-base (121 g, 0.99 mol), HEPES (238 g), Free acid (0.99 mol) and 10 g of sodium dodecyl sulfate, ultra pure (0.03 mol) into a 1L of water. Coomassie blue staining solution was prepared by dissolving coomassie blue G-250 (2 g, 2.3 mmol) in 250 mL of DI water, followed by the addition of 75 mL of glacial acetic acid, 500 mL of ethanol and an additional extra 175 mL of water was required to finish the 1L stain solution. Destain solution was simply prepared by mixing together 850 mL of DI water, 50 mL glycerol and 100 mL glacial acetic acid. Solution was well shaken before used.

Western Blotting Analysis

After the separation of proteins by SDS-PAGE, the stacking gel was cut and discarded and the right corner of the remaining gel cut in order to keep track of its orientation. The gel was then briefly rinsed in distilled water for 2-3 minutes and then equilibrated in Towbin buffer under gentle agitation during 5-10 minutes. Blot paper was

soaked in Towbin buffer, and the anode (bottom of electrode) and the cathode (top of electrode) of the apparatus was also wetted with the Towbin buffer. Two sheets of pre-wetted blot paper were placed on the anode, and a pasteur pipet was rolled over the top of the paper to remove any air bubbles (bubbles were removed in this fashion each time a new layer of paper, membrane or gel was added). After the first sheets of paper, a nitrocellulose blot membrane was added (marked with a pencil at the top left corner at the molecular weight marker position), followed by gel. Finally, two more sheets of pre-wetted blot paper were added (Figure 31).

All the excess of the Towbin buffer was carefully wiped off the anode to avoid leaving bridges of buffer between the two electrodes. Lastly, the cathode was placed carefully, avoiding moving the stack. This procedure took less than 15 minutes, in order to minimize the diffusion of the protein and loss of resolution.

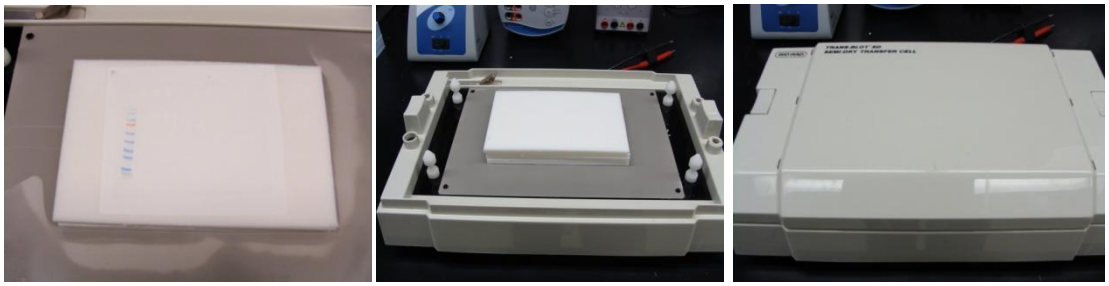

Figure 31. Western blotting apparatus.

The blotting unit was connected to a power supply set to 40V (560 mA) of current for 25 minutes. After that time, the membrane was removed from the transfer apparatus and was blocked by incubation in SuperBlock blocking buffer for 1 hour at room temperature with constant shaking. The membrane was then washed three times for 10 minutes each in wash buffer with agitation. The membrane was then incubated with the

appropriate HRP-conjugate dilution (ImmunoPure Avidin-Horseradish Peroxidase Conjugated) for 1 hour at room temperature with shaking and then washed using wash buffer.

Visualization of the membrane-bound HRP was achieved by preparing a working solution containing equal amounts of stablized peroxide solution and luminol/enhancer solution (typically 2 mL total volume; prepared freshly for each experiment). The working solution was added to the membrane which was shaken to assure all the membrane was covered, and then the membrane was placed in the Ultra Quant imager. The image of the membrane was acquired within seconds after placing the membrane in the imager.

Preparation of the Western Blotting Solutions

Towbin buffer. 3.03 g of Tris base (25 mM), 14.4 g of glycine (192 mM), 100 mL of methanol, and 1 g of sodium dodecyl sulfate (ultra pure) were dissolved in 900 mL of distilled water.

Dilution buffer. 1X TBS.

Wash buffer. 5 mL of 10% Tween-20 was added to 995 mL of 1X TBS.

Blocking reagent. 0.5 mL of 10% Tween-20 was added to 100 mL of SuperBlock blocking buffer. SuperBlock blocking buffer contains a proprietary protein in Tris buffered saline (pH 7.4) and an antimicrobial agent (Kathon). This blocking reagent is appropriate for avidin/biotin systems because it does not contain albumin or milk which contribute to avoid the variable amounts of endogenous biotin.

HRP- conjugated antibody. A stock solution of 1 mg/mL of ImmunoPure Avidin (Horseradish Peroxidase Conjugated) was prepared in dilution buffer. This solution was then diluted to prepare final concentration of 10-50 ng/mL HRP- Avidin in blocking buffer (for example 25 μL of the Avidin-HRP were diluted in 500 mL of SuperBlock blocking buffer to obtain a 50 ng/ mL solution).

Tissue Experiments

Two general approaches were used for the photochemical modification on tissue surfaces. The first approach employed for the tissue experiment consisted in the use of a 24- well plastic plate. Tissue samples (pericardium and meniscus) were cut and placed in the middle of each well, and a stock solution containing naphthalimide derivatives and biotinylated compounds were then added to the tissue surface by using a 10 μL pipettor (to volume of the solution added was 6 μL or less).The light source was positioned ~ 1 cm from the tissue surface which was then exposed for the reported time (Figure 32).

The second approach used a 96-well clear-bottomed white plastic plates with reaction wells filled with 100 μL of a reaction mixture (naphthalimide, biotinylated compounds and DI water). Empty spots were filled out with PBS buffer, and a piece of tissue (bovine pericardium or pig skin) was placed on top of the plate. A glass was then positioned on top of the tissue and fixed by clamps. The entire sandwich was then flipped over, exposing the tissue to the reagents. Tissues were exposed to light by alining the light source ~ 1 cm away from the appropriate positions on the clear bottom of the plate (Figure 33).

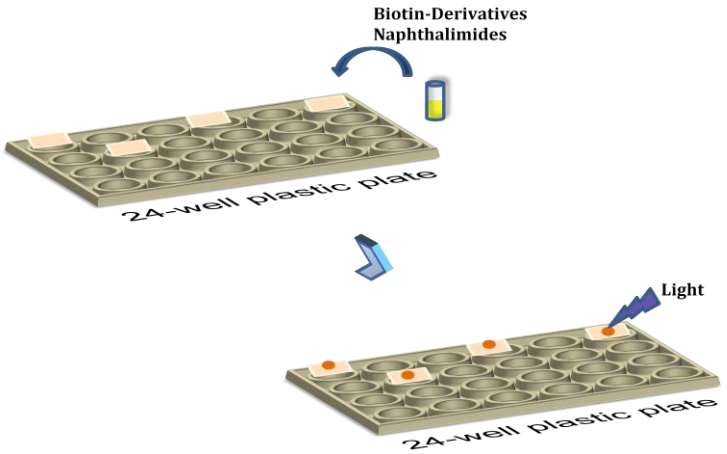

Figure 32. First approach used for the tissue modification experiments.

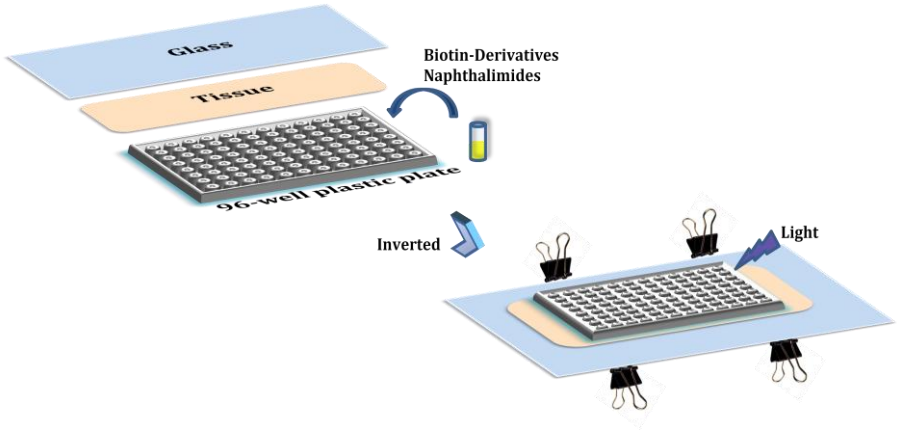

Figure 33. Second approach used for the tissue modification experiments.

Mass Spectral Analysis of Digested RNase A

RNase A samples were digested following the protocol reported by Pierce for use with their in-solution tryptic digestion and guanidination kit. After digestion the samples were subjested to various photochemical modification reactions with naphthalimide **NP8** in the presence of biotin derivatives following the procedure described previously for

protein modification. Immediately after the photochemical reactions the modified peptide samples were submitted for mass spectral analysis at the Baylor University mass spectrometry center.

CHAPTER THREE

Results and Discussion

Synthesis of Sensitizers

The known naphthalimide sensitizers **NP5-NP9** were synthesized by straightforward routes previously described in the literature.[65,73] Scheme 17 shows the synthetic route used for the preparation of the unsubstituted naphthalimide **NP5, NP6,** and **NP7** by the condensation of *N,N*-diethylethylenediamine with 1,8-naphthalene-anhydride using ethanol as solvent.

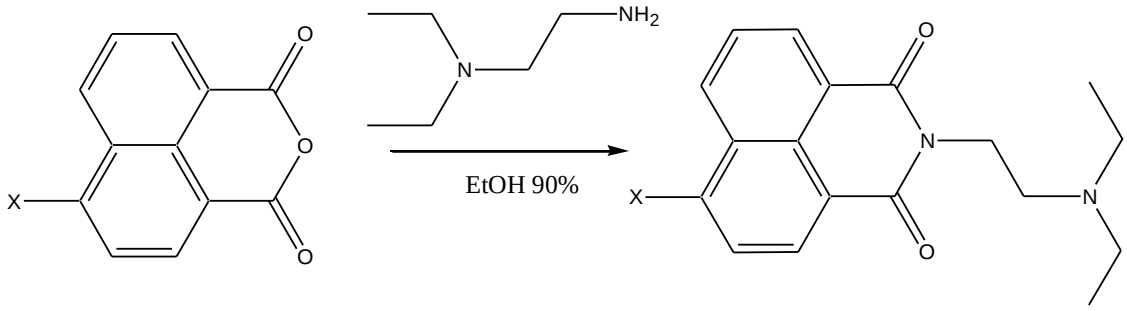

Scheme 17. Synthesis of **NP5** (X=H), **NP6**(X=Br), **NP7**(X=SCH_2CH_3). Average yield 65%

4-Substituted naphthalimide derivatives were synthesized using 4-bromo-1,8-naphthalic anhydride as starting material (Scheme 18-20). Nucleophilic aromatic substitutions before (Scheme 18; **NP7**) or after (Schemes 19 and 20; **NP8, NP9**) imide formation were used to attach the various C-4 substituents.

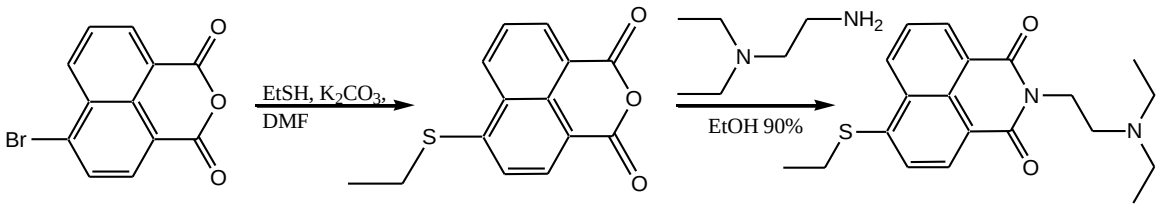

Scheme 18. Synthesis of **NP7**.

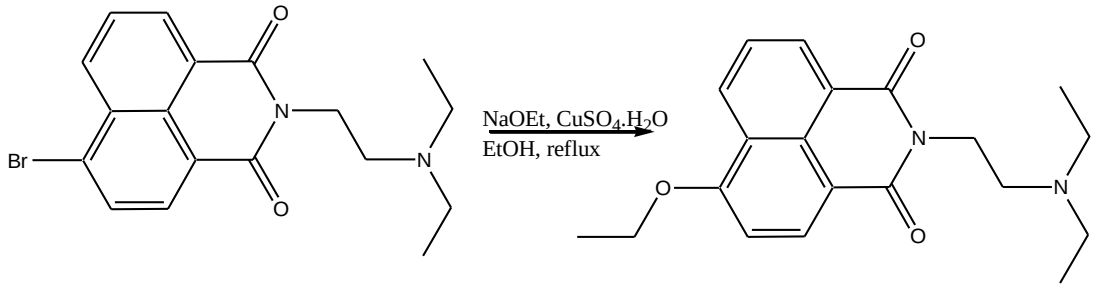

Scheme 19. Synthesis of **NP8**.

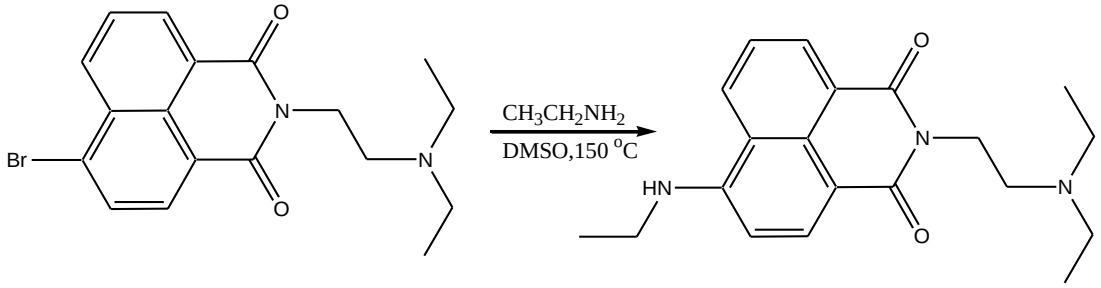

Scheme 20. Synthesis of **NP9**.

Selection of Proteins

It has been reported that the modification of proteins containing certain amino acids as tryptophan, tyramine, histidine and methionine react easier under photochemical conditions.[15] Four proteins were initially selected for testing based on the surface availability or accessibility of those amino acids: RNase A (13700 uma), Aprotinin (6512 uma), Myoglobin (16700 uma), and Lysozyme (14388 uma). Freshly made solutions of

each protein (0.235 mM) were prepared in PBS buffer and **NP5** (0.5 mM final concentration) was added to promote the photochemical crosslinking process. Each protein solution was then irradiated at 2000 mW of light intensity (Hg lamp) for 5 minutes. SDS-PAGE analysis (coomassie blue staining) was used to detect crosslinking of the protein solutions (Figure 34).

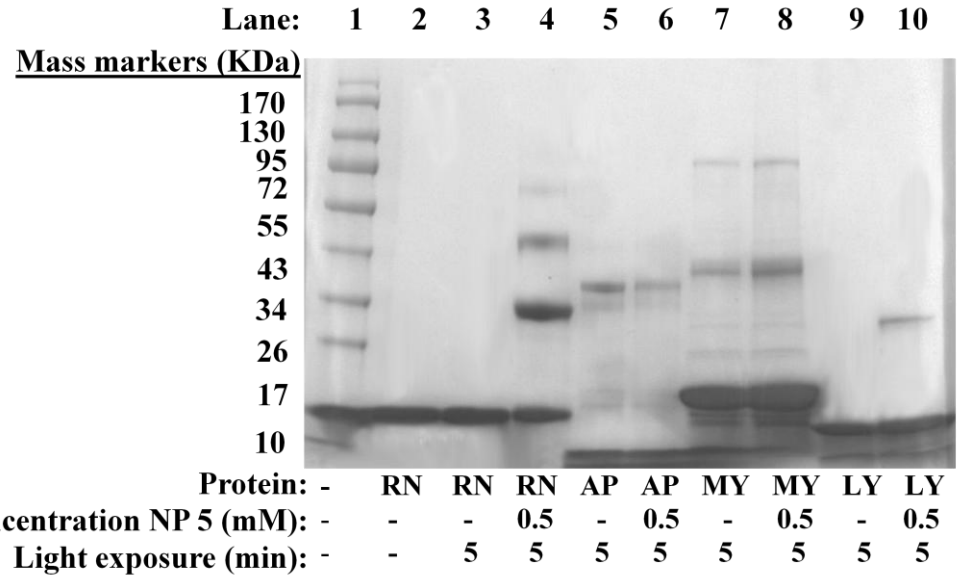

Figure 34. Coomassie blue SDS-PAGE of protein selection studies using RNase A (**RN**), Aprotinin (**AP**), Myoglobin (**MY**), Lysozyme (**LY**) (0.235 mM), **NP5** (0.5 mM), light exposure time: 5 minutes. Lanes 3,5,7,9 were used as protein control lanes in which the exposure of light was made in absence of the sensitizer.

Inspection of this gel reveals that only RNase A and Lysozyme (lanes 4,10) are crosslinked the most under the reaction conditions. Dimer, trimer and larger multimers were formed for RNase A while only a dimer band was formed with lysozyme. No significant change was observed between the control and the reaction lane for aprotinin and myoglobin. It was also clear from this experiment that photo-induced protein crosslinking only occurred when the sensitizer was present.

Modification of RNAse A and Lysozyme with Naphthalimide Derivatives

As an initial SAR study we investigated the relative ability of each of the naphthalimides to catalyze the crosslinking of both proteins. In this experiment we observed (by densitometry on SDS-PAGE gels) that **NP5** and **NP6** were most effective at inducing crosslinking, while **NP9** was the least effective (Figure 35, 36). This result was consistent with previous observations made in our group.[65]

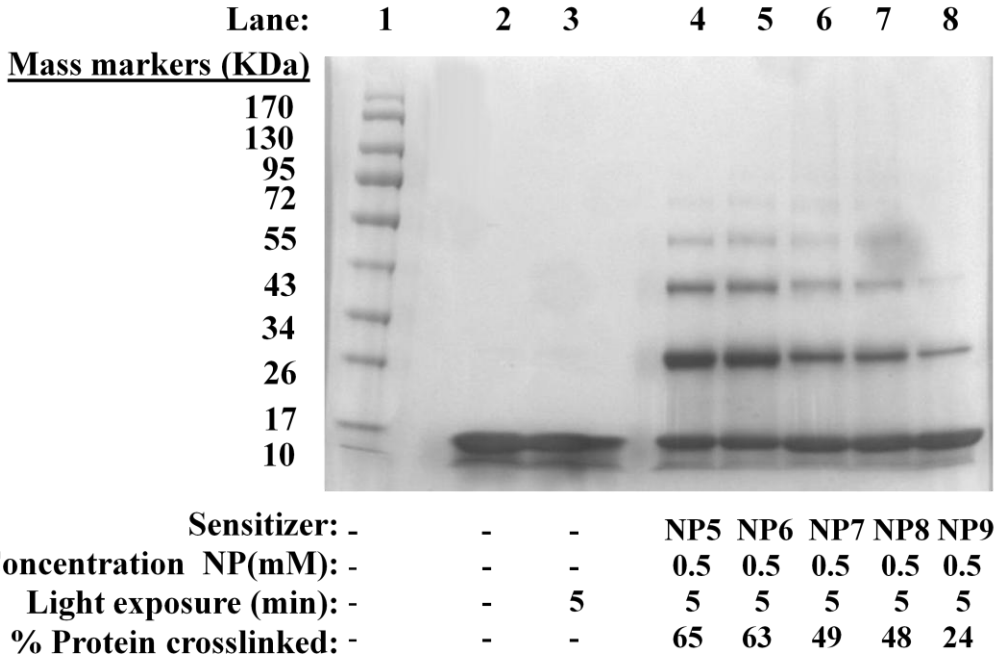

Figure 35. Coomassie blue SDS-PAGE of RNase A (0.235 mM), **NP(5-9)** (0.5 mM), light exposure: 5 minutes, and light intensity: 2000 mW Hg lamp.

The same tendency was observed when the analysis was carried out using an Agilent 2100 bioanalyzer to separate and quantify the crosslinked proteins. The analysis of the proteins was achieved using an Agilent Protein 230 kit that contains a protein chip able to analyze 10 samples per run.

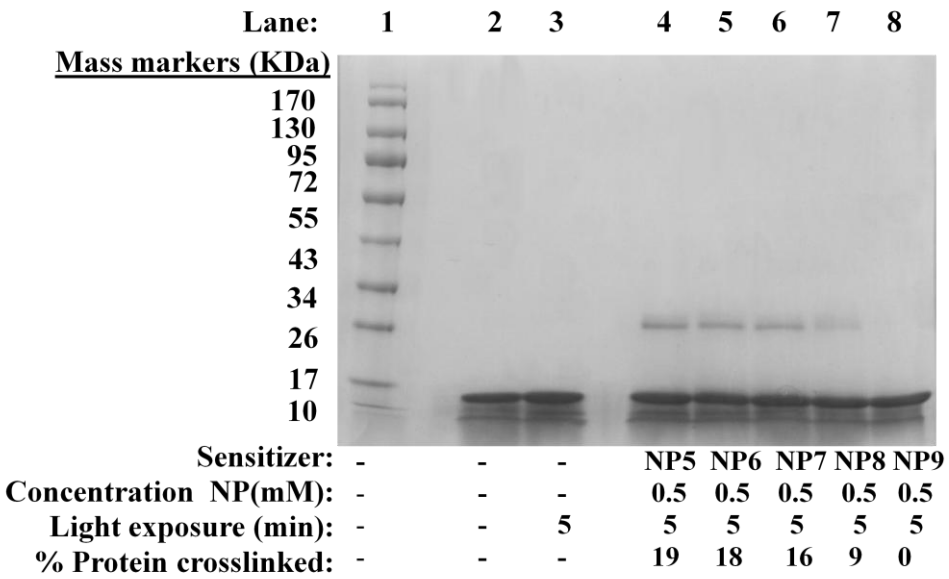

Figure 36. Coomassie blue SDS-PAGE of Lysozyme (0.235 mM), **NP(5-9)** (0.5 mM), light exposure: 5 minutes, and light intensity: 2000 mW Hg lamp.

Figure 37 shows the microchip employed during the experimental work, the experimental procedure can be found as a quick start guide in the protocol repoted by agilent by using http://www.chem.agilent.com/Library/usermanuals/Public/G2938-90008_HiSensProtein250_QSG.pdf). The results of the protein crosslinking experiment are shown in Figures 38 and 39.

Figure 37. Protein Chip provided with the Agilent 2100 bioanalyzer.

(a)

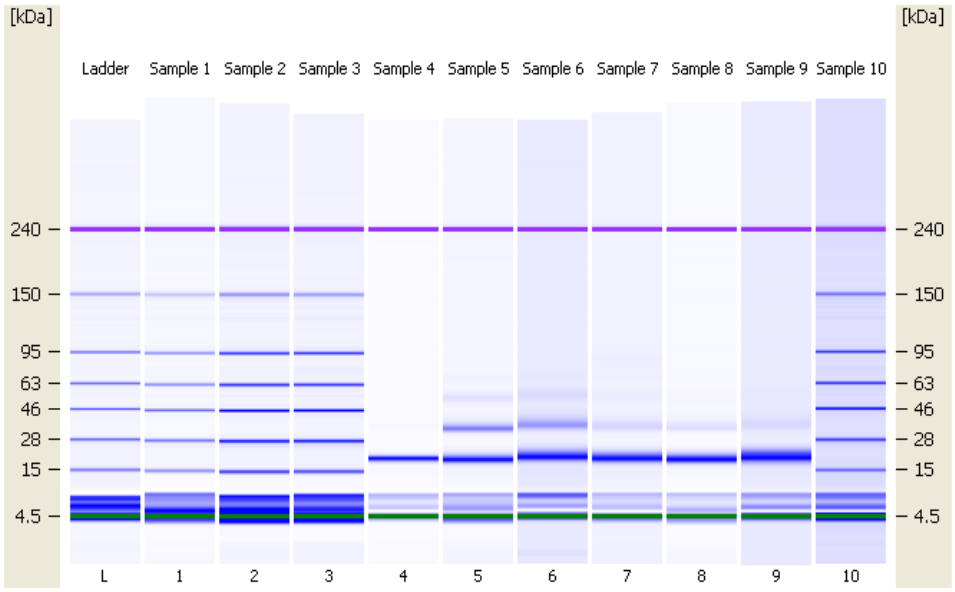

(b)

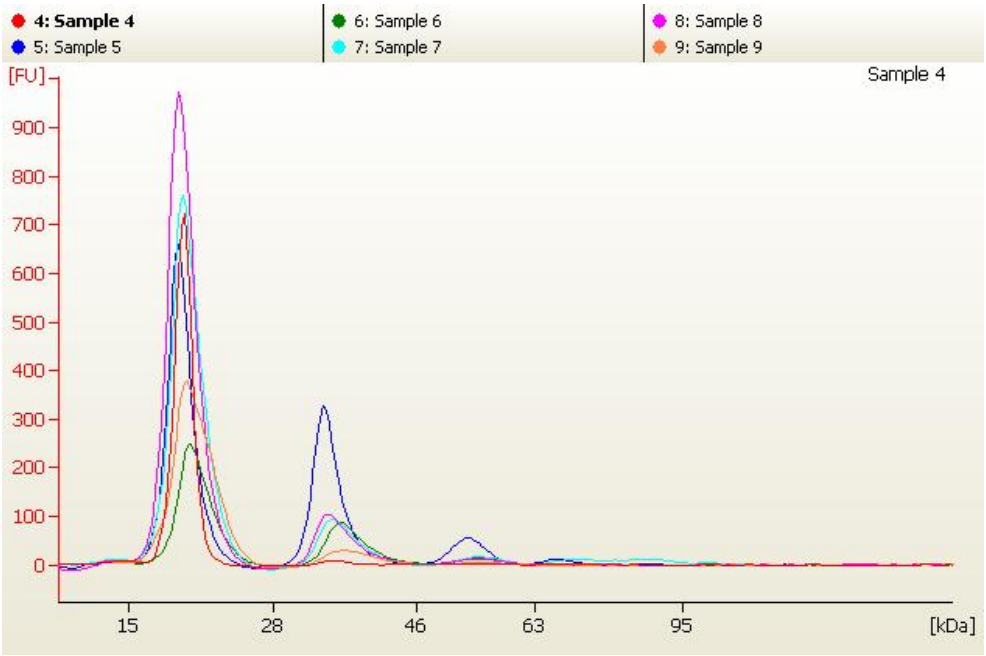

Figure 38. Analysis of RNase A (0.235 mM) crosslinking using Agilent 2100 bioanalyzer. Sample 4 is a control with no naphthalimide; Samples 5-9 include sensitizers **NP5-NP9** (0.5 mM), respectively; light exposure was 5 minutes at 2000 mW. (a) Gel-like representation (b) Electropherogram

(a)

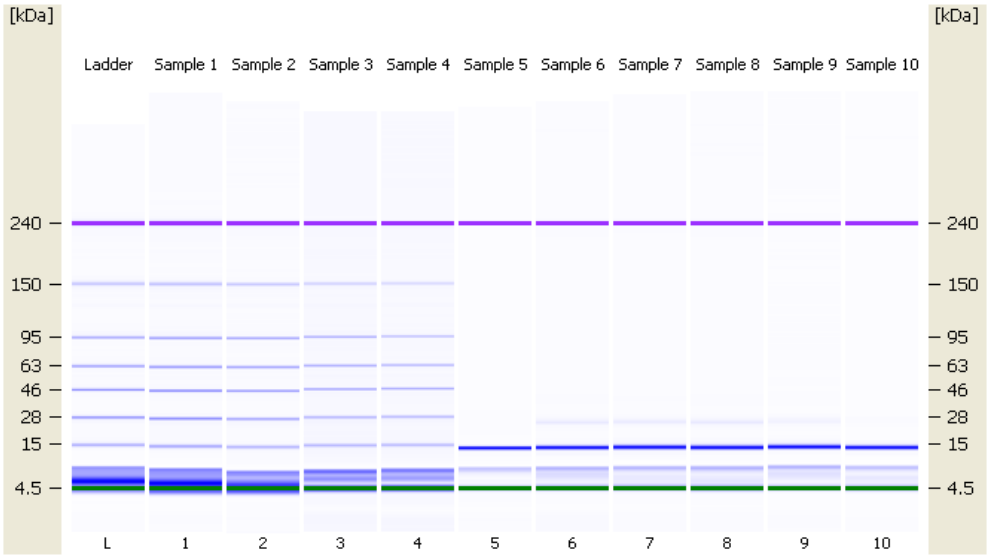

(b)

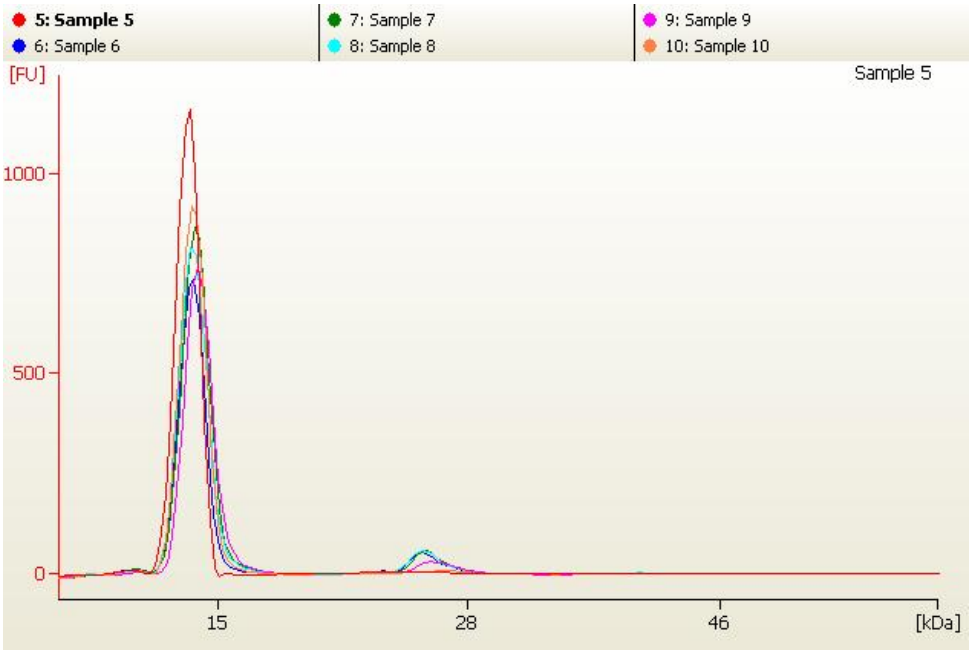

Figure 39. Analysis of Lysozyme (0.235 mM) crosslinking using Agilent 2100 bioanalyzer. Sample 4 is a control with no naphthalimide; Samples 5-9 include sensitizers **NP5**-**NP9** (0.5 mM), respectively; light exposure was 5 minutes at 2000 mW. (a) Gel-like representation (b) Electropherogram

Figure 40 shows data acquired using the two methods placed in juxtaposition, demonstrating that they follow a similar trend, except that the amount of protein crosslinking appears to be lower when analyzed using the protein chips.

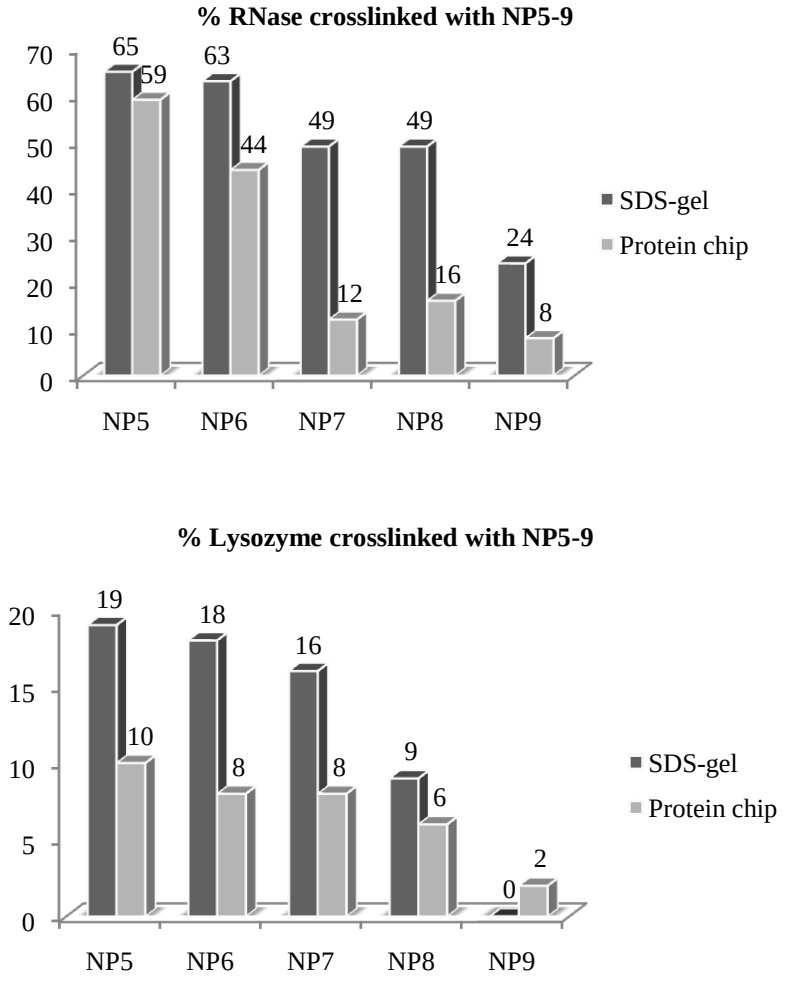

Figure 40. Comparative protein percentage crosslinked for RNase A and Lysozyme when SDS-gel and protein chips were used.

Optimization of Lysozyme Crosslinking

Since the modification reaction seems to be much less effective when crosslinking lysozyme, the reaction conditions were studied in order to optimize the crosslinking of

this protein. Fosusing on one naphthalimide photosensitizer, **NP5**, the consequences of changing the reaction conditions concentration of protein, concentration of sensitizer, and exposure time. Analysis of the coomassie-stained gel from this experiment revealed that the percentage of crosslinked lysozyme can be increased to levels similar to that obtained for RNAse A if the exposure time is increased from 5 to 30 minutes (Figure 41).

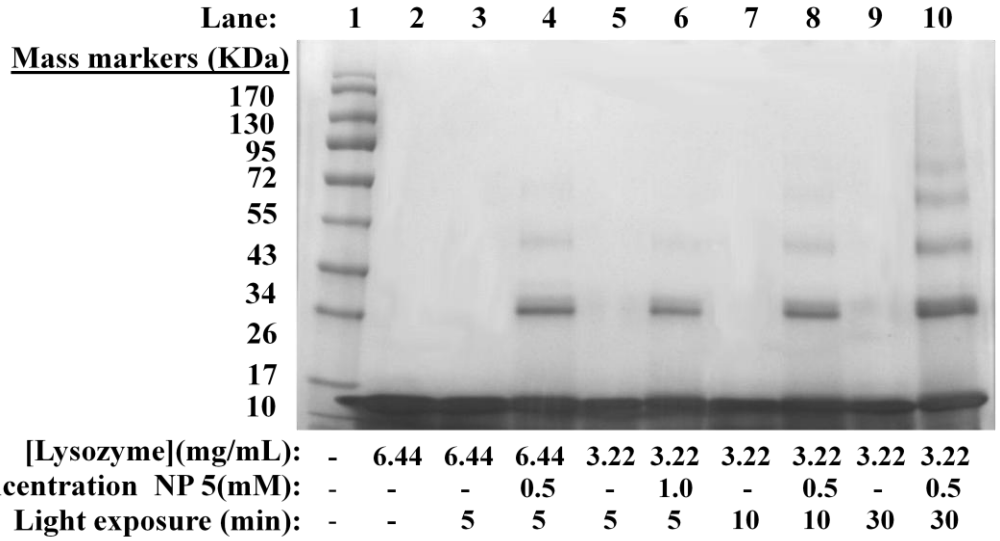

Figure 41. Coomassie blue SDS-PAGE of the reaction of Lysozyme (6.44 mg/mL = 0.448 mM and 3.22 mg/mL = 0.235 mM) with **NP5** (1.0 mM and 0.5 mM), with variying light exposure (5, 10, 30 min at 2000 mW Hg lamp).

Using this extended irradiation time a comparative study of the crosslinking of lysozyme with each of the sensitizers was performed and the resulting gel is shown in Figure 42. Under these conditions lysozyme crosslinking was greatest when **NP7** (thioether-substituted naphathalimide) was employed as the sensitizer, exhibiting a different trend than had been observed for RNase A (Figure 43).

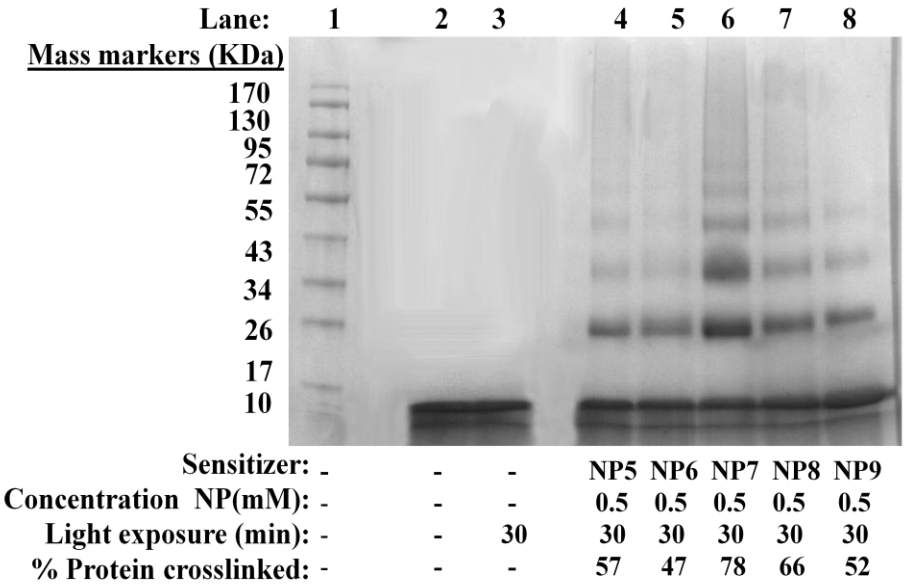

Figure 42. Coomassie blue SDS-PAGE of crosslinking of Lysozyme (0.235 mM) with naphthalimide derivatives **NP(5-9)** (0.5 mM), light exposure: 30 minutes and light intensity: 2000 mW Hg lamp.

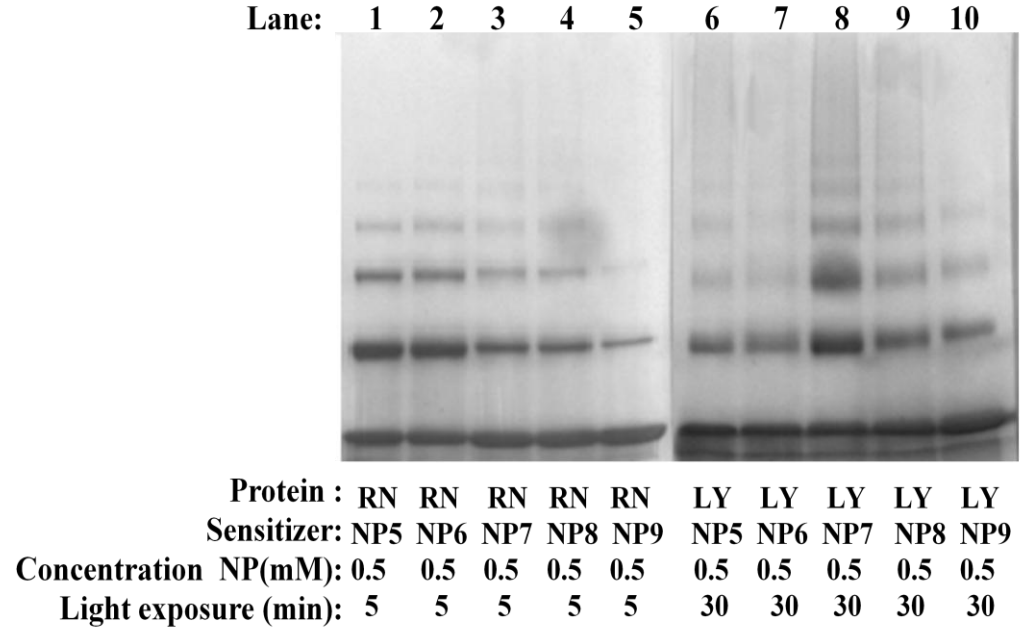

Figure 43. Comparison of crosslinking trends for RNase A and Lysozyme with naphthalimide derivatives.

Effect of Free Amino Acids on Protein Crosslinking

In order to clarify the mechanism(s) responsible for naphthalimide-sensitized photochemical protein crosslinking we chose to examine the participation of specific amino acid residues. Accordingly, exogenous small molecules were added to the protein crosslinking reactions and the effects examined. It was expected that the results would be complicated by the diversity of reactions photoactive naphthalimides exhibit towards biological systems. As previously noted, both Type I and Type II mechanisms are possible; the Type I mechanism involves an excited state of the sensitizer that extracts an electron or a hydrogen atom from a ground state molecule, while in the Type II mechanism the electronic excitation energy is transferred from the excited triplet of the sensitizer to a triplet molecular oxygen, resulting in the return of the sensitizer to its ground state and the production of singlet oxygen.

Amino acids such as tyrosine, tryptophan and histidine have been implicated as key residues in the oxidative crosslinking of proteins[15], and so the study of these amino acids was obviously of interest. However initially it was examined the effect of added dopamine to the photosensitized crosslinking reaction since it is known to be very susceptible to oxidation and includes the functional group primarily responsible for the adhesive properties in proteins adhesives called mussel adhesive proteins (MAPs). As a critical component of MAPs, the DOPA catechol derived from tyrosine participates in intermolecular crosslinking reactions that lead to the formation of a solid adhesive plaque which is responsible for the attachment of mussels to a variety of substrates such as mineral, metal surfaces and wood (Figure 44).[77, 78]

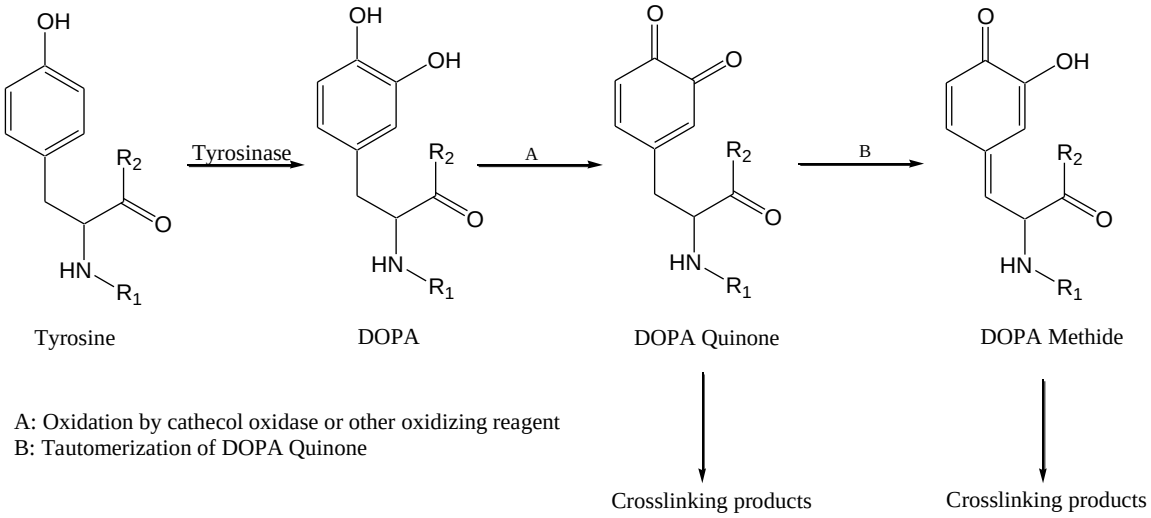

Figure 44. Oxidative reactions and possible crosslinking pathways of tyrosine and DOPA in mussel adhesive proteins.

Accordingly, the naphthalimide-sensitized photochemical crosslinking of RNase A was carried out using **NP5** in presence of five different concentrations of dopamine (0.05 to 1 mM) (Figure 45). Separation by PAGE with coomassie staining revealed that the crosslinking of RNase A was inhibited upon the addition of dopamine and that inhibition was concentration dependent. The photosensitized crosslinking of lysozyme by two naphthalimides (**NP5** and **NP7**) was similarly inhibited by dopamine in a dose-dependent fashion (Figure 46). Potential inhibition mechanisms include excited-state quenching of the sensitizer by the dopamine,[79] the reaction of reactive amino acids on the protein with activated dopamine residues (rather than other protein residues), and the reaction of activated protein with dopamine (rather than additional proteins).

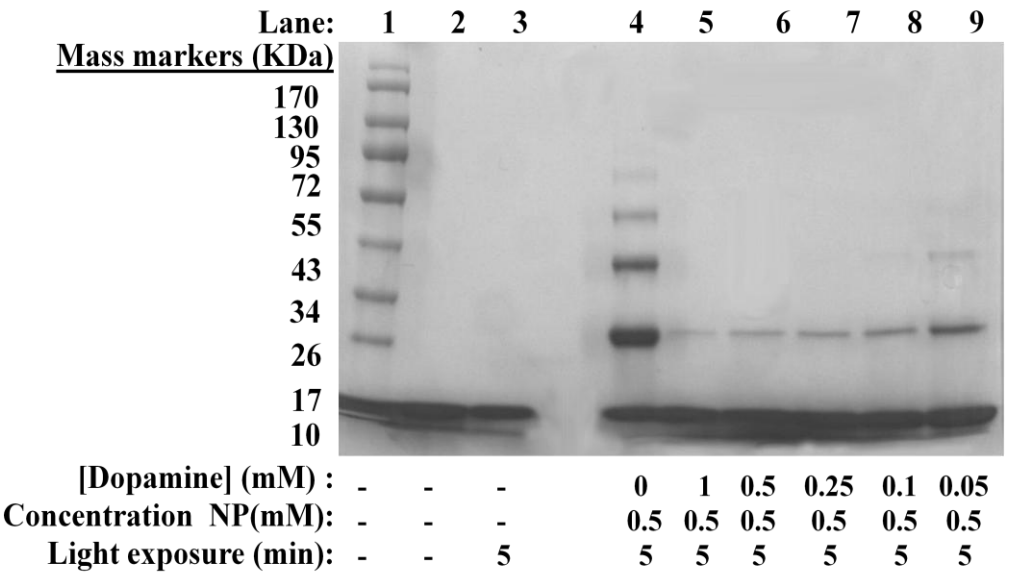

Figure 45. Inhibition of RNase A crosslinking by dopamine. 0.235 mM RNase A; 0.5 mM **NP5**; 0, 0.05, 0.1, 0.25, 0.5, or 1 mM dopamine; 5 min irradiation at 2000 mW.

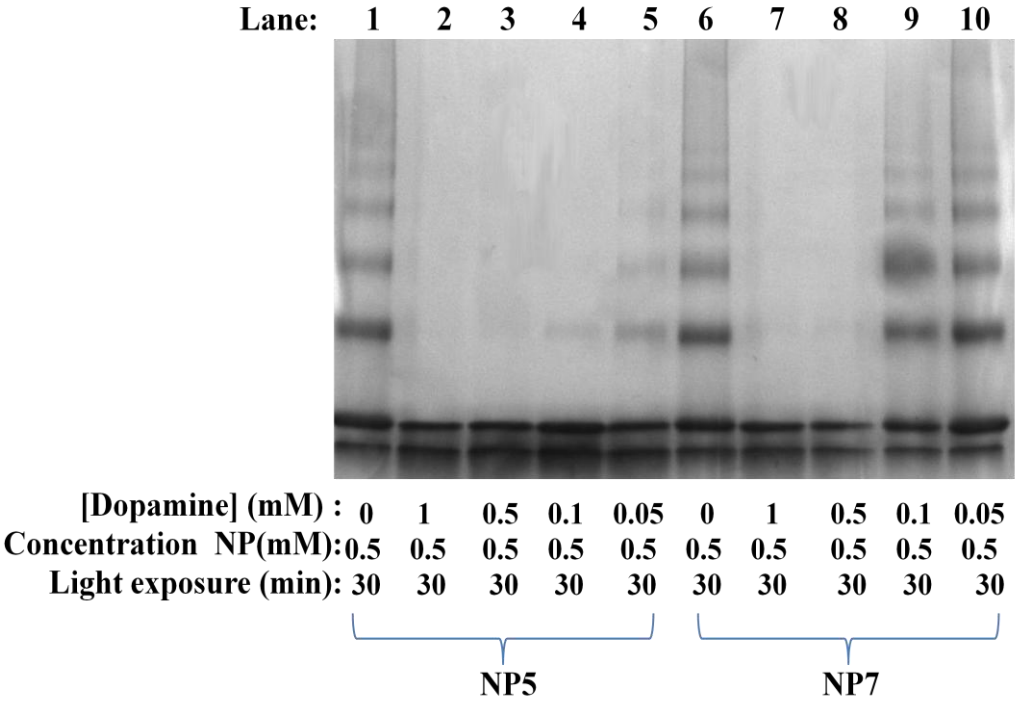

Figure 46. Inhibition of lysozyme crosslinking by dopamine. 0.235 mM lysozyme; 0.5 mM **NP5** or **NP7**; 0, 0.05, 0.1, 0.5, or 1 mM dopamine; 5 min. irradiation at 2000 mW.

RNase A and Lysozyme Inhibition Studies with Amino Acids

In view of the effect of dopamine on naphthalimide-sensitized protein crosslinking a series of experiments using different amino acids (lysine, tryptophan, histidine, tyramine and methionine; Figure 47) was carried out using each of the naphthalimide derivatives and both RNase A and lysozyme. The gels from lysine and histidine inhibition are shown in Figure 48 and 49.

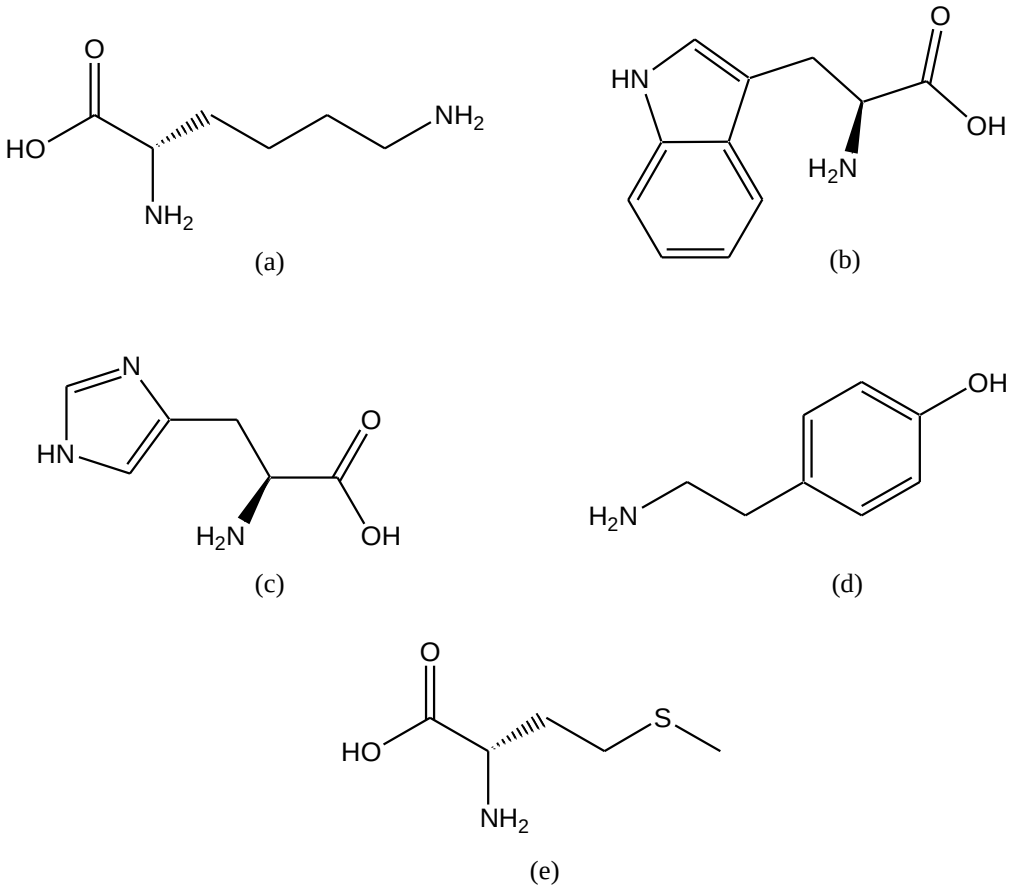

Figure 47. Structure of (a) lysine, (b) tryptophan, (c) histidine, (d) tyramine and (e) methionine

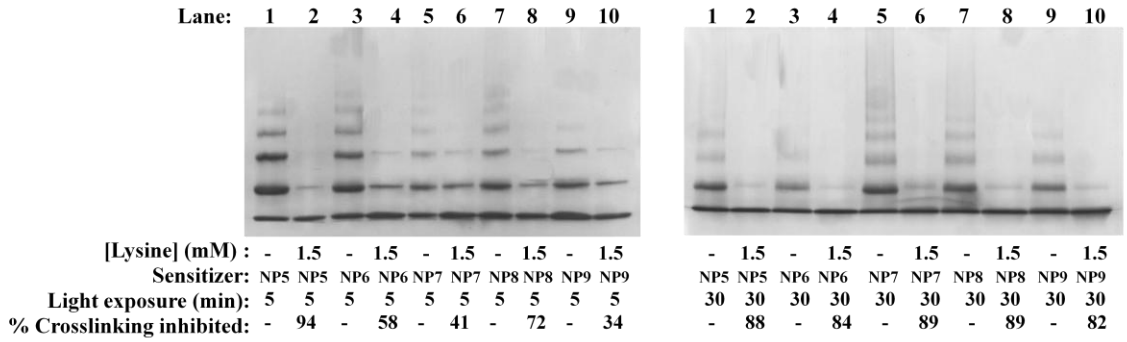

(a) (b)

Figure 48. Crosslinking inhibition studies (a) RNase A (0.235 mM) and (b) lysozyme (0.235 mM); **NP(5-9)** (0.5 mM); lysine (1.5 mM). Photolysis was 5 min for RNase A and 30 min for Lysozyme at 2000 mW.

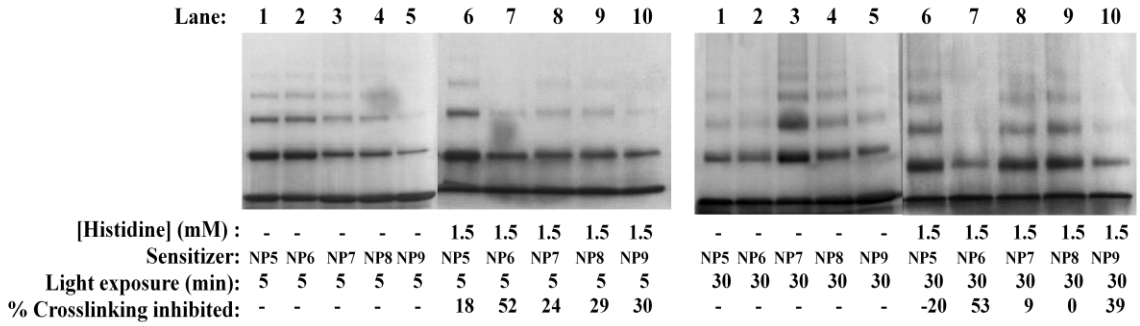

(a) (b)

Figure 49. Crosslinking inhibition studies (a) RNase A (0.235 mM) and (b) lysozyme (0.235 mM); **NP(5-9)** (0.5 mM); histidine (1.5 mM). Photolysis was 5 min for RNase A and 30 min for Lysozyme at 2000 mW.

The decrease in crosslinking compared to controls (lanes 1, 3, 5, 7, and 9 are controls; lanes 2, 4, 6, 8, and 10 include lysine) is clear, with lysozyme consistently exhibiting the greatest inhibition by lysine. On the other hand, histidine gives widely varying results but seems to be generally the poorest inhibitor (and in some combinations stimulates crosslinking). Similar experiments were performed with other amino acids that could potentially be implicated in the photochemical protein crosslinking reaction. The

results of these experiments are tabulated below in Table 3 and Table 4. Inspection of this data suggests that in general **NP7** is the most difficult activator to inhibit.

Table 3. Inhibition of RNase A crosslinking by free amino acids and derivatives

Protein (RNase A)	% Inhibition				
	NP5	NP6	NP7	NP8	NP9
Lysine	94	58	41	72	34
Tryptophan	84	85	59	79	80
Histidine	18	52	24	29	30
Tyramine	84	80	31	45	38
Methionine	79	45	20	31	8

Table 4. Inhibition of lysozyme crosslinking by free amino acids and derivatives

Protein (Lysozyme)	% Inhibition				
	NP5	NP6	NP7	NP8	NP9
Lysine	88	84	89	89	82
Tryptophan	82	76	63	75	98
Histidine	-20	53	9	0	39
Tyramine	88	100	80	84	66
Methionine	98	95	92	88	89

Synthesis of Biotin Labeled Derivatives

After observing the ability of certain amino acid residues to influence photosensitized protein crosslinking we decided to evaluate the incorporation of amino acid functional groups into the proteins. In these experiments (D)-biotin was used as a

marker, since biotin incorporation into proteins can be readily detected using western blotting procedures and the biotin-binding proteins avidin or streptavidin. Biotin labeled derivatives (**BD1-BD9**; Figure 50) were synthesized using BOP-mediated coupling reactions between biotin and the corresponding functionalized amines. For some amino acids the methyl ester derivatives were used in order to protect the carboxylic acids during the coupling reactions, and for these compounds an acidic hydrolysis was used to hydrolyze the esters. Biotin-LC-Hydrazide (**BD1**) was obtained from a commercial source (Pierce) while the rest of the compounds were synthesized in the laboratory. Biotin-dopamine (**BD2**), biotin-tryptophan (**BD4**) and biotin-methionine (**BD6**) have been previously reported,[74-76] and the synthetic routes employed were modified to improve yield and purity of the compounds.

Scheme 21 shows the general procedure for the synthesis of these compounds. The synthetic route involves the activation of the carboxylic acid present in biotin using the BOP reagent, followed by the addition of various amines. The methyl-ester protected compounds (biotin-tryptophan methyl ester (**BD4**) and biotin-hydroxyproline methyl ester (**BD7**)) were hydrolyzed using an acidic solution to afford the carboxylic acid moiety. The final compounds were carefully purified and characterized.

Stability Studies of Biotin Side Amino Acid Chain Compounds

Biotin is a relatively stable compound under physiological conditions but it reacts with oxidants including oxidized unsaturated fatty acids. Partial protection by vitamin E suggests that this reactivity is due to free radical attack on biotin, most likely on the sulfur atom.

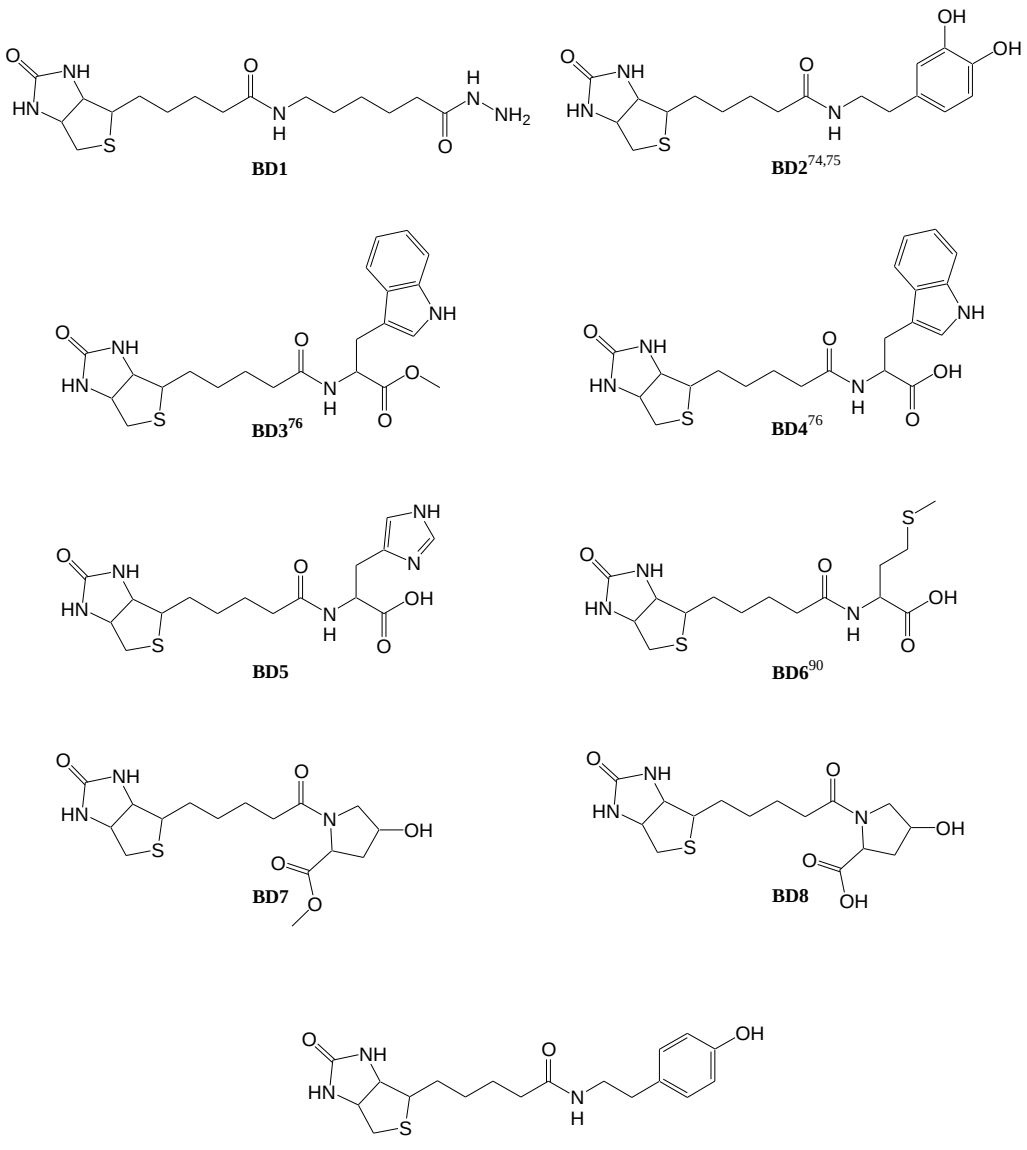

Figure 50. Biotin labeled derivatives (**BD1-BD9**)

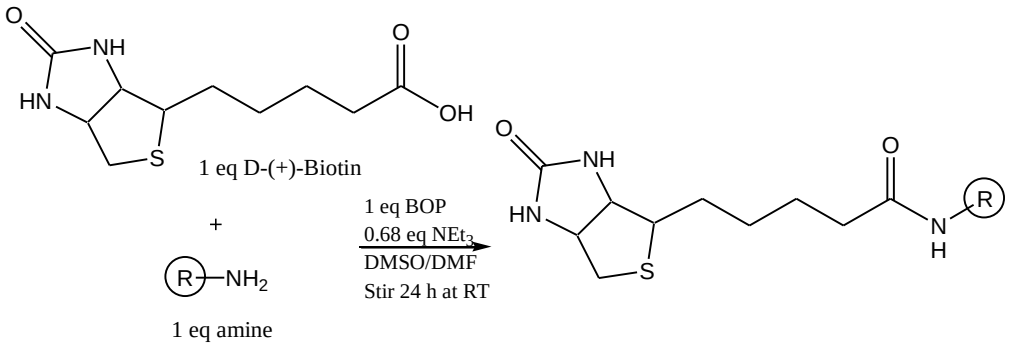

Scheme 21. Synthetic procedure of **BD(2-9)**

Potential S-oxidation products of biotin include the sulfoxide and the sulfone. To ensure that biotin degradation will not greatly reduce our ability to detect the incorporation of biotinylated amino acids into the protein, water-suppressed ^{1}H NMR analysis was used to examine samples of biotin photolysed with each of the sensitizers **(NP5-NP9)** along with the appropriate controls. Since the most susceptible site of biotin is the sulfur atom, we examined the 1H-NMR signals of protons adjacent to the sulfur atom (H_a, H_b, H_c, H_d, H_e; Figure 51) before and after light irradiation. When the control samples (biotin + sensitizer) were compared with the reaction samples (biotin + sensitizer + 5 min hv), the survival of the majority of the biotin was observed (Figure 52) especially the signals for protons Ha and Hb. However, a minor component of oxidized products of biotin were detected after light irradiation, which was evident by the formation of new signals for H_c, H_d, and H_e. This was most evident with **NP6** (Figure 53) and **NP7**, where the intensity of H_c slightly decreased and new signals for H_c, H_d and H_d can also be observed as a result of the formation of oxidized products.

Accordingly, the chemical shifts of H_d, H_e and H_c from δ 1.50, 1.62 and 3.23 ppm to 1.15, 1.29 and 3.05 ppm respectively are the result of the formation of sulfur oxide (sulfoxide) product of the oxidized biotin based on the chemical shift from the ^{1}HNMR result reported by previous members of our group[80] in the oxidation of biotin when reacted with sodium periodate ($NaIO_4$) and hydrogen peroxide (H_2O_2).

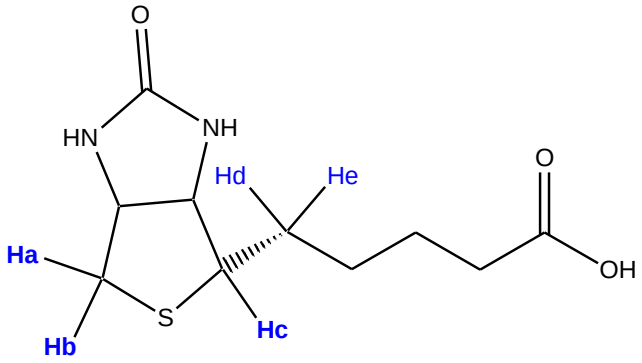

Figure 51. Structure of D-(+)-Biotin

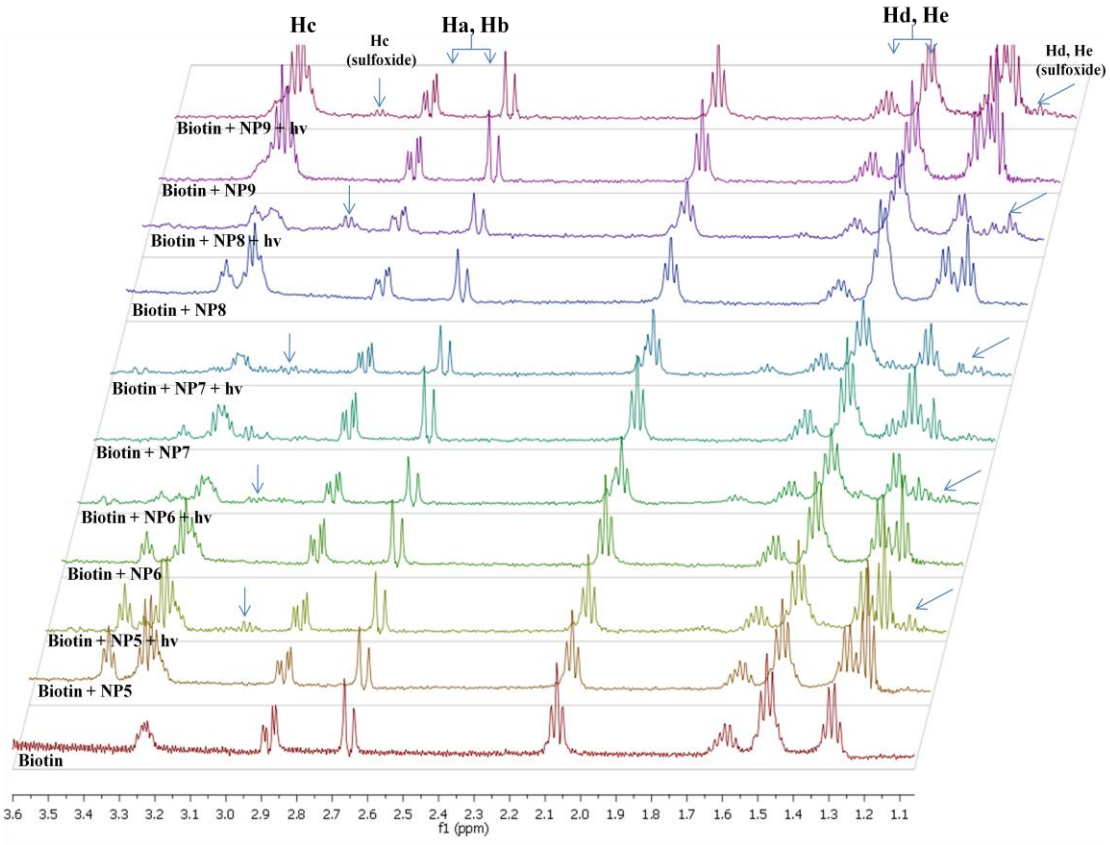

Figure 52. Analysis of biotin stability by ^{1}HNMR . 1 mM Biotin and 0.5 mM sensitizers (**NP5-NP9**) were dissolved in PBS containing 10% D_2O and exposed to 0 or 5 min of light irradiation using Hg lamp (2000 mW).

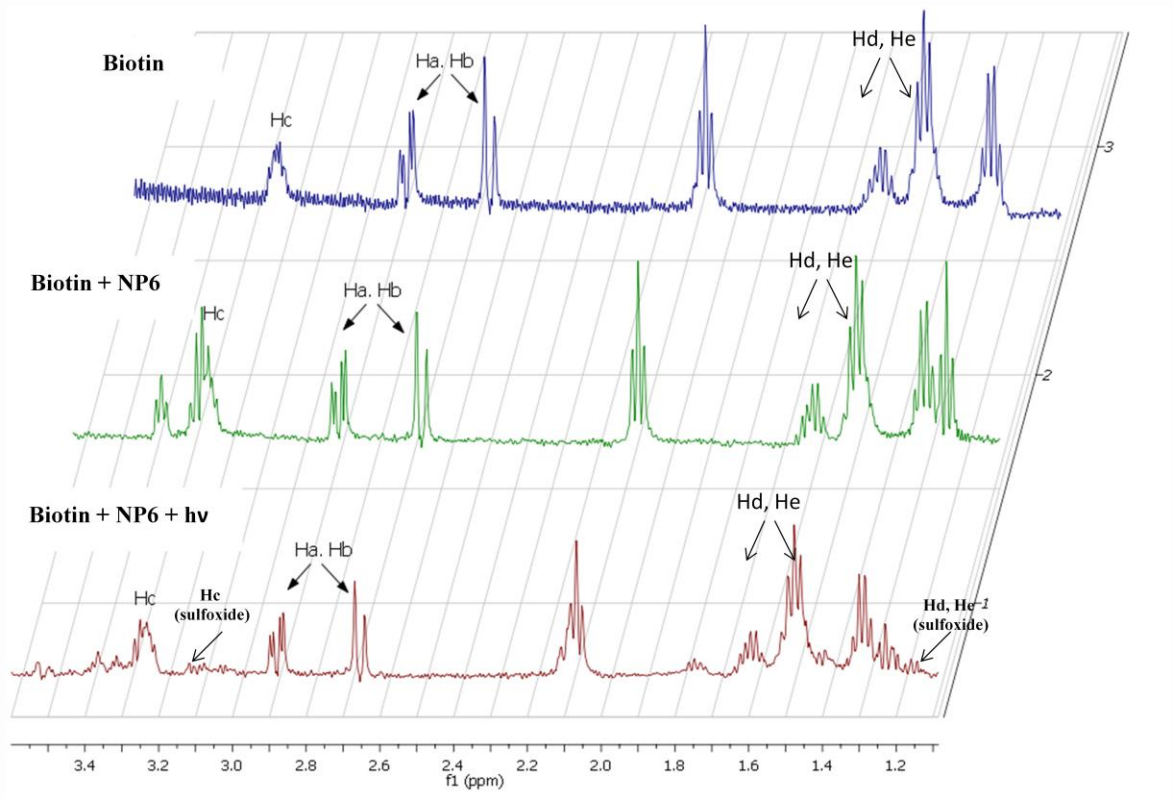

Figure 53. Analysis of biotin stability by ^{1}HNMR . 1 mM Biotin and 0.5 mM sensitizer **NP6** were dissolved in PBS containing 10% D_2O and exposed to 0 or 5 min of light irradiation using Hg lamp (2000 mW). **(1)** Biotin + **NP6** + 5 min hν, **(2)** Biotin + **NP6** + 0 min hν, **(3)** Biotin + 5 min hν.

Incorporation of Biotin Labeled Derivatives into Proteins

In the next set of experiments RNase A and lysozyme were photochemically modified in the presence of seven biotin derivatives – **BD1**, **BD2**, **BD4**, **BD5**, **BD6**, **BD8**, and **BD9** – in order to test the propensity of the various functional groups to get incorporated into the proteins (Scheme 22).

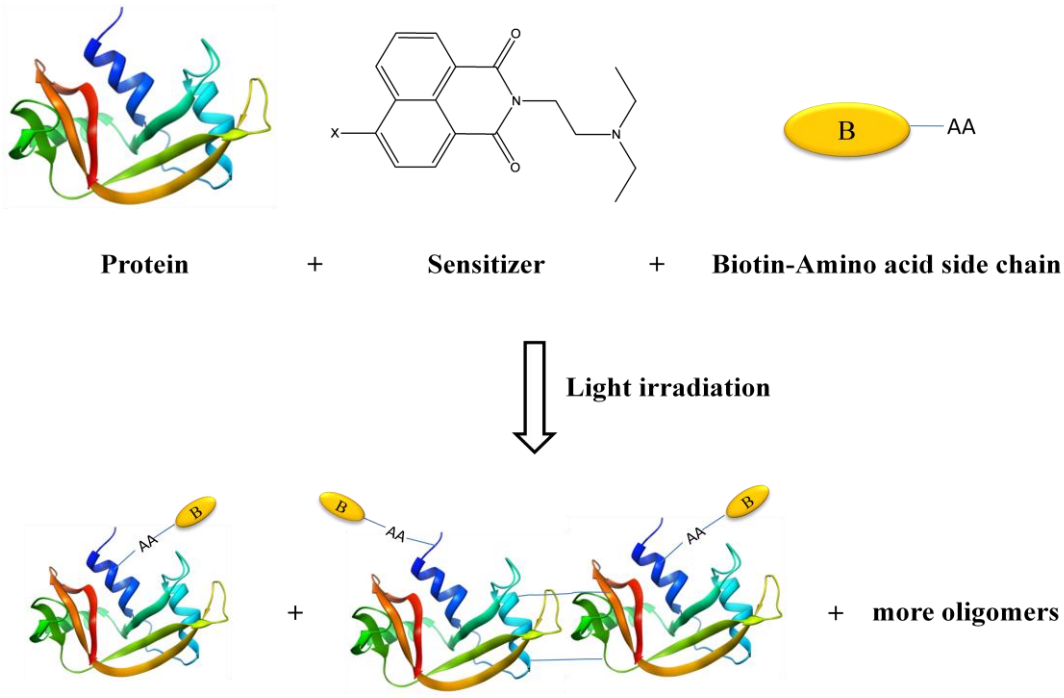

Scheme 22. Involvement of biotinylated compounds in photosensitized reaction.

In these experiments the biotin labeled derivatives are incorporated into the selected proteins and detected by Western-blot analysis of the reaction mixtures. The extent of the biotin incorporation was dependent on the time of irradiation (Figure 54), the concentration of the biotinylated compounds (Figure 55), the functional group attached to the biotin (Figure 56), and the type of sensitizer used (Figures 57 and 58). In general increased incorporation was observed as the time of light irradiation or the concentration of the biotinylated compounds was increased. In addition, these preliminary experiments revealed that in general biotin-tyramine **BD9** is incorporated more effectively into RNase A compared to biotin-dopamine **BD2**, and that **NP7** was most effective at incorporating **BD2** into RNase A while both **NP5** and **NP7** were effective sensitizers for the incorporation of **BD9**.

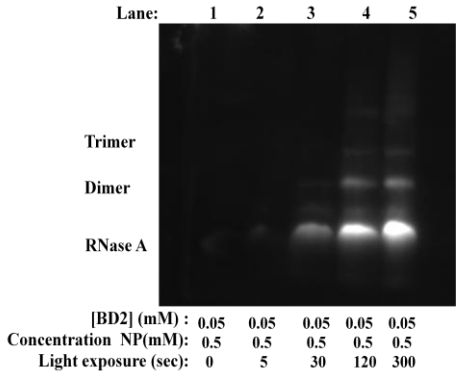

Figure 54. Dependence of biotin- dopamine (**BD2**) incorporation on time of light irradiation. [RNase A]: 0.235 mM, [**NP5**]: 0.5 mM, [**BD2**]: 0.05 mM.

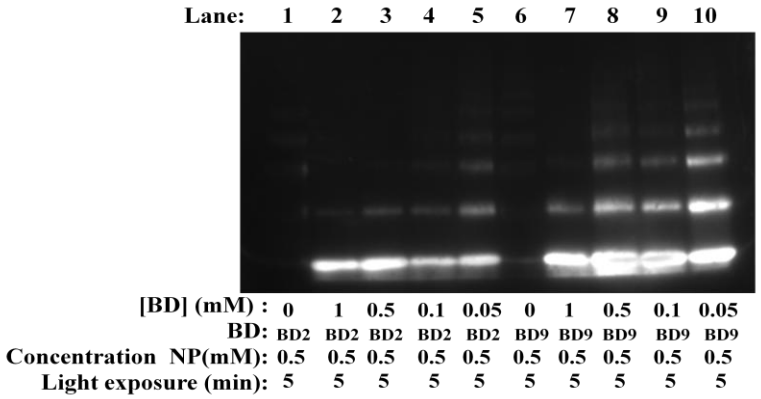

Figure 55. Incorporation of biotin-dopamine (**BD2**) or biotin-tyramine (**BD9**) in RNase A at various concentrations with **NP5** as sensitizer. [RNase A]: 0.235 mM.

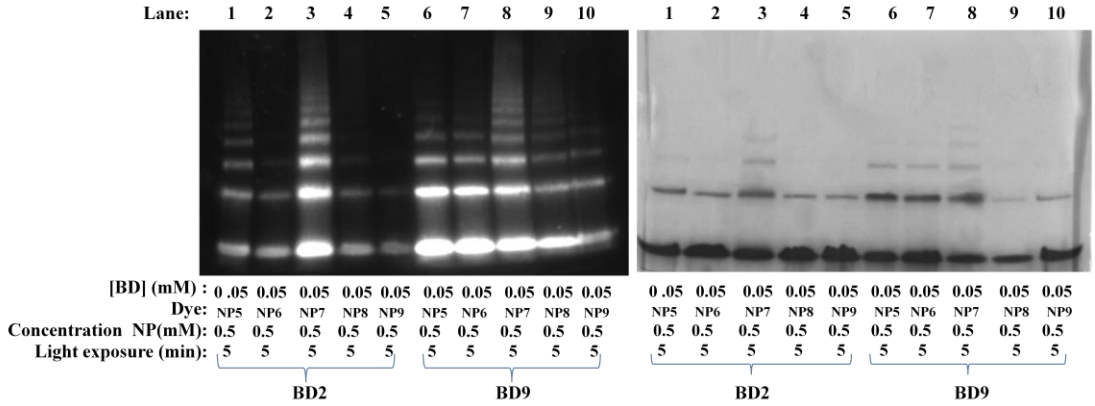

(a) (b)

Figure 56. Dependence of biotin- amino acid side chains incorporation on type of sensitizer. [RNase A]: 0.235 mM, [**NP(5-9)**]: 0.5 mM, [**BD2**],[**BD9**]: 0.05 mM, 5 min light irradiation. (a) Western blot gel, (b) Coomassie blue gel.

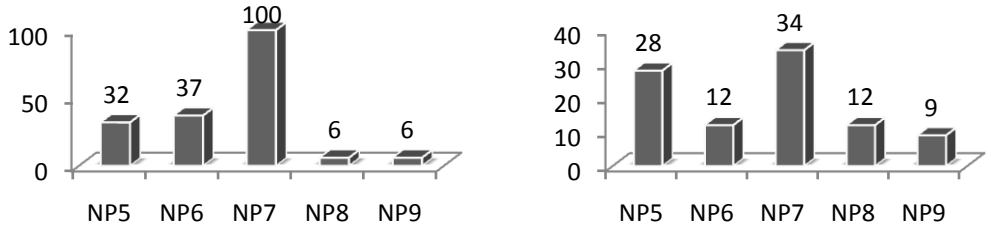

(a) (b)

Figure 57. Dependence of biotin-dopamine incorporation on type of sensitizer. (a) Normalized % **BD2** incorporated into RNase A, (b) % RNase A crosslinked in the presence of biotin-dopamine **BD2**. Calculation of the amount incorporated was normalized based on the maximum value obtained in each experiment.

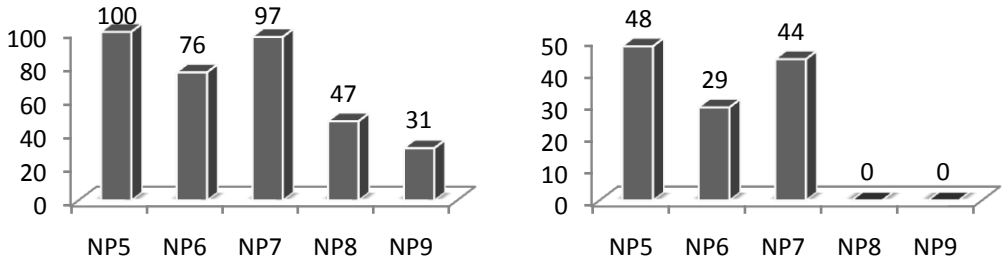

(a) (b)

Figure 58. Dependence of biotin- tyramine incorporation on type of sensitizer. (a) Normalized % of **BD9** incorporated into RNase A; (b) % RNase A crosslinked in the presence of **BD9**.

To determine potential of these biotinylated compounds to be incorporated into the proteins upon photochemical sensitization western blot experiments were performed using each of the sensitizers. As might be expected from the crosslinking experiments, these compounds were generally more effectively incorporated into RNase A (Figure 59a) than into lysozyme (Figure 59b). The hydrazide functionality was universally the most readily incorporated, with the tyramine, dopamine and histidine derivatives incorporated in significant amounts, along with a minor amount of incorporation of the tryptophan derivative. Neither the methionine derivative nor the hydroxyproline derivitive (hydroxyproline was tested as it is found in high concentrations in collagen) were incorporated at all into the proteins under these conditions. One somewhat suprising

observation is that **NP5**, which is the best photosensitizer for RNase crosslinking, was generally the least effective sensitizer for incorporating these biotinylated amino acids.

(a)

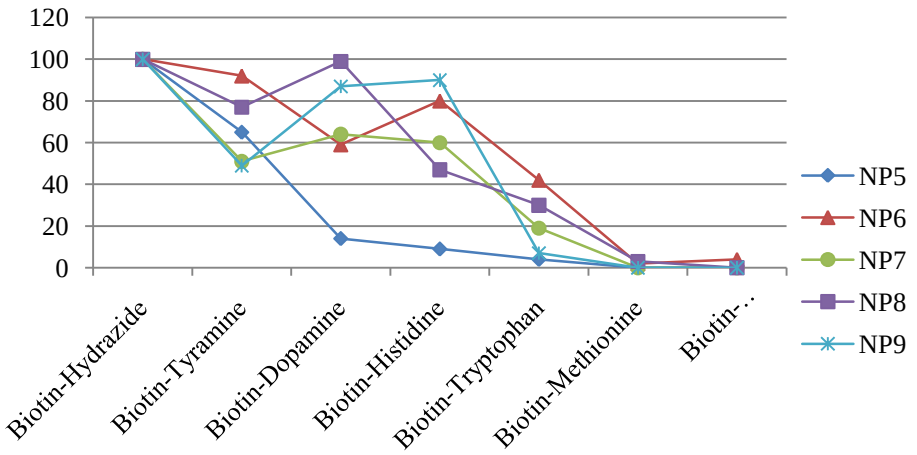

(b)

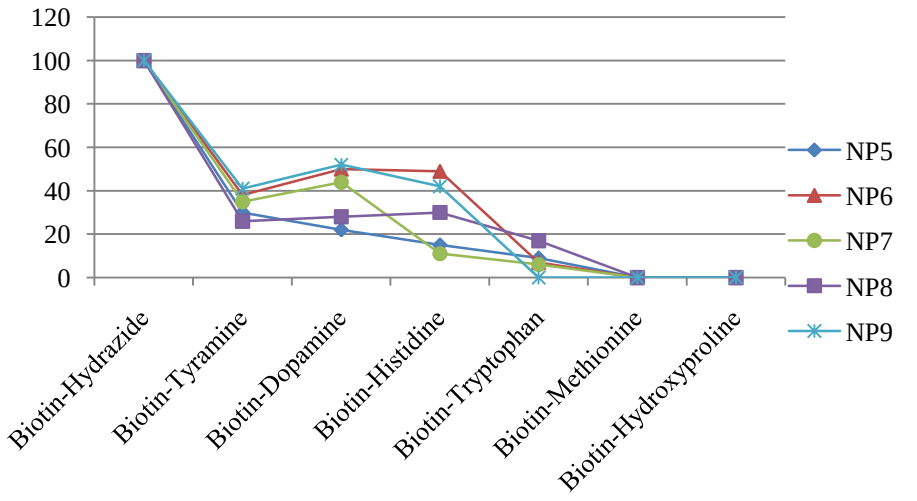

Figure 59. Normalized incorporation of biotin derivatives into proteins; (a) RNase A; (b) lysozyme. [RNase A], [Lysozyme]: 0.235 mM, [**NP5-NP9)**]: 0.5 mM, [**BD**]: 0.025 mM, irradiation 2000 mW for 5 min. for RNase A and 30 min. for lysozyme.

To facilitate the comparison and visualization of the results obtained in these experiments Figure 60 shows as example the incorporation of the biotinylated derivatives when **NP6** was employed as the sensitizer.

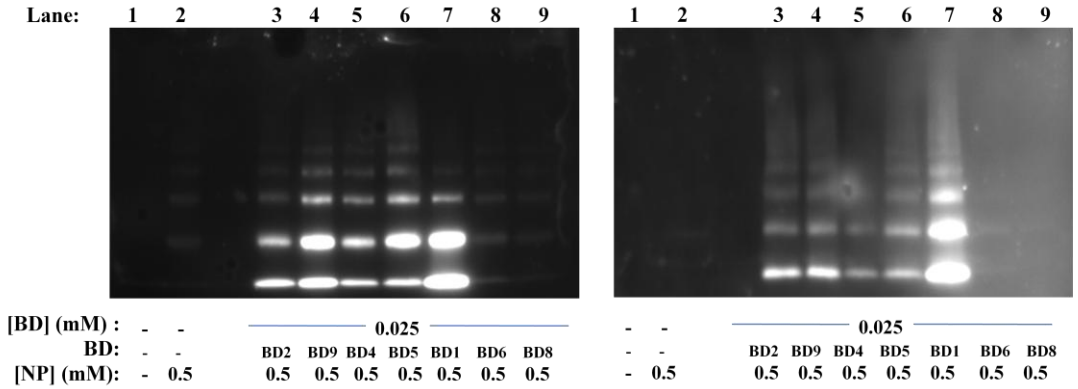

(a) (b)

Figure 60. Incorporation of biotin labeled derivatives using NP6 as sensitizer. a) RNase A, (b) Lysozyme. [protein]: 0.235 mM, [**NP6**]: (0.5 mM), [**BD**]: 0.025 mM, 5 min (RNase A) and 30 min (lysozyme) of light irradiation at 2000 mW.

In order to better understand the inhibition and incorporation results each of the proteins were inspected to identify solvent-accessible amino acids that could potentially participate in the photochemical crosslinking reactions. The numbers of tyrosine, tryptophan, histidine, and lysine residues are shown in Table 5. Inspection of the published crystal structure for RNase A[81] using Jmol[82] reveals that three of its six tyrosine residues are located at the surface of the protein and potentially available for modification and interaction. While lysozyme[83] also has three tyrosine residues relatively close to the solvent surface, it appears that the surface area of the tyrosines present on RNase A is more readily useable and in greater proportion. Histidine is another key amino acid that could play an important role in crosslinking, and RNase A has two of its four histidine residues with reasonably solvent-accessible surfaces whereas lysozyme has

its histidine residue relatively buried. Another amino acid residue that seems to be participating in the modification of these proteins is lysine; both proteins have most of their lysine residues accessible for modification. Finally, lysozyme possesses two of its three tryptophan residues well positioned at the solvent surface (RNase A does not contain tryptophan)(Figures 61 and 62).

Table 5. Potentially reactive amino acid residues present in RNase A and Lysozyme

Protein / Amino acid residues	RNase A	Lysozyme
Tyrosine	6	6
Tryptophan	0	3
Histidine	4	1
Lysine	10	5

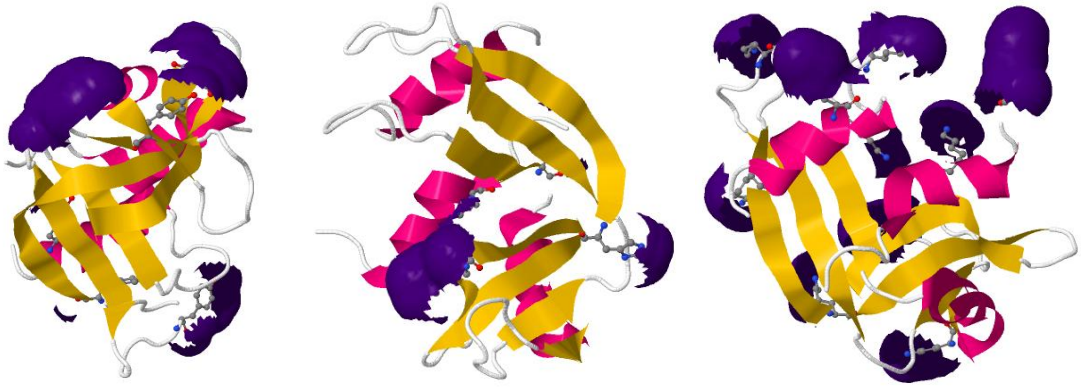

(a) (b) (c)

Figure 61. Solvent-accessible surfaces of amino acid residues in RNase A. (a) Tyrosine; (b) Histidine; (c) Lysine. Images were taken from the protein data bank page (PDB) by simulated the surface of the amino acids in the Jmol image.[83]

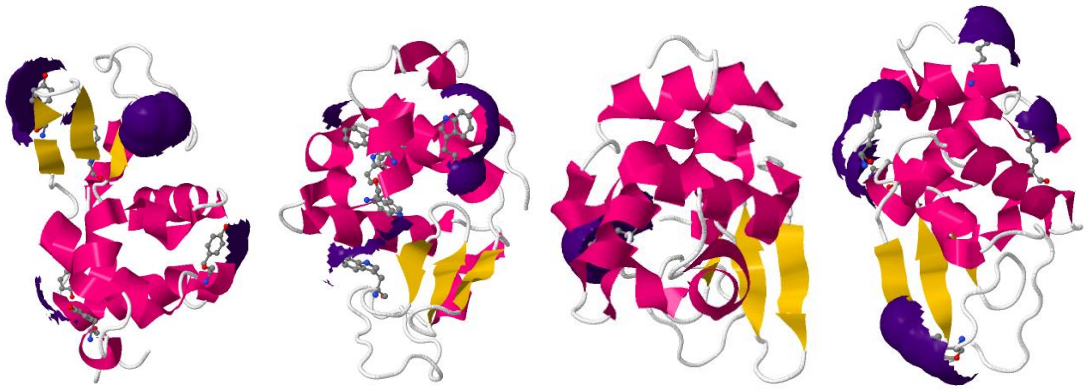

(a) (b) (c) (d)

Figure 62. Solvent-accessible surfaces of amino acid residues in lysozyme. (a) Tyrosine; (b) Tryptophan; (c) Histidine; (d) Lysine.

Inhibition Studies using Biotin Labeled Compounds

With the biotinylated compounds in hand their ability to inhibit the crosslinking of RNase A and lysozyme photosensitized by each of the naphthalimide derivatives was also determined. Two representative crosslinking inhibition experiments using **NP6** as a sensitizer are shown in Figure 63.

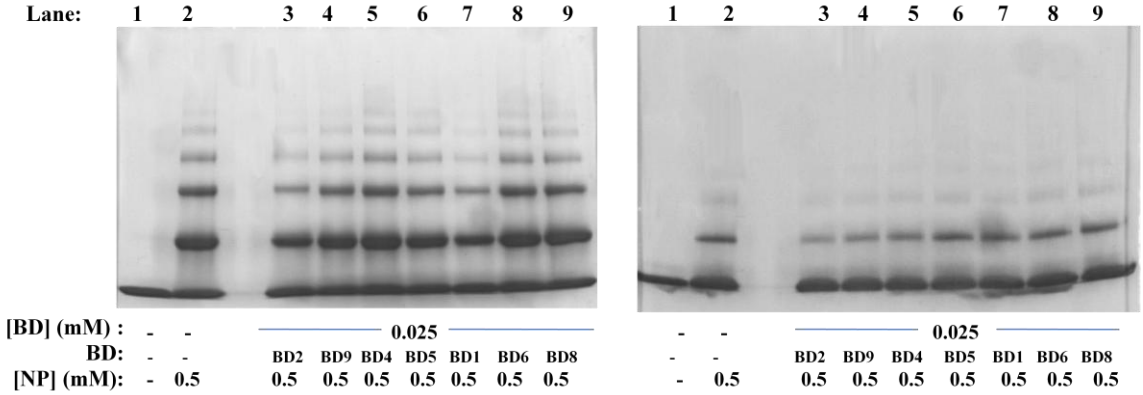

(a) (b)

Figure 63. Inhibition gels of RNase A and lysozyme (0.235 mM) using **NP6** (0.5 mM) as sensitizer, [**BD**]: 0.025 mM and 5 minutes of light exposure.(a) RNase A, (b) lysozyme.

Figures 64 (a) and (b) display the inhibition of RNase A and lysozyme crosslinking by each of the biotinylated derivatives and the sensitizers. In contrast to the results presented in Tables 3 and 4 for the free amino acids, the biotinylated compounds in this experiment exhibit much less inhibition. However, there are two significant differences between the experiments.

First, the concentration of the potential inhibitors is much lower in this experiment - 0.025 mM in this experiment compared to 1.5 mM in the earlier experiment involving free amino acids (the concentration of the proteins was 0.235 in both experiments). Accordingly, any inhibition seen in these experiments suggests that the given functional group is a potent inhibitor. This result only clearly identifies the hydrazide functionality in the biotin-hydrazide compound, and perhaps the catechol residue in the DOPA-biotin derivative, as good inhibitors of photochemically-sensitized RNase A crosslinking inhibition.

A second significant difference is that each of the compounds in the previous experiment had free potentially nucleophilic amines (in addition to the side-chain functional groups), while the biotinylated compounds (with the exception of the biotin-hydrazide) all had amino groups converted into amides (for attaching the biotin residues).

Since biotin-hydrazide (**BD-1**), the only nucleophilic compound, was the overall most effective inhibitor, it may be reasonable to ascribe the primary inhibitory activity from this compound as well as the compounds used previously (Tables 3 & 4) to the nucleophilic amines/hydrazide.

(a)

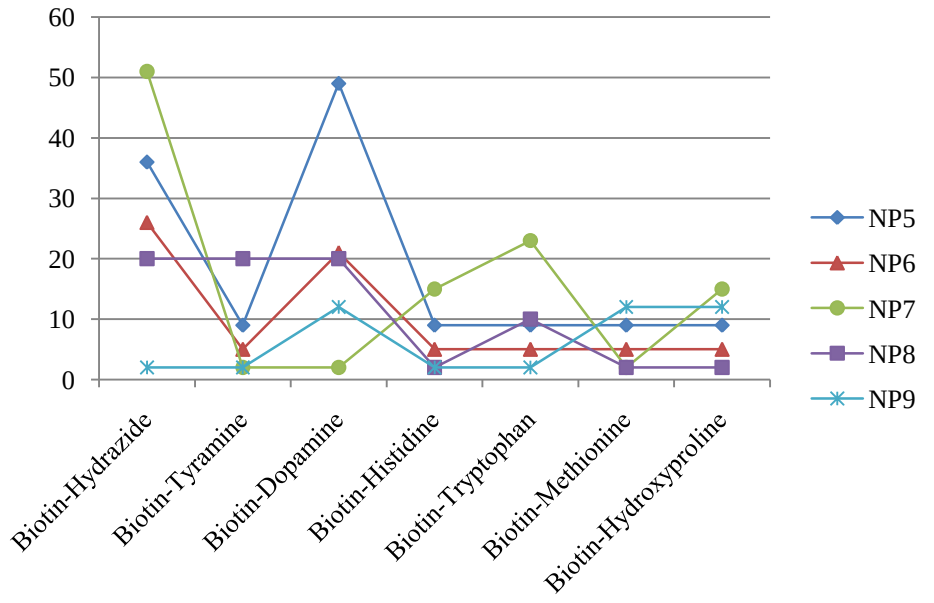

(b)

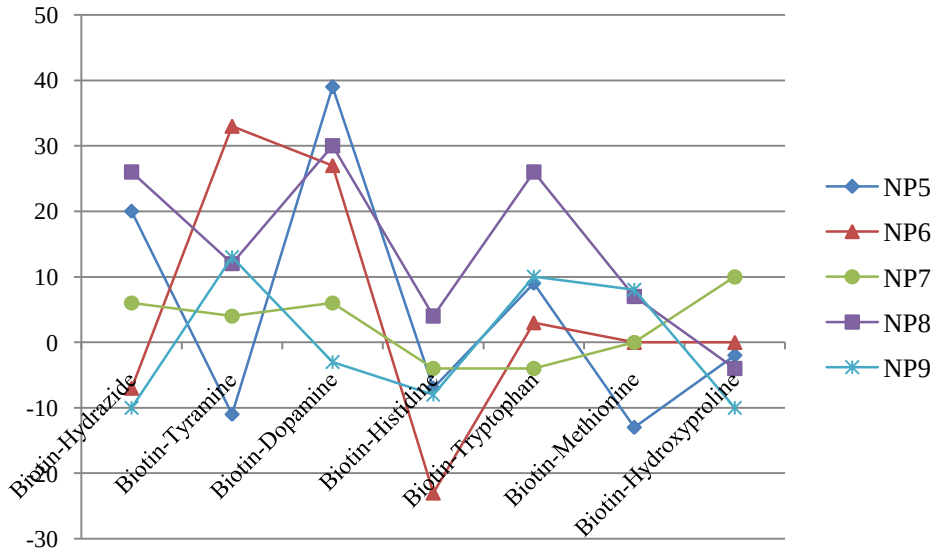

Figure 64. . Inhibition of crosslinking for (a) RNase A; (b) lysozyme. [RNase A], [Lysozyme]: 0.235 mM, [**NP5-NP9**]: 0.5 mM, [**BD**]: 0.025 mM, 5 minutes of light irradiation for RNase A and 30 minutes of exposure for Lysozyme.

Influence of Sodium Azide (NaN_3) and Superoxide Dismutase (SOD) on the Photosensitized Reactions of RNase A and Lysozyme

In an additional set of experiments it was evaluated the effect of added sodium azide (NaN_3) or superoxide dismutase (SOD) on the degree of modification of the proteins. Sodium azide was chosen because of its known propensity to inhibit reactions that proceed by a type II (single oxygen-mediated) reaction. Superoxide dismutase can be useful for determining the role of superoxide radical intermediates during the photochemical modification of proteins since it rapidly deactivates superoxide, preventing it from reacting with the sensitizers, proteins, and other added molecules. The naphthalimides **NP5** and **NP9** were chosen as sensitizers for these experiments since they seemed to possibly represent two mechanistic 'extremes'. Additionally, it had been reported previously in our group[65] that the addition of sodium azide during the crosslinking of RNase A photosensitized by **NP5** and **NP9** produced a decrease in the amount of crosslinked protein. The presence of sodium azide was found to influence the incorporation of biotinylated compounds into the RNase A by naphthalimide photosensitization. Interestingly, **NP5** and **NP9** exhibited different trends (Figure 65). In general, the addition of sodium azide increased the incorporation of the biotin derivatives with **NP5**. This could possible result from the avoidance of unproductive or destructive singlet-oxygen (type II) reactions, and would suggest that this sensitizer potentially operates primarily by a type I mechanism. On the other hand, azide inhibited the incorporation of several compounds (dopamine, histidine, and hydrazide derivatives) in reactions sensitized by **NP9**, suggesting an important role for singlet oxygen in RNase modification using this naphthalimide.

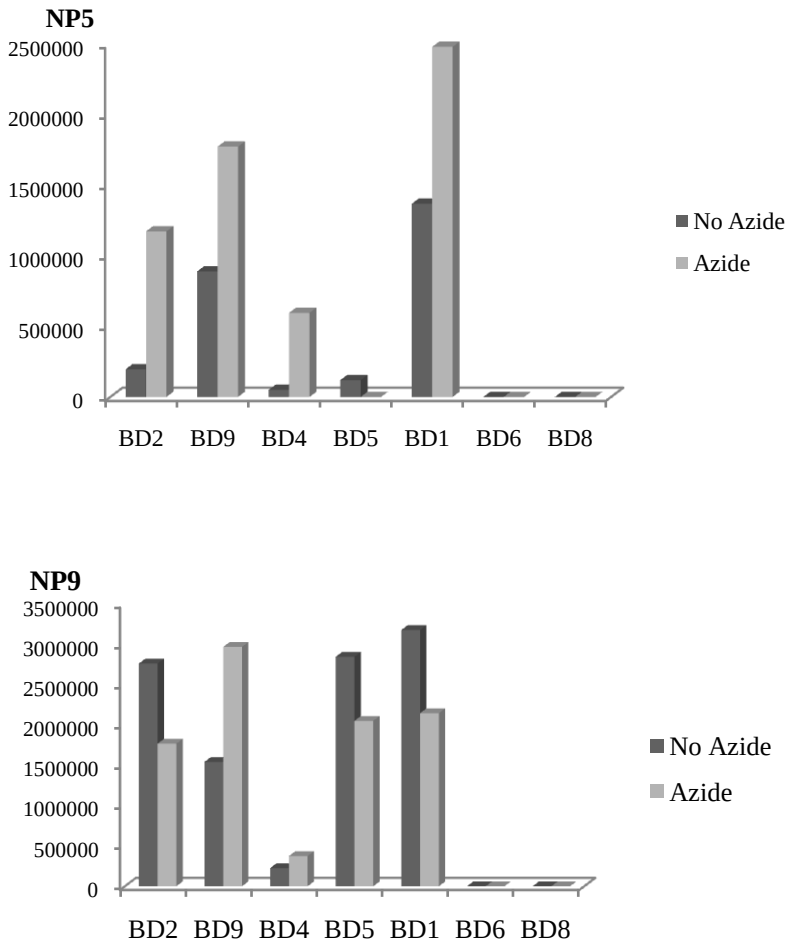

Figure 65 Azide influence on incorporation of biotin derivatives in photosensitized reactions of RNase A using **NP5** and **NP9**. **BD1**: Biotin-Hydrazide, **BD2**: Biotin-Dopamine, **BD4**: Biotin-Tryptophan, **BD5**: Biotin-Histidine, **BD6**: Biotin-Methionine, **BD8**: Biotin-Hydroxyproline, **BD9**: Biotin-Tyramine.

The addition of superoxide dismutase to the naphthalimide-mediated crosslinking of RNase A had previously been shown to stimulate crosslinking. This was confirmed in our hands (Figure 66). One remarkable observation in this experiment was that the addition of a catalytic amount of SOD significantly increased the amount of lysozyme crosslinked – in fact, to the same levels of crosslinking as RNase A at 5 minutes. Additionally, the incorporation of biotin-tyramine **BD9** into lysozyme was significantly enhanced by the addition of SOD (Figure 67). These experiments demonstrate that

lysozyme crosslinking and binding to tyramine is inhibited greatly by superoxide, and suggest the primacy of a type I mechanism for lysozyme with **NP8**.

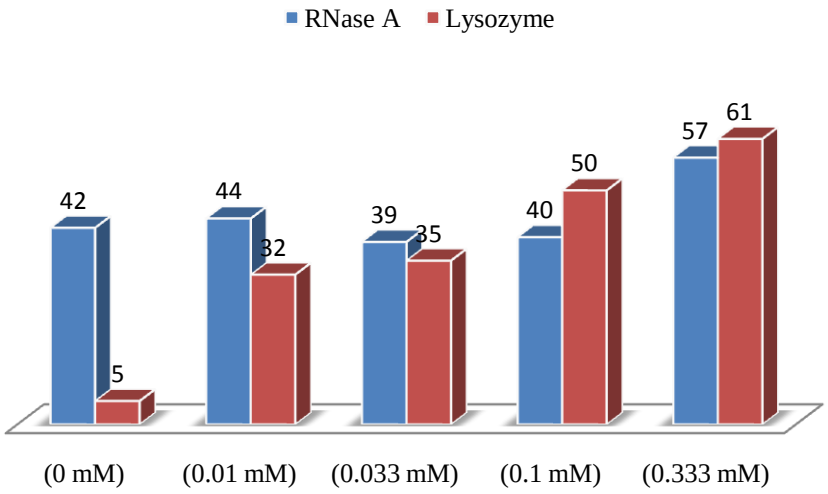

Figure 66. RNase A and lysozyme crosslinking photosensitized by **NP8** in the presence of SOD .

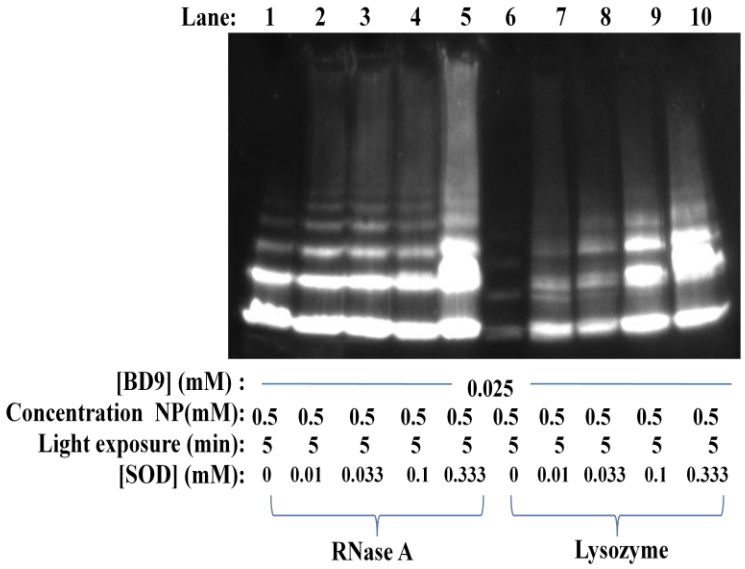

Figure 67. Influence of SOD on incorporation of biotin-tyramine (**BD9**) in RNase A and lysozyme using **NP8.** [**BD9**]: 0.025 mM, [**NP8**]: 0.5 mM, [RNase A] and [Lysozyme]: 0.235 mM.

Previous data reported that the addittion of SOD during the flavin mononucleotide and riboflavin photosensitized oxidation of tyrosine derivatives, dianisidine, and collagen[79,84,85] stimulate crosslinking in these systems supporting our experimental observation. In those reports it is suggested that an increase in protein crosslinking is observed upon addition of SOD because the SOD consumes the superoxide, which is formed in the reaction between the sensitizer and oxygen during the photochemical reaction (Scheme 23). If not removed, the superoxide could react with photo-oxidized amino acid intermediates preventing them from reacting with other amino acid residues in crosslinking reactions.

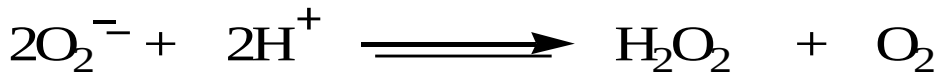

Scheme 23. Superoxide reaction catalyzed by superoxide dismutase (SOD)

Another possibility for the response obtained after addition of SOD in the crosslinking experiments could be the reaction of naphthalimide radical anion with molecular oxygen, which could regenerate the ground state of the naphthalimide (Scheme 24). By regenerating again the ground state; the photosensitizer can undergo futher photochemical processes.

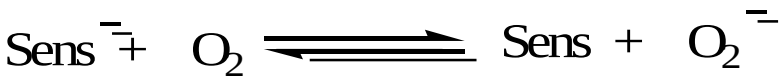

Scheme 24. Oxidation of naphthalimide (Sens) radical anion by oxygen.

Formation of Persistent Reactive Intermediates in the Naphthalimide-Sensitized Photochemical Reactions of RNase A and Lysozyme

In order to determine if persistent intermediates are formed in the photochemical modification of proteins using naphthalimides we examined the reactivity of preactivated biotin derivatives with the proteins RNase A and lysozyme (Scheme 25). In these experiments the biotin derivatives were mixed with the different sensitizers and the mixture irradiated for 5 minutes. Immediately after the exposure to light the proteins were added and the reaction mixture were left to incubate for 1 hour in the dark.

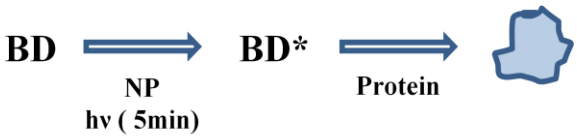

Scheme 25. Procedure of protein modification changing the order of reagent addition

An initial experiment, which also examined the consequence of the preactivation of the proteins, showed very little incorporation of the biotinylated compounds (Figure 68). However, closer examination of the Western blots revealed that a small amount of the pre-activated biotin compounds were in fact incorporated in the protein (lanes 4-6), which not surprisingly was not crosslinked under these conditions. Accordingly, we decided to more closely examine this phenomenon, using each of the sensitizers in combination with each of the biotin derivatives that had previously shown the propensity to be incorporated into the proteins, and using both RNase A and lysozyme (Figure 69).

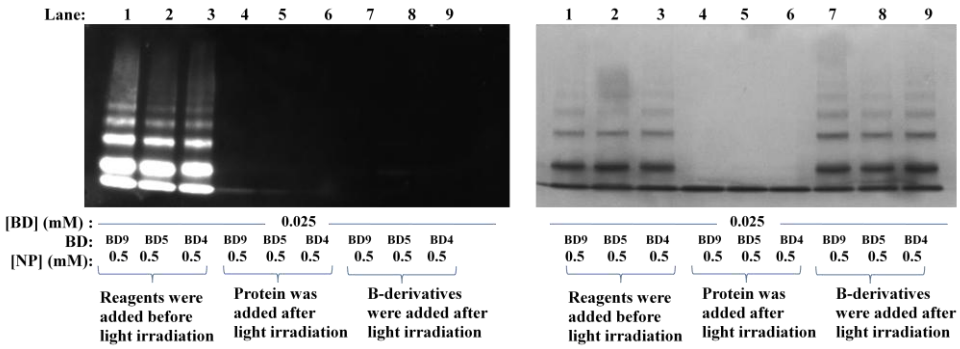

Figure 68. Effect of preactivation on the incorporation of biotin derivatives into RNase A using **NP8** as sensitizer. [**BD**]: 0.025 mM, [**NP8**]: 0.5 mM, [RNase A]: 0.235 mM, 5 min light irradiation for all the lanes followed by 1 hour of incubation after addition of protein (lanes 4-6) or **BD** (lanes 7-9). **BD1**: Biotin-Hydrazide, **BD2**: Biotin-Dopamine, **BD4**: Biotin-Tryptophan, **BD5**: Biotin-Histidine, **BD6**: Biotin-Methionine, **BD8**: Biotin-Hydroxyproline, **BD9**: Biotin-Tyramine.

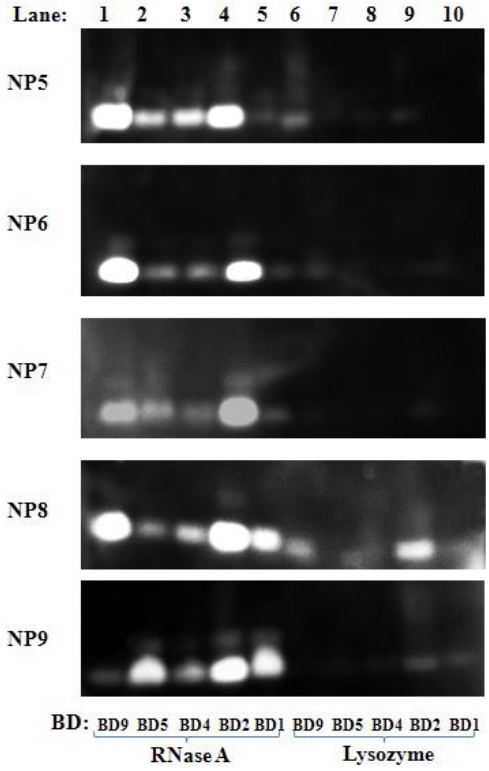

Figure 69. Incorporation of preactivated biotin derivatives into RNase A and lysozyme. [**BD**]: 0.025 mM, [**NP**]: 0.5 mM, [RNase A] and [Lysozyme]: 0.235 mM. A mixture of **BD** and **NP** were irradiated (5 min) after which the protein was added and incubated for 1 hour. **BD1**: Biotin-Hydrazide, **BD2**: Biotin-Dopamine, **BD4**: Biotin-Tryptophan, **BD5**: Biotin-Histidine, **BD9**: Biotin-Tyramine.

Consistent with previous results, lysozyme is much less reactive than RNase A. In this experiment the dopamine derivative was the compound most consistently (and most efficiently) incorporated into RNase, while the tyramine derivative was also incorporated efficiently, although the naphthalimide **NP9** was unable to activate it at all. Tryptophan and histidine were incorporated in small amounts with all of the activators, while the hydrazide derivative was only incorporated when napthalimides **NP8** and **NP9** were used. Once again, **NP8** was the most active at catalyzing the incorporation of the biotin derivatives into the proteins. These results are most consistent with a type I mechanism being primary for **NP5**, **NP6**, and **NP7**, and with the singlet oxygen (type II) mechanism becoming more important with **NP8** and **NP9**.

*Mass Spectral Analysis of Digested RNase A using as Sensitizer Naphthalimide **NP8***

In the hopes of narrowing down the protein modifications that occur in the naphthalimide-sensitized photochemical reactions of RNase A, we decided to order to attempt to apply mass spectroscopy to the problem. Ideally, by inspecting the peptides modified in the naphthalimide reaction the most reactive regions in the protein, and perhaps the most likely reactive amino acids, might be identified. Accordingly, samples of RNase A were digested using an in-solution tryptic digestion and guanidination kit. Trypsin digestion/guanidination is a common tool to identify proteins and post-translational modification by mass spectrometry due to the specificity in the cleavage of peptide bonds at the carboxylic acid side of arginine and lysine residues, while guanidination convert lysines to homoarginines which in general provides a strong signal in the spectrum and minimize any possible N-terminal modification.

The mass spectrum of the digested RNase A (Figure 70) was obtained and four peaks were identified from the full scan TIC MS analysis, with approximate retention times of 14.02, 13.60, 10.93 and 9.91 corresponding to peptides with masses of 742.0334, 651.072, 802.9892 and 479.216 respectively (Figure 71). By using the prospector simulation program (http://prospector.ucsf.edu) for estimating MS-digest peptide sequence in RNase A we were able to identify the peptide sequence for the major four peaks observed in the TIC MS (Figure 72)

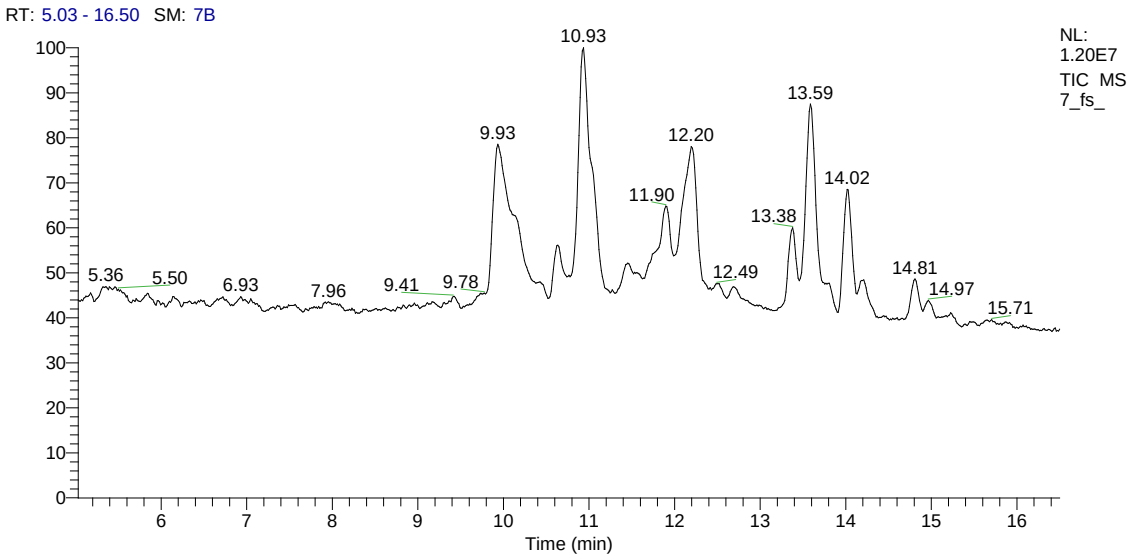

Figure 70. Full scan TIC MS of digested RNase A

Additional samples of the peptide digest were then subjected to the naphthalimide-sensitized photochemical reaction using **NP8** as sensitizer. Three experimental conditions were used for each of the three biotin derivatives examined (biotin-dopamine (**BD2**), biotin-histidine (**BD5**) and biotin-hydrazide (**BD1**)).

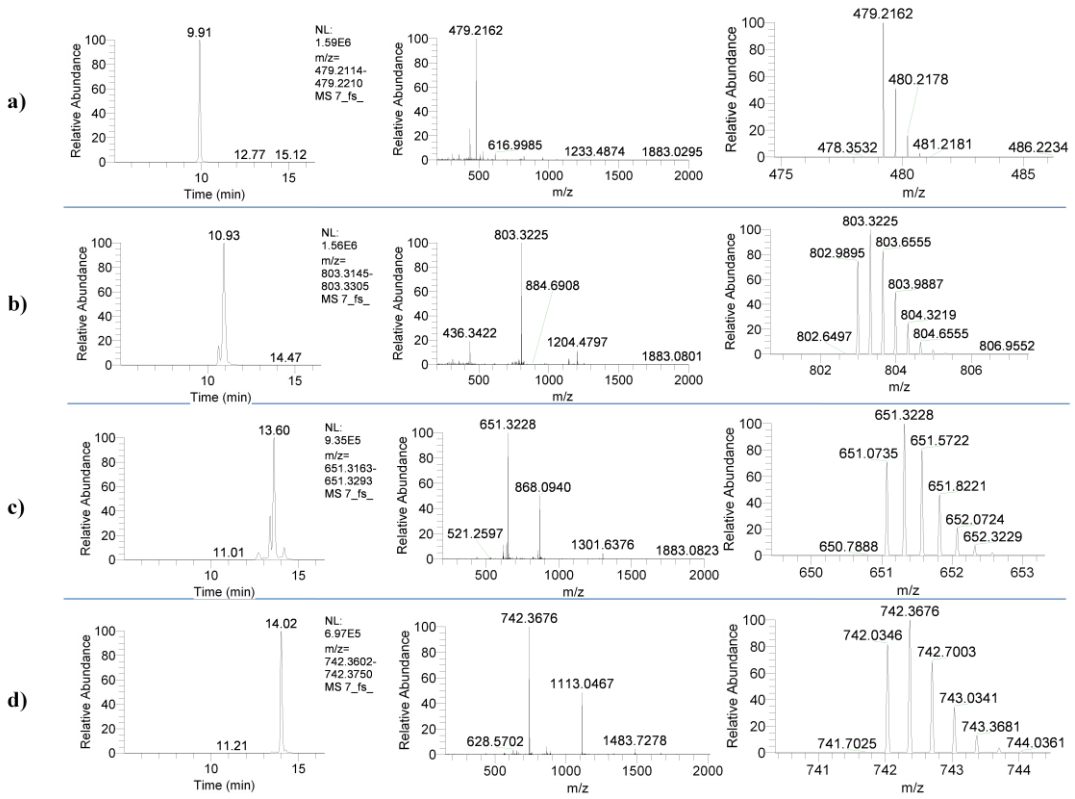

Figure 71. Full scan TIC MS of digested RNase A. Retention times and masses of the major peaks. a) 9.91 min; b) 10.93 min; c) 13.60 min; d) 14.02 min.

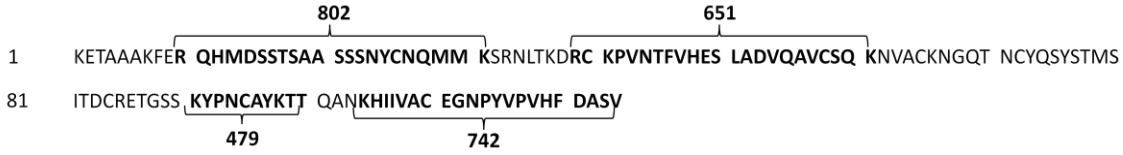

Figure 72. Peptide sequence for the major four peaks identified for digested RNase A

The experimental conditions used were:

1) 2 μL of **NP8** (1mM) and 1 μL of biotin derivative (2mM) were added to the digested RNase A solution followed by 5 min of light irradiation (2000 mW, Hg lamp).

2) 1 μL of biotin derivative (2mM) was preactivated with 2 μL of **NP8** (1 mM) and 5 min of light irradiation (2000 mW, Hg lamp), followed by the immediate

addition of the freshly digested protein. Samples were incubated for 1 hour and then submitted to mass analysis.

3) The RNase A digest was activated first with 2 μL of **NP8** (1 mM) and 5 min of light irradiation (2000 mW, Hg lamp) followed by the addition of 1 μL of biotin labeled derivative (2 mM) and incubation of samples at room temperature for 1 hour.

Biotin-dopamine (**BD2**), biotin-histidine (**BD5**) and biotin-hydrazide (**BD1**) were selected as the biotin-derivatives for these experiments since they showed the most incorporation into RNase A in the Western blotting experiments. It was hoped that as a first foray into the use of MS we would be able to inspect the LC-TIC signature and identify the relatively reactive peptides responsible for the modification on this protein.

Figure 73 shows the mass spectrum resulted from a full scan TIC MS when biotin-dopamine (**BD2**) was used as biotinylated compound under the three experimental conditions mentioned before. a) Control; digested RNase A (144 μg or 0.34 mM), b) amino acid residues of digested RNase A and biotin-dopamine (**BD2**) were activated with the light and the sensitizer at the same time, c) biotin-dopamine (**BD2**) was activated first with light and sensitizers and then reacted with digested RNase A, d) amino acid residues in digested RNase A were activated first with **NP8** and light and then reacted with dopamine derivative (**BD2**). The same studies were done using biotin-histidine (**BD5**) (Figure 74) and biotin-hydrazide (**BD1**) (Figure 75)

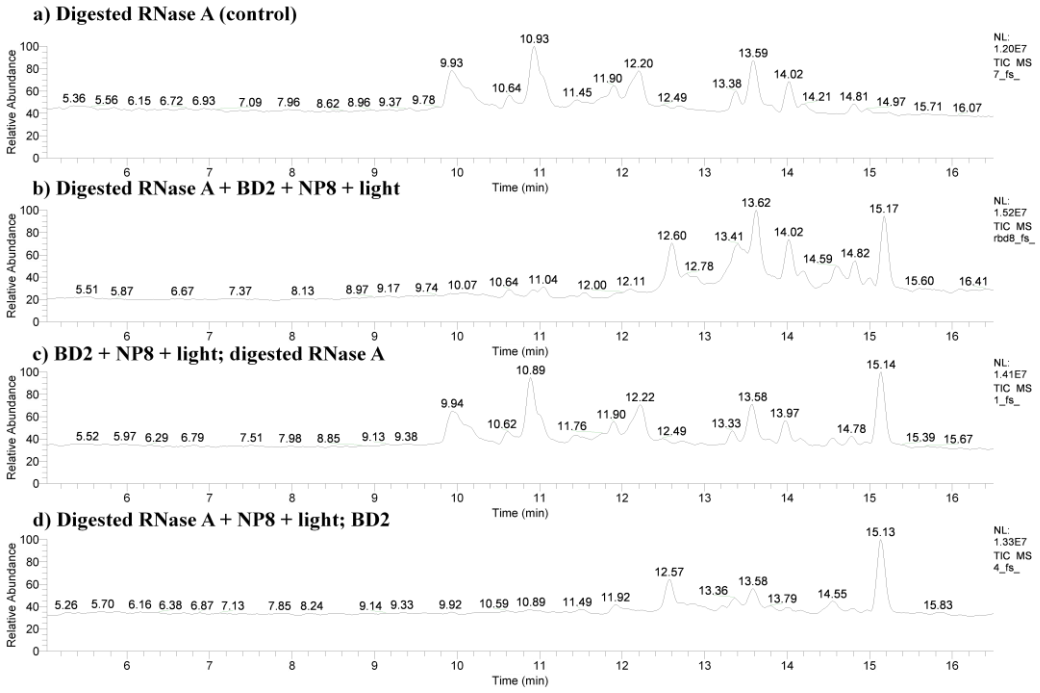

Figure 73. Full scan TIC MS of digested RNase A modified using **NP8** as sensitizer in presence of biotin-dopamine (**BD2**).

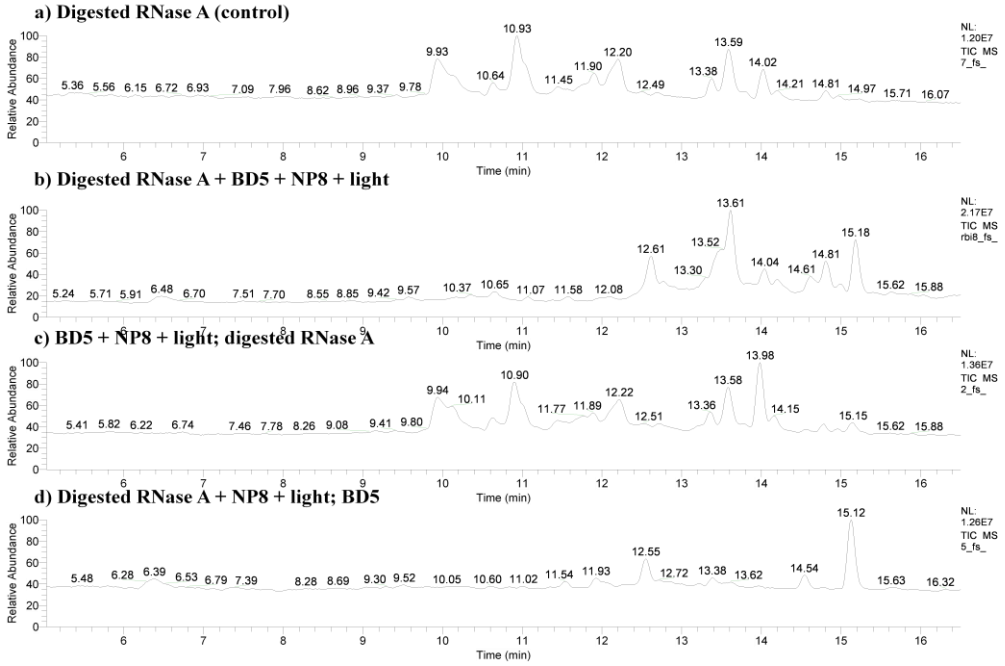

Figure 74. Full scan TIC MS of digested RNase A modified using **NP8** as sensitizer in presence of biotin-histidine (**BD5**).

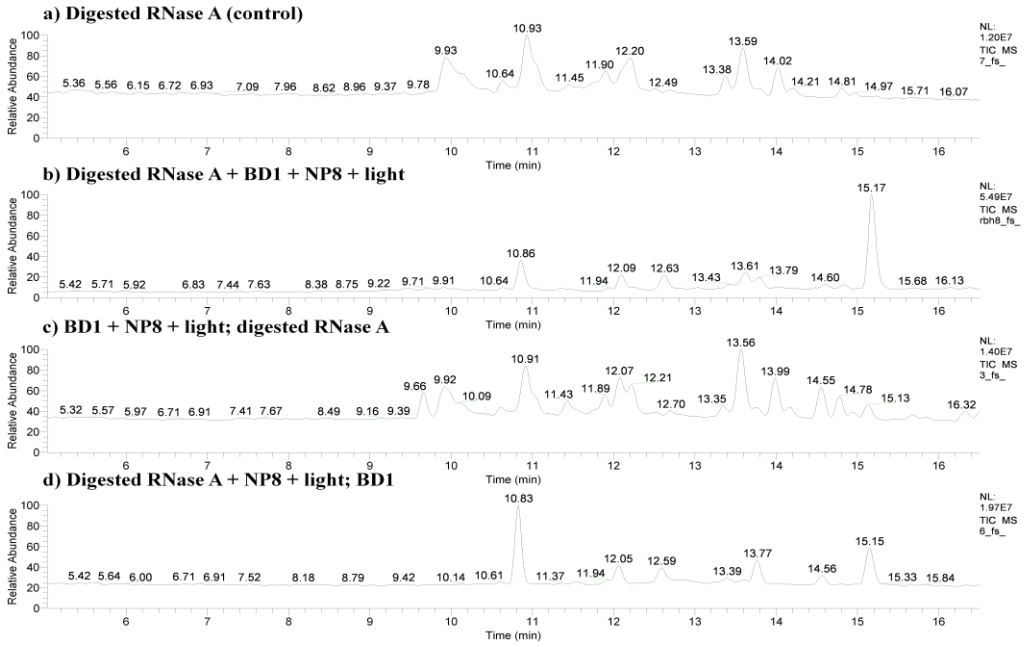

Figure 75. Full scan TIC MS of digested RNase A modified using **NP8** as sensitizer in presence of biotin-hydrazide (**BD1**).

Inspection of the TIC LC-MS spectrum of the digested RNase A modified in the presence of the biotin-derivatives (Figures 73, 74 and 75) reveals a significant decrease in the intensity of the peaks with retention times at 9.93 (479.216) and 10.93 (802.9892). This difference is most noticeable when all the reagents were exposed to light at the same time, but is also found when the amino acid residues of the digested RNase A were also exposed to light prior to addition of biotin labeled derivatives. Notably, treatment with the preactivated biotin derivatives does not seem to alter the composition of the peptide mixture.

The disappearance of the peaks with retention times at 9.93 and 10.93 suggests that these peptides are the most reactive sequences. Figure 76 shows the presence of the amino acid residues with the peaks at 9.89 min (479.216 uma) and 10.93 min (802.9892 uma) which demonstrates that the most reactive peptide sequences has histidine, tyrosine

and lysine residues present in RNase A available for modification. Possibly, these amino acid residues are directly correlated or responsible for modification of RNAse A which gives us additional evidence of the reactivity of tyrosine, lysine and histidine under the photochemical conditions employed for the modification of this protein.

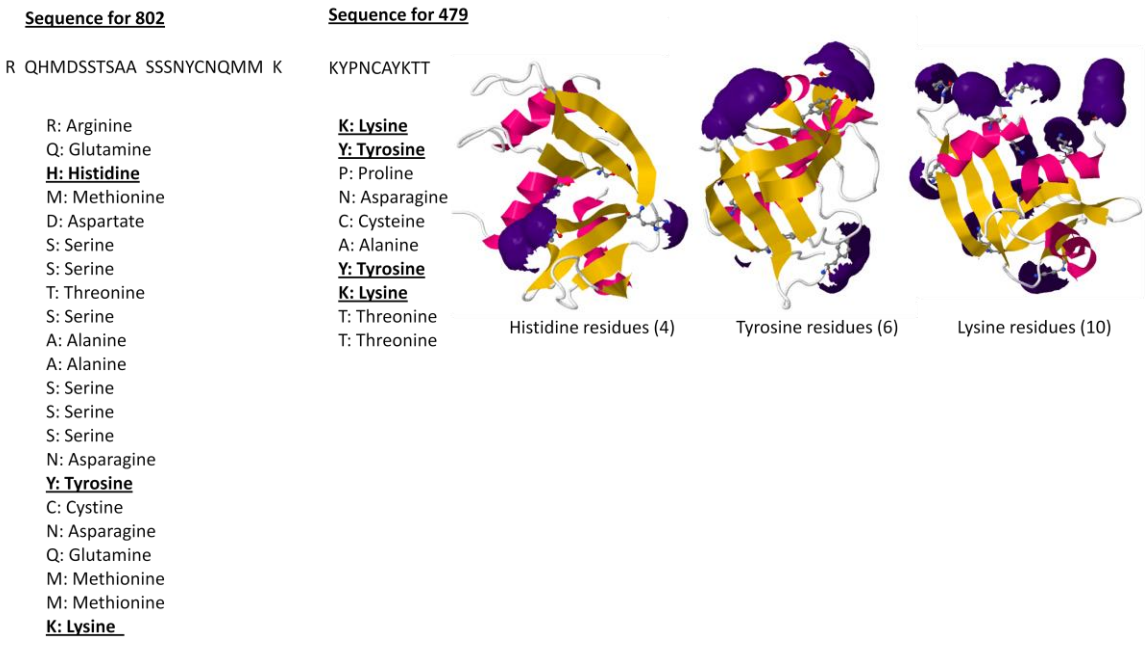

Figure 76. Amino acid residues present in the peptide sequences for peaks with retention time of 9.98 min (479.216 uma) and 10.93 min (802.9892 uma).

Tissue Modification Experiments

The mechanistic studies described in the previous sections were designed with the intention that they would provide guidance for further experimentation in photochemical tissue modification and bonding. Although the use of soluble proteins as model systems provided a reasonable starting point, those experiments are crude model for the processes that occur at the complex tissue interface. Some of the trends and correlations observed for the model studies will prove to have some predictive value in the naphthalimide-

sensitized photochemical modification of tissue surfaces. The promotion of tissue adhesion by covalent bonds between the tissue surfaces potentially represents a powerful tool that could be applied in delicate surgical repairs (cornea, skin grafts, tendons, heart valves), avoiding the presence of foreign materials which potentially slow down the recovery process.

Different types of tissues were used in the tissue-modification studies, including bovine meniscus, bovine pericardium, and pig skin. The protein in these tissues is primarily type 1 collagen. Collagen-based biomaterials, frequently derived from porcine aortic valve, bovine pericardium, dura mater, and autologous pericardium, are being used in medical applications such as nerve regeneration, tissue augmentation, burn and wound dressing, drug delivery system, ocular surface and urinary tract surgery.[86] For example, pericardium tissue patches are widely used to close the pericardial sac after open heart surgery and to repair vascular grafts.[87]

Photochemical Incorporation of Biotin Derivatives into Pericardium Tissue

Initially, tissue experiments were done using unsaturated naphthalimide **NP5** and ethylsulfanyl naphthalimide **NP7** since these sensitizers had shown to be effective at crosslinking RNase A and lysozyme. Using these sensitizers the photosensitized incorporation of biotinylated compounds onto the surface of bovine pericardium was studied. Briefly, solutions containing the naphthalimide sensitizers and the biotin derivatives we spotted on pericardium tissue pieces that had been placed in a 24-well plastic plate, and a small spot on the tissue surface was irradiated. After irradiation and several washes to remove unbound biotin compounds, the samples were visualized by treatment a chemiluminescent assay and imaged. (Figure 77).

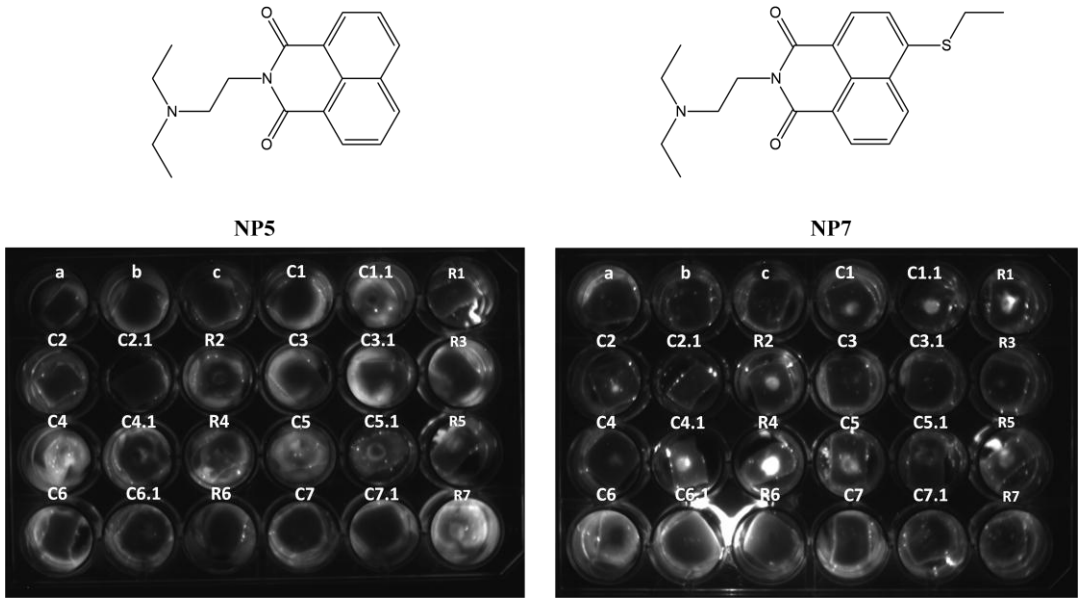

a: Pericardium tissue alone; **b**: Tissue + light; **c**: Tissue + **NP** + light ; **C1**: Tissue + **NP** + biotin-dopamine (**BD2**); **C1.1**: Tissue + biotin-dopamine (**BD2**) + light; **R1**: Tissue + **NP** + biotin-dopamine (**BD2**) + light; **C2**: Tissue + **NP** + biotin-tyramine (**BD9**); **C2.1**: Tissue + biotin-tyramine (**BD9**) + light; **R2**: Tissue + **NP** + biotin-tyramine (**BD9**) + light; **C3**: Tissue + **NP** + biotin-tryptophan (**BD4**); **C3.1**: Tissue + biotin-tryptophan (**BD4**) + light; **R3**: Tissue + **NP** + biotin-tryptophan (**BD4**) + light; **C4**: Tissue + **NP** + biotin-histidine (**BD5**); **C4.1**: Tissue + biotin-histidine (**BD5**) + light; **R4**: Tissue + **NP** + biotin-histidine (**BD5**) + light; **C5**: Tissue + **NP** + biotin-hydrazide (**BD1**); **C5.1**: Tissue + biotin-hydrazide (**BD1**) + light; **R5**: Tissue + **NP** + biotin-hydrazide (**BD1**) + light; **C6**: Tissue + **NP** + biotin-methionine (**BD6**); **C6.1**: Tissue + biotin-methionine (**BD6**) + light; **R6**: Tissue + **NP** + biotin-methionine (**BD6**) + light; **C7**: Tissue + **NP** + biotin-hydroxyproline (**BD8**); **C7.1**: Tissue + biotin-hydroxyproline (**BD8**) + light; **R7**: Tissue + **NP** + biotin-hydroxyproline (**BD8**) + light.

Figure 77. Pericardium tissue coated with a solution of **NP5** or **NP7** (0.5 mM) combined with various biotin derivatives (0.1 mM), irradiated for 5 min. (mercury lamp, 2000 mW).

Examination of the biotin incorporation in this experiment revealed that biotin-tyramine (**BD9**), and biotin-histidine (**BD5**), and biotin-dopamine (**BD2**) were bonded to the tissue when sensitized by **NP7**, but not with **NP5**. The specific compounds incorporated were consistent with protein experiments, although the lack of incorporation of any compound in reactions sensitized using **NP5**, and the lack of incorporation of the biotin-hydrazide with either sensitizer is surprising. Since this experiment verified that

the incorporation of the biotinylated compounds into pericardium was dependent upon on the identities of both the sensitizer and the biotin derivative, the same assays were repeated using **NP6** (Figure 78), **NP8** (Figure 79), and **NP9** (data not shown). No biotin incorporation was detected when **NP9** was used as the photosensitizer, while biotin-dopamine and biotin-histidine were effectively incorporated in reactions promoted by **NP6** and **NP8**.

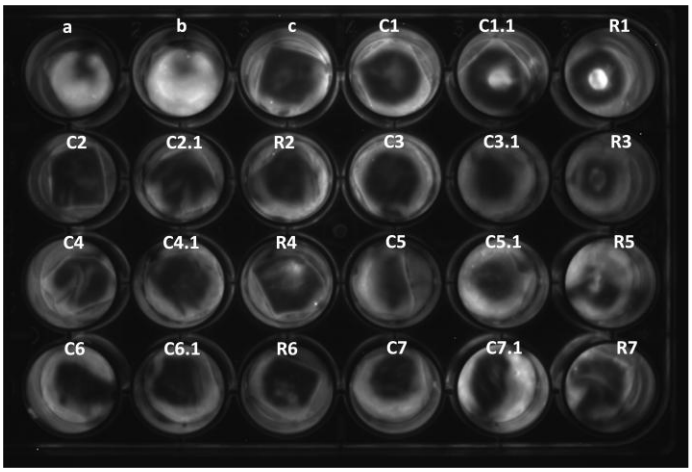

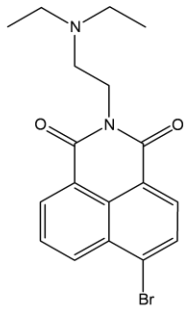

NP6

a: Pericardium tissue alone; **b**: Tissue + light; **c**: Tissue + **NP6** + light ; **C1**: Tissue + **NP6** + biotin-dopamine (**BD2**); **C1.1**: Tissue + biotin-dopamine (**BD2**) + light; **R1**: Tissue + **NP6** + biotin-dopamine (**BD2**) + light; **C2**: Tissue + **NP6** + biotin-tyramine (**BD9**); **C2.1**: Tissue + biotin-tyramine (**BD9**) + light; **R2**: Tissue + **NP6** + biotin-tyramine (**BD9**) + light; **C3**: Tissue + **NP6** + biotin-tryptophan (**BD4**); **C3.1**: Tissue + biotin-tryptophan (**BD4**) + light; **R3**: Tissue + **NP6** + biotin-tryptophan (**BD4**) + light; **C4**: Tissue + **NP6** + biotin-histidine (**BD5**); **C4.1**: Tissue + biotin-histidine (**BD5**) + light; **R4**: Tissue + **NP6** + biotin-histidine (**BD5**) + light; **C5**: Tissue + **NP6** + biotin-hydrazide (**BD1**); **C5.1**: Tissue + biotin-hydrazide (**BD1**) + light; **R5**: Tissue + **NP6** + biotin-hydrazide (**BD1**) + light; **C6**: Tissue + **NP6** + biotin-methionine (**BD6**); **C6.1**: Tissue + biotin-methionine (**BD6**) + light; **R6**: Tissue + **NP6** + biotin-methionine (**BD6**) + light; **C7**: Tissue + **NP6** + biotin-hydroxyproline (**BD8**); **C7.1**: Tissue + biotin-hydroxyproline (**BD8**) + light; **R7**: Tissue + **NP6** + biotin-hydroxyproline (**BD8**) + light.

Figure 78. Pericardium tissue coated with a solution of **NP6** combined with various biotin derivatives (0.1 mM) and irradiated for 5 min. (mercury lamp, 2000 mW).

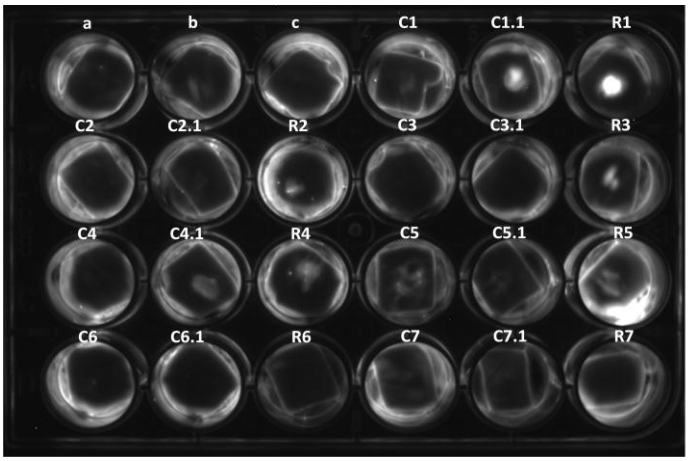

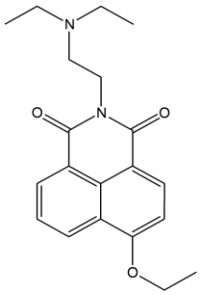

NP8

a: Pericardium tissue alone; **b**: Tissue + light; **c**: Tissue + **NP8** + light ; **C1**: Tissue + **NP8** + biotin-dopamine (**BD2**); **C1.1**: Tissue + biotin-dopamine (**BD2**) + light; **R1**: Tissue + **NP8** + biotin-dopamine (**BD2**) + light; **C2**: Tissue + **NP8** + biotin-tyramine (**BD9**); **C2.1**: Tissue + biotin-tyramine (**BD9**) + light; **R2**: Tissue + **NP8** + biotin-tyramine (**BD9**) + light; **C3**: Tissue + **NP8** + biotin-tryptophan (**BD4**); **C3.1**: Tissue + biotin-tryptophan (**BD4**) + light; **R3**: Tissue + **NP8** + biotin-tryptophan (**BD4**) + light; **C4**: Tissue + **NP8** + biotin-histidine (**BD5**); **C4.1**: Tissue + biotin-histidine (**BD5**) + light; **R4**: Tissue + **NP8** + biotin-histidine (**BD5**) + light; **C5**: Tissue + **NP8** + biotin-hydrazide (**BD1**); **C5.1**: Tissue + biotin-hydrazide (**BD1**) + light; **R5**: Tissue + **NP8** + biotin-hydrazide (**BD1**) + light; **C6**: Tissue + **NP8** + biotin-methionine (**BD6**); **C6.1**: Tissue + biotin-methionine (**BD6**) + light; **R6**: Tissue + **NP8** + biotin-methionine (**BD6**) + light; **C7**: Tissue + **NP8** + biotin-hydroxyproline (**BD8**); **C7.1**: Tissue + biotin-hydroxyproline (**BD8**) + light; **R7**: Tissue + **NP8** + biotin-hydroxyproline (**BD8**) + light.

Figure 79. Pericardium tissue coated with a solution of **NP8** (0.5 mM) combined with various biotin derivatives (0.1 mM) and irradiated for 5 min. (mercury lamp, 2000 mW).

Additional experimentation using **NP8** demonstrated additional incorporation of the biotin-tyramine (**BD9**) derivative when the irradiation time was extended from 5 to 15 minutes or when the concentration of the naphthalimide was increased from 0.5 to 1 mM. **NP5** and **NP9** were then re-examined at the higher concentration (1 mM; still 0.1 mM for the biotin derivatives and 5 min. light). Under these experimental conditions, **NP9** still did not catalyze any incorporation, while **NP5** showed some incorporation for biotin-tyramine, biotin-tryptophan and biotin-histidine (Figure 80).

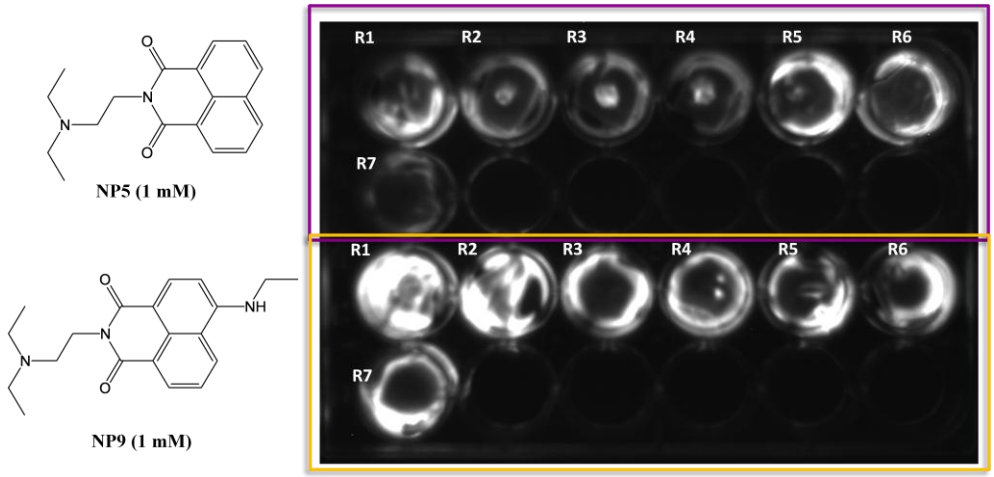

R1: Tissue + **NP** + biotin-dopamine (**BD2**) + light; **R2**: Tissue + **NP** + biotin-tyramine (**BD9**); **R3**: Tissue + **NP** + biotin-tryptophan (**BD4**); **R4**: Tissue + **NP** + biotin-histidine (**BD5**) + light; **R5**: Tissue + **NP** + biotin-hydrazide (**BD1**) + light; **R6**: Tissue + **NP** + biotin-methionine (**BD6**) + light; **R7**: Tissue + **NP** + biotin-hydroxyproline (**BD8**) + light.

Figure 80. Pericardium tissue coated with a solution of **NP5** or **NP9** (1 mM) combined with various biotin derivatives (0.1 mM) and irradiated for 5 min. (mercury lamp, 2000 mW).

Photochemical Incorporation of Biotin Derivatives into Meniscus Tissue

The incorporation of the labeled amino acid was also tested in meniscus tissues. Bovine meniscal tissue was harvested from fresh cow knees supplied by a local slaughterhouse; the meniscus was cut in pieces by slicing it in the middle in order to expose the interior of the cartilage and to expose the collagen network (Figure 81). 24 small pieces were cut and placed in the wells of a 24-well plate.

Reagents were incorporated as reported for the pericardium experiment and tissues were exposed to 5 minutes of light irradiation.

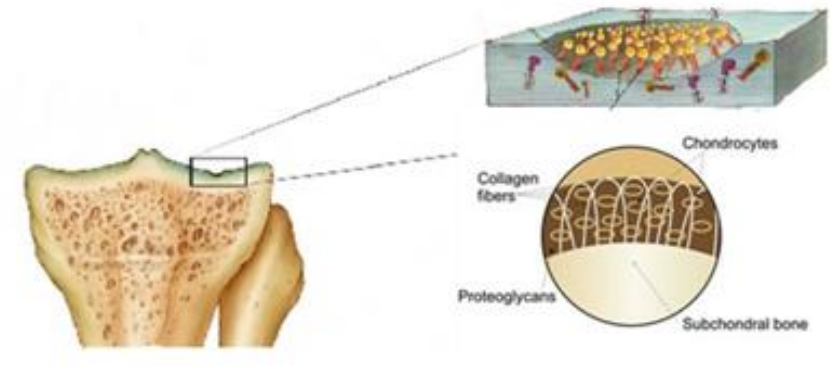

Figure 81. Collagen network in meniscus.[192]

The experiments involving meniscus tissues were not as satisfactory as those using pericardium tissue, and only a slight degree of incorporation of the labeled derivatives was observed, accompanied by significant non-specific background signals possibly resulting from the slow release of non-bound biotin compounds from the tissue matrix (Figure 82). Small amounts of incorporation were observed for biotin-dopamine (**BD2**) when 4-bromo substituted naphthalimide **NP6**, 4-ethylsulfanyl naphthalimide **NP7** and 4-ethoxide naphthalimide **NP8** were employed. No incorporation was observed for the sensitizers **NP5** (unsaturated naphthalimide) and **NP9** (4-ethylenamine naphthalimide) under these reaction conditions.

Meniscal tissue, and cartilage in general, has a complex and dense extracellular matrix.[88] In order to better expose the collagen (presumably the main target in the photochemical oxidation of these tissues) we attempted to remove the surface proteoglycans by treating the tissue with Chondroitinase ABC (chABC).

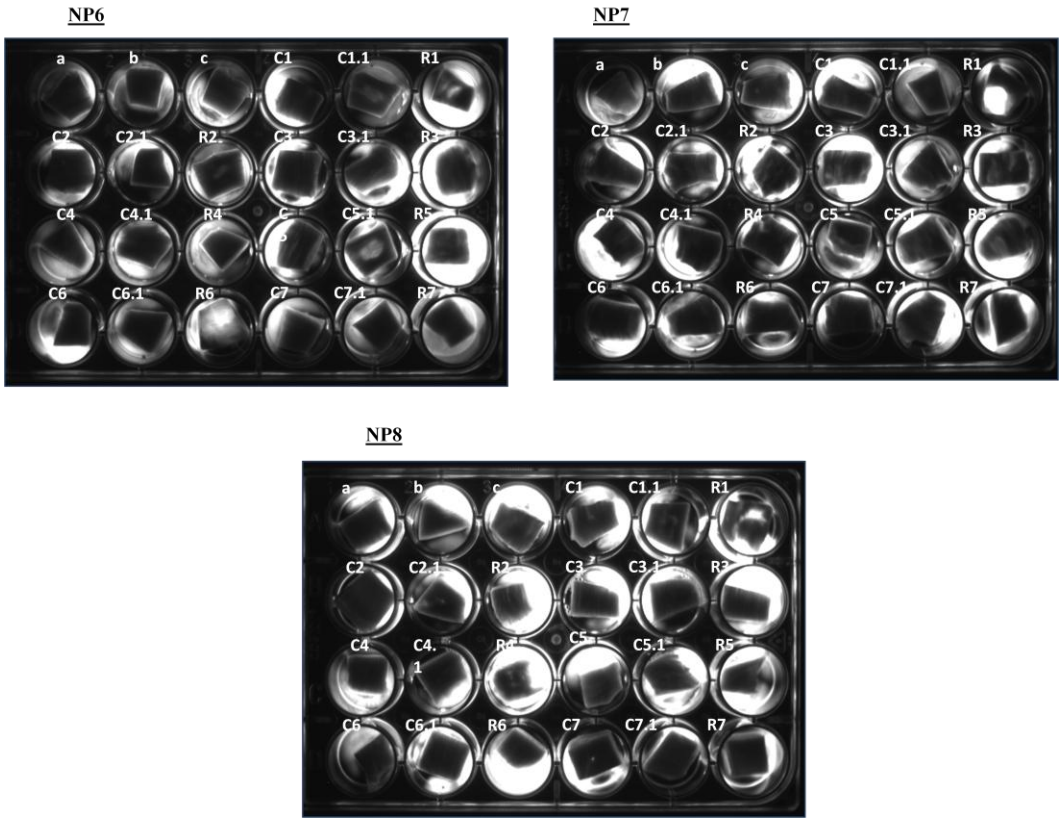

a: Meniscal tissue alone; **b**: Tissue + light; **c**: Tissue + **NP** + light ; **C1**: Tissue + **NP** + biotin-dopamine (**BD2**); **C1.1**: Tissue + biotin-dopamine (**BD2**) + light; **R1**: Tissue + **NP** + biotin-dopamine (**BD2**) + light; **C2**: Tissue + **NP** + biotin-tyramine (**BD9**); **C2.1**: Tissue + biotin-tyramine (**BD9**) + light; **R2**: Tissue + **NP** + biotin-tyramine (**BD9**) + light; **C3**: Tissue + **NP** + biotin-tryptophan (**BD4**); **C3.1**: Tissue + biotin-tryptophan (**BD4**) + light; **R3**: Tissue + **NP** + biotin-tryptophan (**BD4**) + light; **C4**: Tissue + **NP** + biotin-histidine (**BD5**); **C4.1**: Tissue + biotin-histidine (**BD5**) + light; **R4**: Tissue + **NP** + biotin-histidine (**BD5**) + light; **C5**: Tissue + **NP** + biotin-hydrazide (**BD1**); **C5.1**: Tissue + biotin-hydrazide (**BD1**) + light; **R5**: Tissue + **NP** + biotin-hydrazide (**BD1**) + light; **C6**: Tissue + **NP** + biotin-methionine (**BD6**); **C6.1**: Tissue + biotin-methionine (**BD6**) + light; **R6**: Tissue + **NP** + biotin-methionine (**BD6**) + light; **C7**: Tissue + **NP** + biotin-hydroxyproline (**BD8**); **C7.1**: Tissue + biotin-hydroxyproline (**BD8**) + light; **R7**: Tissue + **NP** + biotin-hydroxyproline (**BD8**) + light.

Figure 82. Meniscal tissue coated with a solution of **NP** combined with various biotin derivatives (0.1 mM) and irradiated for 5 min. (mercury lamp, 2000 mW).

Accordingly, 5 units of chABC were dissolved in 1 mL of a freshly made buffer solution containing 50 mM tris, pH: 8.0, with 6 mM sodium acetate and 0.02% bovine serum albumin. The surface of meniscal slices were then treated with this enzyme

solution for 1 hour at 37 ^{o}C. After thoroughly washing the tissue samples they were subjected to the naphthalimide-sensitized photochemical incorporation of biotinylated derivatives as previously described previously.

Figure 83 shows a comparison of the incorporation of the labeled species when **NP5** and **NP9** were used with and without chABC pre-treatment. Two concentrations of naphthalimide derivatives were tested in these assays, 0.5 and 1 mM. While the bonding of the biotin compounds to the tissue is not significantly improved, the background signal is greatly reduced in the wells containing tissue samples pre-treated with chABC.

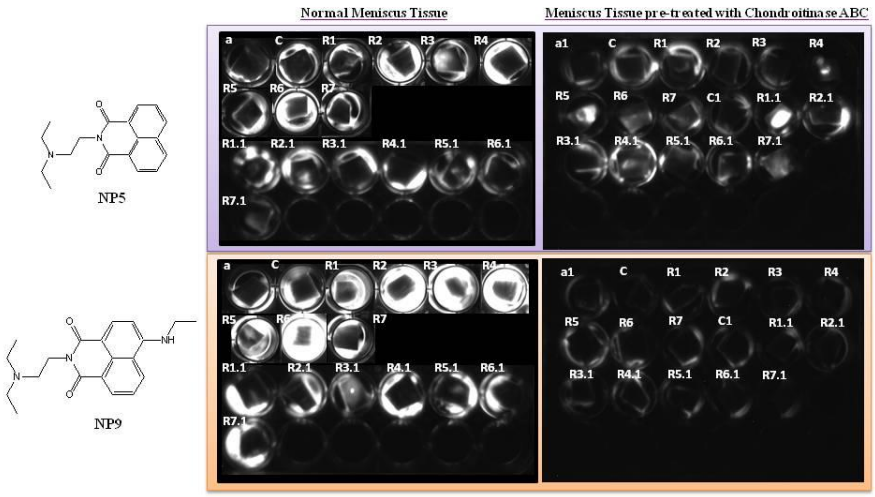

Figure 83. Meniscal tissue, with and without pretreatment using chABC, coated with a solution of **NP5** or **NP9** (0.5 or 1 mM) combined with various biotin derivatives (0.05 mM) and irradiated for 5 min. (mercury lamp, 2000 mW).

From figure 83 the legend is as follow; **a**: Tissue treated with chABC + light; **C**: Tissue + **NP** (0.5 mM) + light; **R1**: Tissue + **NP** (0.5 mM) + biotin-dopamine (**BD2**) + light; **R2**: Tissue + **NP** (0.5 mM) + biotin-tyramine (**BD9**) + light; **R3**: Tissue + **NP** (0.5 mM) + biotin-tryptophan (**BD4**) + light; **R4**: Tissue + **NP** (0.5 mM) + biotin-histidine

(**BD5**) + light; **R5**: Tissue + **NP** (0.5 mM) + biotin-hydrazide (**BD1**) + light; **R6**: Tissue + **NP** (0.5 mM) + biotin-methionine (**BD8**) + light; **R7**: Tissue + **NP** (0.5 mM) + biotin-hydroxyproline (**BD8**) + light. **C1**: Tissue + **NP** (1 mM) + light; **R1.1**: Tissue + **NP** (1 mM) + biotin-dopamine (**BD2**) + light; **R2.1**: Tissue + **NP** (1 mM) + biotin-tyramine (**BD9**) + light; **R3.1**: Tissue + **NP** (1 mM) + biotin-tryptophan (**BD4**) + light; **R4.1**: Tissue + **NP** (1 mM) + biotin-histidine (**BD5**) + light; **R5.1**: Tissue + **NP** (1 mM) + biotin-hydrazide (**BD1**) + light; **R6.1**: Tissue + **NP** (1 mM) + biotin-methionine (**BD8**) + light; **R7.1**: Tissue + **NP** (1 mM) + biotin-hydroxyproline (**BD8**) + light.

Photochemical Incorporation of Biotin Derivatives into Pericardium Tissue – Second Approach

One disadvantage of cutting the pieces of tissues and exposing them individually to the photolysis was that over the course of the experiment it was difficult to remain consistent - some of samples remained hydrated and in good condition while others were almost completely dry. In order to avoid this and increase the reproducibility of the experiment, pericardium tissues were used as a whole piece (the tissues were carefully cleaned), and a 96-well plastic plate was used to allow multiple experiments per piece of tissue. The appropriate wells in the plate were filled with the reaction and buffer solutions, the tissue was stretched over the plate, and a piece of glass was placed on top of the tissue. After carefully clamping the assembly, this “tissue sandwich” was turned over to expose the tissue to the reagents and the tissue ‘trans-illuminated’ by exposing it to light which was shined through the appropriate wells in the 96-well plate (Figure 33).

The first experiment using this set-up was carried out using biotin-dopamine (**BD2**) and naphthalimides 5-9 and 15 minutes of light irradiation. Biotin-dopamine

(**BD2**) was selected as the biotin labeled derivative for this assay since it shown to be one of the most consistent regarding incorporation. Each compound was studied in triplicate in order to determine the reproducibility of the experiment. Figure 84 shows that the biotin-dopamine (**BD2)** is incorporated most efficiently into the tissue when sensitized by the 4-ethoxide naphthalimide **NP8**, although significant incorporation can be detected in the control lane 3 where biotin-dopamine (**BD2**) was photolyzed without any sensitizer.

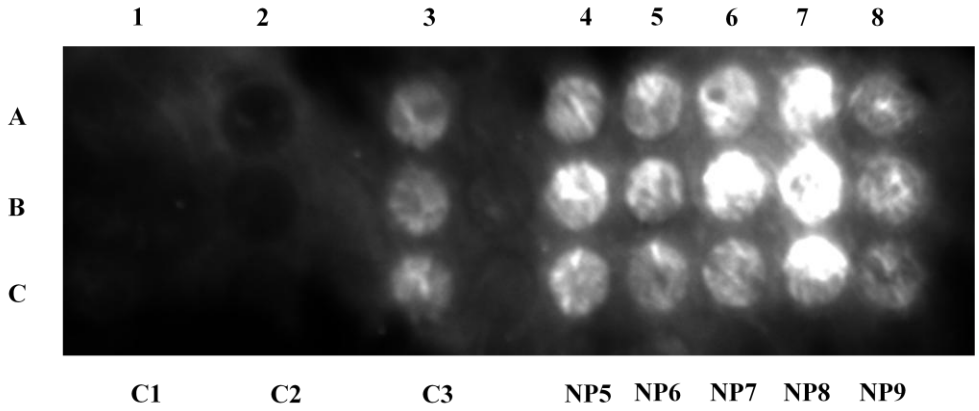

C1: Biotin-dopamine (**BD2**) + **NP9** (0.5 mM); **C2**: **NP9** + light; **C3**: Biotin-dopamine (**BD2**) +light; **NP5**: Biotin-dopamine (**BD2**) + **NP5** + light; **NP6**: Biotin-dopamine (**BD2**) + **NP6** + light; **NP7**: Biotin-dopamine (**BD2**) + **NP7** + light; **NP8**: Biotin-dopamine (**BD2**) + **NP8** + light; **NP9**: Biotin-dopamine (**BD2**) + **NP9** + light.

Figure 84. Incorporation of biotin-dopamine (**BD2**) (0.5 mM) in pericardium tissue using **NP5-NP9** (0.5 mM) and 15 minutes of light irradiation. Lanes 1, 2 and 3 are controls.

Since biotin-histidine, biotin-hydrazide and biotin-tyramine were most commonly incorporated into the proteins in the model studies, these compounds were examined in this tissue model to observe if a similar result would be obtained. Figures 85, 86 and 87 show the result of exposing the surface of the pericardium tissue to biotin-histidine, biotin-tyramine, and biotin-hydrazide using **NP5-NP9** as sensitizers with 15 minutes of light irradiation. In general, these experiments suffered from significant background signals as well as heterogeneity and often signal saturation due to a difficult-to-control

chemiluminescent reaction. The incorporation studies using biotin-tyramine (Figure 85) were the most definitive, showing a consistent strong signal for its incorporation when **NP5** was used as a sensitizer, and one positive signal when using **NP7**. It appears that biotin-histidine (Figure 86) was also incorporated to some extent upon sensitization, although the signals for the control samples (photolysis without a naphthalimide) are rather high. Biotin-hydrazide was observed to incorporate strongly into the tissue sample regardless of the addition of a naphthalimide sensitizer. This experiment in particular resulted in signals that overwhelmed the detector and/or the detection substrate solution (causing dark spots) and so is not interpretable.

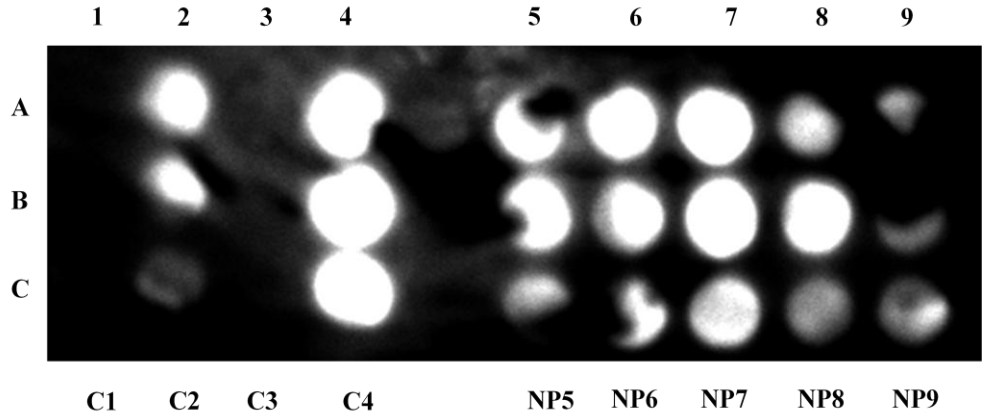

C1: Biotin-histidine (**BD5**) + **NP9** (0.5 mM); **C2**: **NP9** + light; **C3**: Biotin-histidine (**BD5**) +light; **C4**: (Positive control) Biotin-dopamine (**BD2**) + **NP8** + light; **NP5**: Biotin-histidine (**BD5**) + **NP5** + light; **NP6**: Biotin-histidine (**BD5**) + **NP6** + light; **NP7**: Biotin-histidine (**BD5**) + **NP7** + light; **NP8**: Biotin-histidine (**BD5**) + **NP8** + light; **NP9**: Biotin-histidine (**BD5**) + **NP9** + light.

Figure 85. Incorporation of biotin-histidine (**BD5**) in pericardium tissue using **NP5-NP9** and 15 minutes of light irradiation. Lanes 1, 2 and 3 negative controls; Lane 4 is a positive control in which the tissue was reacted with biotin-dopamine (**BD2**) and **NP8**.

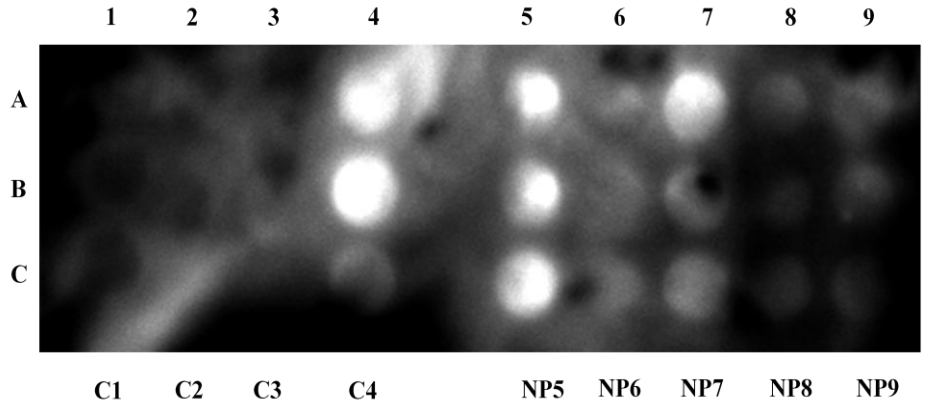

C1: Biotin-tyramine (**BD9**) + **NP9** (0.5 mM); **C2**: **NP9** + light; **C3**: Biotin-tyramine (**BD9**) +light; **C4**: (Positive control) Biotin-dopamine (**BD2**) + **NP8** + light; **NP5**: Biotin-tyramine (**BD9**) + **NP5** + light; **NP6**: Biotin-tyramine (**BD9**) + **NP6** + light; **NP7**: Biotin-tyramine (**BD9**) + **NP7** + light; **NP8**: Biotin-tyramine (**BD9**) + **NP8** + light; **NP9**: Biotin-tyramine (**BD9**) + **NP9** + light.

Figure 86. Incorporation of biotin-tyramine (**BD9**) in pericardium tissue using **NP5-NP9** and 15 minutes of light irradiation. Lanes 1, 2 and 3 negative controls; Lane 4 is a positive control in which the tissue was reacted with biotin-dopamine (**BD2**) and **NP8**.

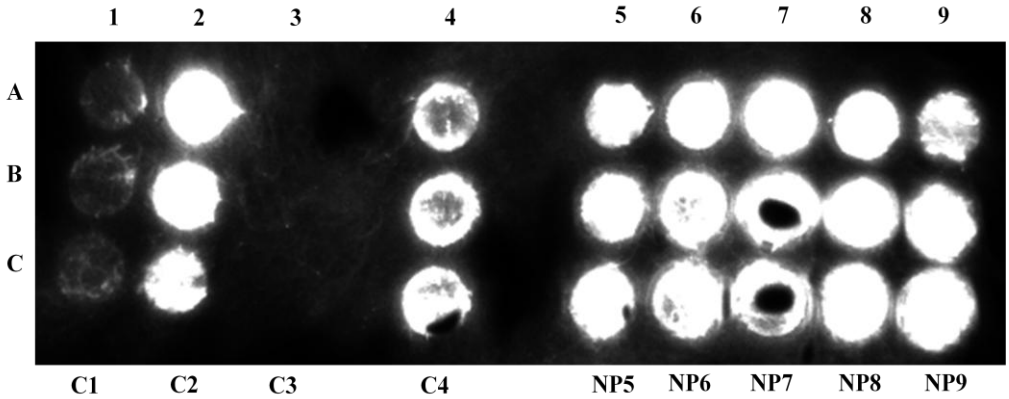

C1: Biotin-hydrazide (**BD1**) + **NP9** (0.5 mM); **C2**: **NP9** + light; **C3**: Biotin-hydrazide (**BD1**) +light; **C4**: (Positive control) Biotin-dopamine (**BD2**) + **NP8** + light; **NP5**: Biotin-hydrazide (**BD9**) + **NP5** + light; **NP6**: Biotin-hydrazide (**BD9**) + **NP6** + light; **NP7**: Biotin-hydrazide (**BD9**) + **NP7** + light; **NP8**: Biotin-hydrazide (**BD9**) + **NP8** + light; **NP9**: Biotin-hydrazide (**BD9**) + **NP9** + light.

Figure 87. Incorporation of biotin-hydrazide (**BD1**) in pericardium tissue using **NP5-NP9** and 15 minutes of light irradiation. Lanes 1, 2 and 3 negative controls; Lane 4 is a positive control in which the tissue was reacted with biotin-dopamine (**BD2**) and **NP8**.

Similarly, the reactivity of biotin-tryptophan and biotin-dopamine catalyzed by the photolysis of naphthalimides **NP7** and **NP8** was examined (Figure 88). Although in this experiment the detector is relatively saturate, it appears due to the size and uniformity of the signals that the incorporation of these compounds into the tissue may have been catalyzed by the naphthalimide photolysis.

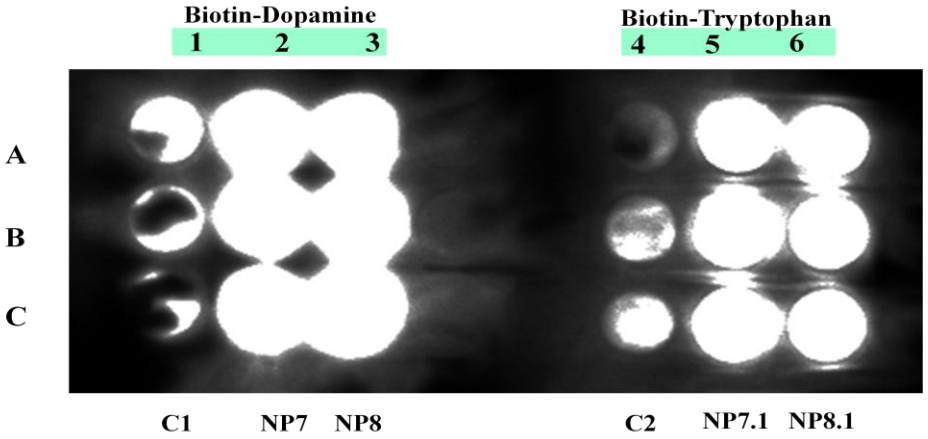

C1: Biotin-dopamine (**BD2**) (0.5 mM) + light; **C2**: Biotin-tryptophan (**BD4**) (0.5 mM) + light; **NP7**: Biotin-dopamine (**BD2**) (0.5 mM) + **NP7** (0.5 mM) + light; **NP8**: Biotin-dopamine (**BD2**) (0.5 mM) + **NP8** (0.5 mM) + light; **NP7.1**: Biotin-tryptophan (**BD4**) (0.5 mM) + **NP7** (0.5 mM) + light; **NP8**: Biotin-tryptophan (**BD4**) (0.5 mM) + **NP8** (0.5 mM) + light.

Figure 88. Incorporation of biotin-dopamine (**BD2**) and biotin-tryptophan (**BD4**) in pericardium tissue using **NP7** and **NP8** as sensitizers and 15 minutes of light irradiation.

In order to try to reduce the background signals and to demonstrate a dose-response type behavior for this reaction, the irradiation time of samples of biotin-dopamine with **NP8** was varied (Figure 89). It is clear from this experiment that more incorporation occurs with more photolysis, and that the naphthalimide catalyzes the reaction (see especially lanes 5 & 6 – 3 minutes photolysis). Similarly, at 1 minute biotin-hydrazide (**BD1**) was effectively incorporated into the pericardium tissue (Figure 90). This experiment also clearly shows the naphthalimide-catalyzed photochemical

incorporation of biotin-dopamine **BD-2** into pericardium, confirming previous experiments.

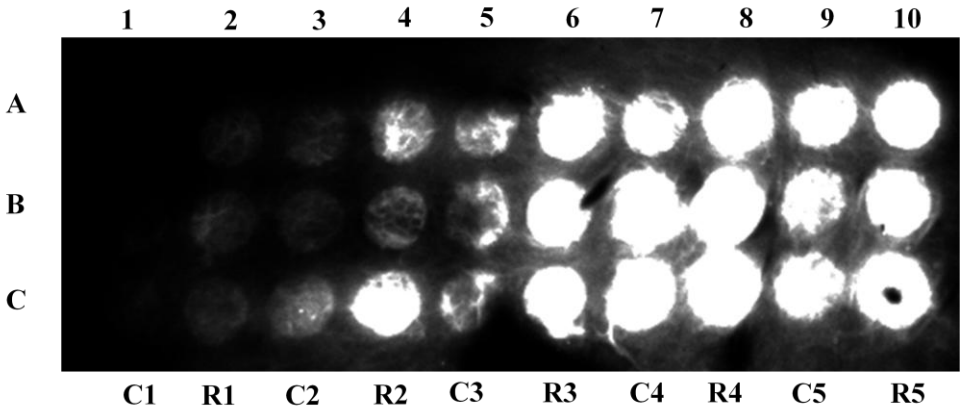

C1: Biotin-dopamine (**BD2**) + 30 sec light; **R1**: Biotin-dopamine (**BD2**) + NP8 + 30 sec light; **C2**: Biotin-dopamine (**BD2**) + 1 min light; **R2**: Biotin-dopamine (**BD2**) + NP8 + 1 min light; **C3**: Biotin-dopamine (**BD2**) + 3 min light; **R3**: Biotin-dopamine (**BD2**) + NP8 + 3 min light; **C4**: Biotin-dopamine (**BD2**) + 5 min light; **R4**: Biotin-dopamine (**BD2**) + NP8 + 5 min light; **C5**: Biotin-dopamine (**BD2**) + 10 min light; **R5**: Biotin-dopamine (**BD2**) + NP8 + 10 min light

Figure 89. Time dependence in the incorporation of biotin-dopamine (**BD2**) (0.5 mM) in pericardium tissue using **NP8** (0.5 mM) as sensitizer.

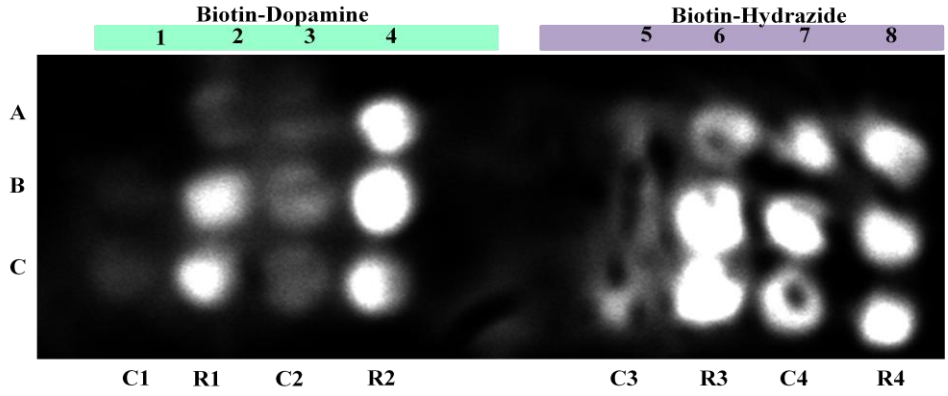

C1: Biotin-dopamine (**BD2**) + 1 min light; **R1**: Biotin-dopamine (**BD2**) + **NP8** + 1 min light; **C2**: Biotin-dopamine (**BD2**) + 3 min light; **R2**: Biotin-dopamine (**BD2**) + **NP8** + 3 min light; **C3**: Biotin-hydrazide (**BD1**) + 1 min light; **R3**: Biotin-hydrazide (**BD1**) + **NP8** + 1 min light; **C4**: Biotin-hydrazide (**BD1**) + 3 min light; **R4**: Biotin-hydrazide (**BD1**) + **NP8** + 3 min light.

Figure 90. Incorporation of biotin-dopamine (**BD2**) (0.5 mM) and biotin-hydrazide (**BD1**) (0.5mM) in pericardium tissue using **NP8** (0.5 mM) as sensitizers.

Photochemical Incorporation of Biotin Derivatives into Fetal Pig Skin

Pig skin was also tested in the incorporation studies with the biotinylated amino acid side chains and the sensitizers. The combination of biotin-dopamine and **NP8** was used initially as this combination was the most consistently active. The results are shown in Figure 91, and it is clear that with irradiation for 3 or 5 minutes that the biotin-dopamine is incorporated in a naphthalimide-dependent fashion. Although the results were less dramatic, biotin-hydrazide (**BD1**) can also be incorporated into pig skin using naphthalimide 8 as the sensitizer (Figure 92). Another experiment revealed that these biotin derivatives are incorporated into pig skin when using a variety of naphthalimide sensitizers (Figure 93), although this particular tissue sample, which upon initial visual inspection appeared to be more hetereogeneous, gave inconsistent results.

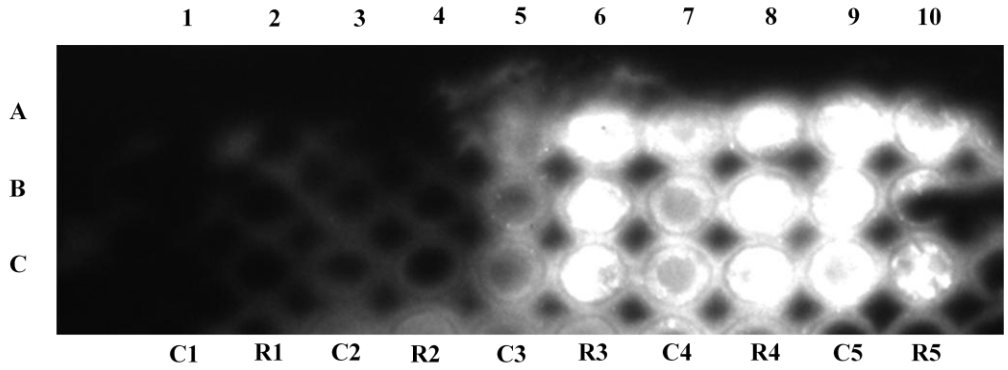

C1: Biotin-dopamine (**BD2**) + 30 sec light; **R1**: Biotin-dopamine (**BD2**) + NP8 + 30 sec light; **C2**: Biotin-dopamine (**BD2**) + 1 min light; **R2**: Biotin-dopamine (**BD2**) + NP8 + 1 min light; **C3**: Biotin-dopamine (**BD2**) + 3 min light; **R3**: Biotin-dopamine (**BD2**) + NP8 + 3 min light; **C4**: Biotin-dopamine (**BD2**) + 5 min light; **R4**: Biotin-dopamine (**BD2**) + NP8 + 5 min light; **C5**: Biotin-dopamine (**BD2**) + 10 min light; **R5**: Biotin-dopamine (**BD2**) + NP8 + 10 min light

Figure 91. The incorporation of **BD2** (0.5 mM) in pig skin using **NP8** (0.5 mM) as sensitizer.

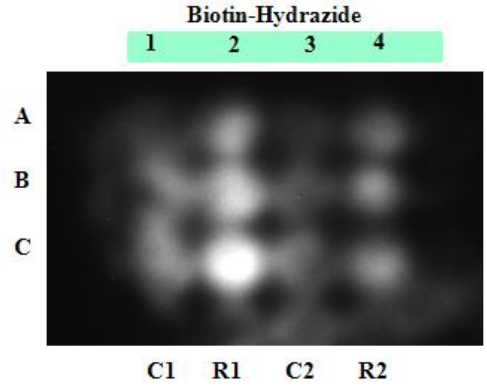

C1: Biotin-hydrazide (**BD1**) + 3 min light; **R1**: Biotin-hydrazide (**BD1**) + **NP8** + 3 min light; **C2**: Biotin-hydrazide (**BD1**) + 1 min light; **R2**: Biotin-hydrazide (**BD1**) + **NP8** + 1 min light.

Figure 92. Incorporation of biotin-hydrazide (**BD1**) (0.5mM) in pig skin using **NP8** (0.5 mM) as sensitizer.

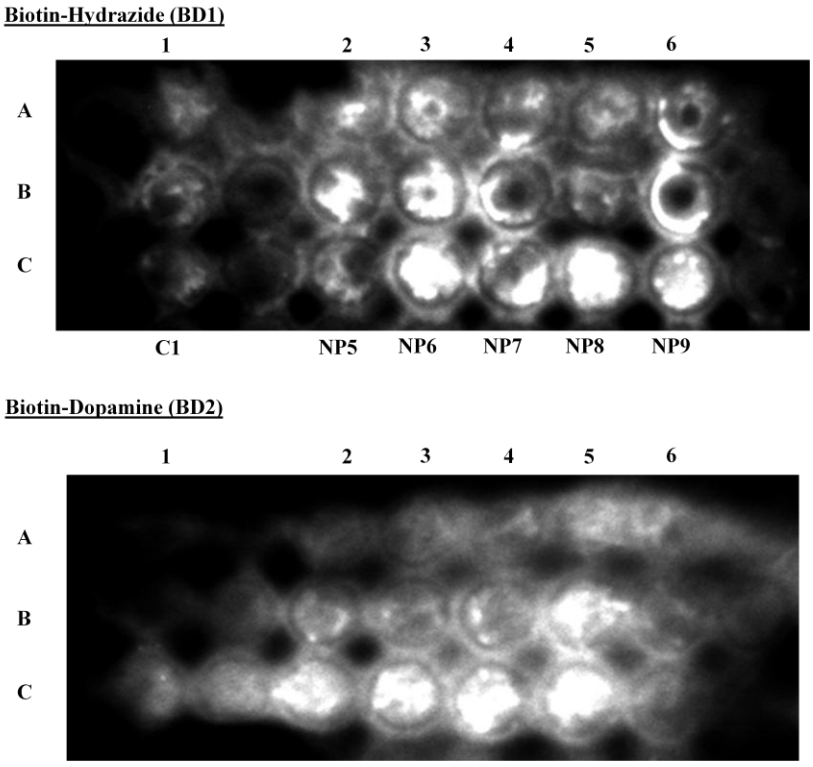

C1: **BD** + 3 min light; **NP5**: **BD** + **NP5** + 3 min light; **NP6**: **BD** + **NP6** + 3 min light; **NP7**: **BD** + **NP7** + 3 min light; **NP8**: **BD** + **NP8** + 3 min light; **NP9**: **BD** + **NP9** + 3 min light.

Figure 93. Incorporation of biotin-hydrazide (**BD1**) (0.5 mM) and biotin-dopamine (**BD2**) (0.5 mM) in pig skin using as sensitizers **NP (5-9)** (0.5 mM) and 3 minutes of light irradiation.

CHAPTER FOUR

Conclusions and Future Directions

Studies for protein modification were carried out using four types of proteins, from which RNase A and Lysozyme were selected as models for studying the effect of the unsubstituted and 4-substituted naphthalimide derivatives. It was observed that under the same photochemical conditions the two proteins showed the same trend with respect to the photosensitizers, where more crosslinking was observed when **NP5** (unsaturated naphthalimide) and the brominated **NP6** were used. A series of biotin labeled derivatives were synthesized to determine the influence of oxidizable amino acid residues such as histidine, tryptophan, tyramine, and methionine, in the mechanism for protein modification. Hydrazide and dopamine derivatives were also tested showing promising results in the protein and tissue models. Incorporation was observed the most for both protein models when biotin-dopamine **BD2**, biotin-histidine **BD5**, biotin-tyamine **BD9** and biotin-hydrazide **BD1** were present in the reaction mixture. In general, biotin-labeled derivatives were more incorporated in RNase A than in Lysozyme which could be intimately associated with the surface accessibility of the most susceptible amino acids residues to photo-oxidation in the proteins; an explanation for this could be cumbersome due to the complexity of the proteins.

From all the naphthalimide tested as photosensitizers in this project, it could be concluded that **NP5** and **NP9** react under different mechanisms depending on the biotin-derivative employed during the photochemical reaction. Reactions of biotin labeled

derivatives in the presence of **NP5** goes more toward a Type I mechanism since the addition of the singlet oxygen quencher sodium azide promoted the incorporation of the biotin-derivatives, while **NP9** seems to be more versatile since it can undergo either a Type II mechanism (biotin-dopamine **BD2**, biotin-histidine **BD5** and biotin-hydrazide **BD1**) or a Type I mechanism (biotin-tyramine **BD9** and biotin-tryptophan **BD4**). The addition of catalytic amounts of superoxide dismutase to the naphthalimide mediated crosslinking of RNase A and lysozyme stimulated the crosslinking in both proteins when **NP8** was employed as the photosensitizer; this influence was more dramatic in the case of lysozyme suggesting the primacy of a type I mechanism for lysozyme when sensitized with **NP8**. Future work exploring the role of oxygen in the modification reaction by studying the influence of sodium azide and SOD dismutase in these protein models using the other naphthalimide derivatives should be done in other to have a better understanding of the mechanism followed by these proteins during the photochemical modification.

It can also be concluded that the crosslinking of proteins and tissues depends on the way the amino acid residues are activated. Crosslinking and incorporation were favored when the amino acids present in the protein and in the biotin derivatives were activated at the same time, and also when the protein was pre-activated followed by addition of the biotin derivatives (not activated under illumination in the presence of sensitizer). According to this, the modification of the protein occurrs mainly by using the amino acid residues present in the protein.

Tissues experiments showed promising results when incorporation in pericardium tissue was observed for biotin-dopamine **BD2**, biotin- histidine **BD5**, biotin-hydrazide

BD1 and biotin-tyramine **BD9**, when unsubstituted and 4-substituted naphthalimide **NP(5-9)** were employed as sensitizers. These results allows to correlate the proteins model with the tissue model, at least in the case of pericardium tissue, since the same biotin labeled derivatives that showed the most activity for RNase A and lysozyme were the most efficient for the tissues experiment as well. Unfortunately, meniscus tissue and pig skin studies did not show satisfactory results which means that more optimization conditions are needed to obtain more efficient and reproducible data.

The mass spectral analysis of the photochemical oxidation of digested RNase A using 4-substituted ethoxy naphthalimide **NP8** as sensitizer in the presence of biotin-dopamine **BD2**, biotin-histidine **BD5** and biotin-hydrazide **BD1** showed the potential of this technique to elucidate the possible mechanism involved during these reactions, and to determine the peptide sequence of the amino acid residues involved during the modification of this protein. Future studies should involve the analysis of the photochemical reaction using only the peptide sequences that were identified and showed a change in the intensity after modification reaction when compared with the control sample.

CHAPTER FIVE

Introduction

DNA Enzymes and In vitro Selection

The technique of "*in vitro* selection" is a powerful approach to identify new catalysts with desired activities from random-sequence pools of candidate molecules. In our laboratory, the use of *in vitro* selection has allowed the identification of deoxyribozymes using organic molecules as cofactors or coenzymes, since deoxyribozymes or DNA enzymes are single-stranded DNA molecules with catalytic capabilities.

Actual evidences indicate that many RNA molecules and proteins are catalytically active for some of the most essential chemical transformations in biological systems. In the case of DNA no naturally occurring enzymes have been found to be composed of deoxyribose nucleic acid. This is not surprising since most DNA exists primarily as double-stranded form or a complete duplex, precluding it from adopting complex secondary or tertiary structures, which obviously lacks the necessary structural intricacy to act as a catalyst.[89] In addition, DNA appears to be less catalytically active than RNA, in part due to the lacks of a 2'-hydroxyl group that can participate in hydrogen bonding acting as both proton donor and acceptor (Figure 94). When compared with proteins, DNA lacks the functional groups found on amino acid side chains that are most commonly recognized as catalytic residues, including the imidazole in histidine, the carboxylate of aspartic acid and glutamic acid, the alkyl amine of lysine and the

sulfhydryl of cysteine (Figure 95). Moreover, at neutral pH, the nucleobases of DNA do not have significant acid/base properties. One could just postulate that DNA is simply not equipped with adequate chemical tools to function as a catalyst. However, when man-made DNA molecule was studied, it was found to possess a catalytic capability.[90]

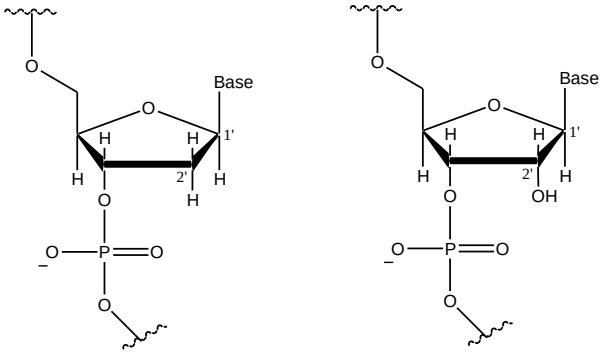

Figure 94. Part of DNA and RNA structure.

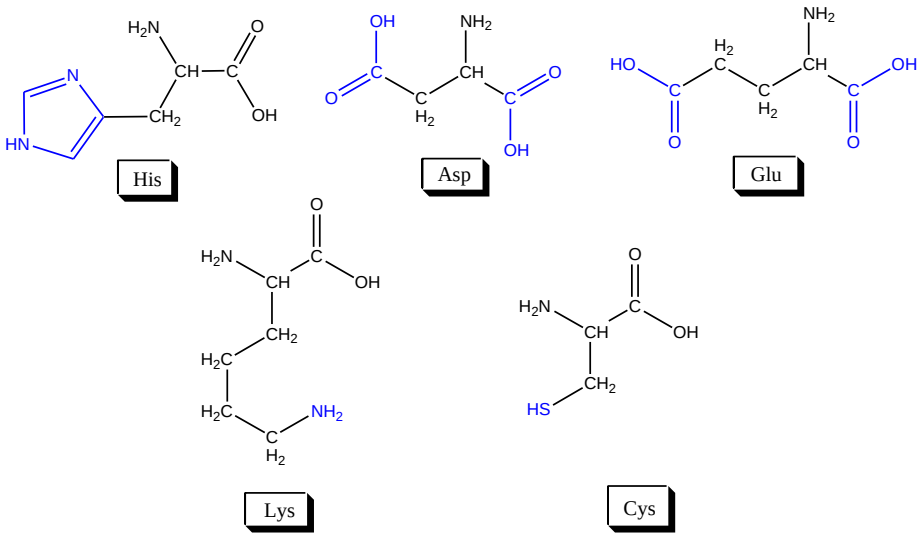

Figure 95. Amino acid side chains that most commonly recognized as catalytic residues.

Since the report of the first DNAzyme, hundreds of DNA sequences have been isolated in many research laboratories around the world to facilitate many chemical

transformations of biological importance. In recent years, considerable efforts have been undertaken to assess a variety of DNA enzymes for innovation-driven applications ranging from biosensors to gene regulators. The DNA enzyme field has been in existence for approximately 16 years. Although significant progress has been made and many catalytic DNA molecules have been generated and studied, there are still many challenges faced by DNA enzyme engineers.

There are several notable advantages of using DNA over RNA or protein, which justifies the practical application of DNA enzymes. First, DNA is more stable to use than RNA and protein. The absence of a 2'-OH group at each phosphodiester linkage makes DNA ~100,000-fold more stable to hydrolysis than RNA under physiological conditions.[91] DNA phosphodiester bonds are also ~1000-fold more resistant to hydrolytic degradation than are peptide bonds.[92] Second, DNA is less expensive and can be easily prepared through solid-phase synthesis. These two preceding properties generally make DNA more versatile and convenient to use. Other practical characteristics of DNA consist that it can be directly amplified by PCR, it can function in solution and on surfaces via immobilization, and it can be chemically modified to increase stability or provide extra functional moieties. Therefore, DNA enzymes can complement and extend the type of applications that may be suitable for synthetic enzymes.[93]

In 1994, Breaker and Joyce described the *in vitro* selection of a DNA enzyme that cleaves a specific RNA linkage within a nucleic strand.[90] They developed a method for rapidly obtaining DNA catalyst and DNA enzymes, starting from random sequences containing a pool of ~10^{14} DNA enzymes including a region of 50 random DNA nucleotides and a RNA phosphodiester position, assisted by a divalent metal cofactor.

After five rounds of *in vitro* selection, they obtained a population of singlet-stranded DNA molecules that catalyze efficient Pb^{2+}-dependent cleavage of a target RNA phosphoester.

Their idea is based on the DNA's property to bind a substrate molecule with high affinity and specificity, which is a prerequisite of a good enzyme. In addition, an enzyme must interact with well-positioned functional groups (either present in the enzyme or from a cofactor) to promote a particular chemical transformation. Furthermore, the enzyme must remain unchanged over the course of the reaction and show catalytic turnover.[94] Since then, many RNA-cleaving deoxyribozymes have been identified, some of which have been applied as practical metal sensors or *in vivo* to degrade messenger RNAs.[94]

Among all the deoxyribozymes made to date, the most efficient ones are metalloenzymes. The known metal-dependent deoxyribozymes have vastly different cation specificities. Some require a particular divalent metal ion to function, while others can make use of a broad range of metal ions.[95-97] Divalent metals ions can facilitate the folding of DNA into higher-order structures, and could potentially act as Lewis acids and general bases (in the form of a metal hydroxide) that can contribute directly to chemical catalysis by stabilizing the attacking and leaving groups.

In addition, it has also been reported the use of amino acid as a cofactor and an active component of an RNA cleavage reaction in *in vitro* selection of catalytic DNA, where a RNA-cleaving DNA enzyme was identified to use the amino acid histidine as a cofactor, from which the imidazole group is suggested to act as a general base.[98]

Most of the RNA cleavage reactions catalyzed by deoxyribozymes have been determined to proceed via a transesterification mechanism (Figure 96).

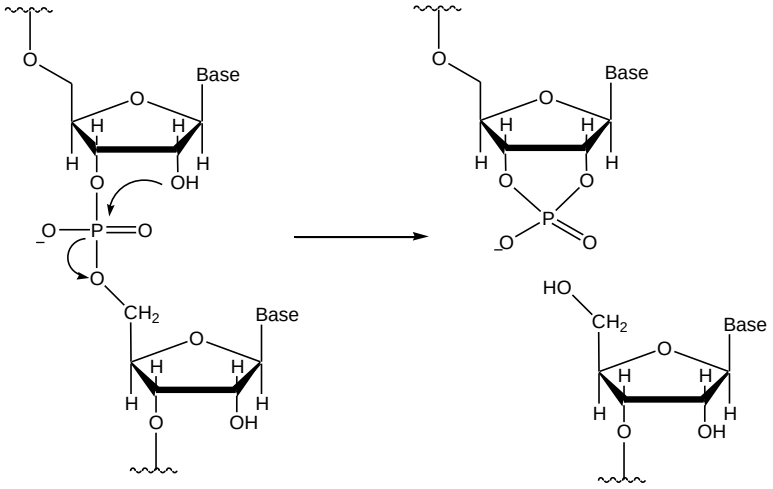

Figure 96. RNA cleavage reaction.

Following Breaker and Joyce discovery, several other deoxyribozymes cleaving similar linkages were also reported.[99-102] Joyce's and Famulok's groups have demonstrated that RNA-cleaving deoxyribozymes can be obtained using divalent metal ions such as Mg^{2+} [99] and Ca^{2+} [100, 103] The dependence of these enzymes on divalent metals can be considered as evidence to support a chemical mechanism involving metal-assisted deprotonation of the 2'-hydroxyl located adjacent to the cleavage site. This would produce a nucleophilic 2'-oxyanion that attacks the adjacent phosphorus, giving as a result the observed cleavage products. The metal may participate in the chemical mechanism of the DNA enzyme either as a metal hydroxide that serve as a general base to assist the deprotonation of the 2'-hydroxyl (Figure 97a) or as a Lewis acid that coordinates directly to the 2'-hydroxyl and enhances its acidity (Figure 97b). The metal

might also play a purely structural role, helping to organize the enzyme into its active conformation.[104]

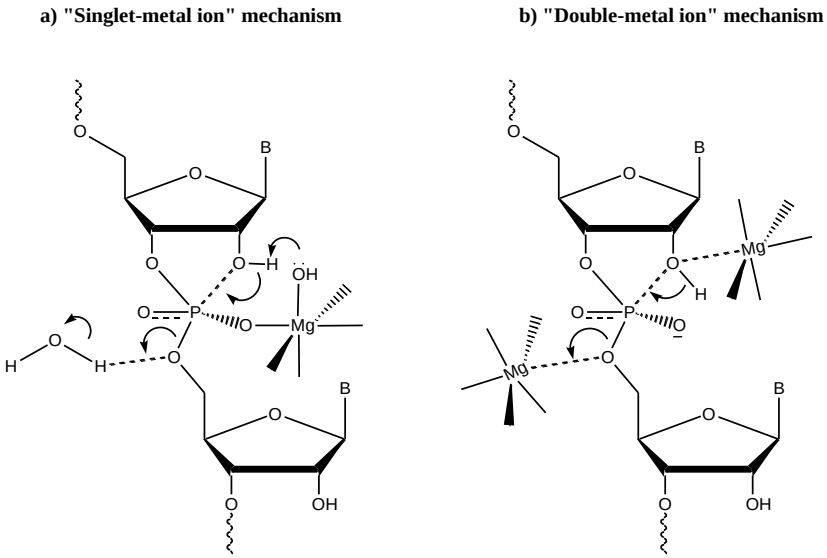

Figure 97. Two hypothetical chemical mechanisms for catalysis of RNA cleavage by divalent metals. a) Mechanism involving a divalent metal hydroxide that functions as a general base. b) Mechanism involving a divalent metal cation that functions as a Lewis acid.

Geyer and Sen later illustrated the intrinsic catalytic capability of DNA by isolating an RNA-cleaving deoxyribozyme whose activity is completely independent of divalent cations.[102] In 1998, Roth and Breaker demonstrated that DNA could take advantage of external chemical functional groups to enhance its catalytic capability by isolating an RNA-cleaving deoxyribozyme that uses histidine as an essential cofactor.[101] These studies, along with several other reports on the isolation of DNA enzymes for other chemical transformations, played an important role in the initial phase of the DNA enzyme study by demonstrating that DNA, possesses a catalytic power like it had been observed for protein and RNA. The RNA-cleaving deoxyribozymes mentioned so far could only cleave an RNA embedded residue placed in the DNA substrate, and fail to

cleave the same linkage within an all-RNA substrate. Joyce's group investigated the use of catalytic DNA in the destruction of viral RNAs by doing experiments *in vivo*. Their study led to the isolation of two remarkably small, yet catalytically efficient, deoxyribozymes that cleave all-RNA substrates.[105] One deoxyribozyme from this study, named '10-23' (Figure 98), can cleave almost any RNA molecule at an R-Y (R = purine; Y = pyrimidine) junction. It cleaves AU and G-U sites with very high proficiency and A-C and GC sites with reduced efficiencies.[104-106] The core of 10-23 is composed of only 15 nucleotides, flanked on each side by a substrate-binding arm of ~7-8 nucleotides. The catalytic efficiency (k_{cat}/K_M) of 10-23 is ~10^9 $M^{-1}min^{-1}$, a value that is limited by the rate of RNA-DNA duplex formation.[104] Under simulated physiological conditions, 10-23 exhibits k_{cat} and K_M values comparable to those of the natural hammer-head ribozyme.[104, 105]

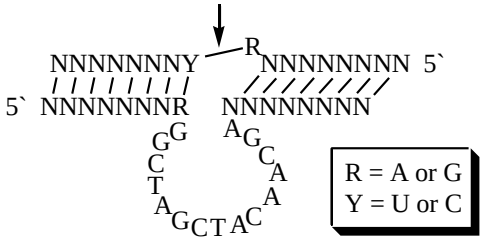

Figure 98. 10-23 RNA cleaving DNA enzyme.

The 10-23 enzyme has been used to power autonomous DNA nanomotors that can perform continuos conformational changes without human interference[93] (Figure 99). The DNA motor is composed by two oligonucleotide strands. One strand (blue) contains 10-23, and the other strand (cyan) contains a donor-acceptor pair of fluorophores, F1 and F2, on opposing ends. The presence of the two fluorophores allows any change in motion to be observed through fluorescence resonance energy transfer (FRET). The motor is fueled

by a chimeric (DNA/RNA) oligonucleotide substrate (red), which is susceptible to cleavage by 10-23. In the absence of the substrate, the motor adopts a ‘‘closed’’ conformation, characterized by a low fluorescence signal. However, when the substrate hybridizes to the DNAzyme, the DNA motor adopts an ‘‘open’’ conformation that leads to an increased fluorescence signal. Cleavage and subsequent dissociation of the substrate allows the DNA motor to once again adopt the closed conformation. This motor continues to cycle between the open and closed states as long as substrate is available.

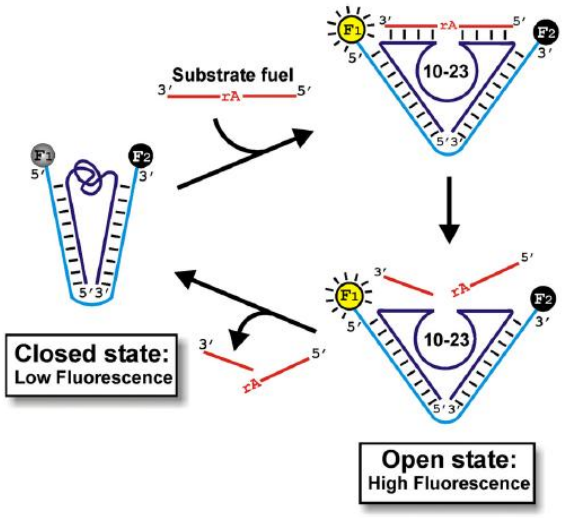

Figure 99. DNA nanomotor based on 10-23.[93]

The chemical stability, high catalytic proficiency and the ease of synthesis of DNA have made 10-23 an attractive alternative to ribozymes for the site-specific cleavage of biological RNA targets.

The 8-17 enzyme was another RNA-cleaving deoxyribozyme isolated alongside with 10-23.[105] Like 10-23, 8-17 is an extremely small DNA enzyme (Figure 100) with a catalytic core of 14-15 nucleotides, flanked by two substrate-binding arms of ~7-8 nucleotides each. 8-17 was initially shown to cleave an A-G junction,[105] and was later

demonstrated to cleave any N-G junction[107] (N stands for all four standard ribonucleotides).

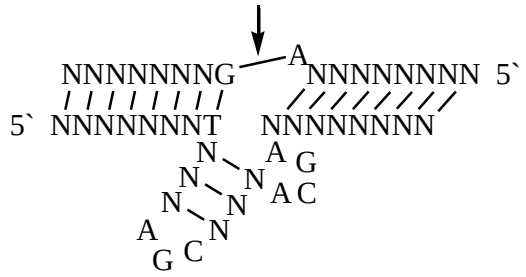

Figure 100. 8-17 RNA cleaving DNA enzyme.

The 8-17 DNA enzyme is able to cleave as many as 14 out of 16 possible RNA-DNA dinucleotide junctions.[108] It is important to point out that this small catalytic motif has been identified from four independent *in vitro* selection experiments.[100, 105-109] The recurrence of the 8-17 motif from four independent selection experiments may reflect its small size, its tolerance to sequence mutations and its catalytic fitness (i.e., high catalytic competency, adaptability to function under various metal ion conditions, and capability to cleave multiple dinucleotide junctions). Although 8-17 has not been shown to be as useful as 10-23 *in vivo*, it has been exploited for many *in vitro* applications, such as analytical devices in order to detect nucleic acids, metal ions, and small organic molecules.

One of the first DNA enzyme biosensors was based on 8-17 enzyme and exploited its Pb^{2+}-dependent RNA cleavage activity (Figure 101).[110] A Pb^{2+} biosensor was constructed with a fluorescent reporting system, by simply labeling the 5' end of the substrate with a fluorophore, and the 3' end of the DNA enzyme strand with a fluorescence quencher. In the uncleaved state, the substrate binds to the DNA enzyme, positioning the fluorophore and quencher in proximity to each other for maximal

fluorescence quenching. When Pb^{2+} is introduced into the solution, the DNA enzyme becomes active and cleaves the substrate, which subsequently dissociates from the DNA enzyme to generate a fluorescence signal.

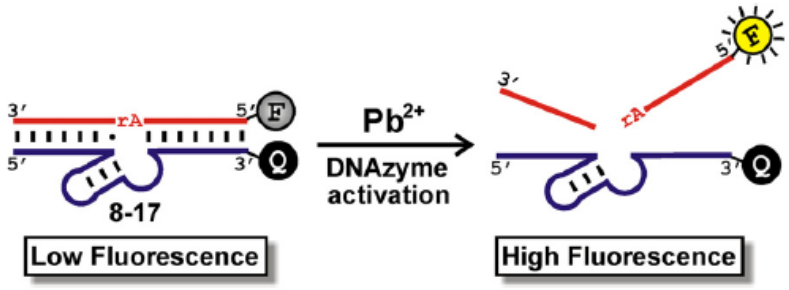

Figure 101. A Pb^{2+} biosensor based on 8-17.[96]

The original design signaling properties were improved by modifying the number, and type of fluorophores and quenchers used.[111, 112] Alternative reporter systems have also been developed based on colorimetric.[113,114] and electrochemical detection methods.[115] Biosensors for other types of toxic metal ions including Cu^{2+},[116,117] Hg^{2+},[118,119] and UO_2^{2+} [120] have also been developed. These biosensors can offer specific and useful sensitivity and selectivity, like in the case of UO_2^{2+} sensor which exhibits parts per trillion sensitivity and million-fold selectivity. [120]

Another deoxyribozyme capable of cleaving an all-RNA substrate denoted "Bipartite II" was reported recently by Sen's group.[121] The initial deoxyribozyme, denoted ‘Bipartite I’, can only cleave a single internal ribonucleotide phosphodiester embedded in a DNA strand. Bipartite II was another DNA enzyme isolated after re-selection of a DNA population containing the sequence of Bipartite I. Bipartite II (Figure 102) contains a 22-nucleotide catalytic core, which is slightly larger than those of 10-23 and 8-17. Similar to 8-17 and 10-23, this enzyme recognizes the RNA substrate by two

flanking binding arms where the arm-sequences can be altered to match a suitable RNA target. Bipartite II is capable of performing multiple-turnover catalysis with a k_{cat} of ~1.4 min^{-1} when a fragment of HIV-1 RNA was used as the substrate *in vitro*. It is not yet clear at the moment whether this DNA enzyme would be useful as a gene-deactivating agent as this enzyme has not been subjected to any *in vivo* study.

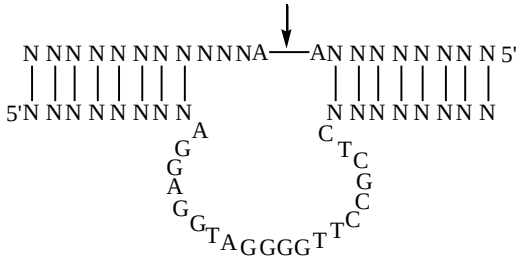

Figure 102. Bipartite II RNA cleaving DNA enzyme.

The first DNA enzyme equipped with foreign chemical functionalities was reported by Joyce and coworkers, who successfully isolated a novel RNA-cleaving deoxyribozyme from a DNA library containing C5-alkylimidazole-modified deoxyuridine (italicized "U" in the structure labeled "16.2-11" in figure 103) moieties in replacement of deoxythymidines.[99] The 16.2-11 enzyme requires three imidazole-modified nucleotides for its activity in addition to the essential metal cofactor, Zn^{2+}. However, it has not been determined whether the imidazole groups play a structural or catalytic role or both for the deoxyribozyme.

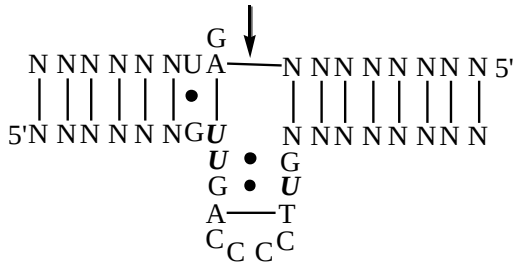

Figure 103. 16.2-11 DNA enzyme.

Subsequently, another group of DNA enzyme engineers have isolated a modified RNA-cleaving deoxyribozyme, termed 9_{25}-11 (Figure 104), which contains two foreign functionalities: an imidazole group placed on deoxyadenosine (italicized "A" in the structure of 9_{25}-11) and an alkylamine attached to deoxyuridine (italicized "U" in the same structure).[122, 123] The 9_{25}-11 enzyme was initially isolated to mimic RNase A. This enzyme is capable of carrying out multiple turnover RNA cleavage in the absence of any cofactors. Although the above efforts have shown that DNA enzymes modified with useful foreign chemical functionalities can be derived by *in vitro* selection, they have not led to the isolation of deoxyribozymes that are significantly more effective than the ones composed of bare DNA. Table 6 provides some perspective on the breadth of applications in which DNA enzyme has participated.[93]

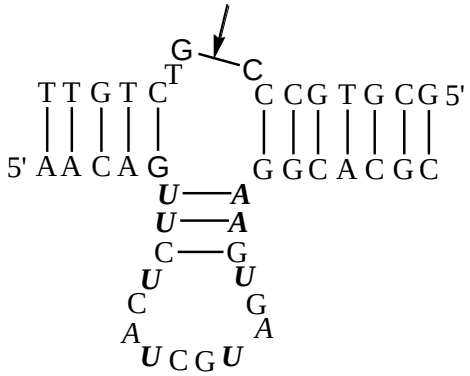

Figure 104. 9_{25}-11 RNA cleaving DNA enzyme.

Amino acids as cofactor for obtaining DNA enzymes

Roth and Breaker[101] identified a class of deoxyribozymes that catalyzed the cleavage of an RNA phosphoester bond by using the amino acid histidine as cofactor. The initial population of DNAs contained 40 random-sequence nucleotides. From the

four sequences classes identified (Figure 105), one class of DNA enzyme demonstrated complete dependence on histidine.

Table 6. Application of DNA enzyme *in vitro* and *in vivo*

Primary Category	Secondary Category	Examples
Molecular biology tools	Practical RNA cleavage[124]/ RNA ligation/RNA labeling[130]	3'-5' linkages,[125] Lariat RNA,[126] Branched RNA[127-129]
Therapeutic agents: mRNA cleavage in vivo	Antiviral, antibacterial, anticancer	Influenza A,[131] Hepatitis C,[132] HIV-1,[133] penicillin-binding protein,[134] VEGFR2,[135] c-Jun,[136,137] Erg1[138-140]
Nanomotors	Opening, closing/walking	10-23 nanomotor[141-143]
Analytical tool: Detection and/or quantification	Proteins, nucleic acids, RNA modifications, small molecules, metal ions[115-119]	Streptavidin,[144] DNA[145] and RNA,[146] 2'-O-methylribose,[147] Adenosine,[148] AMP,[149]ATP,[150] Pb^{2+}, Cu^{2+}, Hg^{2+}, UO_2^{2+}
Computational devices	Boolean function logic gates,[155] Arithmetic operations, automata	Half-adder,[151] full-adder,[152] circuits that play tic-tac-toe.[153,154]

class		Catalytic activity HEPES	histidine
I	(7) GTTGGGTCAC GGTATGGGGT CACTCGACGA AAATGCCGG	+	+
II	(6) AGGATTGGTT CTGGGTGGGT AGGAAGTTAG TGTGAGCCG	-	+
III	(4) CGGGTCGAGG TGGGGAAAAC AGGCAAGGCT GTTCAGGATG	+	+
IV	(3) AGGATTAAGC CGAATTCCAG CACACTGGCG GCCGCTTCAC	+	+

Figure 105. Four classes of histidine-dependent deoxyribozymes.

In orden to improve the catalytic activity of the DNA enzyme, a mutagenized pool based on the histidine dependent class deoxiribozyme was subjected to additional rounds of *in vitro* selection. Individual DNAs isolated from the *in vitro* selection after five rounds of re-selection (e.g., HD1 and HD2) were ~100-fold more active than the original class histidine-dependent deoxyribozyme and show specific patterns of conserved sequence and mutation acquisition that were characteristic of a relatively large and complex tertiary structure.

Experimental data supports a mechanism where the imidazole ring on the histidine participates as a general base in the deprotonation of the 2'-hydroxyl group.[101] This behavior was also observed by He et al. when they reported the DNA enzyme RNA cleavage using RNase A.[156] In the case of the proteinaceous enzyme RNase A, which does not require metal cofactors, the reaction was catalyzed by histidine residues at position 12 (His 12) and at position 119 (His 119) (Figure 106). The acid/base system provided by the two histidine residues in RNase A can, in principle, act in the same manner than "singlet-metal ion mechanism"does.

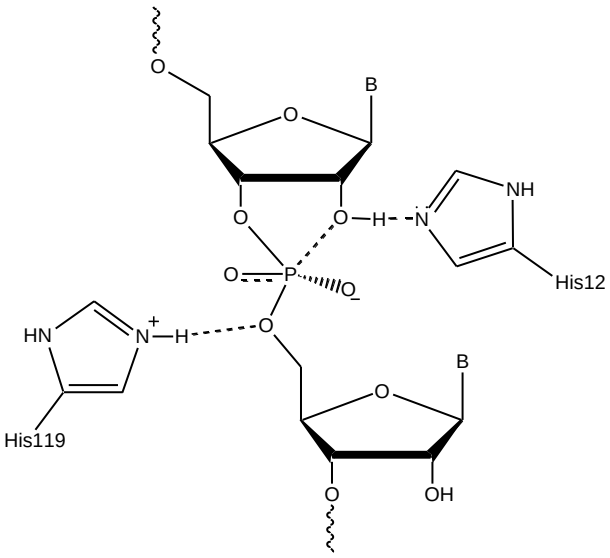

Figure 106. Proposed acid/base mechanism for the cleavage of RNA catalyzed by RNase A.

Due to the chemical repertorie observed in DNA enzymes compared to protein catalysts, several studies have incorporated prostetic groups built into the nucleic acid through the use of modified DNA nucleotides (Figure 107).[157-178]

Imidazole containing groups have also been synthesized and conjugated to oligonucleotides by Verbeure et all.[179] The imidazole moiety was used either unprotected, or protected with a monomethoxytrityl group or a *tert*-butyloxy carbonyl group (Figure 108).

Several small organic molecules designed for cleaving RNA through a hydrolytic pathway via an acid-base catalyzed mechanism have been reported in the past, including simple diamine or polyamine constructs, guanidine derivatives, or imidazole conjugates.[180] Their potential as ribonuclease mimics is attributed to the ability of imidazole rings to coordinate metal ions.[181,182]

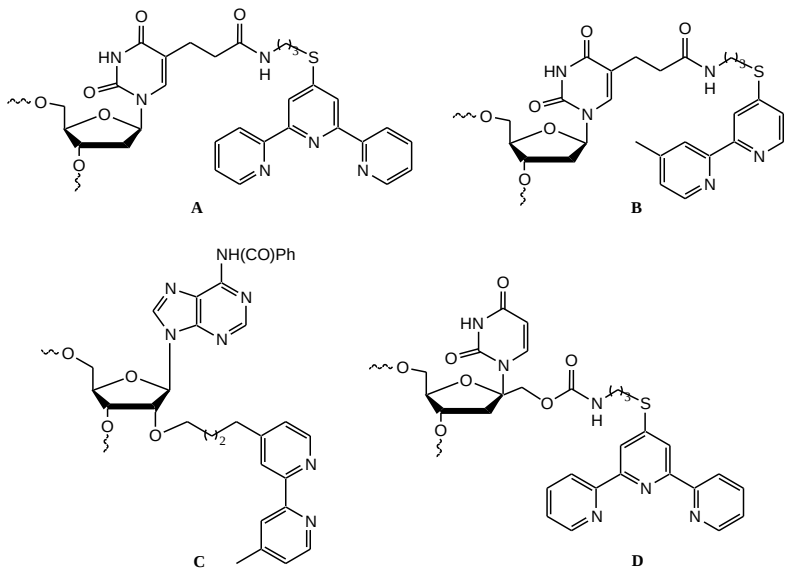

Figure 107. Examples of the catalytic cores of several ribozyme mimics. (A) First example of wholly synthetic ribozyme mimic, a major-groove-directed terpy conjugate. (B) A major-groove-directed bipyridine conjugate. (C) A minor-groove-directed bipyridine conjugate. (D) A minor-groove-directed terpy conjugate.

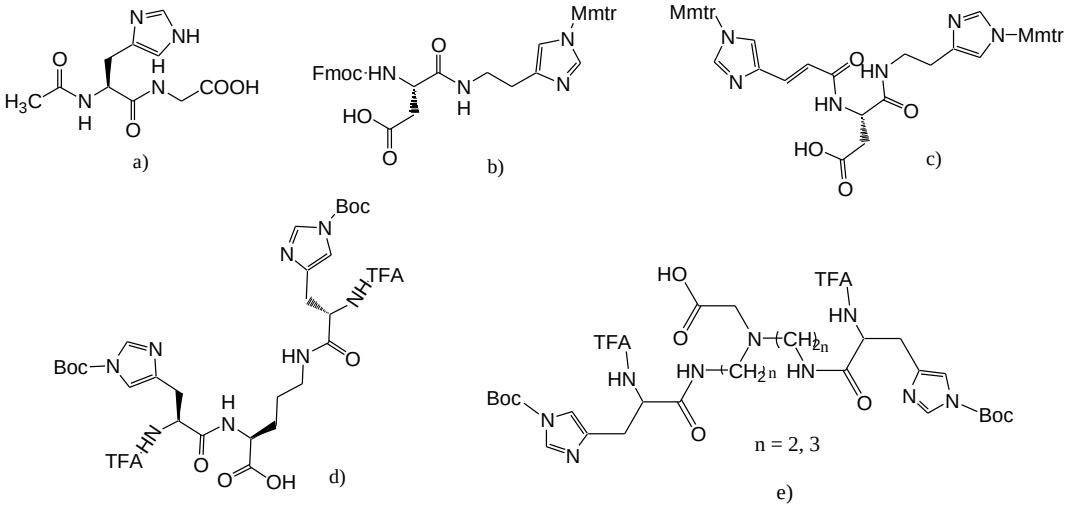

Figure 108. Imidazole ribozyme mimics.

Monoimidazole conjugates of oligonucleotides have previously been reported to exhibit cleaving activity in the absence[183] and presence[184] of metal ions. However, the cleavage process of oligonucleotides bearing a histamine group at the 3'-end in the

presence of Zn^{2+} ions is not very efficient,[184] i.e., 2-5% of RNA is cleaved in 19 h at room temperature. Even though conjugation of a random diimidazole constitute a strand of DNA, the observance of hydrolytic activity is not predictable. For this reason, various backbones bearing juxtaposed functionalities have been used to link the catalytic unit to the oligonucleotide. The amino groups could provide additional charge stabilization on the transition-state or, in its protonated state, improve affinity for the phosphodiester backbone.

Current Research Goals and Strategies

The goal of this research project is the synthesis and study of small organic molecules that can be used as cofactor for the discovery of DNA enzymes using *in vitro* selection technique. Accordingly, it is intended to test different DNA enzymes that can catalyze the cleavage of a ribonucleotide phosphoester substrate embedded in a complete DNA strand, assisted by the synthetic organic cofactors. We also intended to gain a broader understanding of how these cofactors interact during the cleavage process. This may be achieved by testing different organic molecules with different structural characteristics and determining which ones enhance the catalytic activity of the DNA enzymes.

CHAPTER SIX

Materials and Methods

Reagents and Materials

Primers, DNA oligonucleotide template and other oligonucleotides were synthesized by Midland Certified Reagent Co. (Midland, TX) according to our specifications. Table 7 shows the sequence for template and primers used for this project. Taq DNA polymerase, dNTPs, 10X PCR buffers and 15 mM $MgCl_2$ solution were obtained from Promega Corporation and Fermentas. Streptavidin AffinitiTip^{TM} columns were obtained from Genosys Biotechnologies, Inc. Reagents for agarose gel electrophoresis, polyacrylamide gels were purchased from two sources, Ready Gel TBE-Urea Gel 15%, (Bio-Rad) and Ready Gel TBE-Urea Gel 20% (Jule Inc). 10X TBE buffer and TBE-urea sample buffer (89 mM Tris.HCl/89 mM boric acid/2 mM EDTA/7 mM urea/12% Ficoll/0.01% Bromophenol Blue/0.02% Xylene Cyanol FF) were obtained from Bio-Rad Laboratories. 10X TAE buffer was purchased through VWR and MassRuler^{TM} DNA ladder and 6X mass loading dye solution was obtained from Fermentas. Radiaoactive probes, adenosine 5'-triphosphate [γ-^{32}P] ultritide^{TM} 1mCi/mmol; 222 TBq/mmol and deoxyadenosine-5'-triphosphate, [α-^{32}P], 800Ci/mmol, 29.6 TBq/mmol, pH = 7.4-7.5, were purchased from INC Biomedicals. Radiolabeled samples were purified using Mini Quick Spin Oligo Columns from Roche. T4 Polynucleotide Kinase and high quality buffer for radiolabiling of DNA with radioactive material were obtained from Fermentas. Liquid radioactive samples were quantified in

Bio-Safe II liquid scintillation cocktail from Research Products International, Inc. Materials and reagents used during the synthesis of the DNA cofactors were provided by Sigma-Aldrich, VWR, and Acros and used as received. Hexane, chloroform, methanol, and ethyl acetate were obtained from commercial sources and distilled prior to use. DMF and DMSO were used as received. Ethanol for DNA precipitation was obtained as biological degree from VWR. 4-imidazoleacetic acid, 2-mercapto-5-benzimidazole sulfonic acid, L-histidine methyl ester and 4-amino-5-imidazole-carboxamide were purchased from Sigma-Aldrich and used as received.

Table 7. Primers and oligonucleotides used in *in vitro* selection

Primers	Sequences
Template (97 mer): T	5’-CTAATACGACTCACTATAGGAAGAGATGGC GACATCTC$(N)_{40}$GTGAGGTTGGTGTGGTTG-3’
Primer 1 (18 mer): P1	5’-CAACCACACCAACCTCAC-3’
Primer B2 (23 mer): PB2	5’-Biotin-GAATTCTAATACGACTCACTATrA-3’
Primer 2 (38 mer): P2	5’-GAATTCTAATACGACTCACTATAGGAAGA GATGGCGAC-3’
Primer B1 (18 mer): PB1	5’-Biotin-CAACCACACCAACCTCAC-3’
Primer B2rA (23 mer): PB2rA	5’-GAATTCTAATACGACTCACTATrA-3’
Substrate (23 mer): S	5’-CGACTCACATATrAGGAAGAGATG-3’

Instrumentation and Analytical Techniques

Polymerase Chain Reaction (PCR)

PCR reactions were carried out using a Robocycler® Thermocycler from Stratagene. DNA samples were centrifuged using an Eppendorf model 5415R refrigerated microcentrifuge. pH of buffer solutions were adjusted using a Corning pH Meter 430 that has been calibrated to pH values of 4, 7 and 10.

Agarose and PAGE Electrophoresis

Agarose gel was run using a Minicell® Primo^{TM} Thermo EC320 gel apparatus from Fischer Scientific. DNA gels were monitored using a UV transilluminator model LM-20E from VWR. Ten-well Precast 15 and 20 % Urea gels were purchased from Bio-Rad and Jule Inc. Polyacrylamide gel electrophoresis was conducted using a Bio-Rad mini protean 3 cell electrophoresis system connected to a VWR power supply. Gels were photographed using an Omega 10 imager.

Radioactive Labeling of DNA

A Beckman Coulter model LS 6500 Multi-Purpose Scintillation Counter was used to detect and calculate the amount of DNA labeled. Radioactive gels were dried employing a Gel Dryer FBGD45, a vapor trap and a Maxima® C Plus Vacuum Pump from Fischer Scientific. Gels were photographed using Fluor-S^{TM} Multilmager, Personal Molecular Imager FX^{TM} System, Kodak Phosphor storage K screen and Quantity One® quantification software version 4.0 from Bio-Rad.

NMR Analysis

A Bruker 300 MHz NMR was used for ^{1}H, and ^{13}C analysis of the DNA enzymes RNA cleaving cofactors synthesized for the purpose of this investigation.

Synthetic Procedures

Synthesis of DNA Enzyme Cofactors

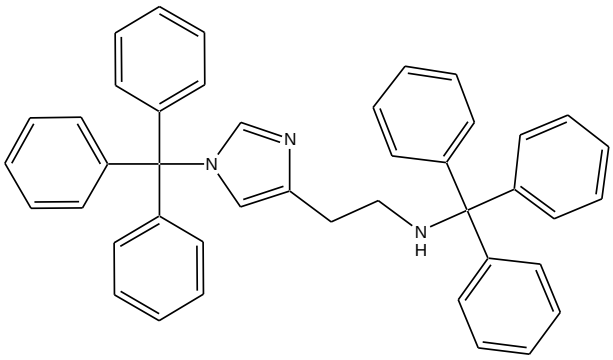

Figure 109. Structure of **C1**.

Trityl-[2-(1-trityl-1H-imidazol-4-yl)-ethyl]-amine (**C1**, Figure 109). (Diprotected histamine). **C1** which has previously been reported by our group,[185] was synthesized by dissolving histamine dihydrochloride (1 equivalent, 1.8 g, 10 mmol) in chloroform (25 mL), with addition of triethylamine (2 equivalents, 2.8 mL, 20 mmol). The solution was then stirred and refluxed for 25 min at 75 ºC. The solution was then cooled down to room temperature with a subsequent dropwise addition of a triphenyl methyl chloride solution in chloroform (4 equivalents, 11.1g, 40 mmol, 20 mL). The reaction was allowed to stir at room temperature for 24 h, followed by removal of the solvents, which afforded a yellow crude product containing the diprotected histamine. The product was purified by column chromatography using silica gel as the stationary phase, and a mixture of

EtOAc/Hex/NH_4OH (80:20:1) as the movil phase. A slightly basic medium (1% of NH_4OH) was required in the column to avoid the removal of the protective species placed in the amine groups of histamine, since silica column conditions are weakly acidic. The final product was collected as a light yellow solid (4.61 g, 78% yield) with R_f = 0.43 UV(+), ninhydrin(+) (EtOAc/Hex/NH_4OH, 50:50:1). ^{1}HNMR ($CDCl_3$, 300 MHz): δ 2.41 (t, 2H, *J* = 6.0 Hz), 2.75 (t, 2H, *J* = 6.0 Hz), 6.50 (s, 1H), 7.39-6.50 (m, 31H).

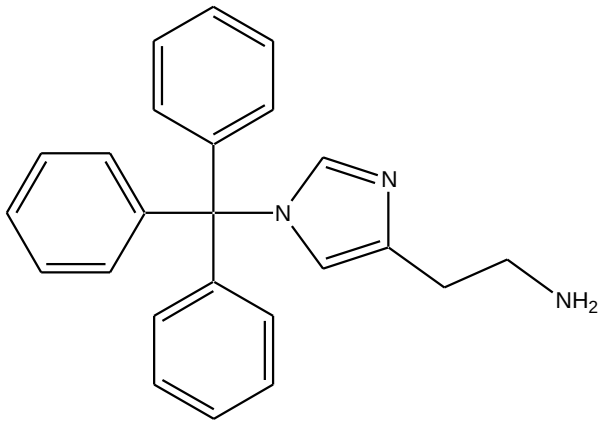

Figure 110. Structure of **C2**.

2-(1-trityl-1H-imidazole-4-yl)-ethylamine (**C2**, Figure 110). (Monoprotected histamine).[185] To a flask containing diprotected histamine compound **C1** (4.63 g, 7.8 mmol) was slowly added 10 mL of 5% trifluoroacetic acid in dichloromethane (v/v) until the solution turned deep yellow and the pH was around 3-4. The solution was stirred for 2 hours at room temperature and checked until reaction completion by TLC using a mixture of EtOAc/hex (20:80). The new derivative showed an R_f = 0.26 UV(+), ninhydrin (+). After complete disappearance of the diprotected histamine with an R_f = 0.43, the reaction was stopped by adding dropwise an 28 % aqueous NH_4OH solution until it turned milky white and the pH was slightly basic (around 7-8). The product was purified by column

chromatography using first a gradient mixture of EtOAc/Hex/NH_4OH (20:80:1), and then a mixture of 50:50:1 to completely elute the product from the column. Vacuum evaporation of the solvents afforded the monoprotected histamine **C2** (3.36 g, 73% yield). ^{1}H NMR (300 MHz,$CDCl_3$): δ 2.18 (s, 2H), 2.70 (t, 2H, *J* = 6.0 Hz), 3.01 (t, 2H, *J* = 6.0 Hz), 6.59 (s, 1H), 7.12-7.34 (m, 16H).

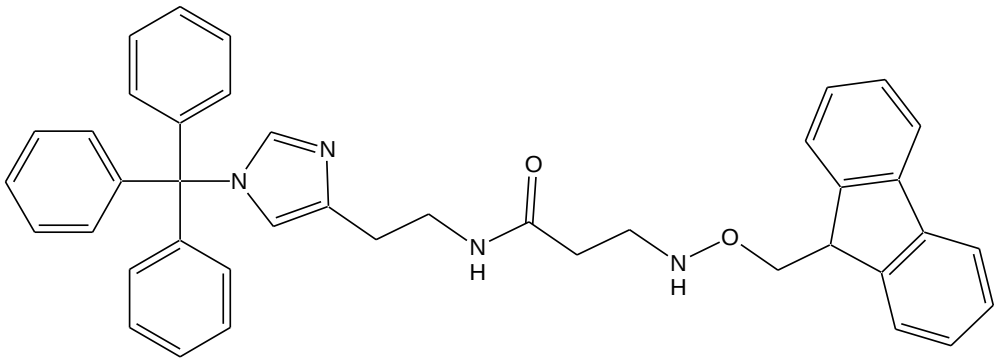

Figure 111. Structure of **C3**.

Fmoc-3-amino-N-[2-(1-trityl-1H-imidazol-4-yl)-ethyl]-propionamide (**C3**, Figure 111).[185] Fmoc-β-ala-OH (0.2 equivalents, 1.0 g, 2.0 mmol) was dissolved in DMF (10 mL), followed by addition of BOP (0.2 equivalents, 1.0 g, 2.0 mmol), The mixture was stirred for 20 minutes at room temperature, and then a solution of monoprotected histamine **C2** (0.44 g, 1.2 mmol) and triethyl amine (0.5 mL, 6.8 mmol) in DMF (5 mL) were added to the solution. The reaction mixture was stirred for 24 hours at room temperature and then washed with water and dichloromethane in a separatory funnel in order to remove the DMF and the impurities soluble in water. The organic layer was then dried with magnesium sulfate and concentrated in *vacuo*. Purification of the compound was achieved by column chromatography using EtOAc (100%). The final product was collected as a yellow solid (0.3 g, 68% yield) with a Rf = 0.75, UV (+), ninhydrin (-)

using a mixture of EtOAc/CH_3OH (9:1) as solvent. ^{1}H NMR (300 MHz, $CDCl_3$): δ 2.40 (t, 2H, *J* = 6.0 Hz), 2.74 (t, 2H, *J* = 6.0 Hz), 3.53 (t, 4H, *J* = 6.0 Hz), 4.13 (t, 1H, *J* = 6.0 Hz), 4.30 (d, 2H, *J* = 6.0 Hz), 6.35 (s, 1H), 6.60 (s, 1H), 6.67 (s, 1H), 7.10 (m, 7H), 7.34 (m, 13H), 7.57 (d, 2H, *J* = 9.0 Hz), 7.76 (d, 2H, *J* = 9.0 Hz).

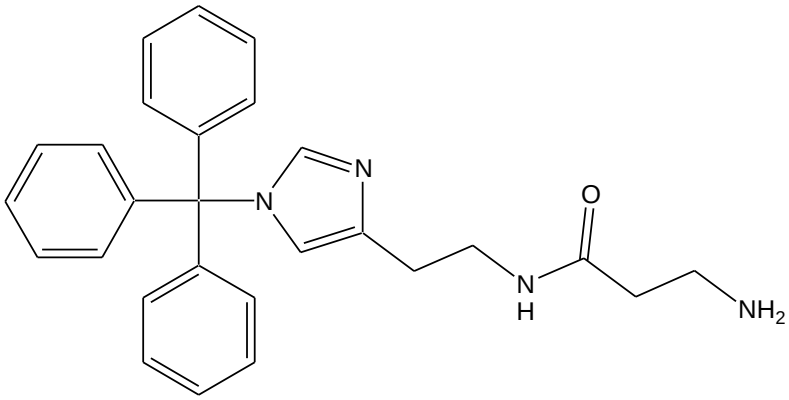

Figure 112. Structure of **C4**.

3-amino-N-[2-(1-trityl-1H-imidazol-4-yl)-ethyl]-propionamide (**C4**, Figure 112).[185] The fmoc protecting group was removed by adding 10 mL of a solution containing 50% piperidine in dichloromethane (v/v) and allowing it to react for 45 minutes at room temperature. Completion of the reaction was confirmed by TLC using a mixture of solvent EtOAc/CH_3OH (90:10): R_f = 0.34. Purification of the compound was achieved by column chromatography using the same mixture of solvents. The desired product was obtained as a yellowish solid (0.26 g, 89% yield). ^{1}H NMR (300 MHz, D_2O): δ 2.55 (t, 2H, *J* = 6.0 Hz), 2.67 (t, 2H, *J* = 6.0 Hz), 3.14 (m, 2H), 3.44 (m, 2H), 6.55 (s, 1H), 7.09 (m, 7H), 7.35 (m, 12H).

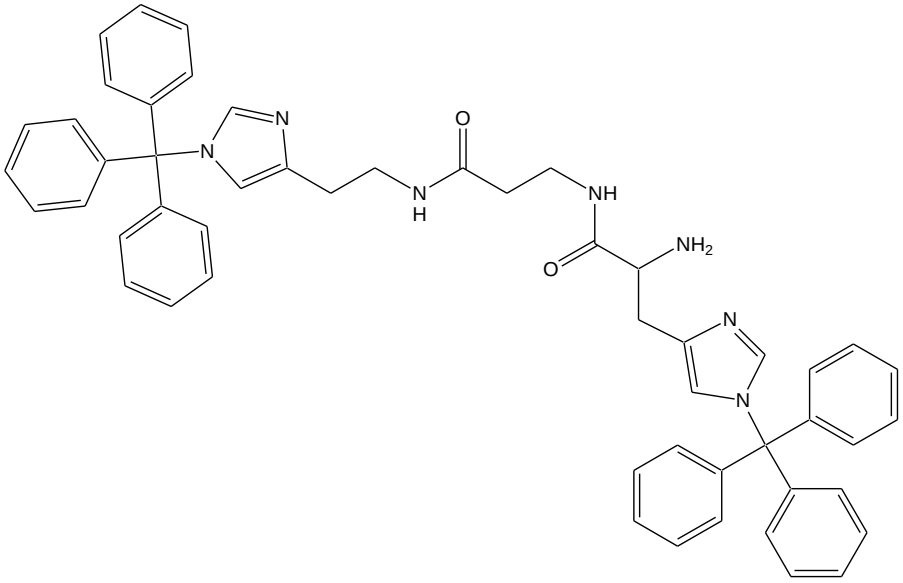

Figure 113. Structure of **C5**.

2-amino-3-(1-trityl-1H-imidazol-4-yl)-N-{2-[2-(1-trityl-1H-imidazol-4-yl)ethylcarbamoyl]-ethyl}-propionamide (**C5**, Figure 113).[185] Fmoc-His(1-Trt)-OH (0.2 equivalents, 1.0 g, 1.6 mmol) was dissolved in DMF (10 mL) followed by addition of 1.0 g of BOP (0.2 equivalents, 2.0 mmol). The mixture was stirred for 20 minutes at room temperature, and then a solution of compound **C4** (0.26 g, 0.62 mmol) and triethyl amine (0.5 mL, 6.8 mmol) in DMF (5 mL) were added to the mixture. The reaction solution was stirred for 24 hours at room temperature under dry N_2. The reaction was then washed with water, and extracted with dichloromethane; the organic layer was dried over sodium sulfate and concentrated in *vacuo*. The crude product was purified by flash chromatography using EtOAc (100%) to afford the desired product (0.16 g, 59% yield), R_f = 0.87, UV(+), ninhydrin (-). The fmoc protecting group was removed by adding 10 mL of a solution containing 50% piperidine in dichloromethane (v/v) and allowing it to react for 45 minutes at room temperature. Completion of the reaction was confirmed by TLC using a mixture of solvent EtOAc/CH_3OH (90:10): R_f = 0.45, UV(+), ninhydrin (+).

Purification by column chromatography afforded the desired product **C5** as a light yellow solid (0.13 g, 80% yield). ^{1}H NMR (300 MHz, $CDCl_3$): δ 2.33 (m, 2H), 2.72 (t, 2H, *J* = 6.0 Hz), 2.89 (dd, 1H, *J* = 15.0, 9.0 Hz), 3.03 (dd, 1H, *J* = 12.0, 6.0 Hz), 3.54 (m, 4H), 3.65 (m, 2H), 3.85 (broad singlet, 2H), 4.16 (m, 1H), 6.61 (s, 1H), 6.64 (1H), 7.13 (m, 12H), 7.37 (m, 21H), 8.25 (t, 1H, *J* = 6.0 Hz).

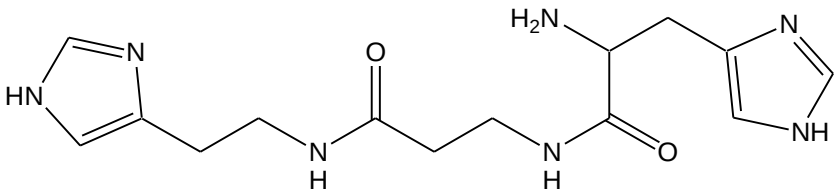

Figure 114. Structure of **C6**

2-Amino-3-(1H-imidazol-4-yl)-N-{2-[2-(1H-imidazol-4-yl)ethylcarbamoyl]-ethyl}-propionamide (**C6**, Figure 114)(histidine cofactor).[185] Compound **5** (0.5 g, 1 equivalent, 0.6 mmol) was mixed with 95% trifluoroacetic acid solution (2 mL) and stirred for 1 hour. Completion of the reaction was confirmed by TLC using a mixture of EtOAc/CH_3OH (90:10) (Rf = 0.25) and then the solution was concentrated *in vacuo*. The crude product was dissolved in water, extracted with chloroform and dried to afford the product histamine-β-alanine-histidine-NH_2 (**C6**) (0.18 g, 93% yield) as a light yellow solid. ^{1}H NMR (300 MHz, D_2O): δ 2.29 (t, 2H, *J* = 6.0 Hz), 2.80 (t, 2H, *J* = 6.0 Hz), 3.27 (m, 3H), 3.35 (m, 3H), 4.13 (t, 1H, *J* = 6.0 Hz), 7.13 (s, 1H), 7.30 (s, 1H), 8.45 (s, 1H), 8.58 (s, 1H). ^{13}C NMR (75 MHz, D_2O): δ 24.01, 26.06, 34.69, 36.07, 38.02, 52.14, 116.17, 118.41, 125.81, 130.72, 133.09, 134.38, 167.71, 173.59.

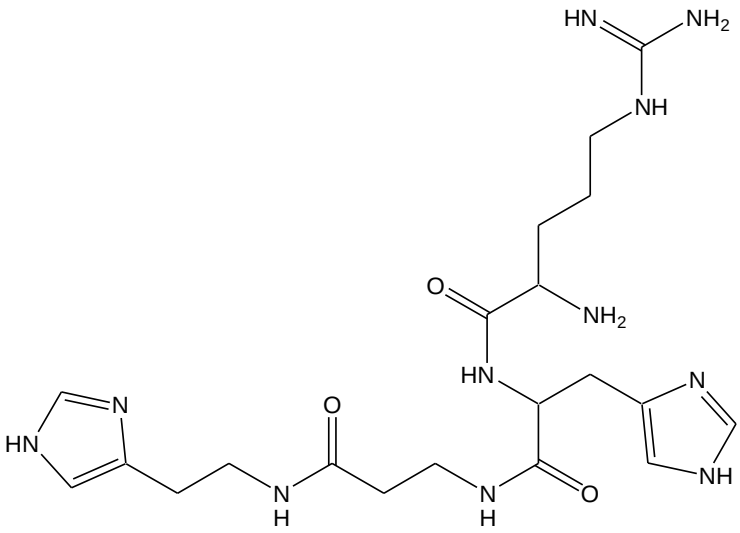

Figure 115. Structure of **C7**.

2-Amino-6-carbamimidoyl-hexanoic acid (2-(1H-imidazol-4-yl)-1-{2-[2-(1H-imidazol-4-yl)-ethylcarbamoyl]-ethylcarbamoyl}-ethyl)-amide (**C7**, Figure 115) (Arginine cofactor).[185] Boc-Arg(Boc)$_2$-OH (1.1 equivalent, 0.15 g, 0.33 mmol) and BOP (0.16 g, 1.1 equivalent, 0.33 mmol) were mixed in anhydrous DMF (5 mL) at 0 °C for 30 minutes. **C5** (0.25 g, 1 equivalent, 0.30 mmol) and triethylamine (1.1 equivalent, 0.05 mL, 0.33 mmol) were then added, and the mixture stirred for 24 hours at room temperature under N_2 atmosphere. Chloroform (10 mL) were added and then the reaction was washed twice with water and once with brine, and the organic layer dried over sodium sulfate and concentrated *in vacuo.* The crude product was purified by flash chromatography using EtOAc (100%) to afford the protected HA-(1-Trt)-β-Ala-His-(1-Trt)-Arg(Boc)$_2$-Boc (0.29 g, 0.23 mmol, 77% yield and Rf = 0.82). The protecting groups (Trt and Boc) were then removed by treatment with 95% trifluoroacetic acid solution (1 mL) in dichloromethane for 2 hours. Reaction completion was confirmed by TLC EtOAc/CH_3OH (90:10) and then concentrated *in vacuo* affording compound **C7**

(Arginine cofactor) (0.10 g, 88% yield, Rf = 0.31) as a white solid: ^{1}H NMR (300 MHz, D_2O): δ 1.55 (m, 2H), 1.83 (m, 2H), 2.30 (t, 2H, *J* = 6.0 Hz), 2.83 (t, 2H, *J* = 6.0 Hz), 3.11 (m, 4H), 3.29 (m, 2H), 3.38 (t, 2H, *J* = 6.0 Hz), 3.96 (s, 1H), 7.17 (s, 1H), 7.24 (s, 1H), 8.49 (s, 1H), 8.54 (s, 1H). ^{13}C NMR (75 MHz, D_2O): δ 23.53, 24.08, 26.44, 28.06, 34.61, 34.96, 35.97, 38.05, 40.41, 52.59, 52.95, 116.20, 117.33, 128.36, 130.75, 133.12, 133.67, 156.73, 169.38, 170.96, 173.61.

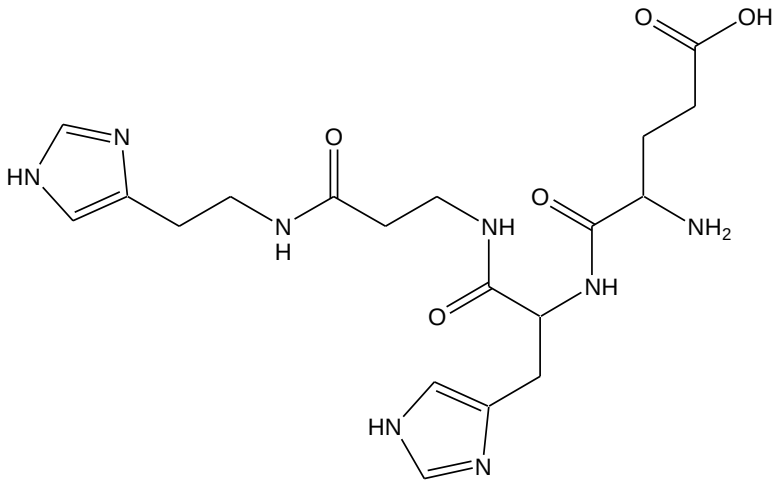

Figure 116. Structure of **C8**.

4-Amino-4-(2-(1H-imidazol-4-yl)-1-{2-[2-(1H-imidazol-4-yl)-ethylcarbamoyl]-ethylcarbamoyl}-ethylcarbamoyl)-butyric acid (**C8**, Figure 116)(Glutamic acid cofactor).[185] Compound **C5** (0.5 g, 1 equivalent, 0.6 mmol), Boc- Glu(OtBu)-OSu (0.24 g, 1 equivalent, 0.6 mmol) and triethylamine (1 equivalent, 80 μL, 0.6 mmol) were dissolved in anhydrous DMF (5 mL) and stirred for 24 hour under N_2 atmosphere. Chloroform (10 mL) were added to the reaction and then washed with water, brine, and the organic layer dried over sodium sulfate and concentrated *in vacuo.* The crude product was purified by flash chromatography using EtOAc (100%) with Rf = 0.76 affording

HA-(1-Trt)-β-Ala-His-(1-Trt)-Glu(OtBu)-Boc (0.4 g, 81% yield). The protecting groups (Trt, Boc and OtBu) were removed by adding 2 mL of 1M HCl in acetone (1:1.5) with 12 hours of reflux at 65 °C. After the reaction mixture was cooled down, acetone was removed *in vacuo* and the remaining aqueous solution was filtered. The water was evaporated *in vacuo* to afford the glutamic acid cofactor **C8** as a light yellow solid (0.21 g, 95% yield). ^{1}H NMR (300 MHz, D_2O): δ 2.03 (m, 2H), 2.26 (t, 2H, *J* = 6.0 Hz), 2.37 (t, 2H, *J* = 6.0 Hz), 2.78 (t, 2H, *J* = 6.0 Hz), 3.08 (m, 2H), 3.25 (t, 2H, *J* = 6.0 Hz), 3.33 (t, 2H, *J* = 6.0 Hz), 3.98 (t, 1H, *J* = 6.0 Hz), 4.51 (t, 1H, *J* = 6.0 Hz), 7.12 (s, 1H), 7.20 (s, 1H), 8.44 (s, 1H), 8.50 (s, 1H). ^{13}C NMR (75 MHz, D_2O): δ 24.04, 25.84, 26.40, 28.97, 34.96, 35.98, 38.03, 52.18, 52.93, 116.18, 117.32, 128.02, 130.72, 133.09, 133.63, 169.08, 170.80, 173.66, 175.87.

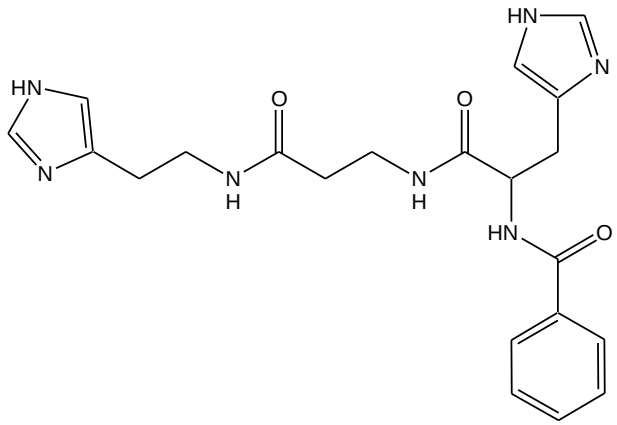

Figure 117. Structure of **C9**.

N-(2-(1H-imidazol-4-yl)-1-{2-[2-(1H-imidazol-4-yl)-ethylcarbamoyl]-ethylcarbamoyl}-ethyl)-isonicotinamide (**C9**, Figure 117) (Isonicotinic cofactor).[185] Isonicotinic acid (1.1 equivalent, 0.04 g, 0.33 mmol) and PyBOP (1.1 equivalent, 0.16 g, 0.33 mmol) were mixed in DMF (5 mL) at 0 °C for 15 min. **C5** (0.25 g, 1 equivalent, 0.3

mmol) and triethylamine (1.1 equivalent, 0.05 mL, 0.03 mmol) were added and stirred at room temperature for 24 hours under N_2 atmosphere. Chloroform (10 mL) were added to the reaction and then washed with water, brine, and the organic layer dried over sodium sulfate and concentrated *in vacuo*. The crude product was purified by flash chromatography using EtOAc (100%, Rf = 0.57) to afford the protected isonicotinamide derivative (0.19 g, 65% yield). The trityl protecting group was removed by treatment with 1 mL of 95% trifluoroacetic acid solution in dichloromethane for 2 hours. Reaction completion was monitored by TLC (Rf = 0.34), and the product purified by column chromatography using as solvent mixture of EtOAc/CH_3OH (90:10). The product was isolated as a yellow solid (0.08 g, 90% yield). ^{1}H NMR (300 MHz, D_2O): δ 2.31 (t, 2H, *J* = 6.0 Hz), 2.80 (t, 2H, *J* = 6.0 Hz), 3.23 (m, 2H), 3.32 (m, 4H), 7.14 (s, 1H), 7.24 (s, 1H), 8.21 (m, 2H), 8.46 (s, 1H), 8.53 (s, 1H), 8.86 (m, 2H). ^{13}C NMR (75 MHz, D_2O): δ 24.04, 26.31, 35.04, 36.06, 38.02, 53.69, 116.17, 117.33, 125.28, 128.34, 130.71, 133.09, 133.69, 142.57, 149.25, 165.07, 170.88, 173.71.

Experimental Conditions for DNA Enzyme Isolation

In vitro Selection Technique

The *in vitro* selection approach that was used with the cofactors to identify RNA-cleaving deoxyribozymes involves the use of a template (**T**) of a single stranded DNA (pool of DNA) that contains 40 random nucleotides, providing 10^{24} possible DNA sequences. This pool of DNA was amplified using the polymerase chain reaction (PCR) in order to obtain double stranded DNA which contains biotin and a single RNA nucleotide in one of the strands. This double stranded DNA is passed through a

streptavidin column, followed by elution using sodium hydroxide to obtain the singlet stranded DNA which contains the potential DNA enzymes, attached to the column. The subsequent addition of the organic molecule as potential cofactor allowed the cleavage of the strand of DNA at the RNA nucleotide position, with the elution of those DNA enzymes that are catalytically active (Figure 118).

Multiple selection rounds were run to get the best catalytic enzymes. Repeating the selection over many rounds enriches the pool in the sequences with substantial catalytic activity. The number of these rounds was varied going from as few as three or as many as ten depending on the variables studied in this project.

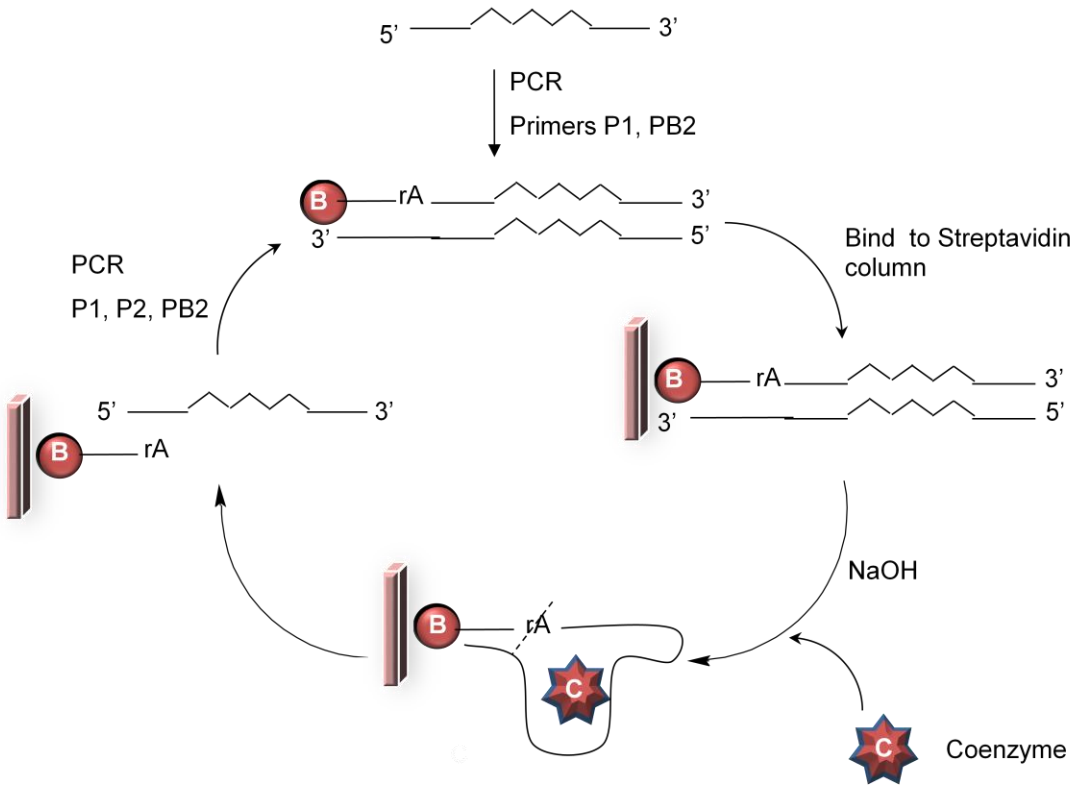

Figure 118. *In vitro* selection using coenzymes.

PCR and In Vitro Selection Conditions using α-dATP ^{32}P as DNA Marker

Table 8 shows the concentrations and reagents employed for the PCR reaction during the *in vitro* selection to obtain radioactive labeled DNA. The *in vitro* selection was conducted in a laboratory that follows strict safety protocols for working with radioactive materials. All the pipette tips were disposed to ^{32}P-solid waste containers.

Table 8. PCR reaction mixture

Reagent	Concentration	Amount	PCR concentration
H_2O	-	To 50 μL	-
DNTPs	2 mM	5 μL (4 μL dATP)	200 μM/each
$MgCl_2$	25 mM	3 μL	1.5 mM
10X TBE buffer	-	5 μL	-
Template	5 μM	1 μL	0.1 μM
Primer B2	10 μM	4 μL	0.8 μM
Primer 1	10 μM	4 μL	0.8 μM
α ^{32}P-dATP	1mCi/100 μL	1 μL	0.2 μCi/100 μL
Taq Poly	5U/μL	1 μL	0.1 U/ μL

The PCR mixture was prepared by adding all the reagents without any particular order, but keeping at last the addition of $MgCl_2$ and α-^{32}P dATP in order to minimize the exposure to the radioactive material. A PCR thermocycler program was used for the first step in the *in vitro* procedure, which consist on four cycles at 94°C (15 sec), 50°C (30 sec), and 72°C (30 sec).

After the four cycles of the PCR reaction are completed, the α-^{32}P labeled DNA was precipitated by adding to the 50 μL PCR mixture, 5 μL of a 3 M sodium acetate solution (pH 5.2) and mixed by vortexing. 165 μL of cold 100 % ethanol were added, mixed by inverting and put in the freezer at 0 ^{o}C overnight. The DNA solution was then centrifuged for 20 minutes at high speed at 4 ^{o}C; the supernatant was poured off into the ^{32}P-liquid waste container, added 100 μL of cold 70 % ethanol, and the solution centrifuged for 5 minutes, and the supernatant discarded again while keeping only the DNA pellet.

The α-^{32}P dATP labeled DNA was dissolved in 60 μL of binding buffer (50 mM HEPES, 0.5 M NaCl, 0.5 M KCl, 0.5 mM EDTA, pH 7.5). 1 μL of the solution was saved for control reading with the scintillation counter while the remaining 59 μL were placed into an activated streptavidin bio-spin chromatography column containing 200 μL of neutravidin slurry which has been washed five times (100 μL each) with binding buffer. The solution buffer containing the amplified α-^{32}P dATP labeled DNA was mixed into the column by carefully vortex the column followed by 30 minutes of incubation inside the column. The solution was then completely removed from the column and 1 μL was saved for control reading with the Scintillation counter. At this point, doublet stranded labeled DNA should be bound in the column by the biotin side, where an extra wash with 100 μL of binding buffer was followed in order to wash any unbound labeled DNA off the column. These solutions washes were disposed in the ^{32}P-liquid waste container.

Non-biotinylated α-^{32}P dATP labeled DNA strand was removed from the column by flushing it three times with 100 μL of 0.2 M NaOH solution. The column was

equilibrated to the pH of the reaction by flushing it once with 100 μL of binding buffer. 60 μL of reaction buffer (50 mM cofactor, 0.5 M NaCl, 0.5 M KCl, 0.5 mM EDTA, pH 7.5) was added to the column and the system was incubated for the designated time of the round. The solution was then collected in a 1.5 ml eppendorf tube and the column washed with 100 μL of binding buffer; this solution was also collected in the 1.5 ml tube (160 μL total volume). After that, 1 μL was kept for control reading in the scintillation counter and the column was discarded in the proper ^{32}P-solid container. The catalytic isolated singlet stranded α-^{32}P dATP labeled DNA was precipitated as was described before by adding 16 μL of sodium acetate and 528 μL of cold 100% ethanol.

Precipitated α-^{32}P dATP containing DNA was amplified by 20 cycles of PCR with thermocycle of 94 ^{o}C (10 sec), 50 ^{o}C (30 sec), 72 ^{o}C (30 sec) as shown in Table 9.

Table 9. Second PCR reaction mixture

Reagent	Concentration	Amount	PCR concentration
H_2O	-	To 50 μL	-
DNTPs	2 mM	5 μL	200 μM/each
$MgCl_2$	25 mM	3 μL	1.5 mM
Primer 2	10 μM	2 μL	0.4 μM
Primer 1	10 μM	2 μL	0.4 μM
Taq Poly	5U/μL	1 μL	0.1 U/ μL

10 μL of the resulting PCR product was taken and re-amplified with primers P1 and PB2 to introduce to the strand of DNA the biotin groups at the 5' position, the ribonucleotide (rA) cleaving moiety, and more of the radioactive alpha-^{32}P dATP since it

tends to decay after each round of selection. Table 10 resumes the new PCR conditions, as the PCR reaction was set to undergo six thermocycle of 94 ^{o}C (10 sec), 50 ^{o}C (30 sec), and 72 ^{o}C (30 sec). The PCR product was precipitated by adding 5 μL of a 3 M sodium acetate solution mixed by vortexing, then 165 μL of cold 100 % ethanol were added, mixed by inverting and put in the freezer at 0 ^{o}C overnight.

Table 10. Third PCR reaction mixture

Reagent	Concentration	Amount	PCR concentration
H_2O	-	To 50 μL	-
DNTPs	2 mM	5 μL (4 μL dATP)	200 μM/each
$MgCl_2$	25 mM	3 μL	1.5 mM
10X TBE buffer	-	7 μL	-
Primer B2	10 μM	5 μL	1.0 μM
Primer 1	10 μM	5 μL	1.0 μM
α ^{32}P-dATP	1mCi/100 μL	1 μL	0.2 μCi/100 μL
Taq Poly	5U/μL	1 μL	0.1 U/ μL

Purification by Agarose Gel of the α-^{32}P dATP Labeled DNA after Third PCR Amplification.

A DNA pellet was dissolved in 20 μL of DI water and 4 μL of loading buffer. A 1.5% low range ultra agarose gel was then prepared in TAE buffer containing 2 μL of ethidium bromide (10 mg/mL).

The Agarose gel was prepared by adding 30 mL of TAE buffer into an Erlenmeyer flask containing 0.45 g of ultra pure agarose, and swirled to mix. The flask

was then weighted and the mixture boiled in a microwave oven (at middle power) until the agarose was completely melted. The initial weight was restored by adding hot water since a significant amount of water evaporates during the process and this step is required to obtain the desired percentage of gel. 2 μL ethidium bromide was added, and the flask heated for an additional minute without boiling. The solution was left to cool to 70 ^{o}C and poured carefully on a clean casting plate with an appropriate comb. Solidification of the gel was achieved after 30 minutes.

The gel was immersed in a TAE buffer and the DNA sample was loaded to the gel and ran along with a low mass DNA ladder. The voltage source was adjusted to 100 mV and the sample was run for approximately 45 minutes. The gel running buffer was discarded to a ^{32}P-liquid waste container and the excess of liquid was removed by gently padding the gel with paper towels. The gel was then placed on top of a saran wrap and in the UV transilluminator (WVR LM-20E). The 100 bases α-^{32}P dATP labeled DNA product was excised and put in a 1.5 mL tube. The DNA was extracted from the gel using QIAEX II (Qiagen) and then 20 μL of purified alpha-^{32}PdATP containing DNA solution was mixed with 20 μL of 2X binding buffer and saved for next round of selection.

QIAEX II Gel Extraction Protocol for Radiolabeled DNA

The DNA band was excised from the agarose gel with a clean, sharp scalpel and the piece was put in a 1.5 ml tube with 300 μL of buffer QX1. 10 μL of QIAEX II was added to the sample followed by incubation at 50°C for 10 min to solubilize the agarose and bind the DNA. The solution was vortex every 2 min to keep the QIAEX II in suspension, centrifuged for 30 seconds and the supernatant was carefully removed with a pipette. The pellet was washed once with 500 μL of Buffer QX1, and twice with 500 μL

of buffer PE. After removal of the supernatant, the pellet was air-dried for 10–15 minutes. To elute the DNA, 20 μL of 10 mM Tris·Cl (pH 8.5) was added and the solution was vortex, allowed it to incubate for 5 minutes at room temperature, centrifuged for 30 seconds and then the supernatant was carefully transferred into a clean tube.

Quantification of Radioactive DNA by Liquid Scintillation Counter

Scintillation vials were filled with 3 mL of Bio-Safe II liquid scintillation cocktail (Research Products International Corp.) using the Hirchmann dispenser. A filter paper was cut to form small squares of 1 cm and 1 μL of sample was placed in the paper. Blank sample (1 μL of buffer or water) was added to a scintillation vial in position 1 of the sample rack, while the rest of the samples were placed in the remaining slots (a sample rack can hold up to 14 vials). The samples were then shaked to mix the radioactive material with the liquid scintillation cocktail. The program card number used for ^{32}P was 9, and the parameter for running the sample was specified in the computer menu. After the counting was complete, the samples were discarded in the corresponding ^{32}P- solid and liquid disposal container.

Labeling of 5' Position of DNA by γ-^{32}P (forward reaction)

Fermentas protocol with some modifications was employed for the radio-labeling of 5'-termini DNA; table 11 resumes the reaction mixtures used for the forward reaction. After mixing all the reagents in a 1.5 mL eppendorf tube, the solution was incubated for 30 minutes at 37 ^{o}C, then 1 μL of 0.5 M EDTA (pH 8.0) was added and then heated at 75 ^{o}C for 10 minutes. Labeled DNA was purified from unincorporated DNA by gel filtration on Sephadex G-50. After purification, the solution was extracted with an equal amount of

chloroform. The chloroform layer was then carefully removed with a pipette and discarded in the appropriate liquid- γ-^{32}P container.

Table 11. Reaction mixture for γ-^{32}P DNA labeling

Reagent	Concentration	Amount
Desphosphorylated DNA (DNA PCR product, Template DNA or Primer)	1-20 pmol	5 μL
10X buffer (Forward Reaction)	-	2.5 μL
γ-^{32}P ATP	40 pmol	2 μL
24% (w/v) PEG 6000 solution	-	4 μL
T4 Polynucleotide kinase	10 U	1.5 μL
Water	-	4 μL

Purification of γ-^{32}P Labeled DNA

A Sephadex column (Bio-Rad) storage at 4 ^{o}C was allowed to warm up to room temperature; the slurry was homogenized by gently inverting the column several times. The top cap of the column was then removed first, followed by the removal of the bottom tip. The column was then placed into a 1.5 mL eppendorf tube and centrifuged at 1,000X gravities for 2 minutes in order to discard the buffer added by the manufacturer company. 50 μL of water were added inside the column and the centrifugation process was repeated. After discarding the solution collected in the tube and while keeping the column in an upright position, 50 μL of the γ-^{32}P labeled DNA sample were added very slowly to the center of the column gel. Centrifugation at 1000X gravities for 4 minutes afforded the purified labeled DNA solution.

DNA Polyacrylamide Gel Electrophoresis

Self and Trans-cleavage experiments of radioactive labeled DNA enzymes were conducted by gel electrophoresis using 10-well precast TBE-Urea Gels (15 and 20%). The gels were placed in the Bio-Rad chamber. 125 mL of 1X TBE buffer were added into the inner chamber and 200 mL of the same running buffer was added to the outer chamber of the electrophoresis apparatus. Precast polyacrylamide gels were warmed prior to use by pre-running them at 80V for 20 minutes. 10 μL of TBE-Urea loading buffer were added to 10 μL of DNA sample; the solution was heated for 5 minutes at 90 ^{o}C. Before loading the sample into the gel, the wells were rinsed with running buffer to remove the residues of urea deposited inside, and then 10 μL of sample were loaded in each well. The gels were run at 80V at the power supply until the dyes separated, and then the current was boosted up to 150V. After observing complete band separation, the gel was removed from the plastic cassette and soaked in 100 mL of a gel-fixing solution that contains 10% ethanol and 10% glacial acetic acid in DI water for 30 minutes.

The gel was then removed from the fixing solution and placed in 3 or 4 sheets of filter papers and covered by a plastic saran wrap. The system was then placed in the dryer unit at 70 ^{o}C for 4 hours. After most of the solvent was dried, gel was removed from the unit and photographed using the autoradiography imager.

Autoradiography of Radioactive Labeled DNA Gel

Due to the radioactivity of the samples loaded in the gel, special considerations and Baylor mandatory training were required to proceed with the protocol. The gel was transferred using a protective plastic box into spring-loaded metal cassette, and a phosphoro screen was placed on top of, it which has been previously activated with light

for 2 minutes. The metallic cassette was closed and the gel was allowed to expose to the screen for 5 minutes. In order to remove the screen from the cassette, the light of the room were turned off since light may activate the phosphoro screen and erase the information it contains. The exposed film was transferred inside the Personal Molecular Imager FX^{TM} System and the autoradiograph and picture were taken using the Quantity One software from Bio-Rad.

CHAPTER SEVEN

Results and Discussion

Synthesis of DNA Enzyme Cofactors

The main objective of this project is to use the synthesized molecules as DNA enzyme cofactors, as they contain functional groups that can cooperate in the cleavage of a RNA substrate. Such functional groups includes amides, that can potentially form hydrogen bonds with nucleobases, the imidazole ring, that can participate in acid/base catalysis, and carboxylic acid groups that can enhance the solubility of the synthetic cofactors.

Imidazole groups were selected as the main moiety present in the cofactor species as they are present in a number of important naturally occurring products, for example histidine (involved in the biochemical reactions of living systems) and purine (forming bases of nucleic acid). Histidine residues are found at the active sites of ribonuclease and of several other enzymes. In some enzymes, they serve as catalysts for proton transfer. The imidazole system can act both as a base and as an acid. The imine nitrogen donates an electron pair and the N-hydrogen, being acidic, is an acceptor. At the physiological pH of 7.4, appreciable concentrations of both protonated and neutral imidazole units are likely to be present. Thus there are species present at the active sites of the enzymes that can act as acids or bases.[186]

The synthetic procedure for intermediate **C1** is shown in Scheme 26, which involves the protection of histamine dihydrochloride with triphenyl chloride; histamine

dihydrochloride was first reacted with triethyl amine to make histamine a better nucleophile that will undergo nucleophilic substitution when reacted with triphenyl chloride thus obtaining the protected histamine species.

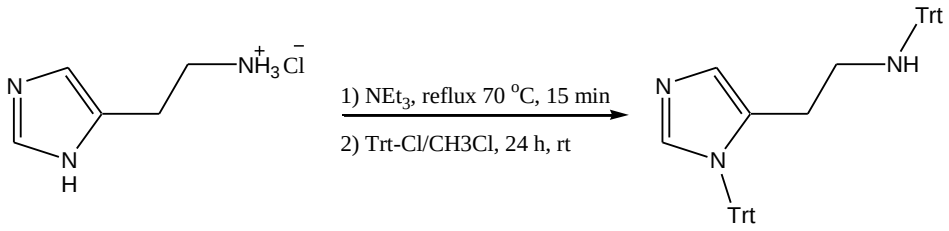

Scheme 26. Protection of histamine dihydrochloride with triphenyl chloride.

Acid hydrolysis of the diprotected histamine (Scheme 27) was achieved with a solution containing trifluoroacetic acid to afford the removal of the triphenyl group from the aliphatic amine to obtain **C2**. Removal of the triphenyl group occurs only at that position since the electrons of the protected nitrogen in the imidazole ring occupies a sp^2-hybridized orbital which possesses more s character, and are therefore more strongly bound and closer to the nucleus than those with less s character. This explains the less basicity of the nitrogen in the imidazole ring while selectively allowing the protonation of the sp^3-hybridized nitrogen lone pairs in the aliphatic amine.

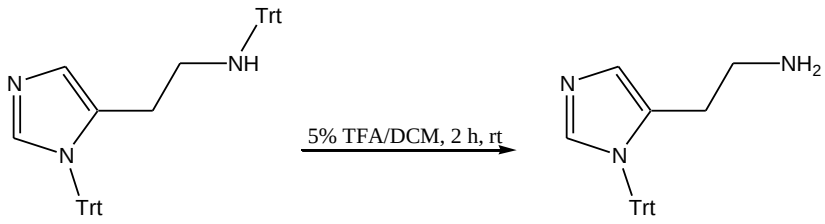

Scheme 27. Diprotection of deprotected histamine.

BOP was used to assist the coupling reaction between the primary amine group in monoprotected histamine **C2** and the carboxylic acid in β-alanine-fmoc, which provided the formation of the fmoc-protected compound **C3** according to Scheme 28.

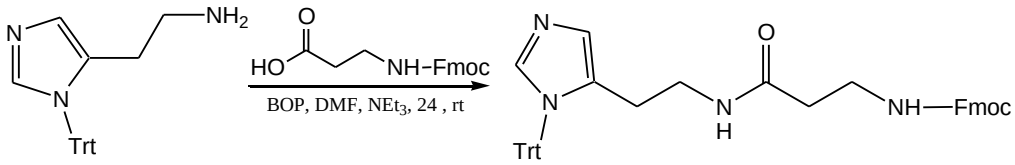

Scheme 28. Coupling reaction with β-alanine-fmoc.

Scheme 29 shows the deprotection of the fmoc protective group using a 50% piperidine solution which allows the formation of compound **C4**. A subsequent BOP mediated coupling reaction of this intermediate with Fmoc-histidine(Trt)-OH, followed by base catalyzed removal of the fmoc afforded the trityl protected intermediate **C5**. This compound is the starting material for the synthesis of the DNA enzymes cofactors used during the *in vitro* selection process.

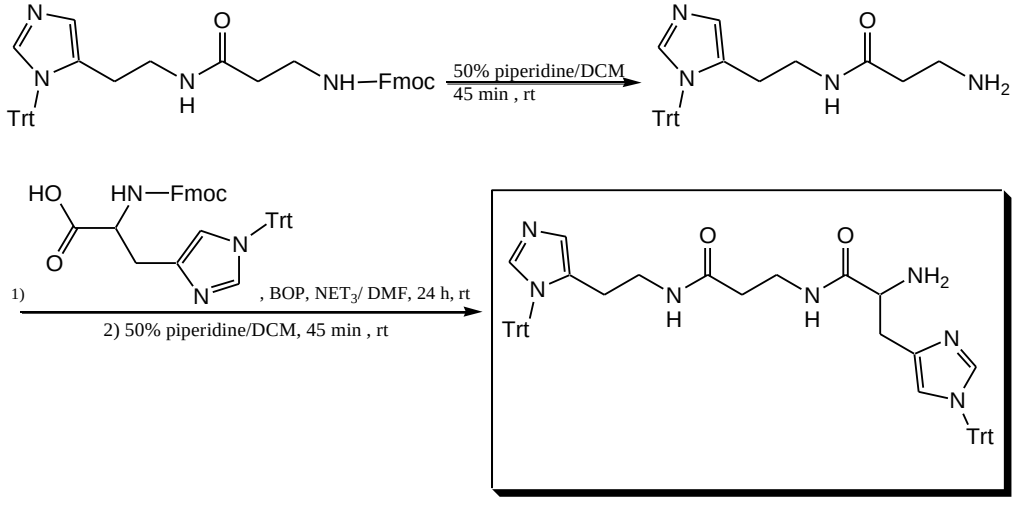

Scheme 29. Synthetic procedure for intermediate **C5**.

Histidine cofactor **C6** was obtained by acidic hydrolysis of the amine groups present in the imidazole rings, which allowed the deprotection of the triphenyl species in intermediate **C5** when a 95% trifluoroacetic acid solution was used (Scheme 30).

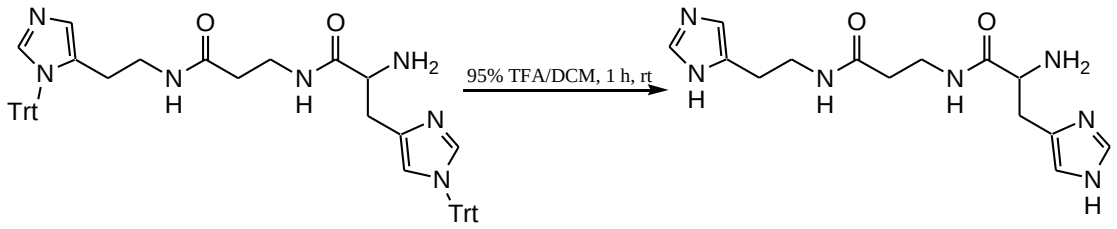

Scheme 30. Synthetic procedure for cofactor **C6**.

In a similar manner cofactor **C7** (arginine cofactor) was synthesized by reacting intermediate **C5** with the commercially available Boc-Arg(Boc)$_2$-OH using the BOP coupling reagent as the promoter of the amide bond formation. After completion of the coupling reaction the new intermediate was deprotected using an acidic solution of 95 % TFA in dichloromethane. The synthetic procedure for this cofactor is illustrated in Scheme 31.

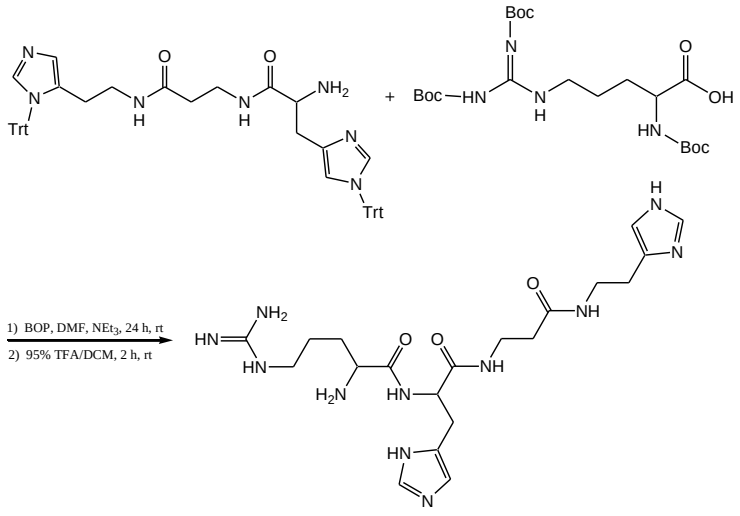

Scheme 31. Synthetic procedure for cofactor **C7**.

Scheme 32 shows the synthetic procedure of glutamic acid cofactor **C8** which was prepared by coupling together intermediate **C5** with Boc-Glu(OtBu)-OSu, followed by removal of the protecting groups using a 1M acidic solution.

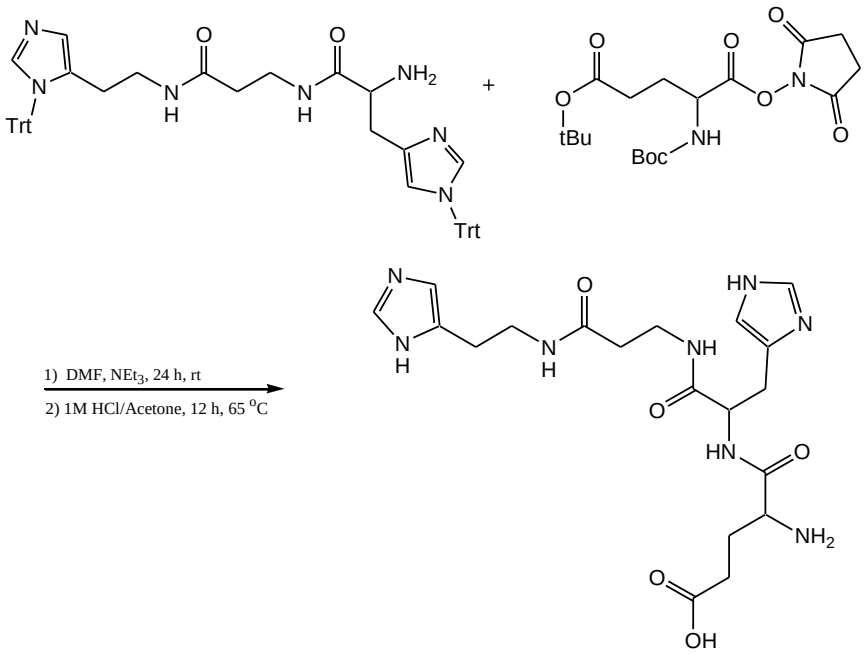

Scheme 32. Synthetic procedure for cofactor **C8**.

Cofactor **C9** (Scheme 33), which contains the isonicotinic moiety, was synthesized by condensation of isonicotinic acid with intermediate **C5** in presence of the coupling promoter PyBOP. Deprotection of Boc and the Trt groups were achieved by stirring the protected cofactor for 2 hours in a 95% TFA solution.

*In Vitro Selection Studies using Glutamic Acid Cofactor **C8** (DNA **R1**)*

In order to study the effectiveness of cofactor **C8** in the cleavage of DNA, an *in vitro* selection was carried out to isolate the best DNA sequences that can utilize this cofactor.

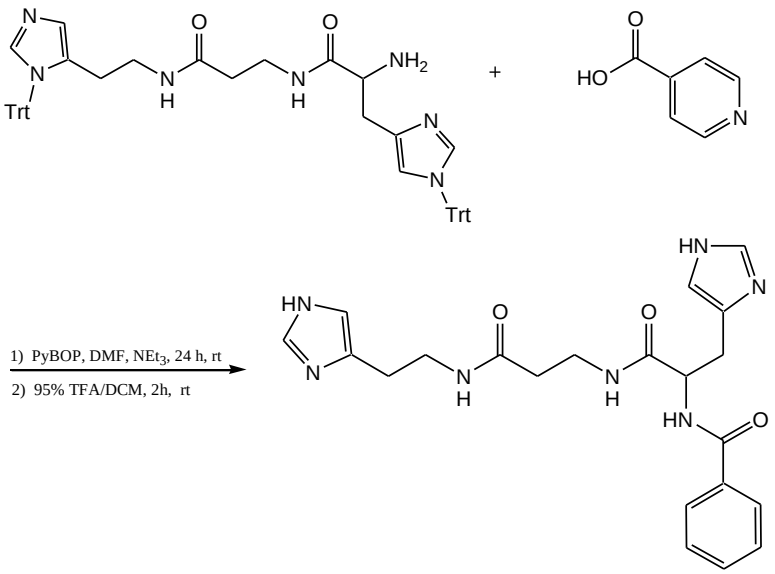

Scheme 33. Synthetic procedure for cofactor **C9**.

The objective was to assess the influence of the glutamic acid cofactor in the selection process by using a solution containing 50 mM of cofactor **C8**, 0.5 M NaCl, 0.5 M KCl, 0.5 mM EDTA, and pH = 7.5. In this study, the sequence diversity was constrained depending only in the incubation time of the cofactor while its concentration was kept constant during the rounds of selection. Ten rounds of selection were carried out in order to enrich the pool in the sequences with substantial catalytic activity. The time of incubation during the first five rounds of selection was set to 5 hours, while the time of incubation was decreased starting from round six. Table 12 summarizes the time of incubation used during this *in vitro* selection experiment. Rounds of selection were started using a DNA template (97 mer) possessing 40 random nucleotides equivalent to 4^{40} or 10^{24} potential sequences. This pool of DNA (20 pmol) was amplified by PCR using primers **P1** and **PB2** to obtain a double-stranded DNA containing a 5'-biotin and a single embedded ribonucleotide. Traces amounts of [α-^{32}P]-dATP were included in the reaction mixture to monitor the amount of DNA in the process. Immobilization on a streptavidin

column and subsequently denatured, produced a matrix that display single-stranded molecules. After the incubation time, the single stranded DNA molecules were then incubated with reaction buffer containing 50 mM of **C8** for various period of time. Those molecules able to catalyze their cleavage were then eluted of the column and amplified using **P1** and **P2**. Reincorporation of the biotin and the ribonucleotide moieties into the DNA strand were achieved by amplifying 10 μL of the previous PCR product with primer **P1** and **PB2**. The extended PCR product was gel purified and saved for the next round of selection.

Table 12. Incubation time used in the *in vitro* selection experiment when 50 mM of cofactor **C8** was employed for isolating DNA enzymes.

Round	1	2	3	4	5	6	7	8	9	10
Time	5 h	5h	5h	5h	5h	2h	1h	10 min	1 min	10 s

Figure 119 shows the percentage of catalytic active single stranded DNA obtained after each round of selection. The calculation was based on the scintillation counter result recorded by measuring the amount of radioactive material incorporated into the strand of DNA. A blank experiment was conducted using only HEPES buffer, where the amount of cleaved DNA was substrated from the total amount of DNA obtained when the cofactor was used.

The first three rounds of selection shows minimum cleavage of the DNA enzyme when cofactor **C8** was incubated for 5 hours. However, after exposing the next rounds (4 and 5) to the cofactor solution, it was observed how the pool of DNA was progressively enriched with catalytically active oligonucleotides. When the time of the reaction was

constrained from 5 to 2 hours, the amount of DNA cleaved was lower since not all of the enzymes that were catalytic active at 5 hours are necessary active after only 2 hours. The same behavior was observed in the following rounds. DNA cleaved or isolated in this *in vitro* selection will be called DNA-**R1**.

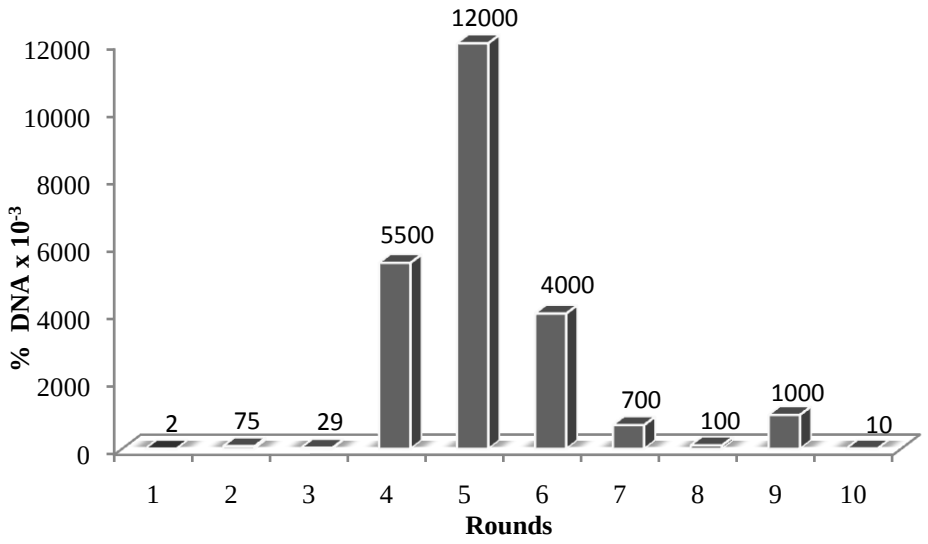

Figure 119. Percentage of DNA-**R1** cleaved per round of selection in the *in vitro* selection experiment of DNA enzymes with cofactor **C8**.

In Vitro Selection of DNA Enzyme using Imidazole Moiety Cofactors

Imidazoles containing small molecules were employed in order to study the possibility of utilizing a library of potential cofactors, since Roth and Breaker reported the use of histidine derivatives as coenzymes, showing promising results in the isolation of DNA enzymes.[101] The idea was to expose the potential catalytic enzymes to several cofactors and determine the influence of these mixtures in the selection process. The molecules for these experiment were chosen based on their solubility in aqueous solution at the pH selected for the *in vitro* conditions (pH 7.5), and also for the presence of the imidazole ring that can potentially participate in the isolation of the DNA enzyme that are

catalytically active. Molecules selected are shown in Figure 120 which included the 4-imidazoleacetic acid (cofactor **C10)**, 2-mercapto-5-benzimidazole sulfonic acid (cofactor **C11**), L-histidine methyl ester (cofactor **C12**), and 4-amino-5-imidazole-carboxamide (cofactor **C13**).

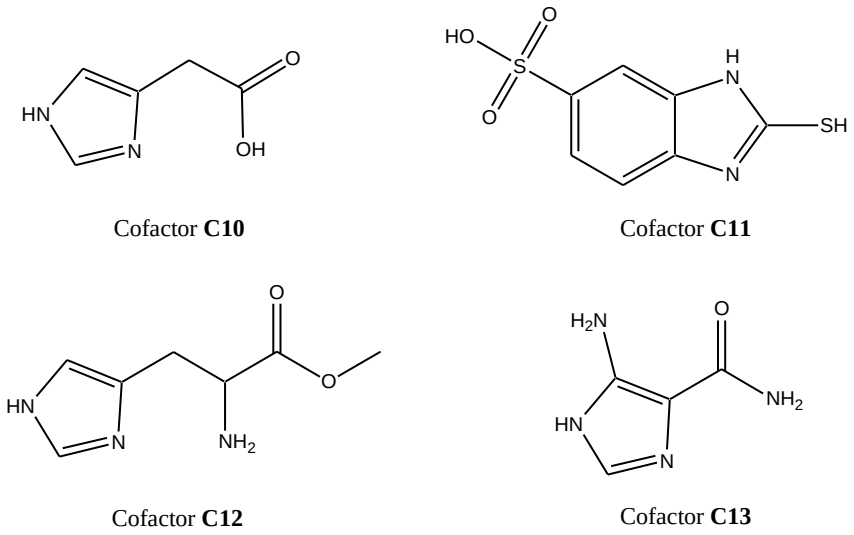

Cofactor **C10** Cofactor **C11**

Cofactor **C12** Cofactor **C13**

Figure 120. Imidazole cofactors.

Figure 121 shows the percentage of DNA-**R2** cleaved after ten rounds of *in vitro* selection when a mixture of cofactors **C10-C13** was used having a concentration of 50 mM. The *in vitro* selection was conducted by initially incubating the system using 5 hours during the first five rounds of the process, followed by a progressive decrease of the incubation time for the remainder rounds. Table 13 shows the variation of time employed for this *in vitro* selection when a reaction buffer containing 50 mM of cofactor **C10-C13**, 0.5 M NaCl, 0.5 M KCl, and 0.5 mM EDTA (pH = 7.5). The results showed a drop of the amount of DNA cleaved after decreasing the time of the cofactor mixture incubation.

Table 13. Reaction time used in the *in vitro* selection used for 50 mM of cofactor **C10-C13**

Round	1	2	3	4	5	6	7	8	9	10
Time	5 h	5h	5h	5h	5h	2h	1h	10 min	1 min	10 s

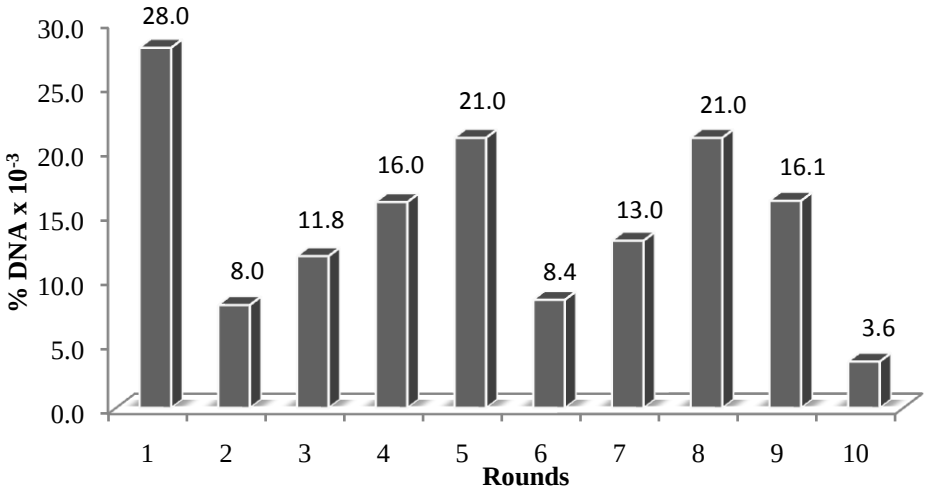

Figure 121. Percentage of DNA cleaved during the *in vitro* selection of DNA-**R2** enzymes by mixture of cofactor **C10-C13** (50 mM of cofactors concentration).

A subsequent *in vitro* selection was performed using the same cofactors mixtures (50 mM **C10-C13**) while keeping the reaction time constant (2 hours), and decreasing the concentration of the cofactors after the fifth round of selection. This could drastically alter the outcome of the isolated deoxyribozymes obtained during the *in vitro* selection which will potentially give rise to DNA enzymes whose activity depends on the concentration of these cofactors. Additionally, this experiment will allow us to determine which concentration of these cofactors may be the best for the cleavage of DNA.

Table 14 and Figure 122 show the conditions and the result of this *in vitro* selection that allow the isolation of DNA-**R3**. A reaction buffer containing a mixture of

the four cofactors were varied from a more concentrated solution (50 mM, rounds 1-5) to a less concentrated one (0.1mM, rounds 6-10). In this experiment, the time of the reaction from round 1 to 5 was kept constant at 5 hours while for the rest of the rounds 2 hours were used. Some constrains of time was needed to be applied since the isolation of the most active catalytic enzymes was desired.

Table 14. Conditions used in the *in vitro* selection of DNA **R3** by mixture of cofactor **C10-C13**

Round	1	2	3	4	5	6	7	8	9	10
Time (h)	5	5	5	5	5	2	2	2	2	2
[Cofactors C10-C13] (mM)	50	50	50	50	50	25	12	5	1	0.1

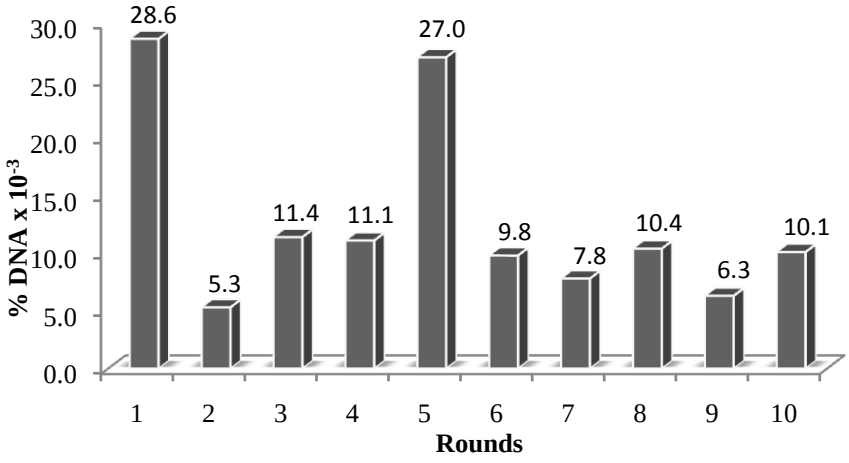

Figure 122. Percentage of DNA-**R3** cleaved during the *in vitro* selection of DNA enzymes by variation of mixture of cofactor **C10-13** concentration.

Comparing the results of rounds 1 to 5 of the two experiments (Figures 121 and 122), a similar amount of DNA was cleaved by the mixture of the organic molecules. On the other hand, from round 6 to 10 a totally different behavior was observed for the two

in vitro selection results. A more radical change was observed when the time of incubation of the cofactor mixture was decreased, than when the concentration of the mixture was varied. This suggests a possible saturation of the active site of the enzyme at higher concentration of cofactors, which indicates that the enzymatic reaction has reached its maximum velocity producing a constant rate of product formation.

*Self Cleavage Experiment using Pool of DNA **R2** and DNA **R3**.*

In order to determine which of these cofactors were involved in the cleavage of the DNA enzymes, self cleavage experiments were conducted using each cofactor individually.

In these self cleavage experiments (Figure 123) the DNA was isolated after the 10^{th} round of selection with primers **P1** and primers **P2** to generate again the double strand of DNA; 10 μL of this solution was reamplified using primers **P2rA** and **PB1** followed by sodium acetate/ethanol precipitation. The DNA was then dissolved in 60 μL of binding buffer and the solution was passed through a streptavidin column allowing it to incubate for 30 minutes. This incubation time was necessary since it would assure that most of the DNA population gets attached to the streptavidin column. Catalytic single stranded DNA containing the ribonucleotide was isolated by adding 20 μL of 0.1 M NaOH solution, which was then collected in a tube containing 2 μL of a 3M sodium acetate solution. Subsequent rapid addition of cold ethanol was followed in order to avoid the DNA population containing the RNA position be affected by the excessive exposure to the sodium hydroxide solution, which could cleave the DNA before reacting it with the cofactor. After DNA precipitation the pellet was dissolved and then radiolabeled with γ-

^{32}P at the 5'-terminal position by following the radioactive protocol that has been described early in this project.

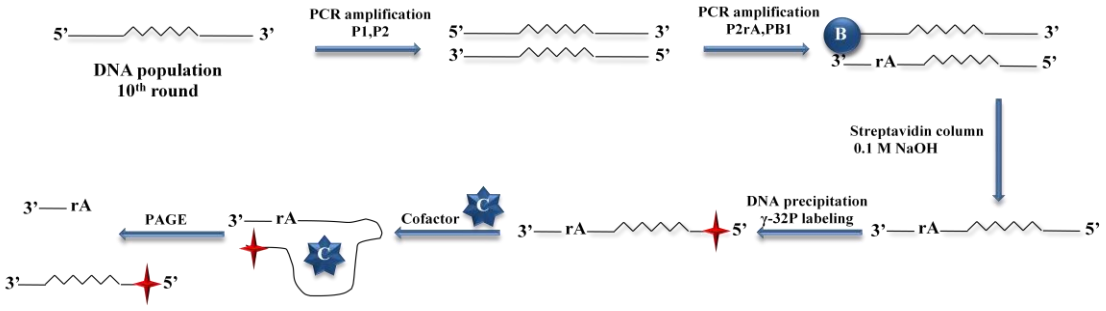

Figure 123. Self cleavage procedure.

Radioactive DNA pools were subjected to a self cleaving reaction in the presence of 50 mM of each cofactor solution. 10 µL of the radioactive labeled DNA pool was heated, denatured for 30 seconds at 90 ^{o}C, cooled to room temperature, and then reaction was started by adding 10 µL of the reaction buffer (100 mM cofactor in 2X binding buffer). The samples were incubated for 4 hours followed by addition of 10 µL of TBE-urea sample buffer. The solutions were then heated at 90 ^{o}C for 5 minutes, loaded and ran in a precast 15% polyacrylamide TBE-urea gel.

Unfortunately, the results we obtained were unable to be interpreted because of the poor resolution and inconsistencies of the data that arose from difficulties faced while handeling the radioactive gels.

In Vitro Selection Studies using Metal-Cofactors

Based on the poor results obtained when the imidazole derivatives were employed during the isolation of DNA enzyme; a new approach was investigated by testing the isolation of the DNA enzymes using metal-cofactors since it has been reported that some

of the most important DNA enzymes isolated are metallo-dependent such as the enzymes 10-23 and 8-17. In addition, it has also been shown that lanthanide ions and their complexes are very active for the hydrolysis of RNA.[187-190] Three *in vitro* selection studies were conducted using lanthanide chloride (Lu^{3+}) in the presence of (carbamoylmethyl-carboxymethyl-amino)-acetic acid (ADA, Figure 124) at two different concentrations and time of cofactor incubation (the DNA pool used for these *in vitro* selection experiments were labeled as DNA-**R4**, DNA-**R5**, and DNA-**R6**).

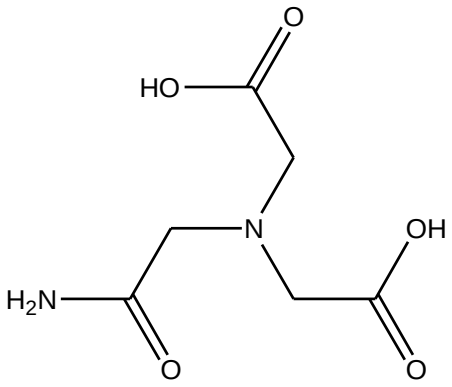

Figure 124. Structure of ADA.

The use of lanthanide complexes as coenzymes was previously reported by Matsumara[191] and co-worker who observed a sequence-selective hydrolysis of RNA by lanthanide complexes bound to an iminodiacetate-attached DNA oligomer (DNA-IDA). In this study, they reported the hydrolysis of the substrate RNA at 37 ^{o}C in a pH 8 tris buffer was initiated by the addition of the RNA to the mixture of DNA-IDA and lanthanide (III) chloride. The total conversion of the RNA hydrolysis was 7.3 mol% at 4 hours and 17 mol% for 8 hours.

*In Vitro Selection Studies using Lu(III)/ADA Complex as Cofactor (DNA-**R4**).*

An *in vitro* selection study was carried out using as cofactor a solution containing 10 μM ADA, 10 μM Lu(III), 1M NaCl, 10 mM Tris, pH 8.0; The conditions for the *in vitro* selection are described in Table 15. After 10 rounds of selection using this lanthanide/ADA complex it was observed a trend similar to that for DNA **R1**, in which the pool of DNA gets richer in those rounds of selection that utilizes 5 hours of incubation with the cofactor. On the other hand, a decrease of the percentage of cleaved DNA was detected just right after the 6th round of selection when the time of incubation of the coenzyme complex was constrained (Figure 125).

Table 15. Reaction time used in the *in vitro* selection used for 10 μM of cofactor Lu(III)/ADA

Round	1	2	3	4	5	6	7	8	9	10
Time	5 h	5h	5h	5h	5h	2h	1h	10 min	1 min	10 s

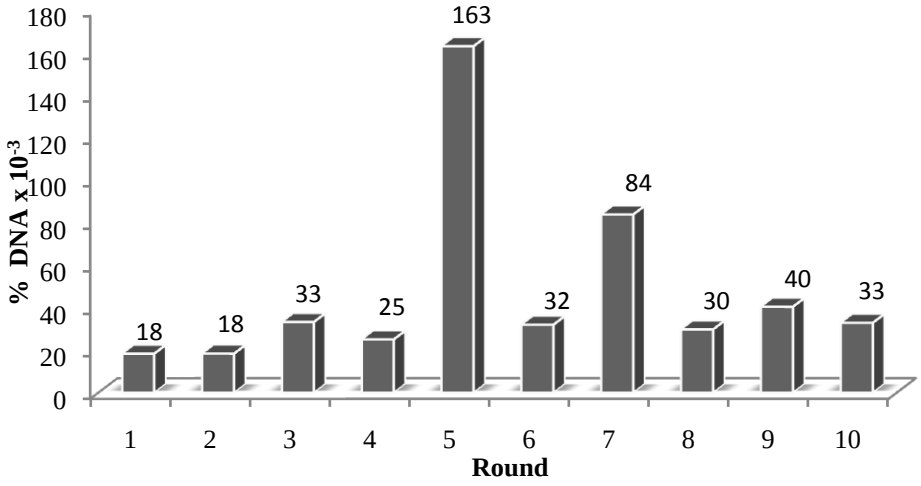

Figure 125. Percentage of DNA cleaved during the *in vitro* selection of DNA-**R4** enzymes by Lu(III)/ADA complex when the incubation time was varied after the 6th round.

*In Vitro Selection Studies using Lu(III)/ADA Complex as Cofactor (DNA-**R5**).*

A cofactor solution containing 10 μM ADA, 10 μM Lu(III), 1M NaCl, and 10 mM Tris, with pH 8.0 was used for the isolation of DNA enzymes. The template of DNA was incubated for 16 hours with the cofactor complex for over 11 rounds of selection. The time of reaction was kept constant during all the *in vitro* process. With this experiment it was intended to observe the influence of the cofactor incubation time in the isolation of DNA enzymes. In theory, it would be expected that the longer the time of incubation of cofactor with the DNA pool, the higher the probability of isolating catalytic active DNA enzymes

Figure 126 shows the percentage of DNA detected after each round of selection, where the activity did not increased lineary over a longer period of time of incubation, but rather a fluctuating tendency was observed.

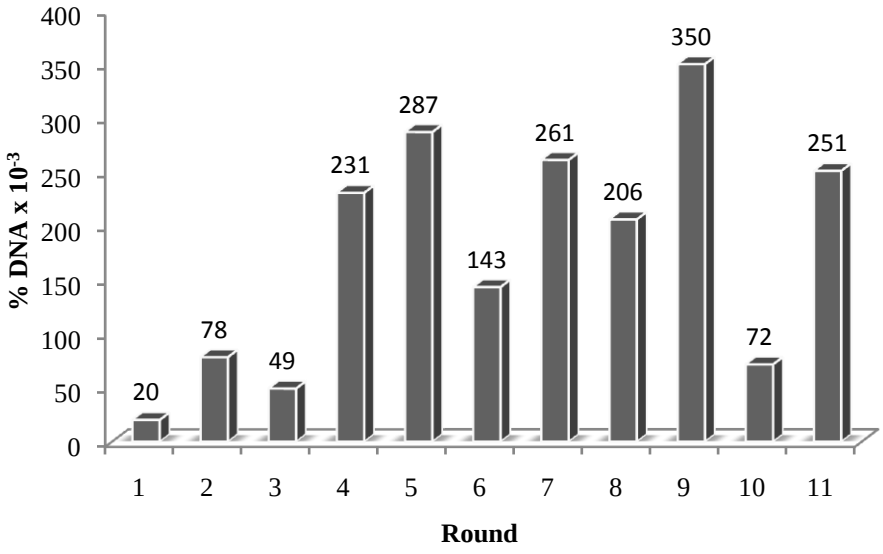

Figure 126. Percentage of DNA-**R5** cleaved during the *in vitro* selection of DNA enzymes by Lu(III)/ADA complex (10 μM cofactor, 16 hours incubation).

*In Vitro Selection Studies using Lu(III)/ADA Complex as Cofactor (DNA-**R6**).*

In order to assess the influence of the concentration of the metal cofactor in the isolation of DNA enzymes, a solution with 1mM of Lu(III)/ADA (1 mM ADA, 1 mM Lu(III), 1M NaCl, 10 mM Tris, pH 8.0) was prepared and 11 rounds of *in vitro* selection were conducted while keeping the incubation time constant for 16 hours during the whole experiment (Figure 127). The percentage of pool of DNA-**R6** detected shows a gradual enrichment of the DNA population from rounds 1 to 7. For the subsequent rounds a saturation point is reached of the active site of the enzyme, possibly due to the effect of the more concentrated cofactor solution used in this experiment.

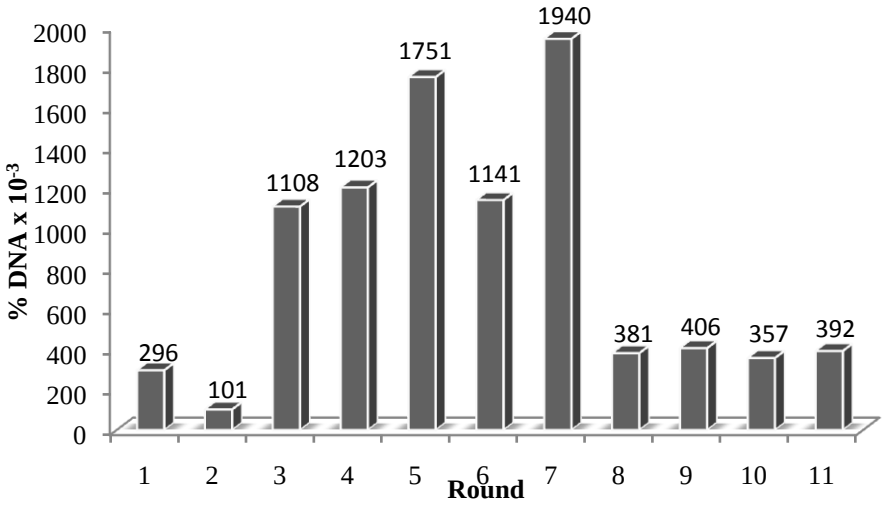

Figure 127. Percentage of DNA-**R6** cleaved during the *in vitro* selection of DNA enzymes by Lu(III)/ADA complex (1 mM cofactor, 16 hours incubation).

*Comparative Data of In Vitro Selection Results for Pools of DNA **R4**, **R5** and **R6***

Comparing the percentages of DNA detected from each of the different *in vitro* selection experiments, it is rather difficult to determine the influence of the different conditions on the isolation of these DNA enzymes. Figure 128 shows that the amount of

DNA obtained were improved by increasing the concentration of the cofactor complex. In addition it could be observed that the DNA isolation process depends on the period of time of cofactor incubation that was used during the selection process. Accordingly, the longer the time of exposure of the DNA to the cofactor, the more DNA was detected. This can be noted when comparing the two *in vitro* selection results using the 10 μM cofactor solutions (DNA **R4**, DNA **R5**).

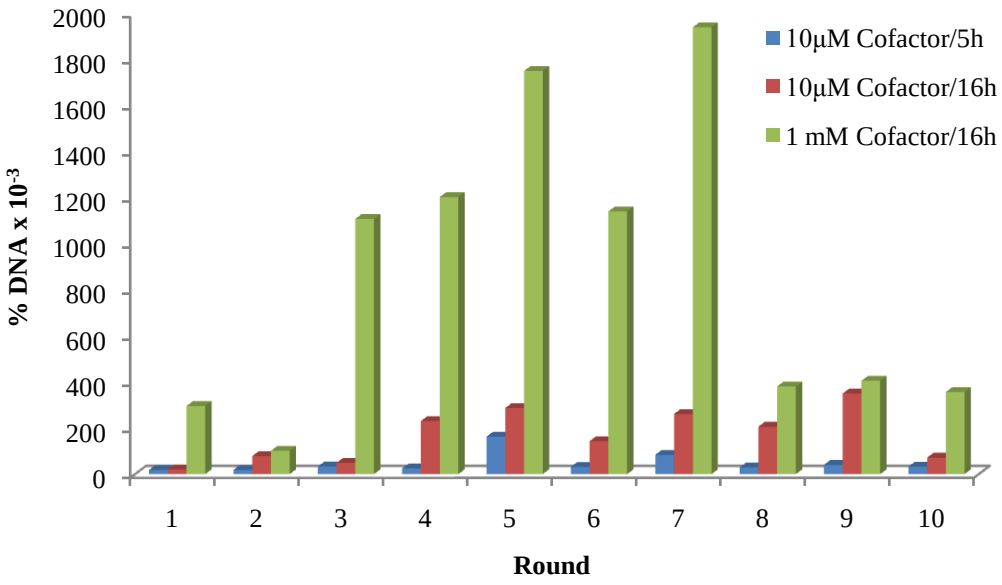

Figure 128. Comparative plot of percentage of DNA cleaved for pool of DNA enzymes **R4**, **R5**, and **R6**.

CHAPTER EIGHT

Conclusions and Future Directions

These studies have demonstrated how the *in vitro* selection process is influenced by the conditions employed during the experiments. Concentration and the time of interaction of the cofactors (imidazole derivatives and metallo-cofactor) affected the percentage of DNA enzymes isolated after each round of selection. Unfortunately the data obtained from the catalytic experiments could not be concluded since self cleavage experiments (*cis* cleavage) did not give positive results.

APPENDIX

APPENDIX

Selected NMR Spectra

Spectra 1. ^{1}HNMR (500 MHz, $CDCl_3$) of **NP5** 180

Spectra 2. ^{13}CNMR (500 MHz, $CDCl_3$) of **NP5** 180

Spectra 3. Gcosy NMR (500 MHz, $CDCl_3$) of **NP5** 181

Spectra 4. ^{1}HNMR (500 MHz, $CDCl_3$) of **NP6** 182

Spectra 5. ^{13}CNMR (500 MHz, $CDCl_3$) of **NP6** 182

Spectra 6. Gcosy NMR (500 MHz, $CDCl_3$) of **NP6** 183

Spectra 7. ^{1}HNMR (500 MHz, $CDCl_3$) of **NP7** 184

Spectra 8. ^{13}CNMR (500 MHz, $CDCl_3$) of **NP7** 184

Spectra 9. Gcosy NMR (500 MHz, $CDCl_3$) of **NP7** 185

Spectra 10. ^{1}HNMR (500 MHz, $CDCl_3$) of **NP8** 186

Spectra 11. ^{13}CNMR (500 MHz, $CDCl_3$) of **NP8** 186

Spectra 12. Gcosy NMR (500 MHz, $CDCl_3$) of **NP8** 187

Spectra 13. ^{1}HNMR (500 MHz, $CDCl_3$) of **NP9** 188

Spectra 14. ^{13}CNMR (500 MHz, DMSO) of **NP9** 188

Spectra 15. Gcosy NMR (500 MHz, $CDCl_3$) of **NP9** 189

Spectra 16. ^{1}HNMR (500 MHz, DMSO) of **BD2** 190

Spectra 17. ^{13}CNMR (500 MHz, DMSO) of **BD2** 190

Spectra 18. Gcosy NMR (500 MHz, DMSO) of **BD2** 191

Spectra 19. ^{1}HNMR (500 MHz, DMSO) of **BD3** 192

Spectra 20. ^{13}CNMR (500 MHz, DMSO) of **BD3** ……. 192

Spectra 21. Gcosy NMR (500 MHz, DMSO) of **BD3** ……...…… 193

Spectra 22. ^{1}HNMR (500 MHz, DMSO) of **BD4** ……...……..……. 194

Spectra 23. ^{13}CNMR (500 MHz, DMSO) of **BD4** ……. 194

Spectra 24. Gcosy NMR (500 MHz, DMSO) of **BD4** ……...…… 195

Spectra 25. ^{1}HNMR (500 MHz, DMSO) of **BD5** ……...……...… 196

Spectra 26. ^{13}CNMR (500 MHz, DMSO) of **BD5** ……..… 196

Spectra 27. Gcosy NMR (500 MHz, DMSO) of **BD5** ……...… 197

Spectra 28. ^{1}HNMR (500 MHz, D_2O) of **BD6** ……..…… 198

Spectra 29. ^{13}CNMR (500 MHz, D_2O) of **BD6** ……..…… 198

Spectra 30. Gcosy NMR (500 MHz, D_2O) of **BD6** ……...…… 199

Spectra 31. ^{1}HNMR (500 MHz, DMSO) of **BD7** ……..…… 200

Spectra 32. ^{13}CNMR (500 MHz, DMSO) of **BD7** ……..… 200

Spectra 33. ^{1}HNMR (500 MHz, D_2O) of **BD8** ……..…… 201

Spectra 34. ^{13}CNMR (500 MHz, D_2O) of **BD8** ……..…… 201

Spectra 35. Gcosy NMR (500 MHz, D_2O) of **BD8** ……...…… 202

Spectra 36. ^{1}HNMR (500 MHz, DMSO) of **BD9** ……..…… 203

Spectra 37. ^{13}CNMR (500 MHz, DMSO) of **BD9** ……..… 203

Spectra 38. Gcosy NMR (500 MHz, DMSO) of **BD9** ……...… 204

Spectra 39. ^{1}HNMR (300 MHz, $CDCl_3$) of **C1** ……..... 205

Spectra 40. ^{1}HNMR (300 MHz, $CDCl_3$) of **C2** ……. 205

Spectra 41. ^{1}HNMR (300 MHz, $CDCl_3$) of **C3** ……. 206

Spectra 42. ^{1}HNMR (300 MHz, $CDCl_3$) of **C4** ……. 206

Spectra 43. ^{1}HNMR (300 MHz, $CDCl_3$) of **C5** …… 207

Spectra 44. ^{1}HNMR (300 MHz, D_2O) of **C6** …… 208

Spectra 45. ^{1}CNMR (75 MHz, D_2O) of **C6** ……... 208

Spectra 46. ^{1}HNMR (300 MHz, D_2O) of **C7** …… 209

Spectra 47. ^{1}CNMR (75 MHz, D_2O) of **C7** ……... 209

Spectra 48. ^{1}HNMR (300 MHz, D_2O) of **C8** …… 210

Spectra 49. ^{1}CNMR (75 MHz, D_2O) of **C8** ……... 210

Spectra 50. ^{1}HNMR (300 MHz, D_2O) of **C9** …… 211

Spectra 51. ^{1}CNMR (75 MHz, D_2O) of **C9** ……... 211

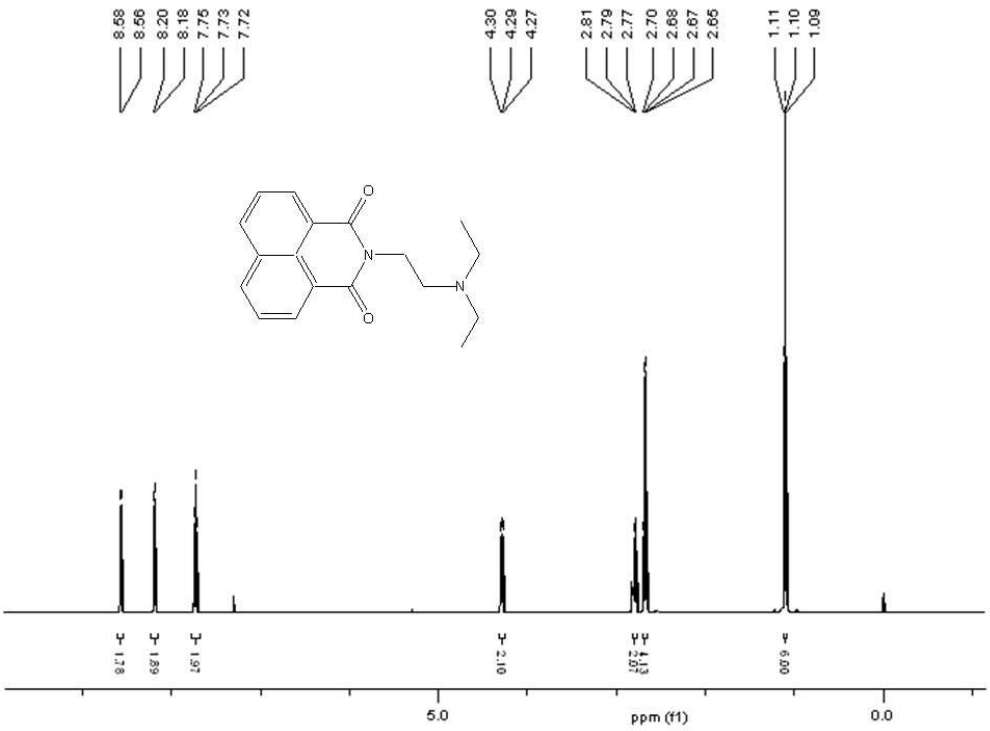

Spectra 1. ^{1}HNMR (500 MHz, $CDCl_3$) of **NP5**

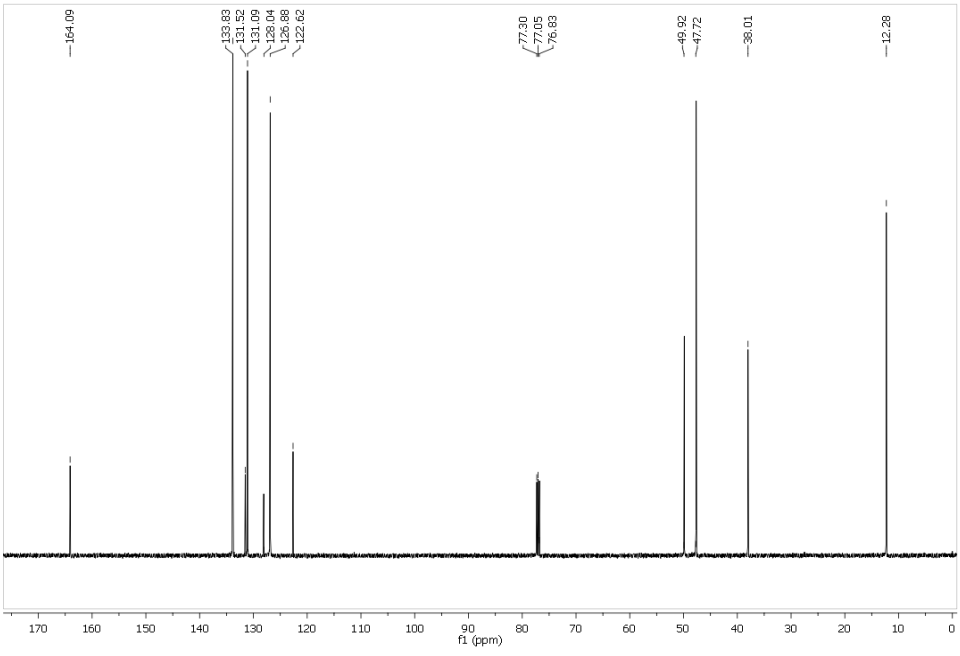

Spectra 2. ^{1}CNMR (125 MHz, $CDCl_3$) of **NP5**

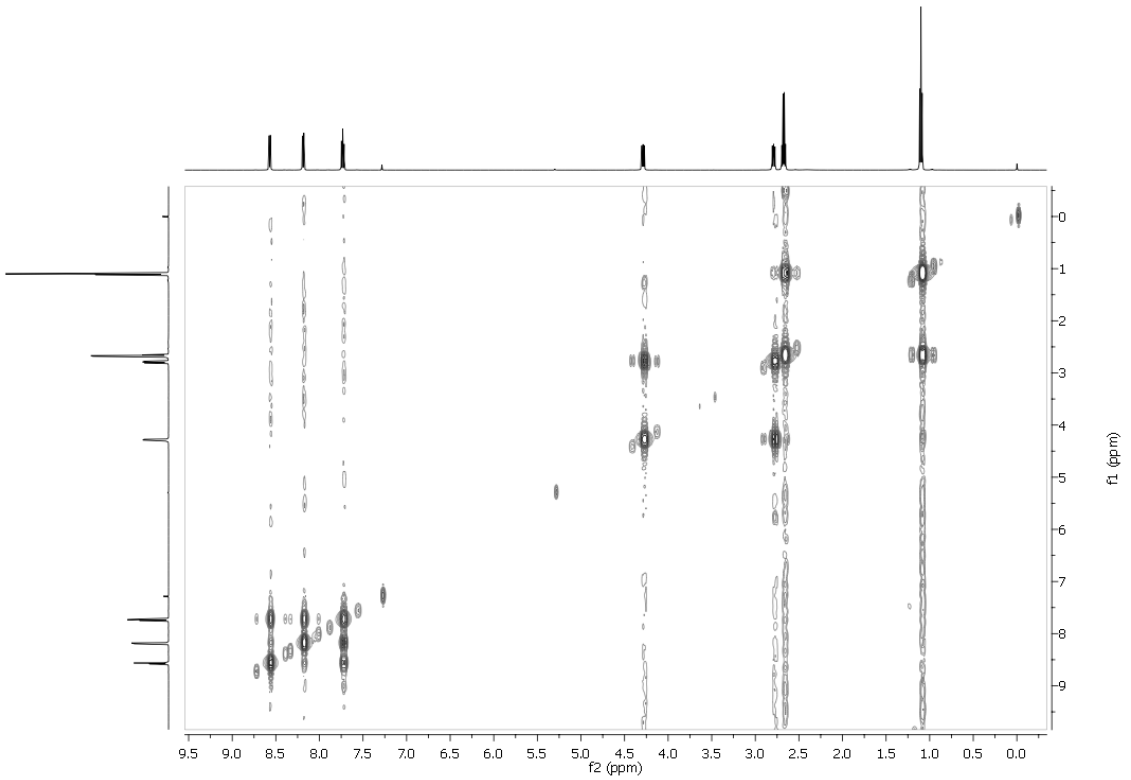

Spectra 3. Gcosy NMR (500 MHz, $CDCl_3$) of **NP5**

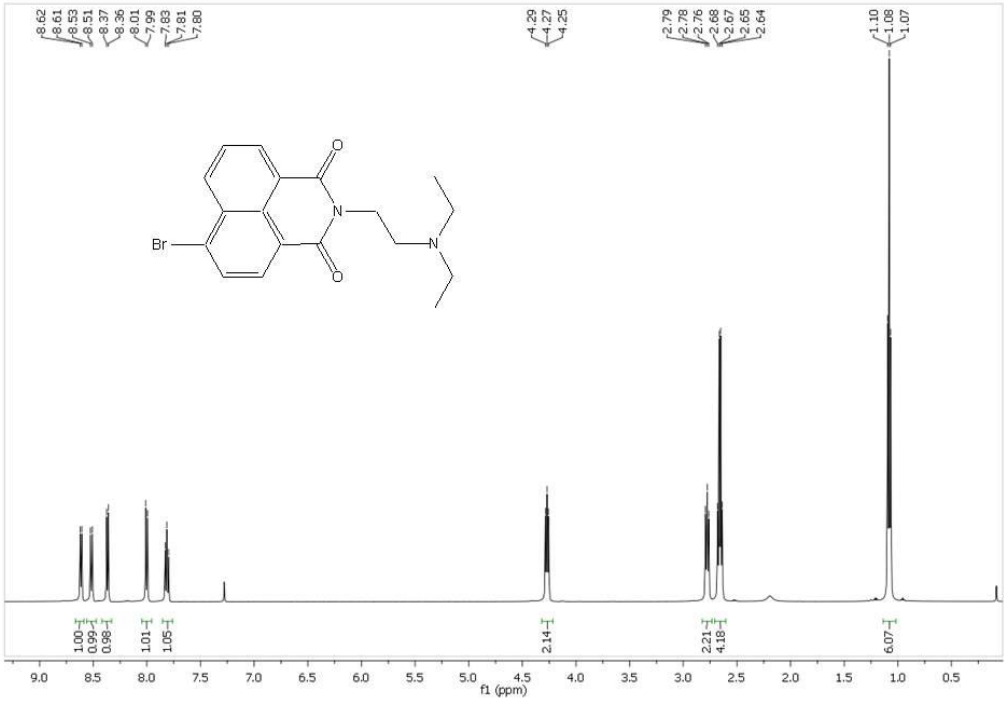

Spectra 4. ^{1}HNMR (500 MHz, $CDCl_3$) of **NP6**

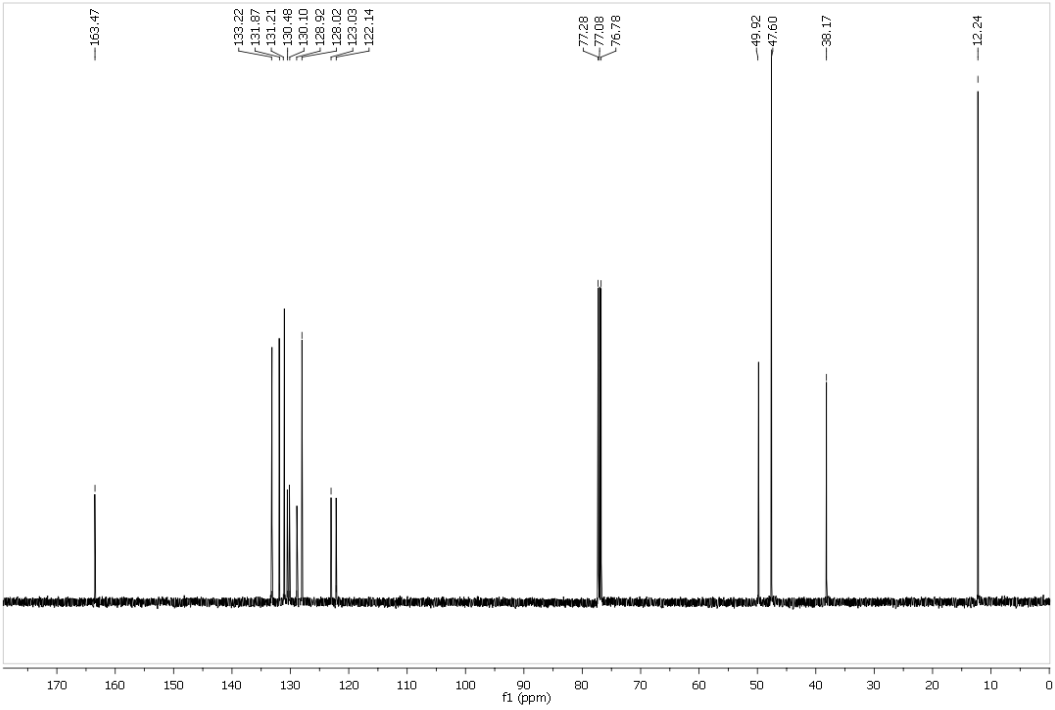

Spectra 5. ^{1}CNMR (125 MHz, $CDCl_3$) of **NP6**

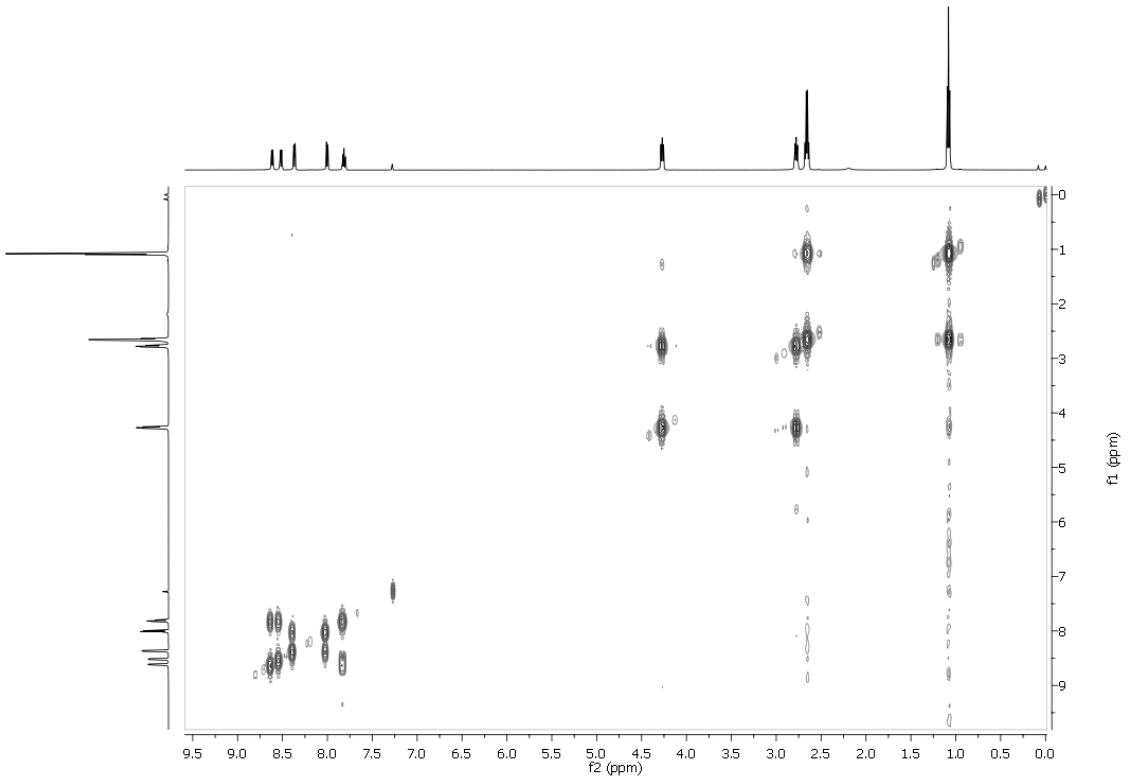

Spectra 6. Gcosy NMR (500 MHz, $CDCl_3$) of **NP6**

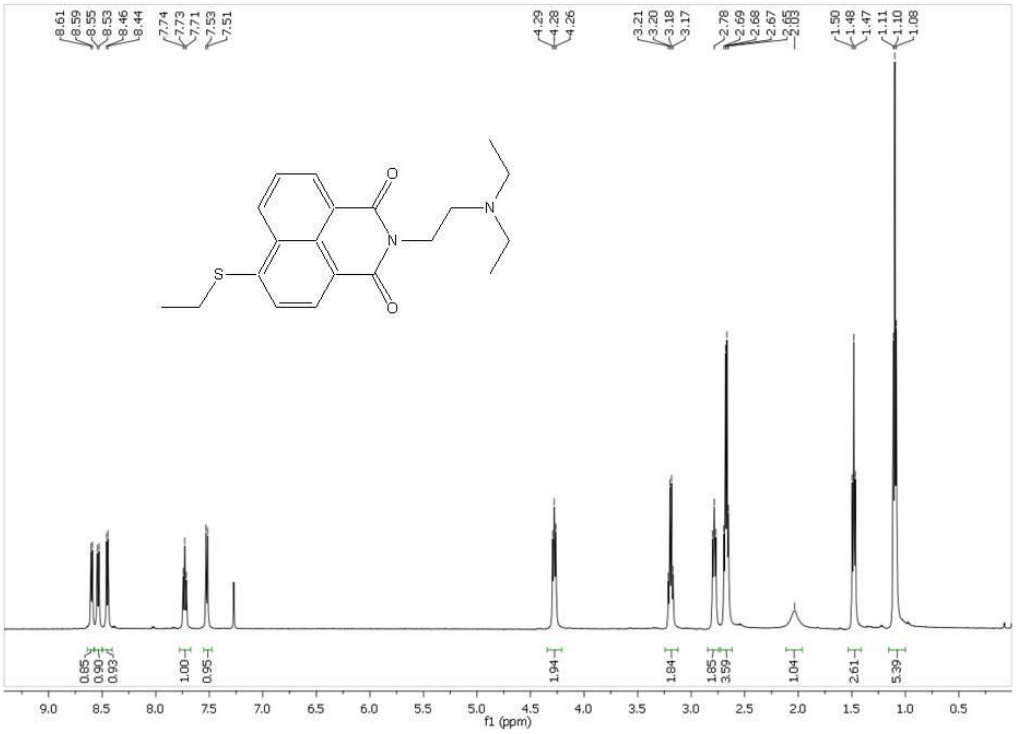

Spectra 7. ^{1}HNMR (500 MHz, $CDCl_3$) of **NP7**

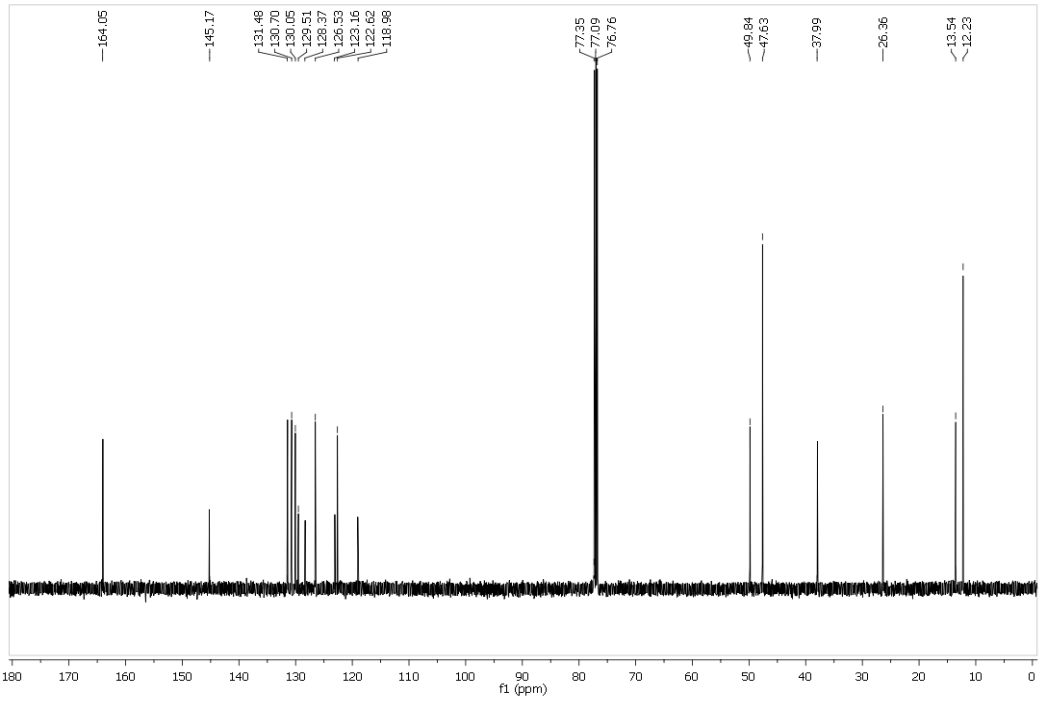

Spectra 8. ^{1}CNMR (125 MHz, $CDCl_3$) of **NP7**

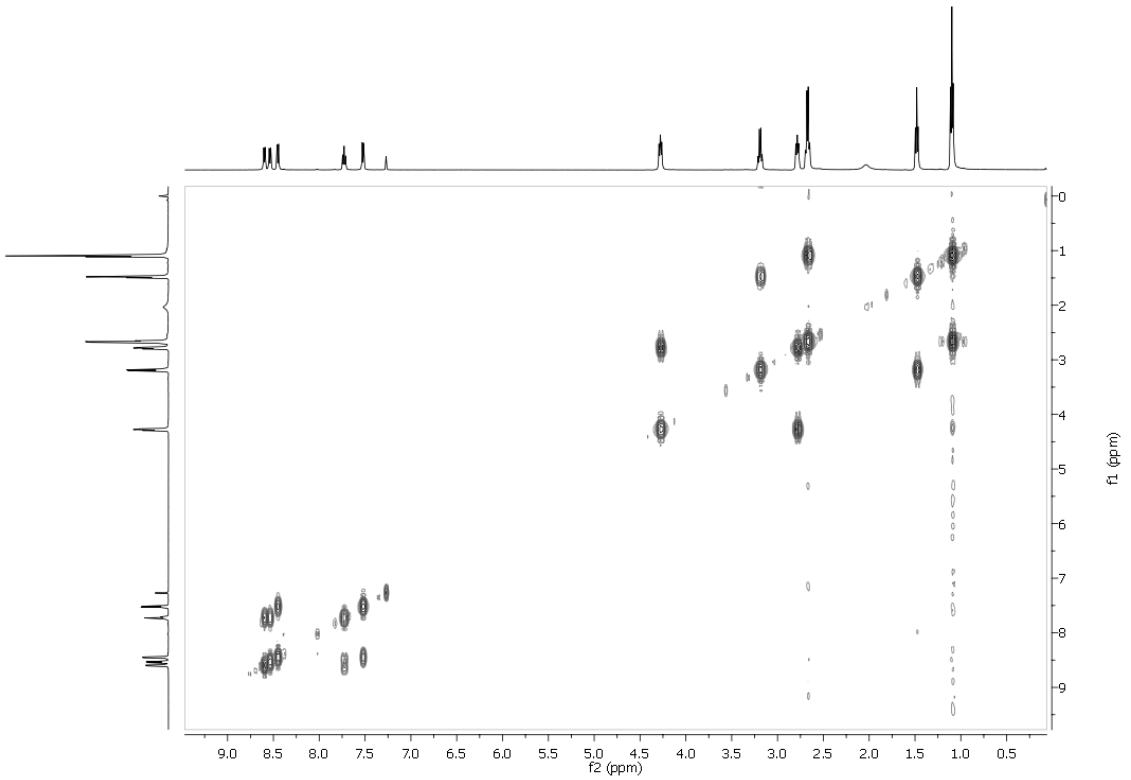

Spectra 9. Gcosy NMR (500 MHz, $CDCl_3$) of **NP7**

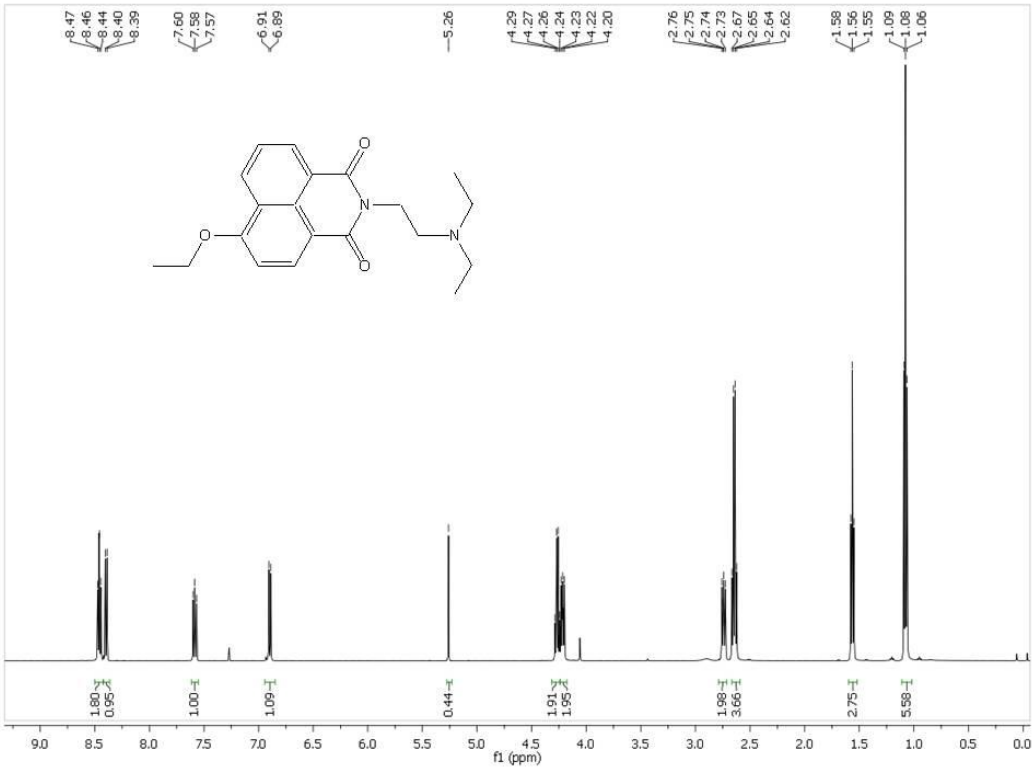

Spectra 10. ^{1}HNMR (500 MHz, $CDCl_3$) of **NP8**

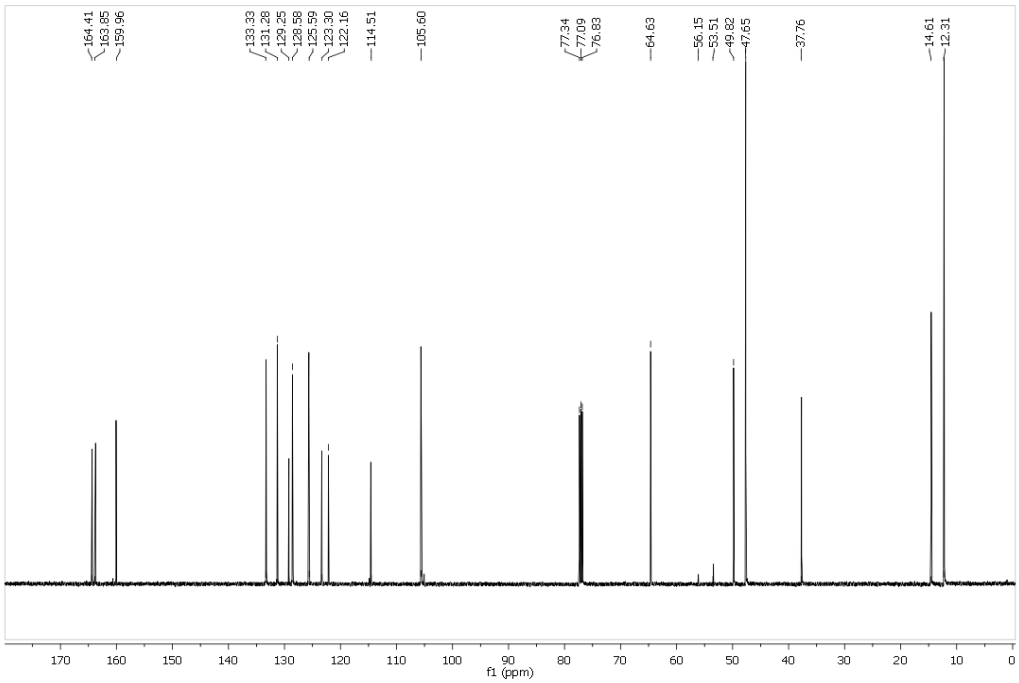

Spectra 11. ^{1}CNMR (125 MHz, $CDCl_3$) of **NP8**

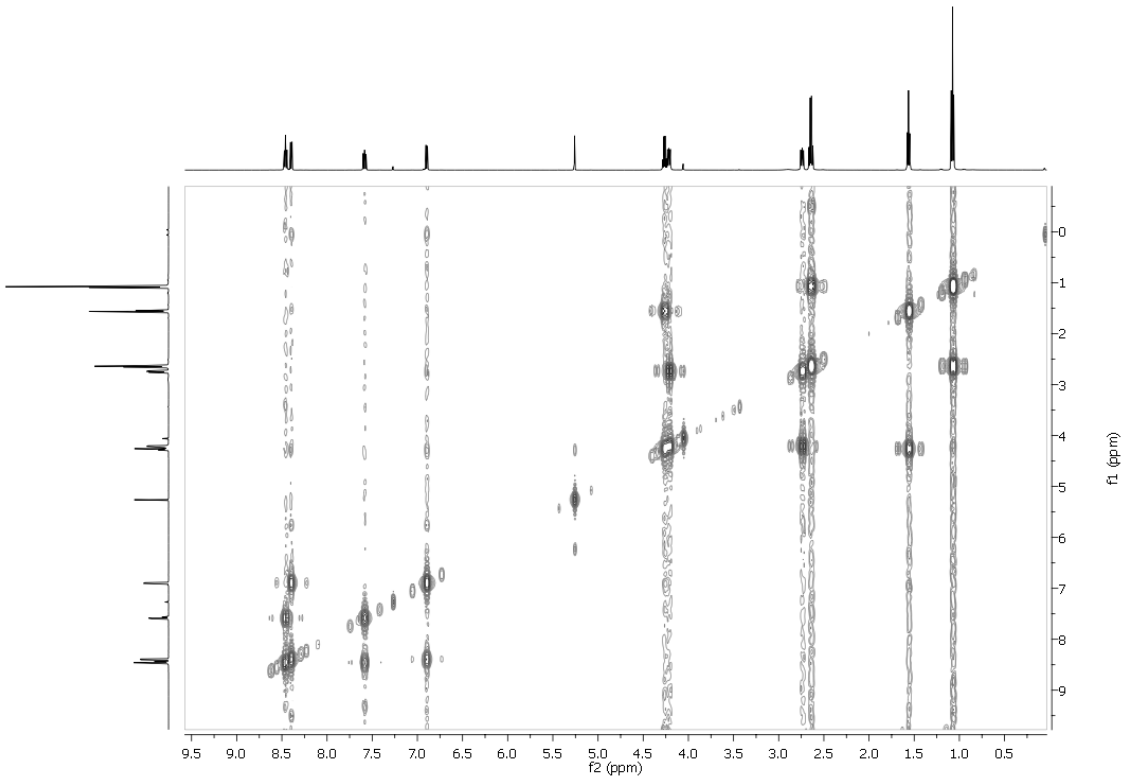

Spectra 12. Gcosy NMR (500 MHz, $CDCl_3$) of **NP8**

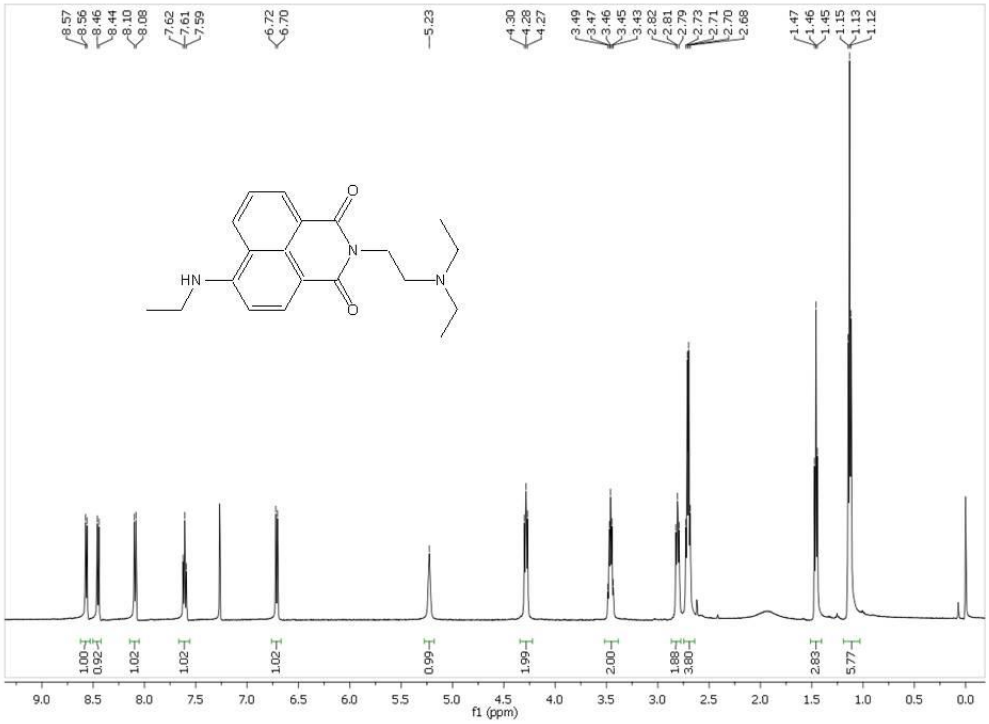

Spectra 13. ^{1}HNMR (500 MHz, $CDCl_3$) of **NP9**

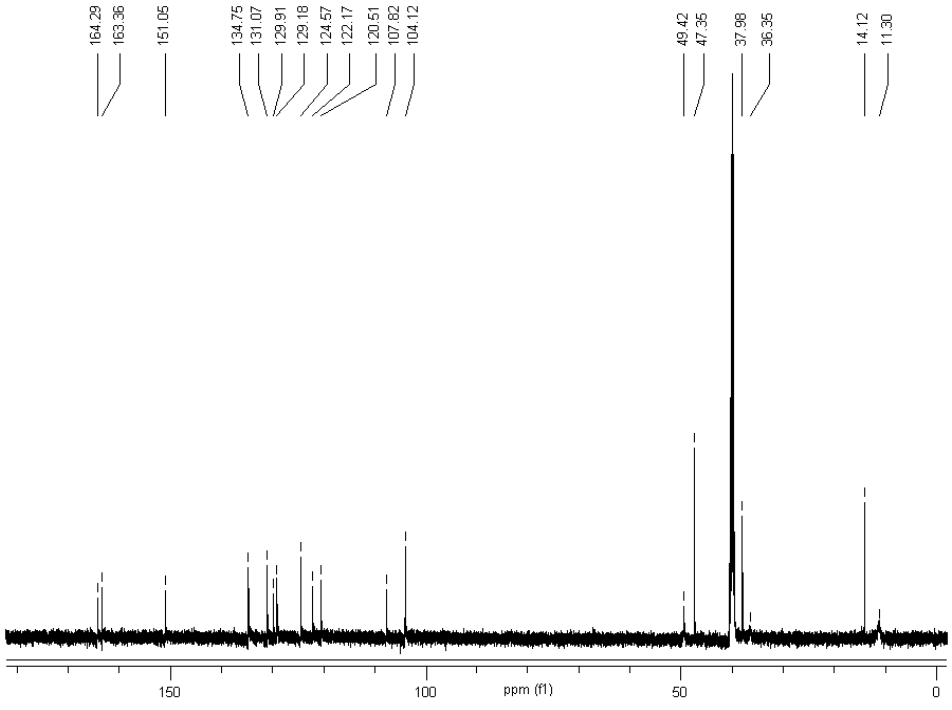

Spectra 14. ^{1}CNMR (125 MHz, DMSO) of **NP9**

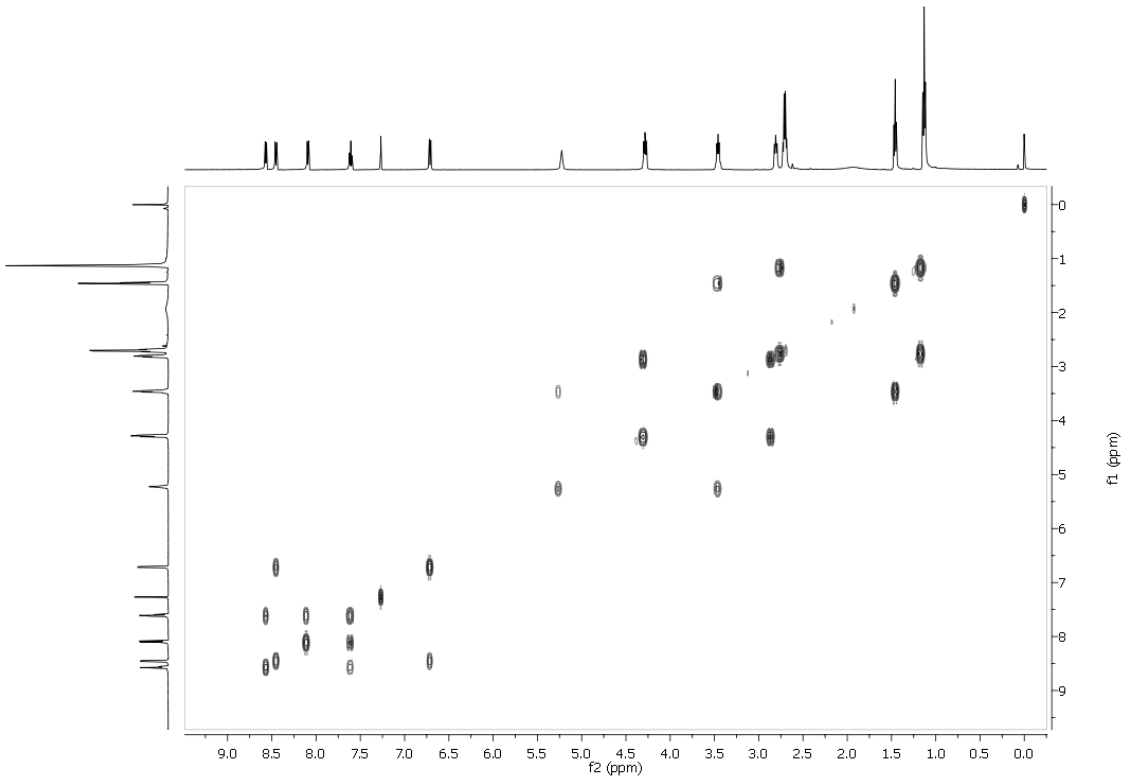

Spectra 15. Gcosy NMR (500 MHz, $CDCl_3$) of **NP9**

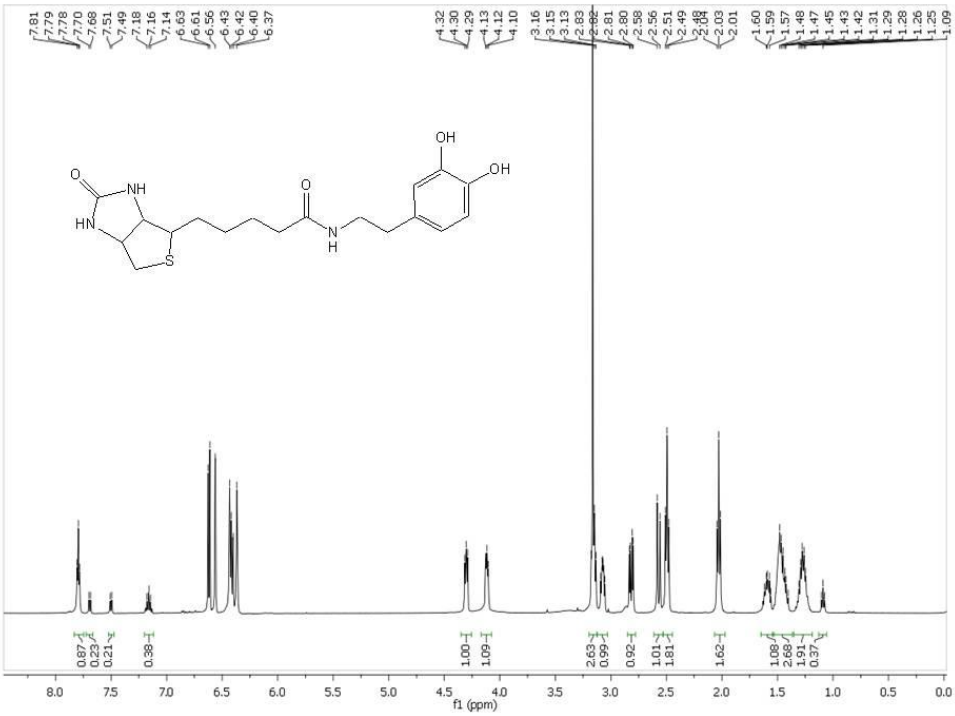

Spectra 16. ^{1}HNMR (500 MHz, DMSO) of **BD2**

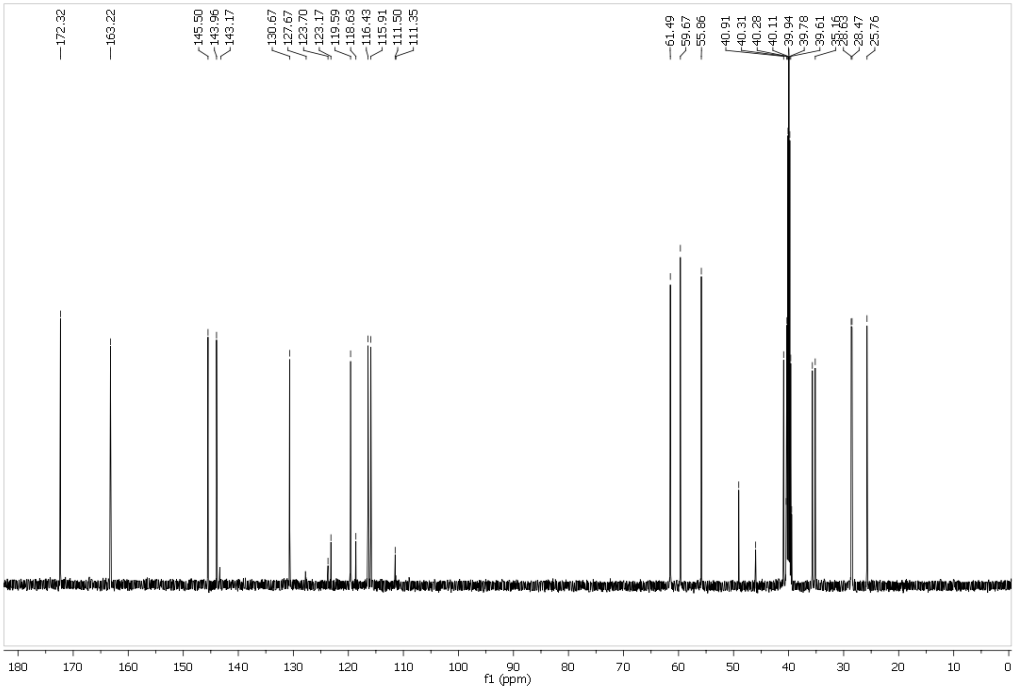

Spectra 17. ^{1}CNMR (125 MHz, DMSO) of **BD2**

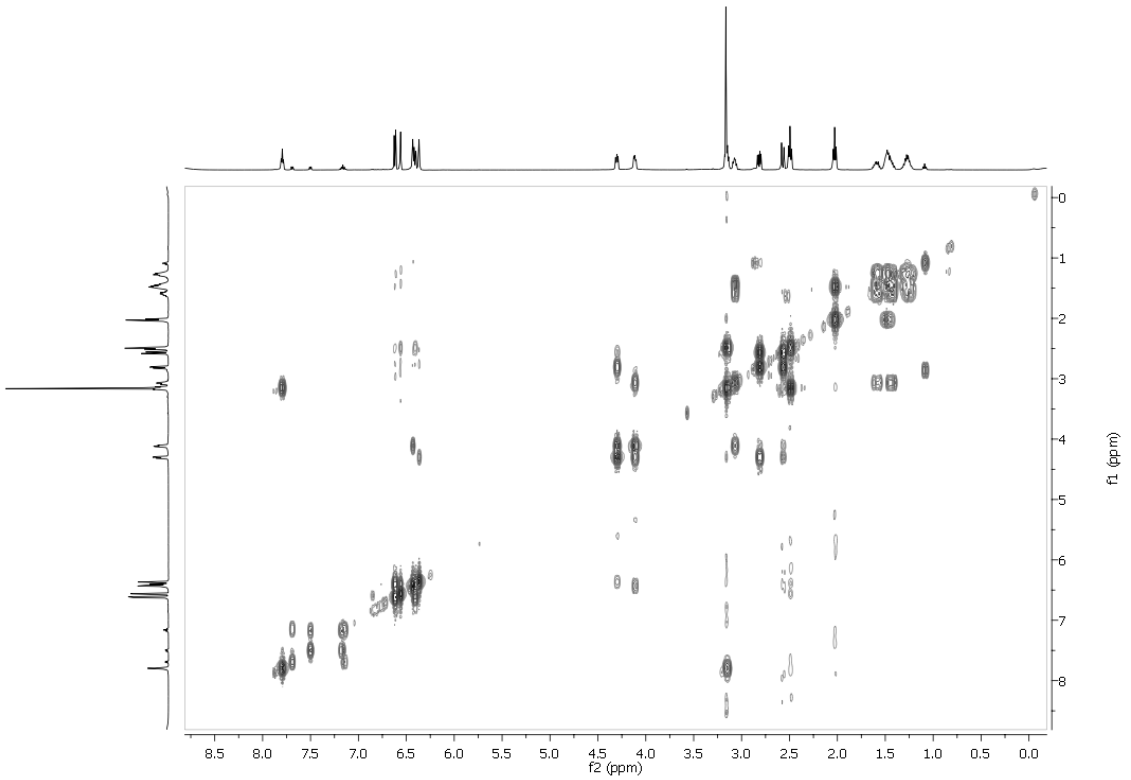

Spectra 18. Gcosy NMR (500 MHz, DMSO) of **BD2**

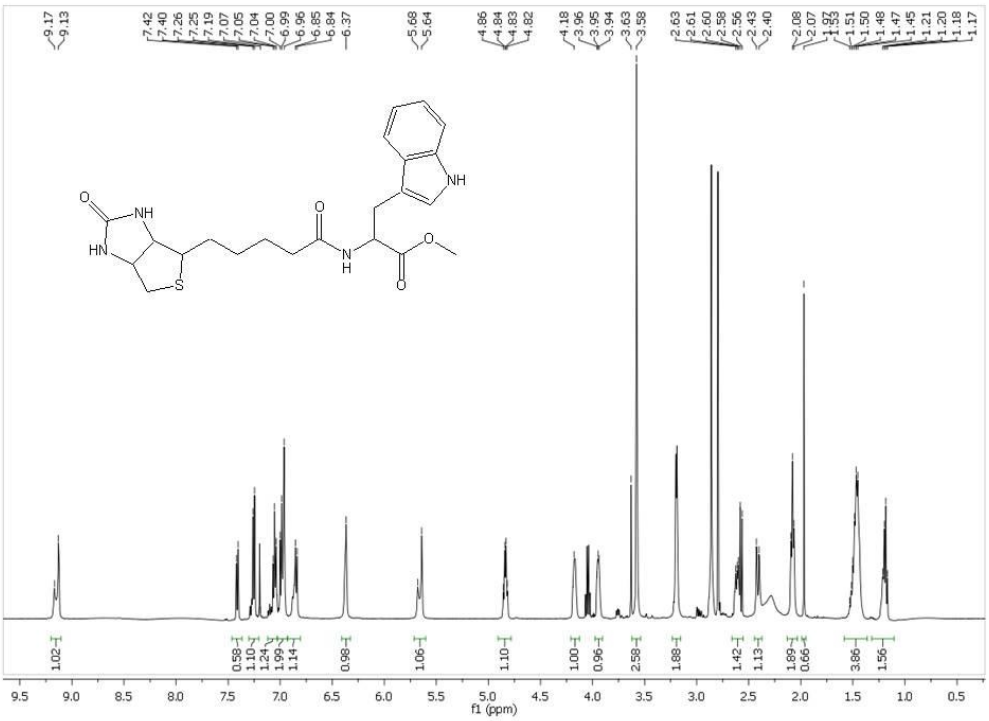

Spectra 19. ^{1}HNMR (500 MHz, DMSO) of **BD3**

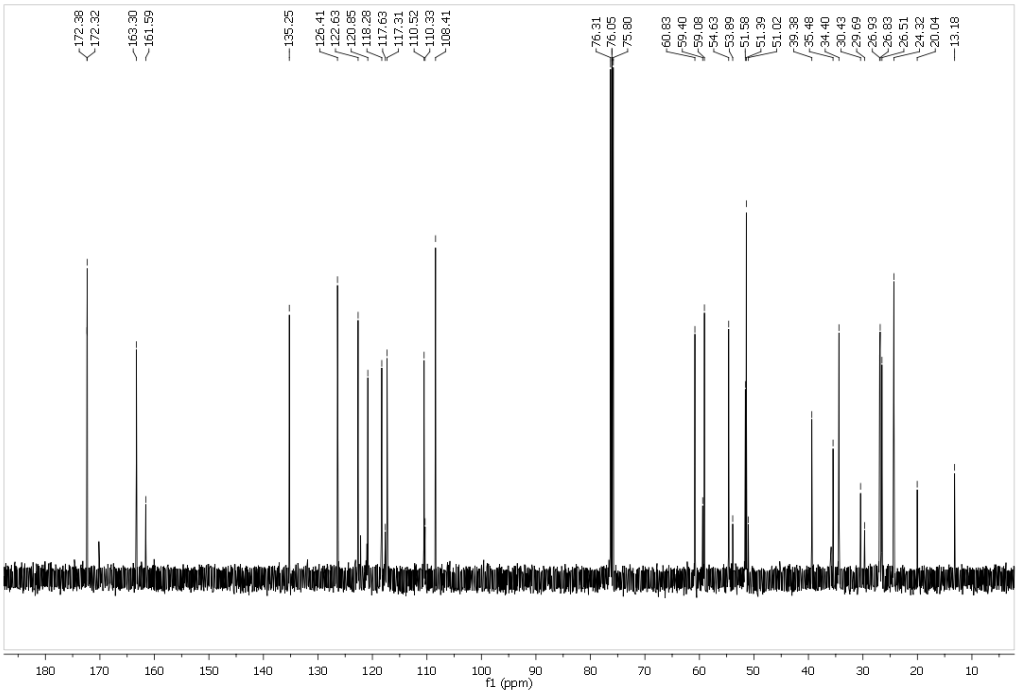

Spectra 20. ^{1}CNMR (125 MHz, DMSO) of **BD3**

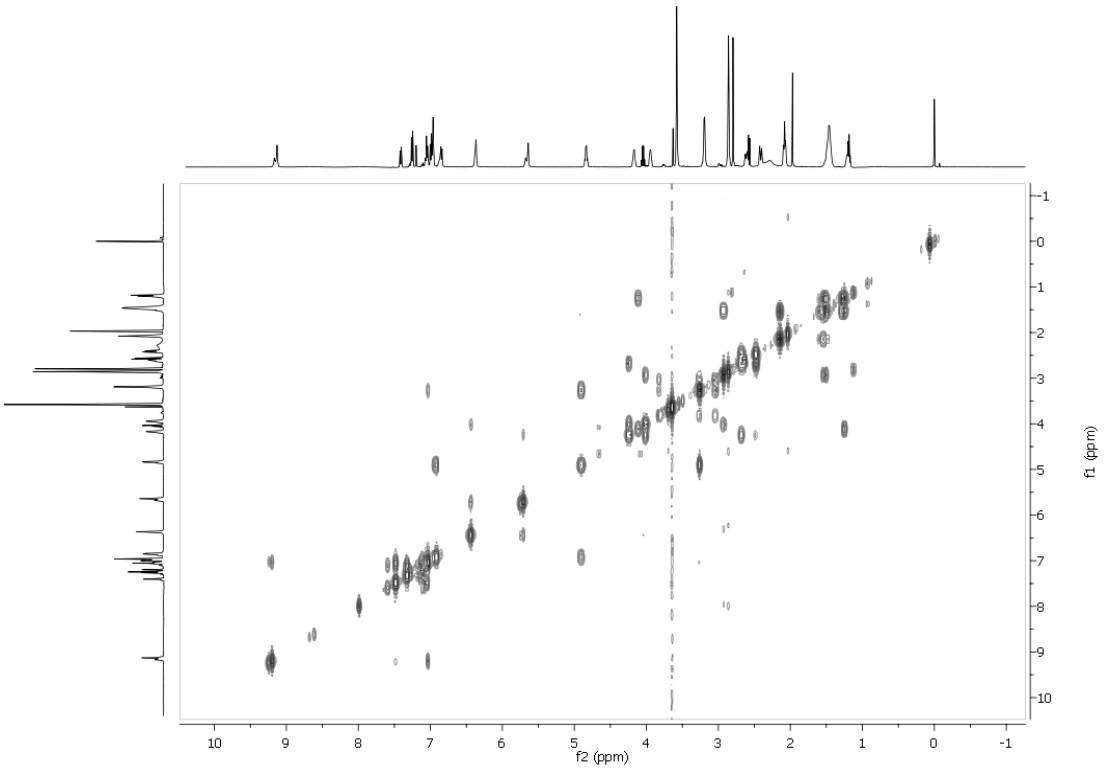

Spectra 21. Gcosy NMR (500 MHz, DMSO) of **BD3**

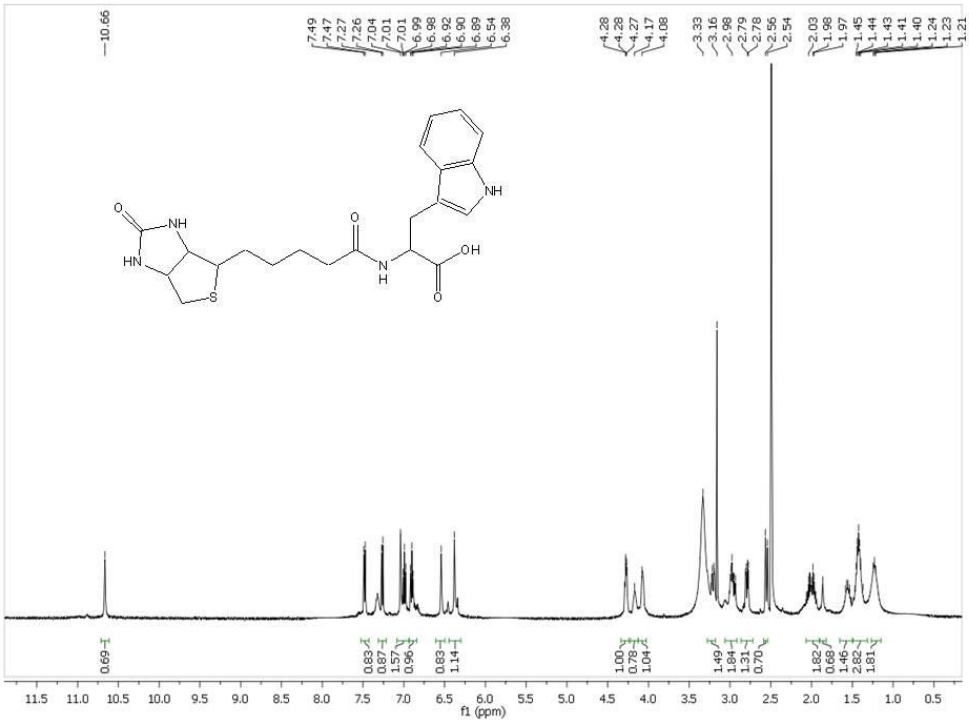

Spectra 22. [1]HNMR (500 MHz, DMSO) of **BD4**

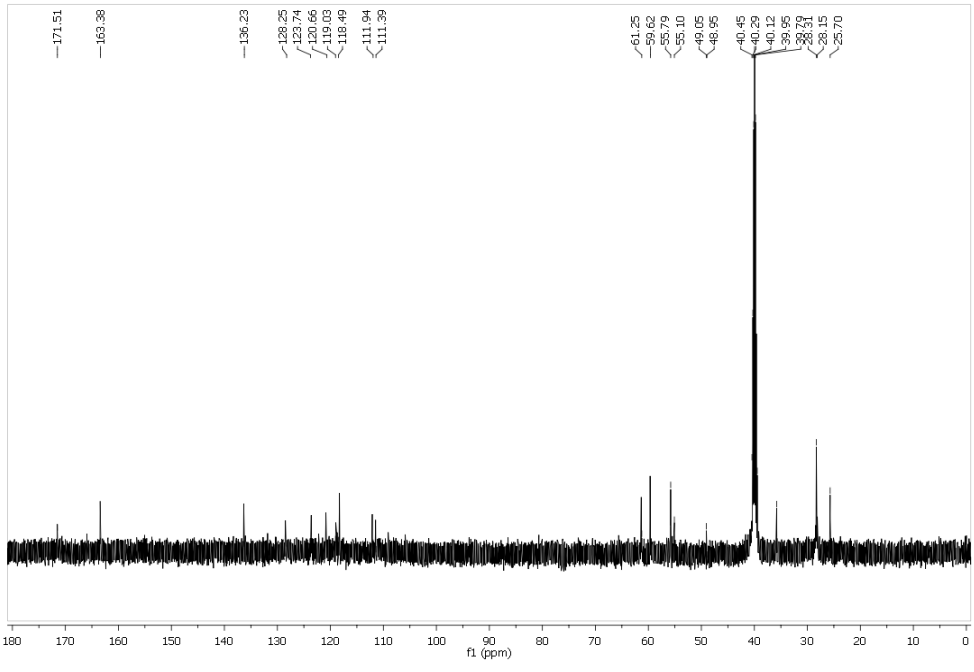

Spectra 23. [1]CNMR (125 MHz, DMSO) of **BD4**

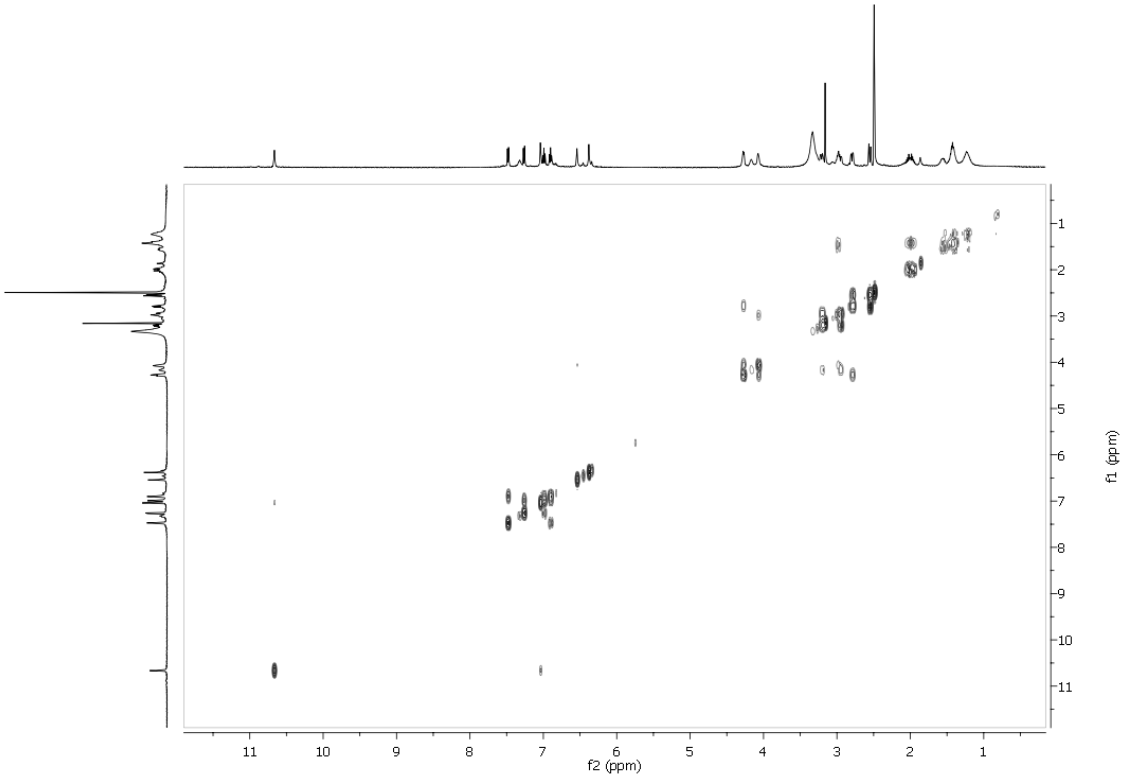

Spectra 24. Gcosy NMR (500 MHz, DMSO) of **BD4**

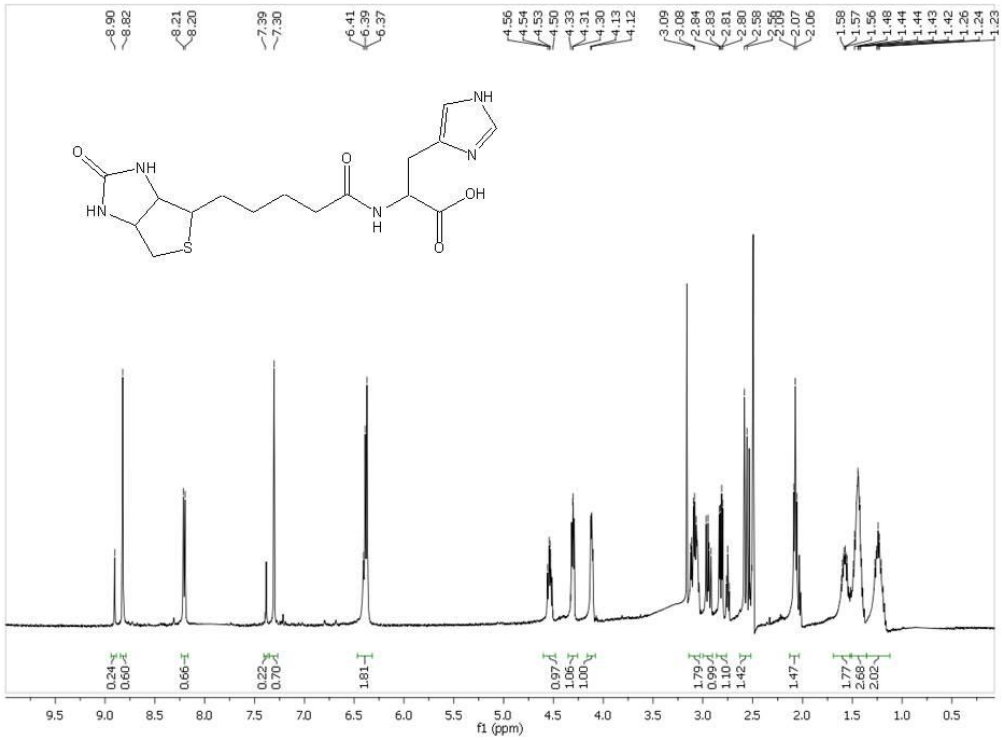

Spectra 25. [1]HNMR (500 MHz, DMSO) of **BD5**

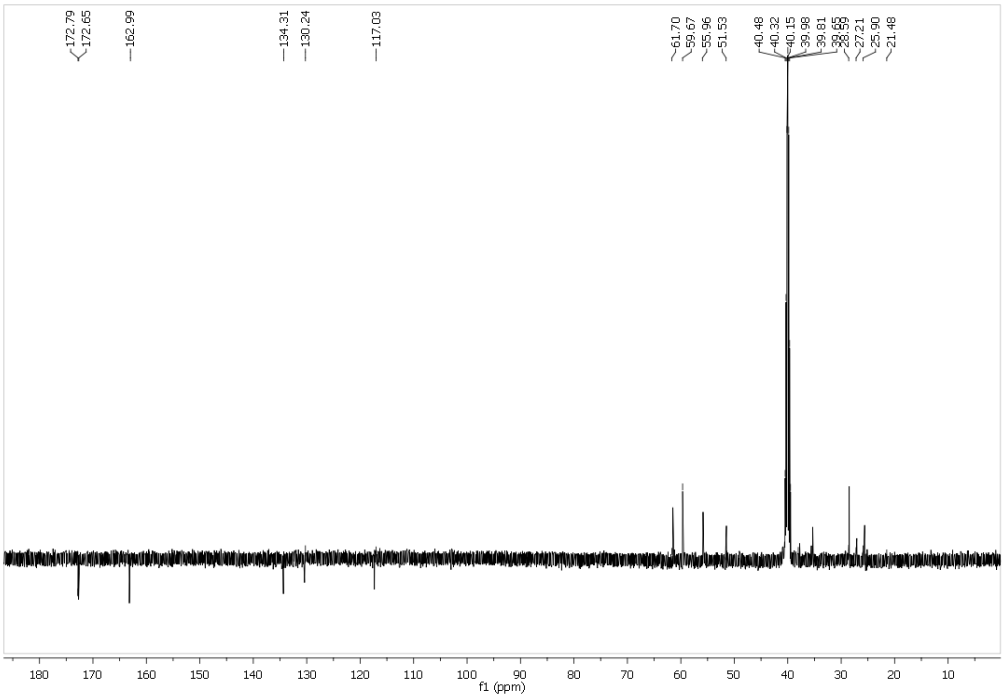

Spectra 26. [1]CNMR (125 MHz, DMSO) of **BD5**

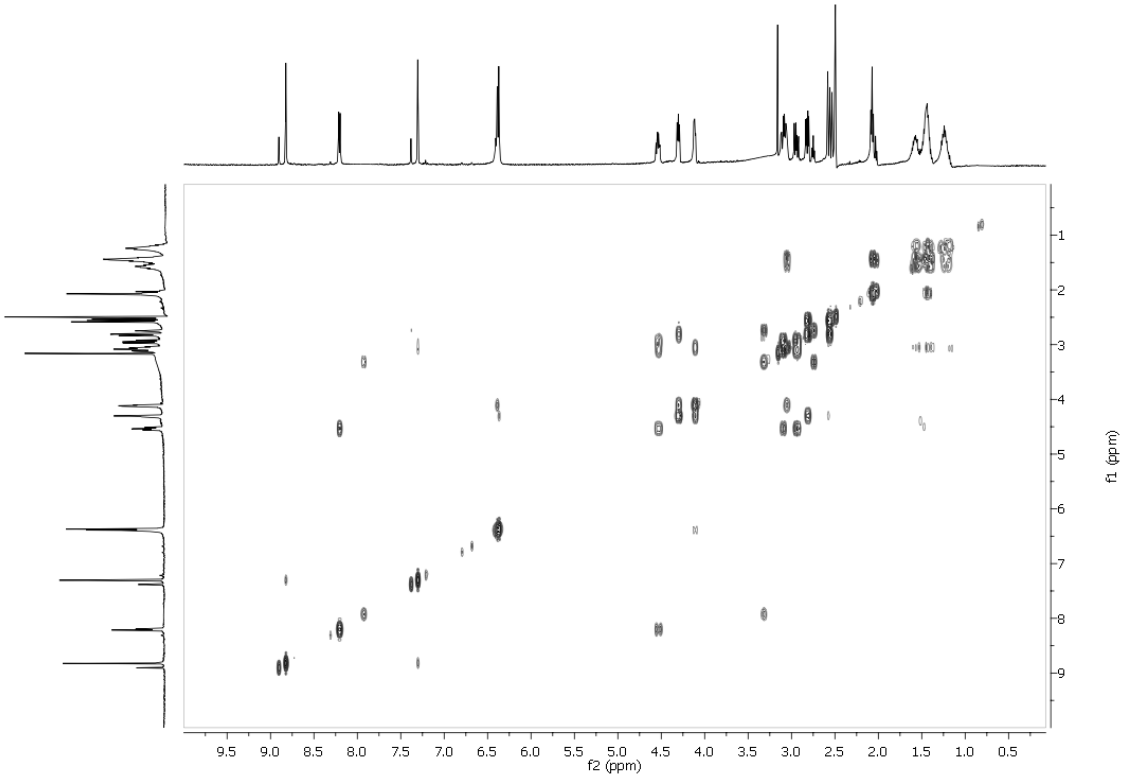

Spectra 27. Gcosy NMR (500 MHz, DMSO) of **BD5**

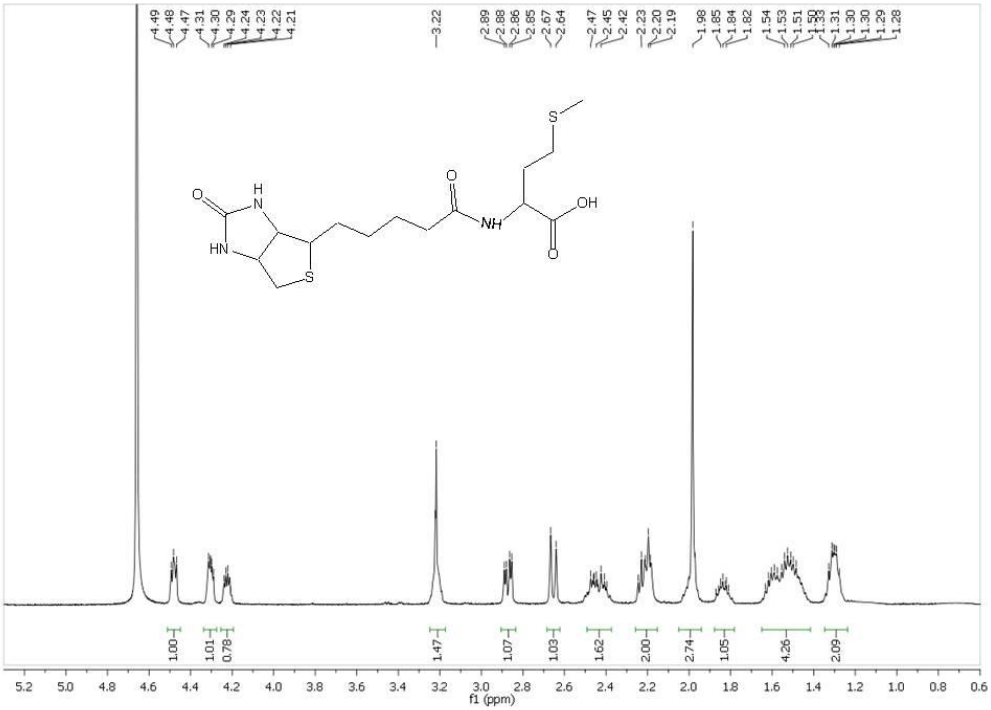

Spectra 28. ^{1}HNMR (500 MHz, D_2O) of **BD6**

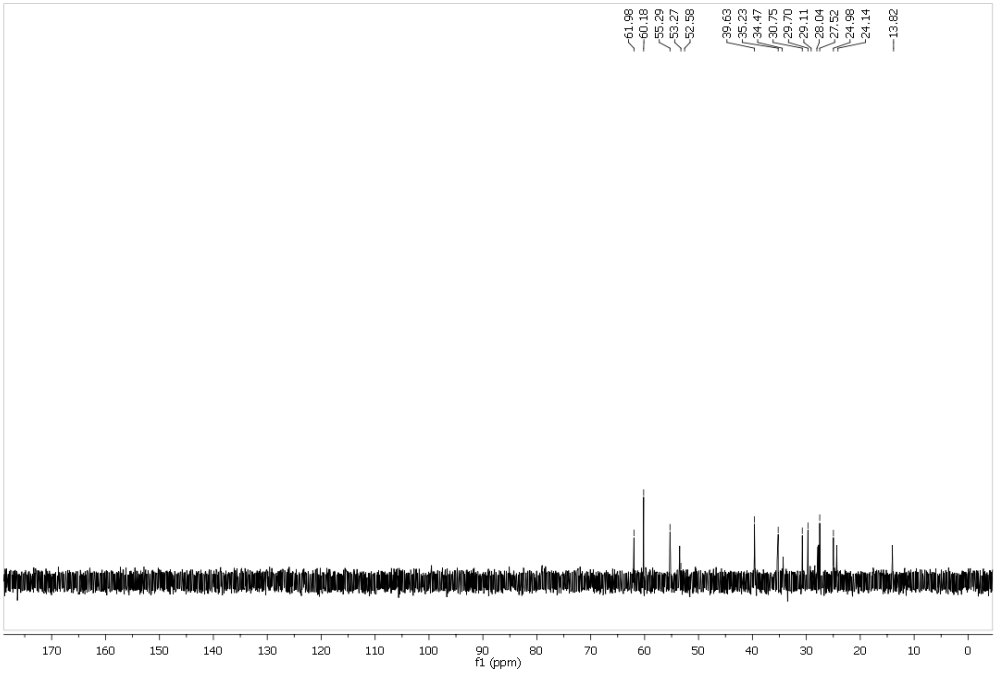

Spectra 29. ^{1}CNMR (125 MHz, D_2O) of **BD6**

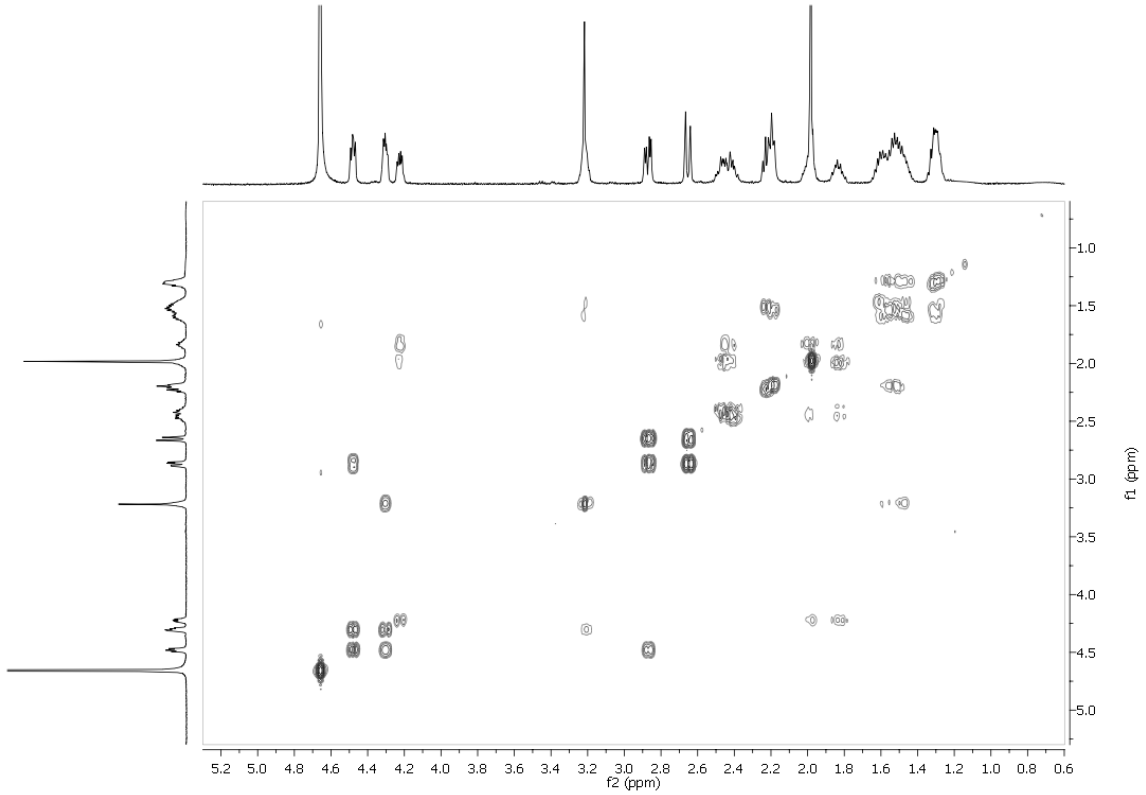

Spectra 30. Gcosy NMR (500 MHz, D_2O) of **BD6**

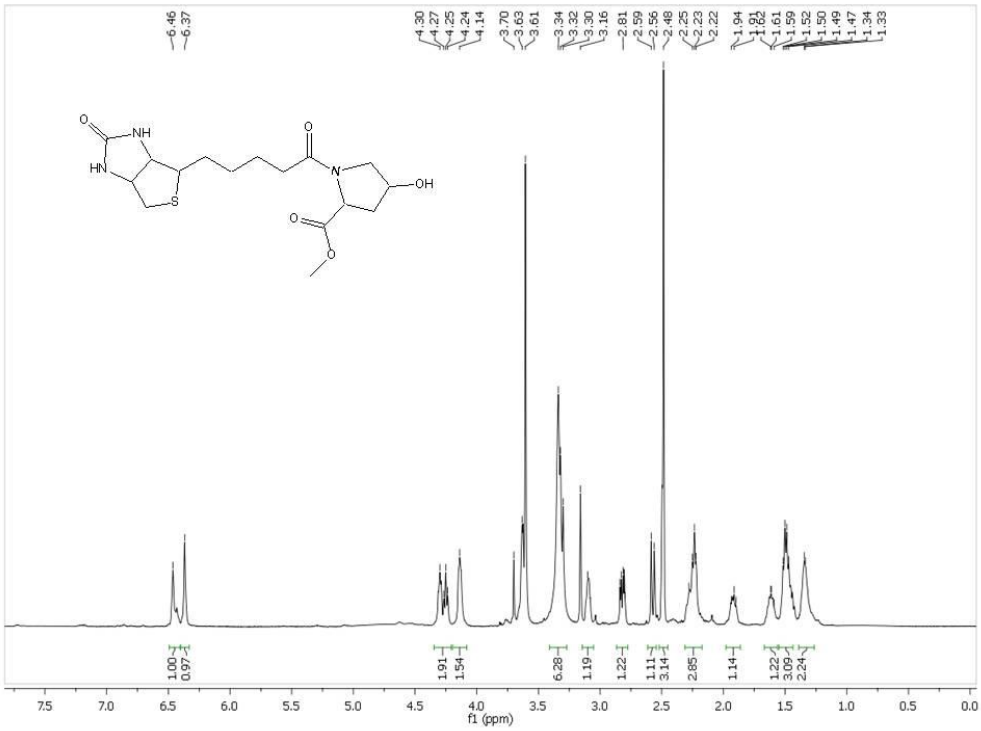

Spectra 31. ^{1}HNMR (500 MHz, DMSO) of **BD7**

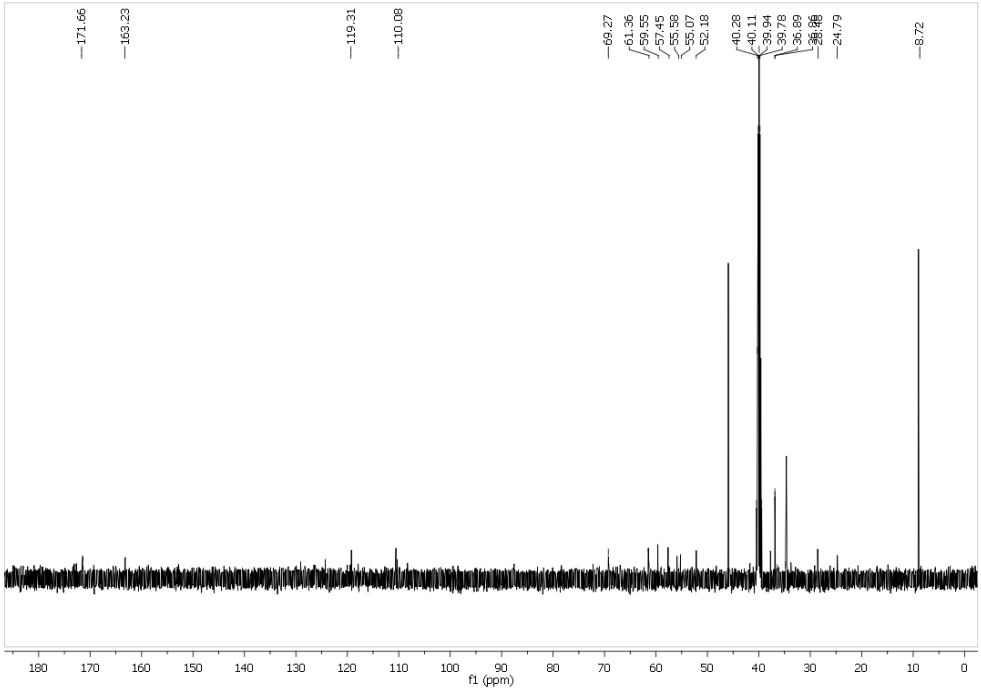

Spectra 32. ^{1}CNMR (125 MHz, DMSO) of **BD7**

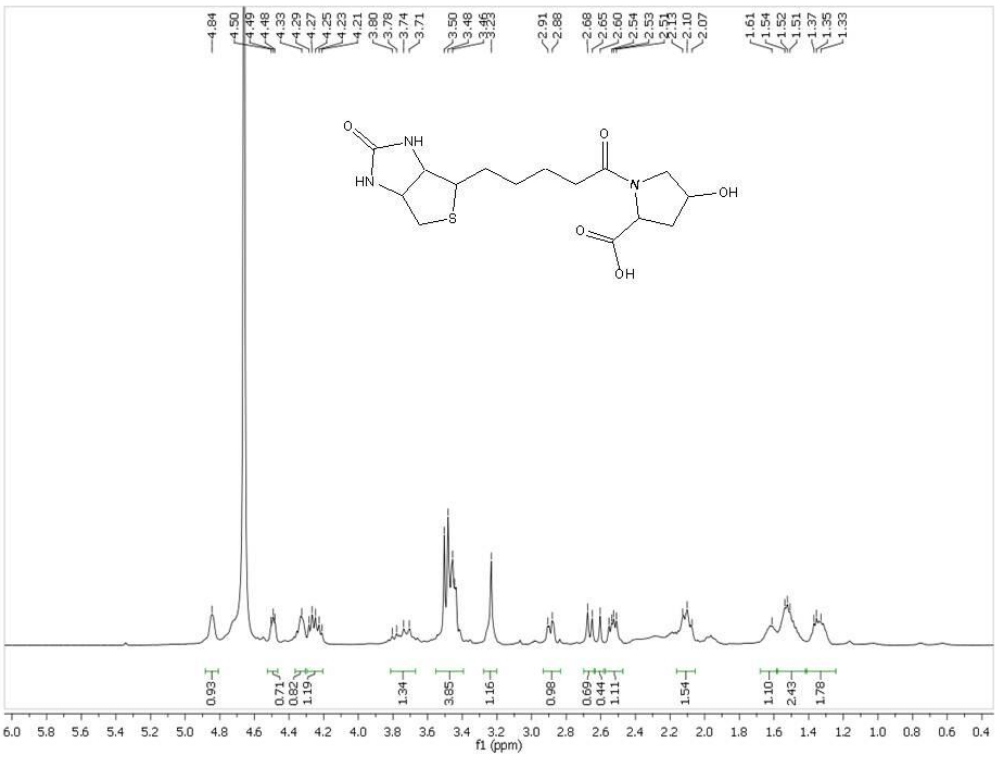

Spectra 33. ^{1}HNMR (500 MHz, D_2O) of **BD8**

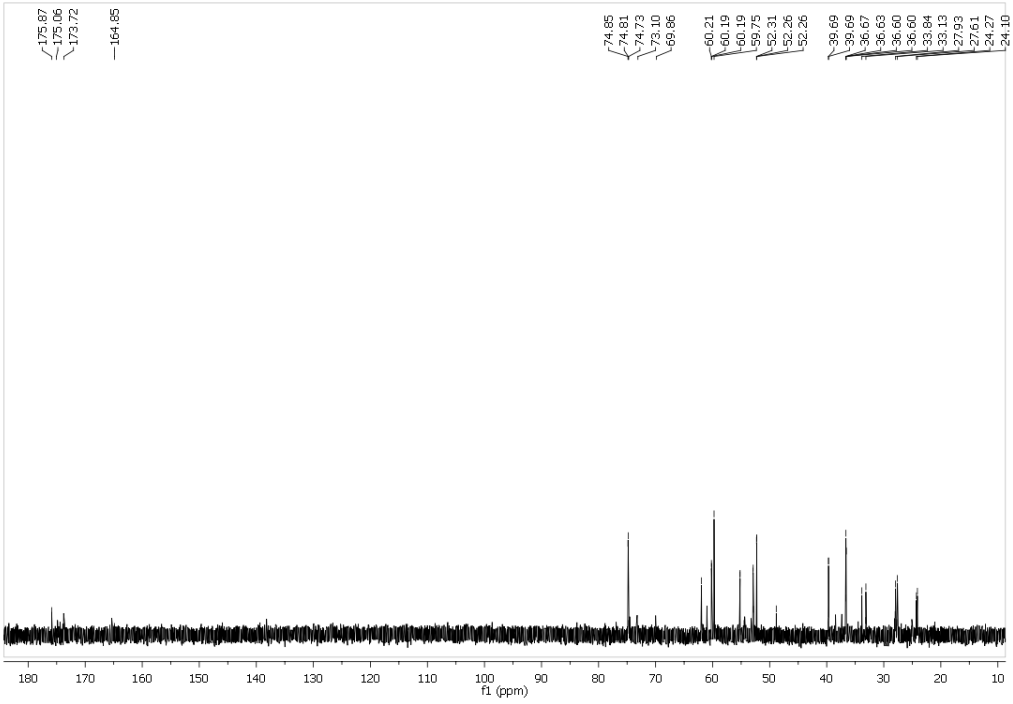

Spectra 34. ^{1}CNMR (125 MHz, D_2O) of **BD8**

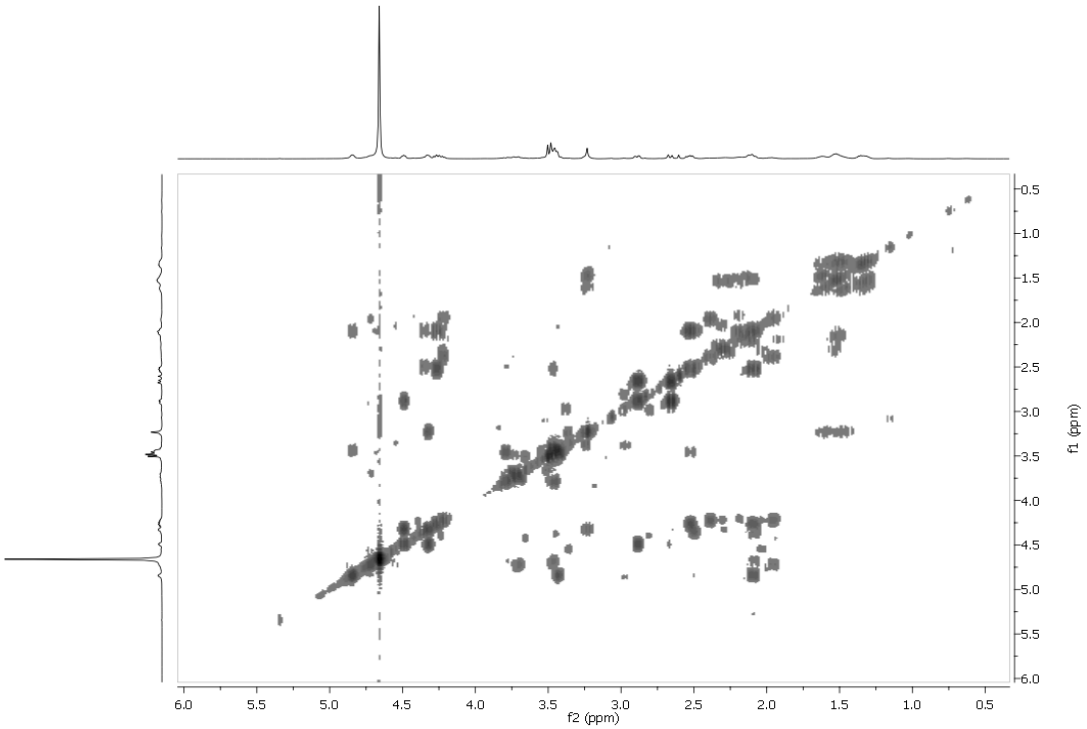

Spectra 35. Gcosy NMR (500 MHz, D_2O) of **BD8**

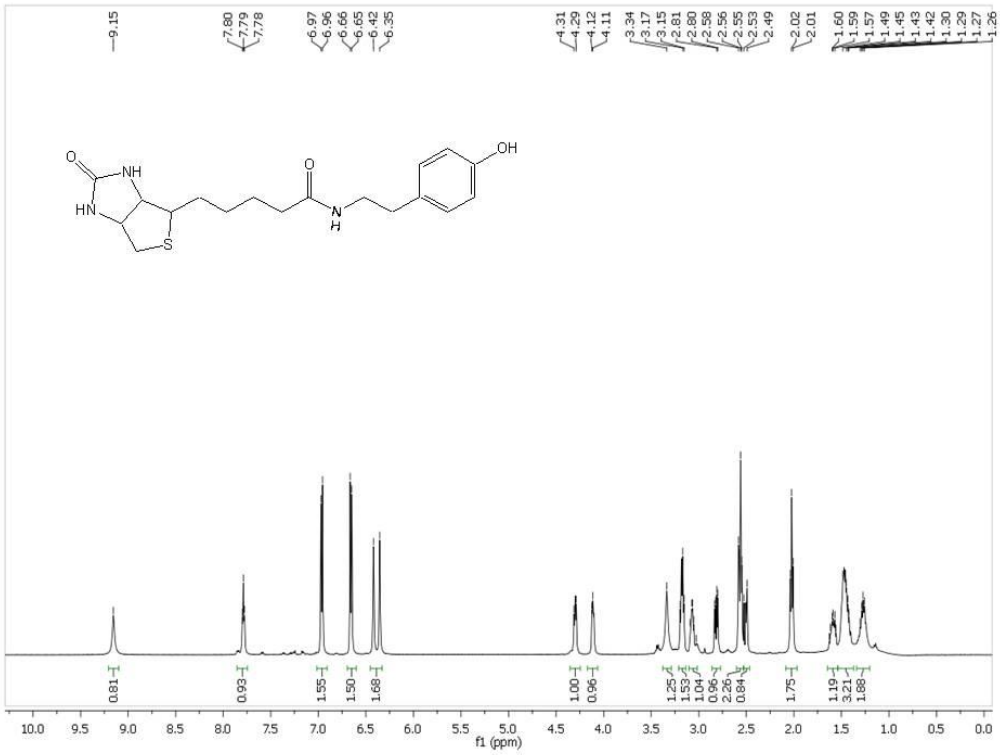

Spectra 36. [1]HNMR (500 MHz, DMSO) of **BD9**

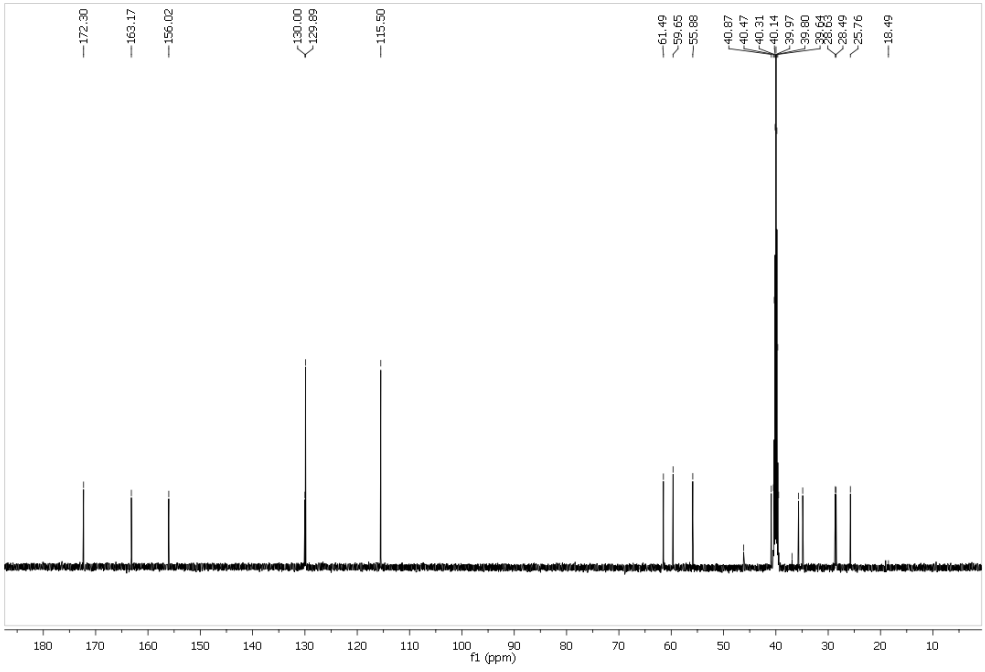

Spectra 37. [1]CNMR (125 MHz, DMSO) of **BD9**

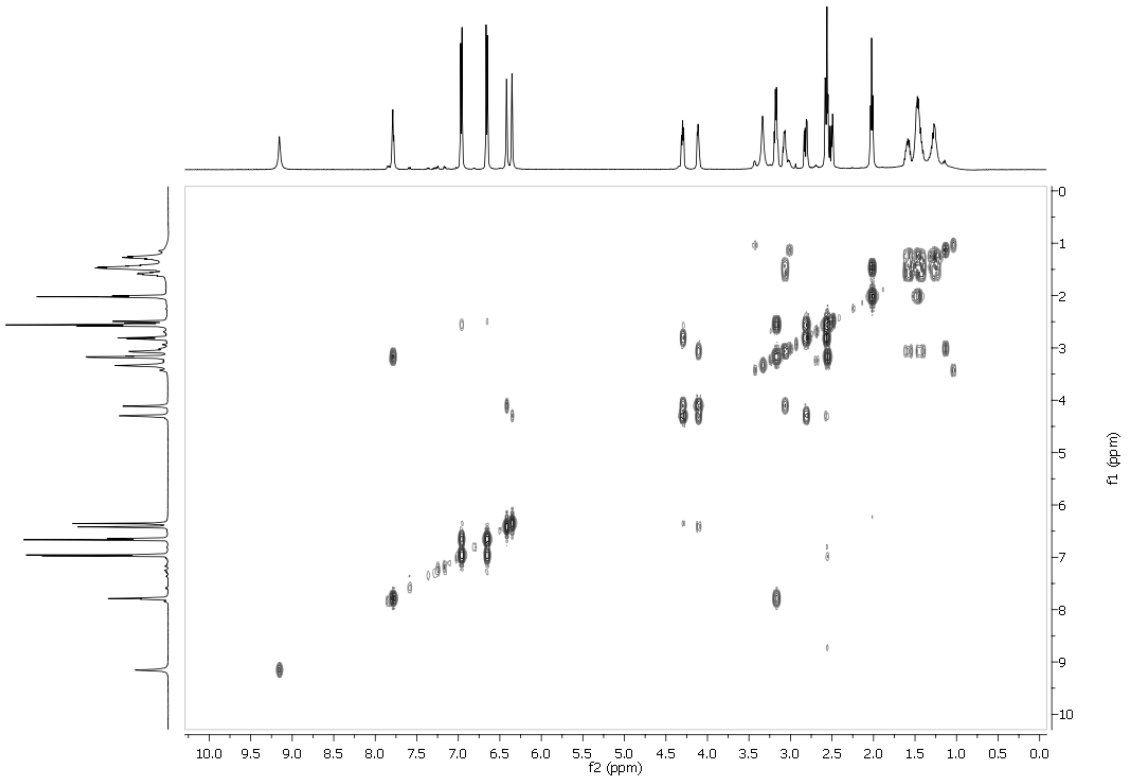

Spectra 38. Gcosy NMR (500 MHz, DMSO) of **BD9**

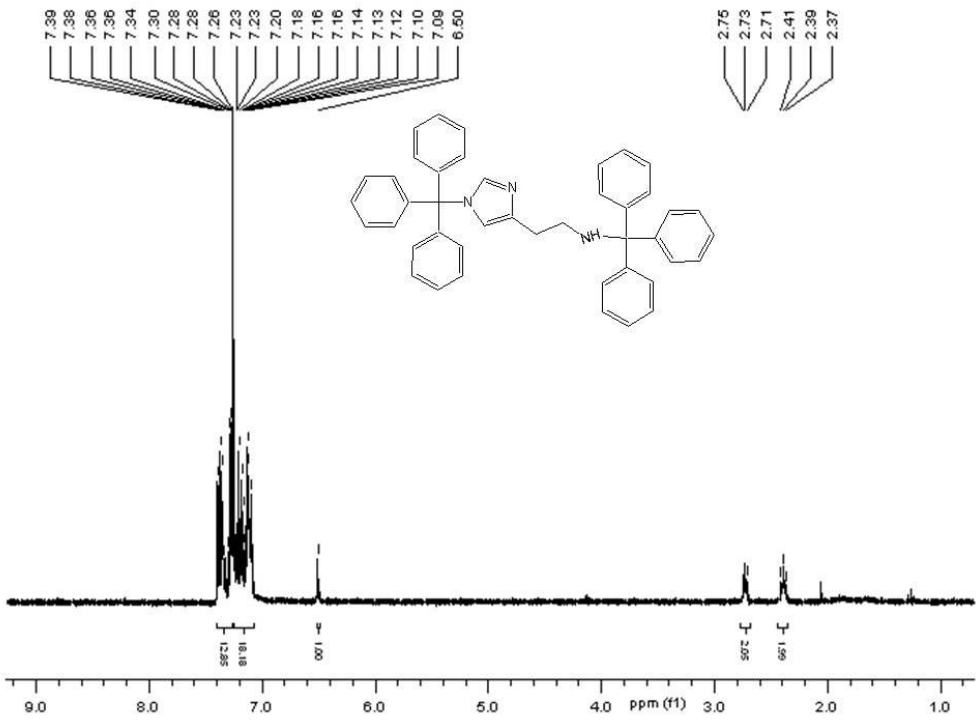

Spectra 39. ^{1}HNMR (300 MHz, $CDCl_3$) of **C1**

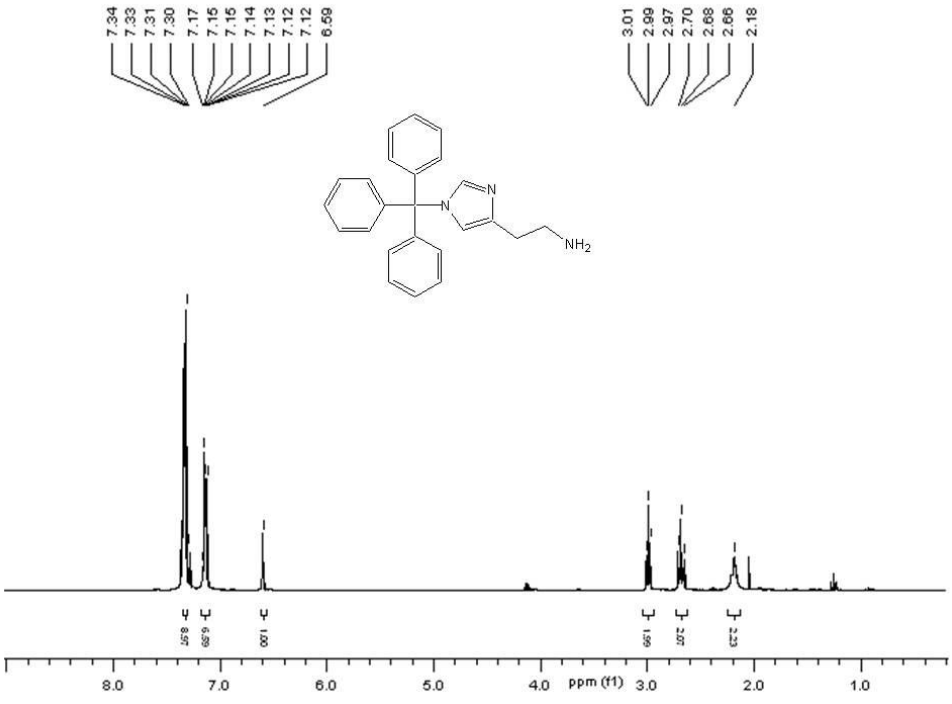

Spectra 40. ^{1}HNMR (300 MHz, $CDCl_3$) of **C2**

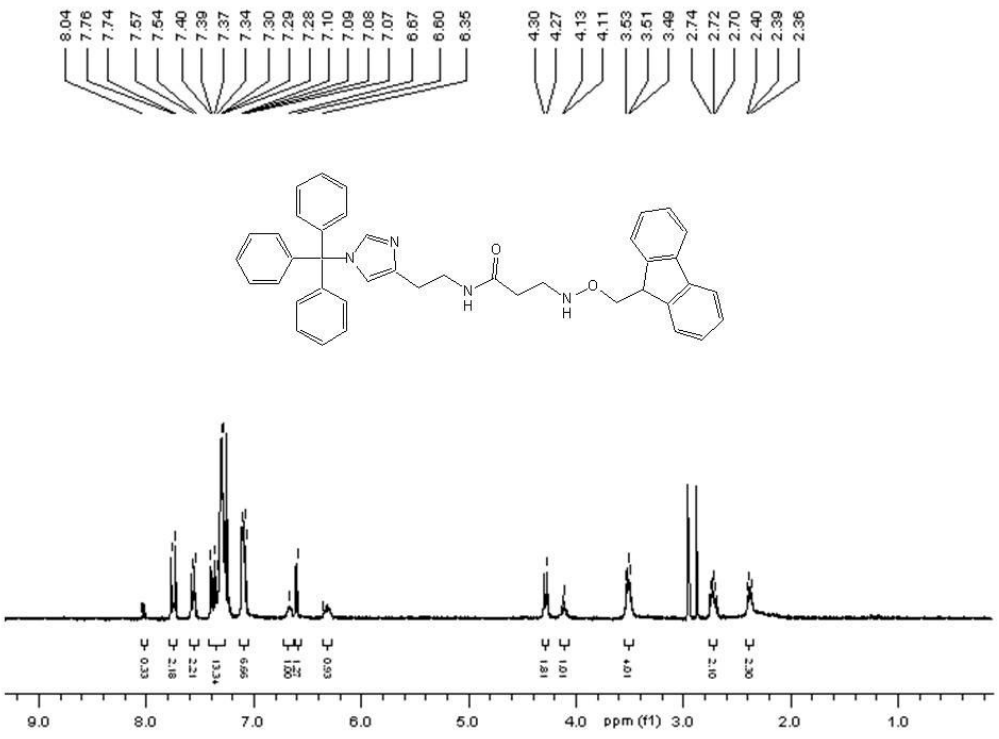

Spectra 41. ^{1}HNMR (300 MHz, $CDCl_3$) of **C3**

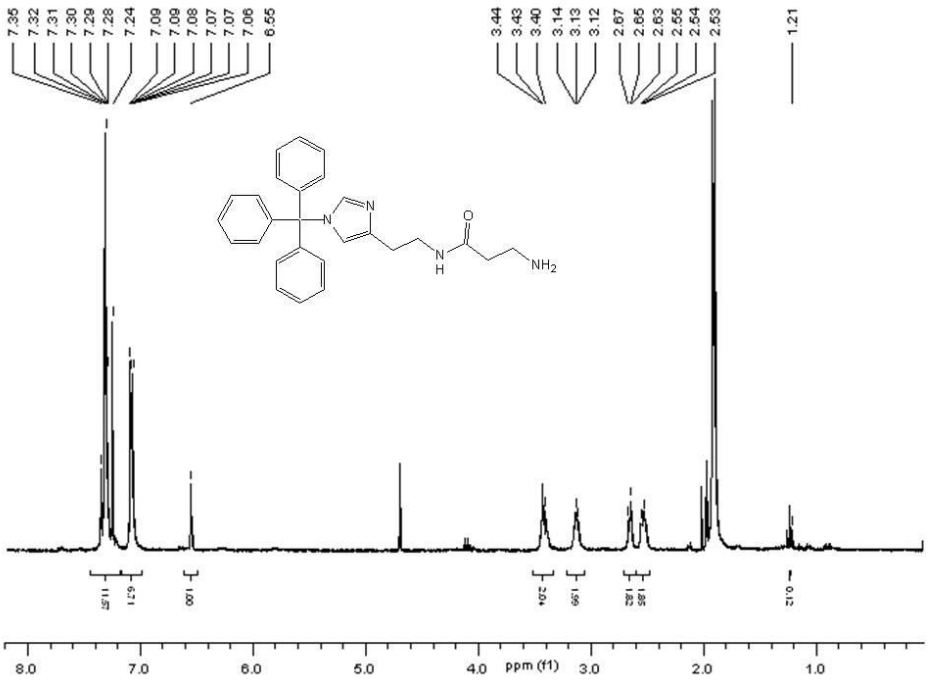

Spectra 42. ^{1}HNMR (300 MHz, $CDCl_3$) of **C4**

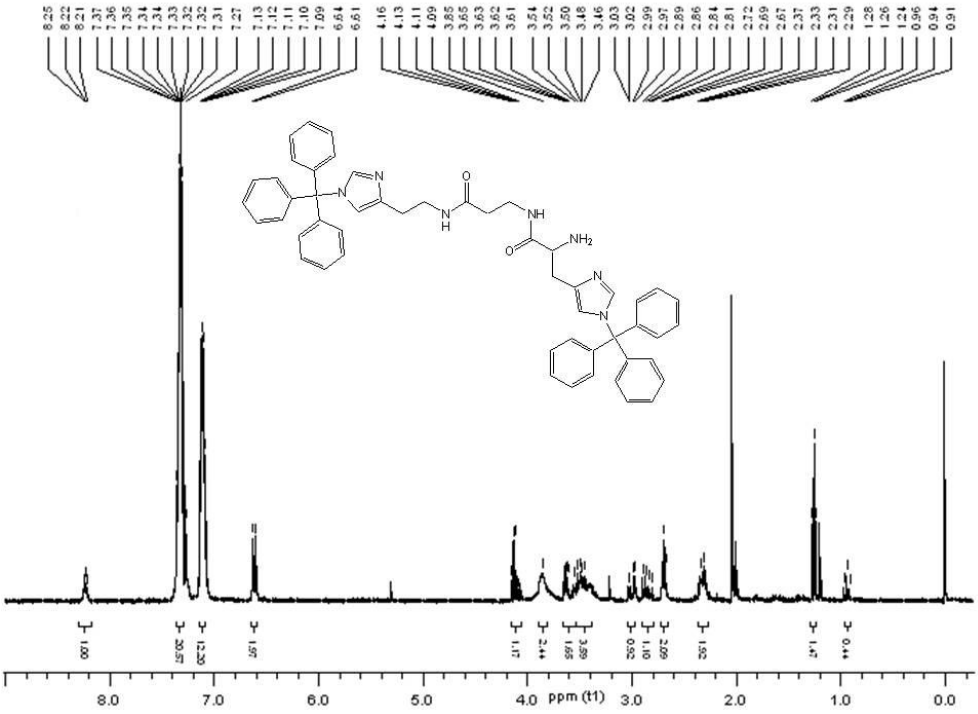

Spectra 43. ^{1}HNMR (300 MHz, $CDCl_3$) of **C5**

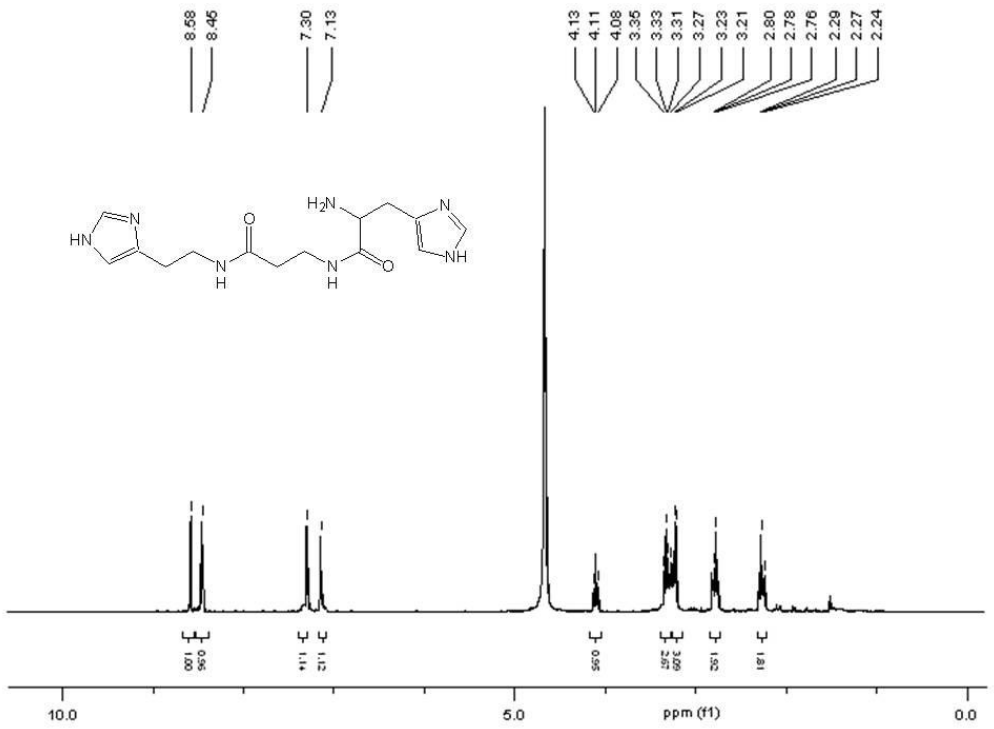

Spectra 44. ^{1}HNMR (300 MHz, D_2O) of **C6**

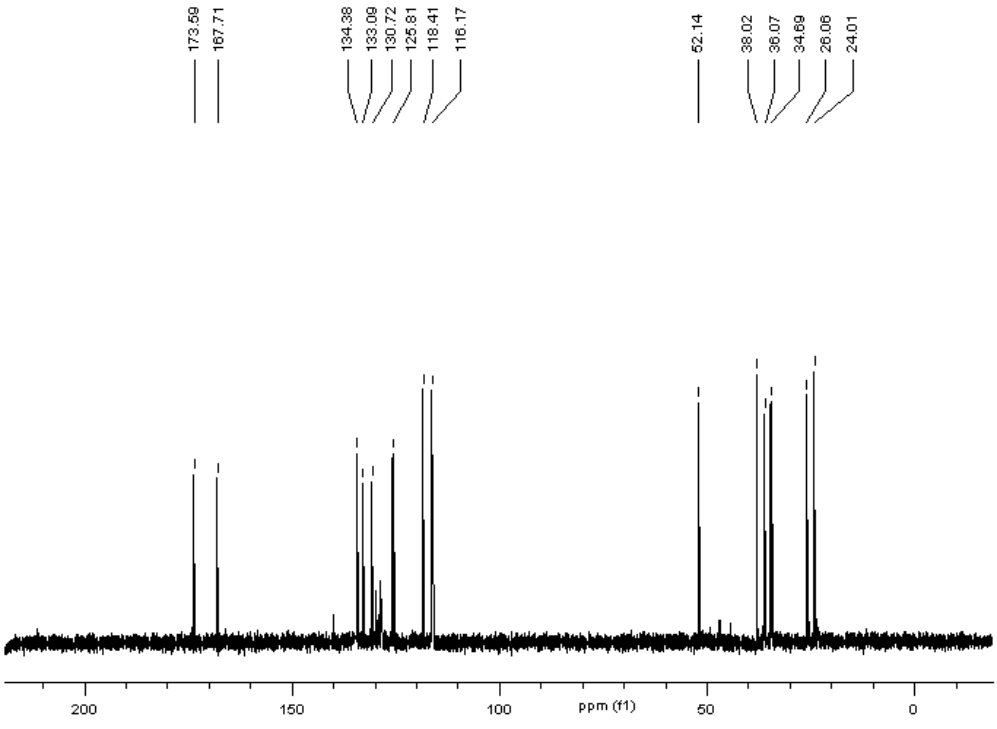

Spectra 45. ^{1}CNMR (75 MHz, D_2O) of **C6**

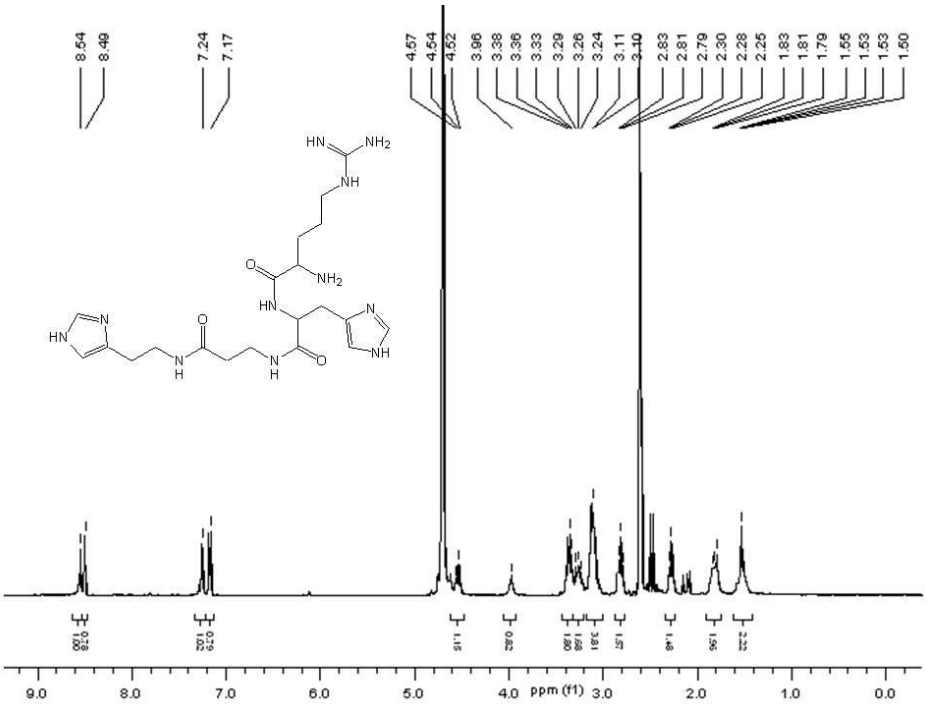

Spectra 46. ^{1}HNMR (300 MHz, D_2O) of **C7**

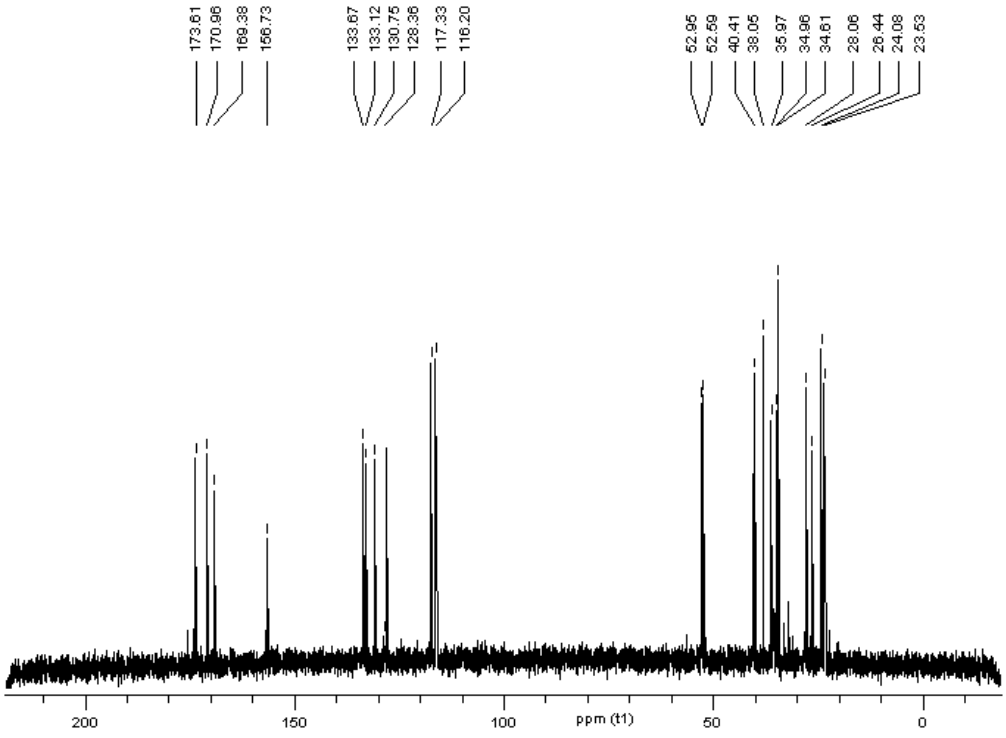

Spectra 47. ^{1}CNMR (75 MHz, D_2O) of **C7**

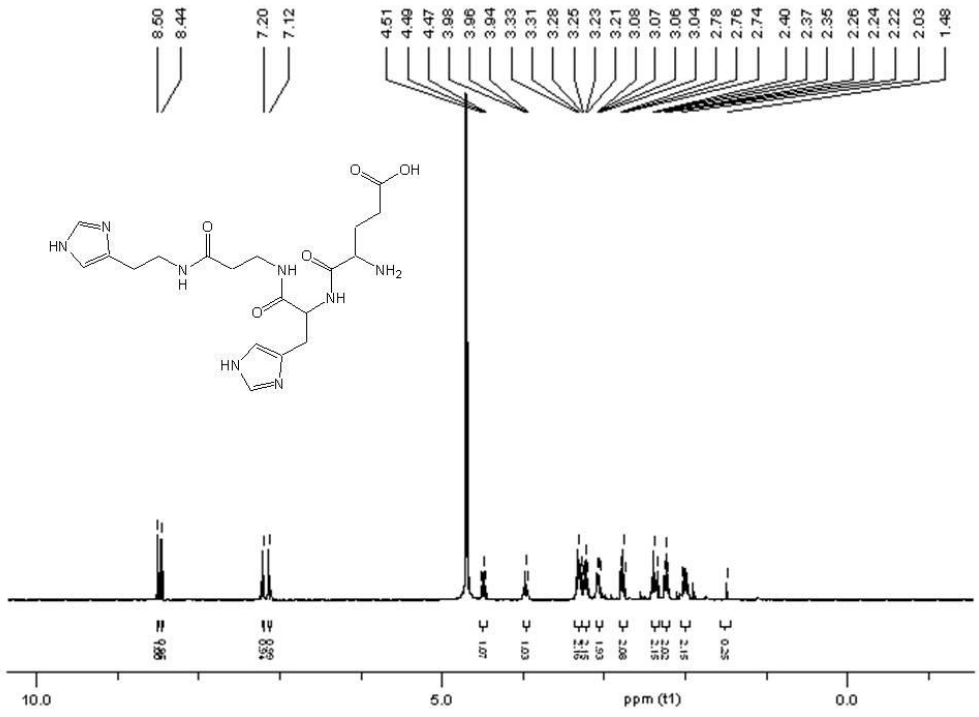

Spectra 48. ^{1}HNMR (300 MHz, D_2O) of **C8**

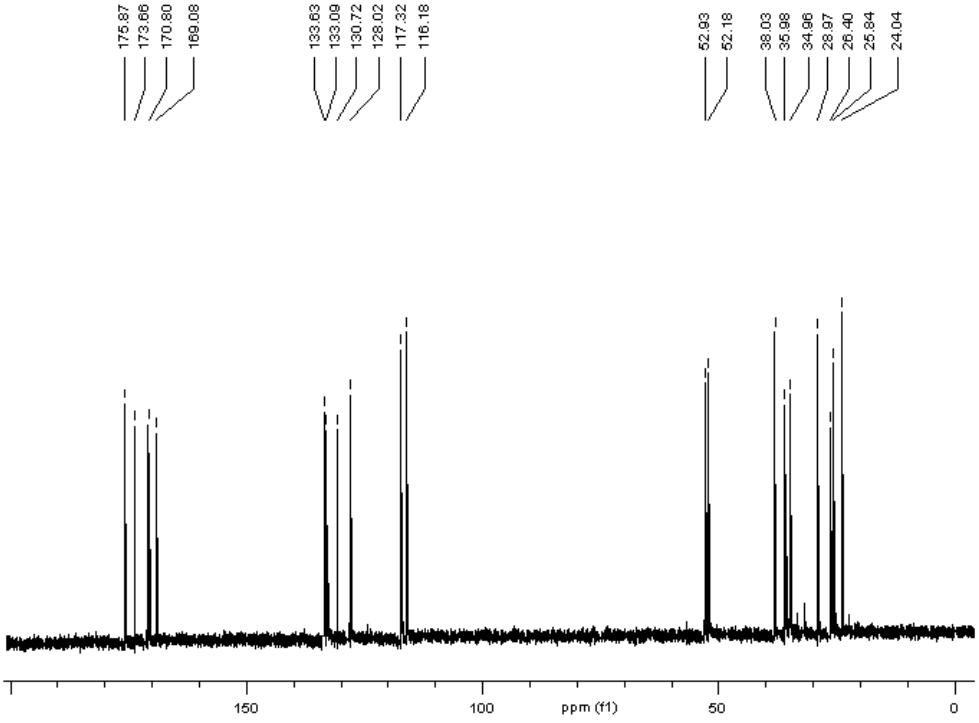

Spectra 49. ^{1}CNMR (75 MHz, D_2O) of **C8**

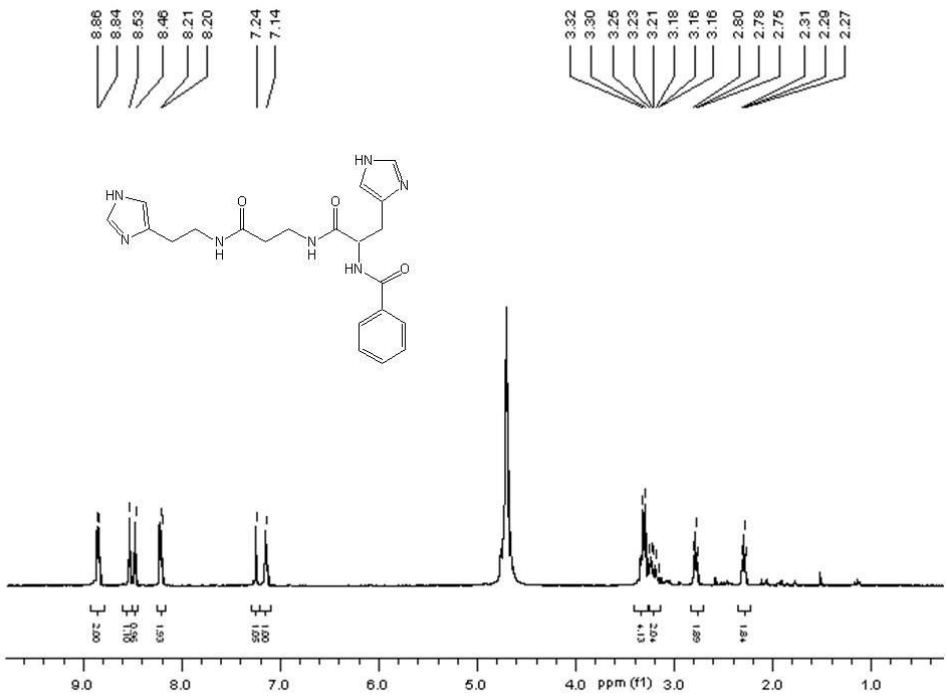

Spectra 50. ^{1}HNMR (300 MHz, D_2O) of **C9**

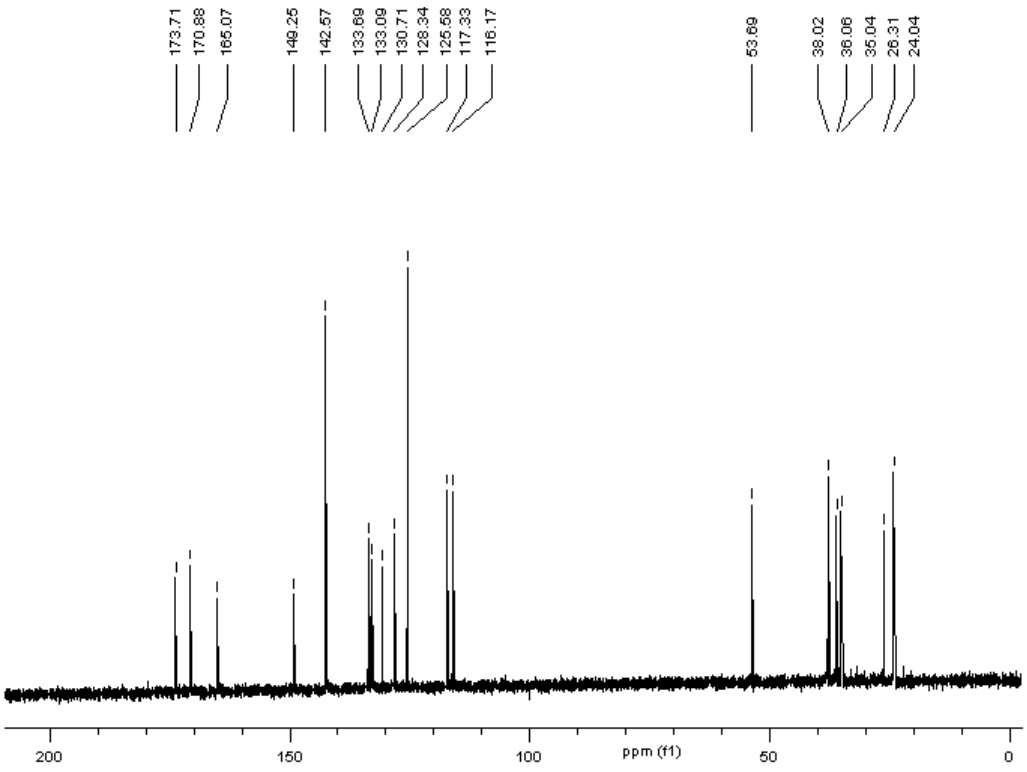

Spectra 51. ^{1}CNMR (75 MHz, D_2O) of **C9**

REFERENCES

1) Means, G. E.; Freeney, R. E. Chemical Modification of Proteins; Holden-Day: San Francisco, 1971.

2) Hirs, C.H.W.; Timasheff, S. N., Eds. Methods Enzymol. 1972, 25.

3) Ibid., 1977, 47

4) Glazer, A. N.; DeLange, R. J.; Sigman, D.S. Chemical Modification of Proteins: Selected methods and Analytical procedures; North-Holland/American Elsevier: Amsterdam, 1975.

5) Stadtman, R. *Annu. Rev. Biochem*. **1993**, *62*, 797-821.

6) Skipper, P. *Chem. Res. Toxicol*. **1996**, *9*, 918-923.

7) Lundblad, R. Modification of proteins. Chemical reagents for protein modification. Third edition, CRC press, Boca Raton, Florida 2005. Chapter 1.

8) Trejo-Gonzalez, A.; Feria-Morales, A.; Wild-Altamirano, C. Modification of proteins. Food, nutritional and pharmacological aspects. Advances in chemistry series 198, American Chemical Society, Washington, D.C. 1982. Chapter 9

9) Freeney, R. E.; Blankenhorn, G.; Dixon, H. B. F. *Adv. Protein Chem*. **1975**, *29*, 135.

10) Metz, B.; Kersten, G.; Baart, G.; Jong, A.; Meiring, H.; Hove, H.; van Steenbergen, M.; Hennink, W.; Crommelin, D.; Jiskoot, W. *Bioconjugate Chem.* **2006,** *17*, 815-822.

11) Seiler, N.; Jung, M. J.; Eds. Enzyme-Activated irreversible inhibitors. Elsevier/North Holland Biomedical: Amsterdam,1978.

12) Metcalf, B. W. *ACS Symp. Ser*. **1980**, *123*, 1.

13) Benisek, W. F.; Orgez, J. R.; Smith, S.B. Modification of proteins. Food, nutritional and pharmacological aspects. Advances in chemistry series 198, American Chemical Society, Washington, D.C. 1982. Chapter 10.

14) Harkness, D. R.; *Trends Biochem. Sci*. **1976**, *1*, 73.

15) Raymond Bonnett, Chemical aspect of photodynamic therapy. Advanced chemistry texts; v.1, 2000, Gordon and Breach science publishers, Amsterdam, pages 57-79.

16) Hott J. L.; Borkman R. F. *Photochem Photobiol.* **1992**, *56*, 257-263.

17) Adams, A.; Talman E.; Cambpell, L.; McIlroy, B.; Moore, M. *J Biomed Mater Res*. **2001**, *57*, 582-587.

18) Chan, B.; Kochevar I.; Redmond R. *J. Surg. Res*. **2002**, *108*, 77-84.

19) Chan, B.; Amann C.; Yaroslavsky A.; Title, C.; Smink, D.; Zarins, B.; Kochevar, I. *J Surg Res.* **2005**.

20) Chan, B.; Sato, M.; Vacanti J.; Kochevar I.; Redmond R. Photochemical bonding of epithelial cell-seeded collagen lattice to rat muscle layer for esophageal tissue ingeneering. Procedings of the photonics west, SPIE 2005, 22-27 January 2005b. San Jose, California, USA.

21) Vogelmann, E.; and Kramer, H. *Photochem. Photobiol.* **1976**, *24*, 595-597.

22) Pathak, M. *J. Natl. Cancer Inst.* **1982**, *69*, 163-170.

23) Oschsner, M. *J. Photochem. Photobiol. B.* **1997**, *39*, 1-18.

24) Vemeersch, G.; Ronfard-Haret, J., Bazin, M., Carillet, V.; Morliere, P.; and

25) Santus, R. *Photochem. Photobiol*. **1991**, *54*, 661-666.

26) Balasubramanian, D.; Du, X.; Zigler J.S. Jr. *Photochem. Photobiol.* **1990**, *52*, 761-768.

27) Inoue, K; Matsuura, T; and Saito, I. *Bull. Chem. Soc. Japan* **1982**, *55*, 2959.

28) Moan, J.; and Berg, K. *Photochem. Photobiol.* **1991**, *53*, 549-553.

29) Schwartz, S.; Absolon, K.; and Vermund, H. *Univ. Minnesota Med. Bull.* **1955**, *7*, 7-13.

30) Lipson, R.; Aldes, E.; and Olsen, A. *J. Natl. Cancer Inst.* **1961**, *1*, 1-11.

31) Dougherty, T.; Gomer, C.; Henderson, B.; Jori, G.; Kessel, D.; Korbelik, M.; Moan, J.; Peng, Q. *J. Natl. Cancer Inst.* **1998**, *90*, 889-905.

32) Garbo, G. *J. Photochem. Photobiol. B.* **1996**, *34*, 109-116.

33) Diwu, Z.; and Lown, J. *Pharmacol. Ther.* **1994**, *63*, 1-35.

34) Anderson, C.; Hrabovsky, S.; McKinley, Y.; Tubesing, K.; Tang, H.; Dunbar, R.; Mukhtar, H.; Elmets, C. *Photochem. Photobiol.* **1997**, *65*, 895-901.

35) Delaey, E.; van Laar, F.; De Vos, D.; Kamuhabwa, A.; Jacobs, P.; de Witte, P. *J. Photochem. Photobiol. B.* **2000**, *55*, 27-36.

36) Pandey, R.; Bellnier, D.; Smith, K.; Dougherty, T. *Photochem. Photobiol.* **1991**, *53*, 65-72.

37) Arnold, D. R.; Baird N.C; Bolton, J. R.; Brand, J.C.; Jacobs, P. W.; de Mayo, P.; Ware, W.R. Academic Press Inc. New York and London 1974. Cap 1.

38) Dennis, E.; Dolmans, G.; Fukumura, D.; Jain, R. *Nat. Rev. Cancer* **2003**, *3*, 380-387.

39) Brana, M. F.; Castellano, J. M.; Moran, M.; Perez de Vega, M. J.; Romerdahl, C. R.; Qian, X.-D.; Bousquet, P.; Emling, F.; Schlick, E. *Anti-Cancer Drug Design* **1993**, *8*, 257-268.

40) Brana, M. F.; Castellano, J. M.; Roldan, C. M.; Santos, A.; Vazquez, D.; Jimenez, A. *Cancer Chemother. Pharmacol.* **1980**, *4*, 61-66.

41) Brana, M. F.; Castellano, J. M.; Sanz, A. M.; Roldan, C. M.; Roldan, C. *Eur. J. Med. Chem.* **1981**, *16*, 207-212.

42) Bousquet, P. F.; Brana, M. F.; Conlon, D.; Fitzgerald, K. M.; Perron, D.; Cocchiaro, C.; Miller, R.; Moran, M.; George, J.; Qian, X.-D.; Keilhauer, G.; Romerdahl, C. A. *Cancer Res.* **1995**, *55*, 1176-1180.

43) Waring, M. J.; Gonzalez, A.; Jimenez, A.; Vazquez, D. *Nucleic Acids Res.* **1979**, *7*, 217-233.

44) Rideout, D.; Schinazi, R.; Pauza, C. D.; Lovelace, K.; Chiang, L.C.; Calogeropoulou, T.; McCarthy, M.; Elder, J. H. *J. Cell. Biochem.* **1993**, *51*, 446-457.

45) Chanh, T. C.; Lewis, D. E.; Allan, J. S.; Sogandares-Bernal, F.; Judy, M. M.; Utecht, R. E.; Matthews, J. L. *AIDS Res. Hum. Retro*V*iruses* **1993**, *9*, 891-896.

46) Chanh, T. C.; Archer, B. J.; Utecht, R. E.; Lewis, D. E.; Judy, M. M.; Matthews, J. L. *Biomed. Chem. Lett.* **1993**, *3*, 555-556.

47) Judy, M. M.; Nosir, H.; Jackson, R. W.; Matthews, J. L.; Lewis, D. E.; Utecht, R. E.; Yuan, D. *Proc. SPIEsInt. Soc. Opt. Eng.* **1996**, *2671*, 251-255.

48) Bailly, C.; Brana, M.; Waring, M. J. *Eur. J. Biochem.* **1996**, *240*,195-208.

49) Mehrotra, J.; Misra, K.; Mishra, R. K. *Nucleosides Nucleotides* **1994**, *13*, 963-978.

50) Saito, I.; Takayama, M.; Sakurai, T. *J. Am. Chem. Soc.* **1994**, *116*, 2653-2654.

51) Saito, I.; Takayama, M.; Suyiyama, H.; Nakatani, K. *J. Am. Chem. Soc.* **1995**, *117*, 6406-6407.

52) Chanh, T. C.; Lewis, D. E.; Judy, M. M.; Sogandares-Bernal, F.; Michalek, G. R.; Utecht, R. E.; Skiles, H.; Chang, S. C.; Matthews, J. L. *Anti*V*iral Res*. **1994**, *25*, 133-146.

53) Judy, M. M.; Matthews, J. L.; Boriak, R. L.; Berlacu, A.; Lewis, D. E.; Utecht, R. E. *Proc. Int. Conf. Lasers* **1993**, *15*, 774-776.

54) Judy, M. M.; Matthews, J. L.; Boriak, A.; Burlacu, A. *Proc. SPIEsInt. Soc. Opt. Eng.* **1993**, *1882*, 305-308.

55) Judy, M. M.; Fuh, L.; Matthews, J. L.; Lewis, D. E.; Utecht, R. *Proc. SPIEsInt. Soc. Opt. Eng.* **1994**, *2128*, 506-509.

56) Judy, M. M.; Matthews, J. L.; Boriak, R. L.; Burlacu, A.; Lewis, D. E.; Utecht, R. E. *Proc. SPIEsInt. Soc. Opt. Eng.* **1993**, *1876*, 175-179.

57) Johnson, S.; O'Neill, A.; Motarjem, P.; Amann, C.; Nguyen, T.; Randolph, M.; Winograd, J.; Kochevar, I.; Redmond, R. *Journal of Surgical Research* **2003**, *143*, 224-229.

58) Merguerian, P.A.; Pugach, J.L.; Lilge, L.D. *SPIE Proc.* **1999**, *3590*, 194.

59) Judy, M. M.; Jackson, R. W.; Nosir, H. R.; Matthews, J. L.; Loyd, J. D.; Lewis, D. E.; Utecht, R. E.; Yuan, D. *SPIE Proc.* **1997**, *2970*, 257.

60) Judy, M.M.; Jackson, R.W.; Nosir, H.R.; Matthews, J.L.; Lewis, D.E.; Utecht, R.E.; Yuan, D. *SPIE Proc.* **1996**, *2922*, 436.

61) Zhang, J.; Woods, J.; Brown, P.; Mowery, R.; Kane, R. *Journal of Biomedical Optics* **2004**, *9*, 1089-1092.

62) Becker,R.; Starke, C.; Heymann,M.; Nebelung W. *Clin. Orthop. Relat. Res.* **2001**, *400*, 236–245.

63) Judy,M.; Nosir, R. R.; Jackson, R.W; Matthews, J.L; Utecht, R.; Lewis,D.; Yuan,D. *Proc. SPIE* **1998**, *3195*, 21–24.

64) Saito, I.; Takayama, M.; Kawanishi, S. *J. Am. Chem. Soc.* **1995**, *117*, 5590-5591.

65) Woods, R. J. Photochemical crosslinking of protein by 1,8-naphthalimides. Ph.D. diss., Baylor University, **2003**.

66) de Silva, A. P.; Gunaratne, H. Q. N.; Habib-Jiwan, J. L.; McCoy, C. P.; Rice, T. E.; Soumillion, J. P. *Angew. Chem. Int. Ed. Engl.* **1995**, *34*, 1728.

67) Hansch, C; Leo, A.; Taft, R. W. *Chem. Rev*. **1991**, *91*(2), 165.

68) Alexiou, M. S.; Tychopoulos, V.; Ghorbanian, S.; Tyman, J. H. P.; Brown, R. G.; Brittain, P. I. *J. Chem. Soc.-Perkin Trans. 2* **1990**, 837–842.

69) Hasharoni, K.; Levanon, H.; Greenfield, S. R.; Gosztola, D. J.; Svec, W. A.; Wasielewski, M. R. *J. Am. Chem. Soc.* **1996**, *118*, 10228–10235.

70) Ramachandram, B.; Saroja, G.; Sankaran, B.; Samanta, A. *J. Phys. Chem. B* **2000**, *104*, 11824–11832.

71) Wintgens, V.; Valat, P.; Kossanyi, J.; Biczok, L.; Demeter, A.; Berces, T. *J. Chem. Soc.-Faraday Trans.* **1994**, *90*, 411–421.

72) Pardo, A.; Martin, E.; Poyato, J. M. L.; Camacho, J. J.; Brana, M. F.; Castellano, J. M. *J. Photochem. Photobiol., A* **1987**, *41*, 69–78.

73) Adam, W.; Qian, X.; Saha-Möller, C.R. *Tetrahedron* **1993**, *49*, 417.

74) Dubbelman, T.; De Goeij, A.; Van Steveninck, J. *Biochim. Byophis. Acta* **1978**, *511*, 141-151.

75) Aoki, S.; Matsuo, N.; Hanaya, K.; Yamada,Y.; Kageyama, Y. *Bioorganic & Medicinal Chemistry* **2009**, *17*, 3405-3413.

76) Gu, H.; Yang, Z.; Gao, J.; Chang, C.; Xu, B. *J. Am. Chem. Soc.* **2005**, *127*, 34-35.

77) Lee, B.; Dalsin, J.; Messersmith, P. *Biomacromolecules* **2002**, *3*, 1038-1048.

78) Hu, B.; Messersmith, B. *Tetrahedron letters* **2000**, 41, 5795-5798.

79) Abraham, B.; Kelly, L. *J. Phys. Chem. B.* **2003**, *17*, 12534-12541.

80) Kang, A. G. Mechanistic studies of photochemical protein modification using 1,8-naphthalimides. M.S. diss., Baylor University, **2009**.

81) Dechene, M.; Wink, G.; Smith, M.; Swartz, P, Mattos, C. *Proteins* **2009**, *76*, 861-881.

82) PDB; http://www.rcsb.org/pdb/explore/explore.do?structureId=3EV3.

83) Wine, Y.; Cohen-Hadar, N.; Freeman, A.; FroloW, F.; *Biotechnol. Bioeng*. **2007**, *98*, 711-718.

84) Straigth, R.; Spikes, J. In Singlet O_2; Frimer, A.; Ed.; CRC: Boca Raton, Florida, 1985; Vol. 4, ch 2.

85) Shen, H.; Spikes, J.; Cameron, K.; Kopeck, J. *J. Photochem. Photobiol. A*. **2000**, *130*, 1-6.

86) Spikes, J.; Shen, H.; Kopeckova, P. *Photochem. Photobiol*. **1999**, *70*, 130-137.

87) Misra, H.; Fridovich, I. *Arch. Biochem. Biophys*. **1977**, *181*, 308-312.

88) Kato, Y.; Uchida, K.; Kawakishi, S. *Photochem. Photobiol*. **1994**, *59*, 343-349.

89) Achenbach J.C.; Chiuman, W.; Cruz, R.P.; Li, Y. *Current Pharmaceutical Biotechnology*. **2004**, *5*, 321.

90) Breaker R. R; and Joyce, G. F. *Chem. Biol.* **1994**, *1*, 223-229.

91) Li, Y.; Breaker, R. R. *J. Am. Chem. Soc*. **1999**, *121*, 5364–5372.

92) Smith, R. M.; Hansen, D. E. *J. Am. Chem. Soc.* **1998**, *120*, 8910–8913.

93) Schlosser, K.; Li, Y. *Chemistry & Biology*. **2009**, *16*, 311-322.

94) Albery, W. J.; Knowles, J.R. *Biochemistry*. **1976**, *15*, 5631-5640.

95) Silverman, S. *Org. Biomol. Chem.* **2004**, *2*, 2701.

96) Wang, W.; Billen, L. P.; and Li, Y. *Chemistry and Biology*. **2002**, *9*, 507.

97) Feldman, A.; and Sen, D. *J. Mol. Biol.* **2001**, *313*, 283.

98) Faulhammer, D.; Famulok, M. *J. Mol. Biol.* **1997**, *269*,188.

99) Breaker, R. R.; Joyce, G. F. *Chem. Biol.* **1995**, *2*, 655-660.

100) Faulhammer, D.; Famulok, M. *Angew. Chem. Int. Ed.Engl.*, **1996**, *35*, 2809-2813.

101) Roth, A.; Breaker, R. R. *Proc. Natl. Acad. Sci. USA.* **1998**, *95*, 6027-6031.

102) Geyer, C. R.; Sen, D. *Chem. Biol.* **1997**, *4*, 579-593.

103) Faulhammer, D.; Famulok, M. *J. Mol. Biol.* **1997**, *269*,188-202.

104) Santoro, S.W.; Joyce, G.F. *Biochemistry.* **1998**, *37*, 13330-13342.

105) Santoro, S.W.; Joyce, G.F. *Proc. Natl. Acad. Sci. USA.* **1997**, *94*, 4262-4266.

106) Cairns, M.J.; King, A.; Sun, L.Q. *Nucleic Acids Res.* **2003**, *31*, 2883-2889.

107) Li, J.; Zheng, W.; Kwon, A.H.; Lu, Y. *Nucleic Acids Res.* **2000**, *28*, 481-488.

108) Cruz, R.P.G.; Withers, J.W.; Li, Y. *Chem. Biol.* **2003**, *11*, 57-67.

109) Peracchi, A. *J. Biol. Chem.* **2000**, *275*, 11693-11697.

110) Li, J.; Lu, Y. *J. Am. Chem. Soc.* **2000**, *122*, 10466–10467.

111) Chiuman, W.; Li, Y. *Nucleic Acids Res.* **2007**, *35*, 401–405.

112) Liu, J.; Lu, Y. *Anal. Chem*. **2003**, *75*, 6666–6672.

113) Liu, J.; Lu, Y. *J. Am. Chem. Soc*. **2003**, *125*, 6642–6643.

114) Liu, J.; Lu, Y. *J. Fluoresc*. **2004**, *14*, 343–354.

115) Xiao, Y.; Rowe, A. A.; and Plaxco, K.W. *J. Am. Chem. Soc.* **2007**, *129*, 262–263.

116) Liu, J.; Lu, Y. *Chem. Commun. (Camb.)* **2007**, 4872–4874.

117) Liu, J.; Lu, Y. *J. Am. Chem. Soc*. **2007**, *129*, 9838–9839.

118) Liu, J.; Lu, Y. *Angew. Chem. Int. Ed. Engl*. **2007**, *46*, 7587–7590.

119) Hollenstein, M.; Hipolito, C.; Lam, C.; Dietrich, D.; and Perrin, D.M. *Angew. Chem. Int. Ed. Engl*. **2008**, *47*, 4346–4350.

120) Liu, J.; Brown, A. K.; Meng, X.; Cropek, D. M.; Istok, J. D.; Watson, D. B.; Lu, Y. *Proc. Natl. Acad. Sci. USA* **2007**, *104*, 2056-2061.

121) Feldman, A. R.; Sen, D. *J. Mol. Biol.* **2001**, *313*, 283-294.

122) Lermer, L.; Roupioz, Y.; Ting, R.; Perrin, D. M. *J. Am .Chem. Soc.* **2002**, *124*, 9960-9961.

123) Perrin, D. M.; Garestier, T.; Helene, C. *J. Am. Chem. Soc.* **2001**, *123*, 1556-1563.

124) Pyle, A. M.; Chu, V. T.; Jankowsky, E.; Boudvillain, M.; *Methods Enzymol.* **2000**, *317*, 140–146.

125) Purtha, W. E.; Coppins, R.L.; Smalley, M. K.; Silverman, S.K. *J. Am. Chem. Soc.* **2005**, *127*, 13124–13125.

126) Wang, Y.; Silverman, S. K. *Angew. Chem. Int. Ed. Engl.* **2005**, *44*, 5863–5866.

127) Pratico, E. D.; Silverman, S. K. *RNA* **2007**, *13*, 1528–1536.

128) Pratico, E. D.; Wang, Y.; Silverman, S. K. *Nucleic Acids Res.* **2005**, *33*, 3503–3512.

129) Wang, Y.; Silverman, S. K. *ACS Chem. Biol.* **2006**, *1*, 316–324.

130) Baum, D.A.; Silverman, S. K. *Angew. Chem. Int. Ed. Engl.* **2007**, *46*, 3502–3504.

131) Takahashi, H.; Hamazaki, H.; Habu, Y.; Hayashi, M.; Abe, T.; Miyano, N.; Takaku, H. FEBS Lett. **2004**, *560*, 69-74.

132) Kurosaki, N.; Takaku, H. *FEBS Lett.* **2004**, *570*, 72–74.

133) Trepanier, J.; Tanner, J. E.; Momparler, R. L.; Le, O. N.; Alvarez, F.; Alfieri, C. *J. Viral Hepat.* **2006**, *13*, 131–138.

134) Chakraborti, S.; Banerjea, A. C. *Mol. Ther*. **2003**, *7*, 817–826.

135) Hou, Z.; Meng, J.R.; Niu, C.; Wang, H.F.; Liu, J.; Hu, B. Q.; Jia, M.; Luo, X. *Clin. Exp. Pharmacol. Physiol*. **2007**, *34*, 1160–1164.

136) Zhang, L.; Gasper, W. J.; Stass, S. A.; Ioffe, O. B.; Davis, M. A.; Mixson, A. J. *Cancer Res*. **2002**, *62*, 5463–5469.

137) Fahmy, R. G.; Waldman, A.; Zhang, G.; Mitchell, A.; Tedla, N.; Cai, H.; Geczy, C. R.; Chesterman, C. N.; Perry, M.; Khachigian, L. M. *Nat. Biotechnol.* **2006**, *24*, 856–863.

138) Zhang, G.; Dass, C. R.; Sumithran, E.; Di Girolamo, N.; Sun, L. Q.; Khachigian, L.M. *J. Natl. Cancer Inst.* **2004**, *96*, 683–696.

139) Bhindi, R.; Khachigian, L. M.; Lowe, H.C. *J. Thromb. Haemost*. **2006**, *4*, 1479–1483.

140) Mitchell, A.; Dass, C. R.; Sun, L. Q.; Khachigian, L.M. *Nucleic Acids Res.* **2004**, *32*, 3065–3069.

141) Santiago, F. S.; Lowe, H. C.; Kavurma, M. M.; Chesterman, C. N.; Baker, A.; Atkins, D.G.; Khachigian, L.M. *Nat. Med.* **1999**, *5*, 1264–1269.

142) Chen, Y.; and Mao, C. *J. Am. Chem. Soc.* **2004**, *126*, 8626–8627.

143) Chen, Y.; Wang, M.; Mao, C. *Angew. Chem. Int. Ed. Engl.* **2004**, *43*, 3554–3557.

144) Tian, Y.; Mao, C. *Talanta* **2005**, *67*, 532–537.

145) Stojanovic, M. N.; de Prada, P.; Landry, D. W. *Nucleic Acids Res*. **2000**, *28*, 2915–2918.

146) Sando, S.; Sasaki, T.; Kanatani, K.; Aoyama, Y. *J. Am. Chem. Soc.* **2003**, *125*, 15720–15721.

147) Suenaga, H., Liu, R., Shiramasa, Y., and Kanagawa, T. *Appl. Environ. Microbiol*. **2005**, *71*, 4879–4884.

148) Buchhaupt, M.; Peifer, C.; Entian, K.D. *Anal. Biochem*. **2007**, *361*, 102–108.

149) Liu, J.; Lu, Y. *Anal. Chem*. **2004**, *76*, 1627–1632.

150) Li, D.; Shlyahovsky, B.; Elbaz, J.; Willner, I. *J. Am. Chem. Soc*. **2007**, *129*, 5804–5805.

151) Cho, E. J.; Yang, L.; Levy, M.; Ellington, A. D. *J. Am. Chem. Soc.* **2005**, *127*, 2022–2023.

152) Stojanovic, M. N., and Stefanovic, D. *J. Am. Chem. Soc.* **2003**, *125*, 6673–6676.

153) Lederman, H.; Macdonald, J.; Stefanovic, D.; Stojanovic, M. N. *Biochemistry.* **2006**, *45*, 1194–1199.

154) Macdonald, J.; Li, Y.; Sutovic, M.; Lederman, H.; Pendri, K.; Lu, W.; Andrews, B.L.; Stefanovic, D.; Stojanovic, M. N. *Nano Lett.* **2006**, *6*, 2598–2603.

155) Stojanovic, M. N.; Stefanovic, D. *Nat. Biotechnol.* **2003**, *21*, 1069–1074.

156) Breaker, R. R.; Joyce, G. F. *Trends Biotechnol.* **1994**. *12*, 268–275.

157) He, Q.; Zhou, J.; Zhou, D.; Nakamatsu, Y.; Baba, T.; Taira, K. *Biomacromolecules* **2002**, *3*, 69-83.

158) Dreyer, G. B.; Dervan, P. B. *Proc. Natl Acad. Sci. USA* **1995**, *82*, 968-972.

159) Dervan, P. B. *Nature* **1992**, *359*, 87-88.

160) Meijler, M. M; Zelenko, O.; Sigman, D. S. *J. Am. Chem. Soc.* **1997**, *119*, 1135-1136.

161) Sigman, D. S. *Acc. Chem. Res.* **1986**, *19*, 180-186.

162) Sigman, D. S.; Mazumder, A.; Perrin, D. M. *Chem. Rev.* **1993**, *93*, 2295-2316.

163) Basile, L. A.; Barton, J. K. *J. Am. Chem. Soc.* **1987**, *109*, 7548-7550.

164) Basile, L. A.; Raphael, A. L.; Barton, J. K. *J. Am. Chem. Soc.* **1987**, *109*, 7550.

165) Gallagher, J.; Chen, C. B.; Pan, C. Q.; Perrin, D. M.; Cho, Y.; Sigman, D. S. *Bioconj. Chem.* **1996**, *7*, 413-420.

166) Trawick, B. N.; Daniher, A. T.; Bashkin, J. K. *Chem. Rev.* **1998**, *98*, 939-960.

167) Baskin, J. K.; Xie, J.; Daniher, A. T.; Jenkins, L. A.; Yeh, G. C. *Nato Asi Ser. Ser. C*. **1996**, *479*, 355-366.

168) Cech, T. R.; *J. Am. Med. Assoc.* **1988**, *260*, 3030-3034.

169) Cohen, J. S. *Oligonucleotides* **1989**, CRC press, Boca Raton, FL.

170) Hanner, R.; Hall, J. *Antisense Nucleic Acid Drug Dev*. **1997**, *7*, 423-430.

171) Morrow, J. R.; Buttrey, L. A.; Shelton, V. M.; Berback, K. A. *J. Am. Chem. Soc*. **1992**, *114*, 1903-1905.

172) Putnam, W.; Daniher, A. T.; Trawick, B. N.; Bashkin, J. K. *Nucleic Acids Research* **2001**, *29*, 2199-2204.

173) Liu, S.; Hamilton, A. D. *Tet. Lett.* **1997**, *38*, 1107-1110.

174) LInkletter, B.; Chin, J. *Angew. Chem. Int. Ed. Engl*. **1995**, *34*, 472-474.

175) Stern, M. K.; Bashkin, J. K.; Sall, E. D. *J. Am. Chem. Soc.* **1990**, *112*, 5357.

176) Modak, A. S.; Gard, J. K.; Merriman, M. C.; Winkeler, K. A.; Bashkin, J. K.; Stern, M. K. *J. Am. Chem. Soc.* **1991**, *113*, 283.

177) Jenkins, L. A.; Bashkin, J. K.; Pennock, J. D.; Florian, J.; Washel, A. *Inorg. Chem.* **1999**, *38*, 3215-3222.

178) Jenkins, L. A.; Bashkin, J. K.; Autry, M. E. *J. Am. Chem. Soc.* **1996**, *118*, 6822-6825.

179) Jenkins, L. A.; Bashkin, J. K. *Inorg. Chim. Acta* **1997**, *263*, 49-52.

180) Verbeure, B.; Lacey, C. J.; Froeyen, M.; Rozenski, J.; Herdewijn, P. *Bioconjugate Chem.* **2002**, *13*, 333-350.

181) Breslow, R., Dong, S. D., Webb, Y., and Xu, R. J. *J. Am. Chem. Soc.* **1996**, *118*, 6588.

182) Reynolds, M. A.; Beck, J. A.; Say, P. B.; Dweye, B. P.; Daily, W. J.; Vaghefi, M. M.; Metzler, M. D.; Klem, R. E.; Arnold, L. J., Jr. *Nucleic Acids Res.* **1996**, *24*, 760-765.

183) Kuusela, S.; Rantanen, M.; Lonnberg, H. *J. Chem. Soc. Perkin Trans.* **1995**, *2*, 2269-2273.

184) Zhdan, N. S.; Kuznetsova, I. L.; Vlasov, A. V.; Sil'nikov, V. N.; Zenkova, M. A.; Vlasov, V. V. *Bioorg Khim.* **1999**, *25*, 723-732.

185) Carranza, D. L. Coenzymes for *in vitro* selection of DNA enzymes. Ph.D. diss., Baylor University, **2006**.

186) Theophil, E.; Siegfried, H. The Chemistry of Heterocycles: Structure, Reactions, Syntheses, and Applications, 2003, 2nd edition, John Wiley and Sons, 166.

187) Breslow, R.; Huang, D. *Proc. Natl. Acad. Sci. USA* **1991**, *88*, 4080.

188) Komiyama, M.; Matsumura, K.; Matsumoto, Y. *J. Chem. Soc., Chem. Commun.* **1992**, 640.

189) Morrow, J.; Buttrey, L.; Shelton, V.; Berback, K. *J. Am. Chem. Soc*. **1992**, *114*, 1903.

190) Takasaki, B.; Chin, J. *J. Am. Chem. Soc.* **1994**, *116*, 1121.

191) Yoshinari, K.; Yamazaki, K.; Komiyama, M. *J. Am. Chem. Soc.* **1991**, *113*, 5899.

192) http://www.genacolphilippines.com/collagene/collagene_cartilage.html